Towards an integrated microalgal biorefinery

Frederik Lloyd Zitzmann

Doctor of Philosophy

University of York

Chemistry

January 2023

Abstract

This research explores the valorisation of a proprietary microalgal strain (ALG01, provided by AlgaeCytes Ltd.) as a renewable, biobased feedstock into chemicals, materials and (bio)energy within the context of a zero-waste biorefinery. Four main areas of research are reported, namely: i. the preliminary characterisation of ALG01; ii. the isolation, purification, and characterisation of water-based microalgal proteins; iii. the tandem production of defibrillated celluloses and protein isolation from hydrolysates via acid-free hydrothermal microwave processing and their subsequent characterisation and, iv. The production and characterisation of bio-oils and bio-chars via microwave pyrolysis processing.

Water-soluble proteins were isolated successfully using ultrafiltration with up to 5% yield (weight of extracted protein-containing fraction/ initial weight of biomass) and 70% purity (percentage of protein of the overall protein-containing fraction) for the spent biomass protein retentates obtained at 180^{o}C microwave processing.

A range of defibrillated cellulose were successfully produced using acid-free hydrothermal processing with materials processed at 200^{o}C and 220^{o}C forming hydrogels. Confocal Laser Microscopy using Carbotrace 480, a fluorescent optotracer, shed more light on the spatial distribution of cellulose in the samples with cellulose congregating in lumps of small grains. Clear links have been established between the capability of forming hydrogels and the amount of cellulose present in the samples, with higher amounts of cellulose present resulting in better hydrogel formation capability. Two publications have resulted from the work on defibrillated celluloses.

The residual biomass left after protein extraction was subsequently valorised through microwave pyrolysis, yielding bio-chars, which achieved energy densification of up to 37% for spray dried biomass derived chars, and a 65% higher HHV (higher heating value) for spent biomass derived chars. The bio-oils mostly consisted of saturated fatty acids such as myristic, palmitic and stearic acid.

Overall, this research has resulted in significant new knowledge in the development of microalgal zero-waste biorefineries.

Table of Contents

List of Figures

List of Tables

Abbreviations

AA	Amino Acid
ALG01	Proprietary strain of AlgaeCytes microalgae used in this thesis
ALG15	Proprietary strain of AlgaeCytes diatom microalgae for fucoxanthin extraction
ATR IR	Attenuated total reflection infrared spectroscopy
BSA	Bovine Serum Albinum
CPM09	Abbreviation for Spent biomass peptides used for bioactivity testing
CrI	Crystallinity index
CT480	Carbotrace 480
DES	Deep eutectic solvent
DFC	Defibrillated cellulose
DHA	Docosahexaenoic acid
D.P.	Double pyrolysis
EC	Emulsion capacity
EHP	Enzymatically hydrolysed peptides
EPA	Eicosapentaenoic acid
ES	Emulsion stability
FC	Foaming capacity
FS	Foaming stability
GC-MS	Gas Chromatography- Mass Spectrometry
LC-MS	Liquid Chromatography – Mass Spectrometry
MF	Microfiltration
MFC	Micro-fibrillated cellulose
MG	Manual grinding
MW	Microwave
PBS	Phosphate-buffered saline
SEM	Scanning electron microscopy
SS NMR	Solid State NMR
TEM	Transmission electron microscopy
TGA	Thermogravimetric analysis
UF	Ultrafiltration

US	Ultrasound
WHC	Water-holding capacity
XRD	X-ray diffraction

Acknowledgment

First and foremost, I want to thank Professor Avtar Matharu for his supervision over the last four and a half years, throughout my MSc and PhD. There have been so many instances where he guided me in terms of improving my scientific progress and prowess in the lab, where he gave me valuable input for data analysis, polishing write-up, being professional in presentation as well as teaching me essential skills that made me a more developed scientist than I was before. I also must thank him a lot for being such an understanding person, giving us the freedom we need to fulfil not just our PhD projects, but also our time outside the lab.

This whole PhD also would not have been possible without the industrial partners at AlgaeCytes Ltd. providing me with my daily dose of 'green friends' ALG01 that I have come to know so well over the last years. Thanks to Donal McGee for all the knowledge transfer on microalgae and the countless conversations and expertise that helped me shape my experiments and interpret results. Further thanks also go to Yat-Keung Lee and Christopher Gadenne at AlgaeCytes for their roles in helping me with my PhD, organising logistics and letting me visit AlgaeCytes in Kent twice, I have really enjoyed the collaboration! All your input on the industrial side of things has helped me a lot in extending my field of vision beyond academia towards potential scale-up, implications and difficulties of potentially implementing my bench-top research into larger-scale and the insight into an algal business.

Within the GCCE, a massive thank you to Richard Gammons and Suranjana Bose and the technical team, who have helped me so much over the past years, may it be equipment-related, experiment-design related or a much-needed chat about literally anything. You guys really invest so much into helping us, may the issue be large or small and I really appreciate all the help I have received, without which the PhD would have been so much more difficult!

Beyond Chemistry, I have spent countless mornings and afternoons at the Department of Biology. Thank you to Chris Taylor at Proteomics, who taught me everything about running protein gels, and whose little tips and tricks saved me a lot of time and enhanced the quality of my gels considerably! Special thanks also go to Joanne Marrison and Grant Calder for assisting me in performing Confocal Laser Spectroscopy and testing out the Carbotrace

molecules, which led to two publications. Generally, every person I have worked with at the University regardless of the Department has been extraordinarily kind and helpful, thus a big thank you to everyone who has not been mentioned by name.

A person who must be named, is Dr. Tony Wild, whose Wild Fund has enabled me to pursue my PhD here at the GCCE through his generous funding and who has gifted me such a wonderful time over the last few years!

Back home, my parents have always been full of unwavering support for me and my studies, enabling me to study abroad and fulfil my dreams of pursuing a PhD and living such a beautiful time, which I have had at York throughout the years!

And finally, thanks to all the great friends I have made at the GCCE, you have made the time so much more enjoyable and fun! From chats at our office seats, to helping each other within the lab, going for lunch or dinner in the evening, strolling through York or cooking together, all of you contributed to a fantastic time which I will certainly miss dearly.

Declaration

I declare that this thesis is a presentation of original work, and I am the sole author. This work has not previously been presented for an award at this, or any other, University. All sources are acknowledged as References.

Work on the bioactivity testing of spent peptides, enzymatically hydrolysed peptides and microwaved peptides has been conducted by Aelius Biotech at the University of Newcastle, from whose reports the appropriate graphs have been taken.

Parts of this research have been published in peer-reviewed journals:

Publication 1:

Zitzmann, F.L.; Ward, E.; Meng, X.; Matharu, A.S. Microwave-Assisted Defibrillation of Microalgae. *Molecules* **2021**, *26*, 4972. https://doi.org/10.3390/molecules26164972

Publication 2:

Zitzmann, F.L.; Ward, E.; Matharu, A.S. Use of Carbotrace 480 as a Probe for Cellulose and Hydrogel Formation from Defibrillated Microalgae. *Gels* **2022**, *8*, 383. https://doi.org/10.3390/gels8060383

This research has also been presented at the following conferences:

1. 'Youth and Climate Change' organised by The Culture and Education Section of British Embassy in Moscow/British Council Russia on 18/02/2022.
2. 'Advances in Green Chemistry and Sustainable Technology', Goa University and Syngenta, India on 31/09/2021.
3. 'PhD Student Poster Presentation', University of York, Department of Chemistry, on 24/03/2022.

„In den Wissenschaften ist viel Gewisses, sobald man sich von den Ausnahmen nicht irremachen lässt und die Probleme zu ehren weiß.“

Johann Wolfgang von Goethe

Chapter 1

General Introduction

1.1 Contextualisation

Our planet and all life on it are in the middle of an unsustainable transition connected to global warming and climate change. Anthropogenic or human-induced activity associated with increased industrialisation, urbanisation and, historically, unsustainable manufacturing processes through the overuse of fossil fuels are directly linked to climate change.[1,2] As global population continues to rise, currently at 8 billion and expected to reach 10 billion by the middle of this century, our needs for chemicals, materials and energy will also increase commensurately.[3] Chemical manufacturing processes have led to resource depletion both mineral and organic (fossil), pollution and increased waste. The chemical industry itself contributes to approximately 7% of global greenhouse gas emissions.[4]

Thus, we need to change our mindset from being oil-reliant (unsustainable) to renewable resource-reliant (sustainable) and explore waste reutilisation or valorisation.[1,2,5] Fossil fuels will no longer play a major role in the future for our chemicals, materials and energy needs, after decades of basing our complete economies, infrastructure and way of living on them.[6,7] Instead, non-food competitive vegetal biomass (either terrestrial or aquatic), especially where it exists as waste, residual or is underutilised, is a promising alternative as it is a carbon-neutral feedstock, reduces waste and positively impacts on global carbon dioxide emissions.[8,9] The transition from traditional petroleum refineries to biorefineries coupled with the concepts of green chemistry, the United Nations (UN) Sustainable Development Goals (SDG) and circular (cradle to cradle) economy principles, is envisaged to combat climate change and support a carbon-neutral, zero-waste, sustainable 21st century.[10]

1.2 Green Chemistry and Sustainable Development Goals

Anastas and Warner first introduced the term 'Green Chemistry' in the late 1990s.[11] Green chemistry is the design of chemical products and processes that reduce or eliminate the use or generation of hazardous substances. The practice of green chemistry is guided by a framework or operating rules known as the 12 Principles of Green Chemistry (Table 1),[7] which is contextualised with respect to this research later in this thesis (see Section 1.5). However, at this juncture it is already evident that the use of microalgae as a feedstock complies with green chemistry principle 7 (use of renewable feedstocks).

Green chemistry in combination with the UN SDGs is pivotal to achieving improved sustainability.[12–14] The UN SDGs focus on targets that set out to fight the most urgent global problems to combat climate change and limit the increase in global warming to within 1.5°C with respect to pre-industrialisation levels.[12,15,16] Although many SDGs may be linked to green chemistry, SDG12 (Responsible Production and Consumption) probably links closest as it conceives to reduce waste, increase resource efficiency (doing more with less), decouples economic growth from environmental pollution (seeks alternatives to crude oil) and promotes sustainable lifestyles through circular economy principles.[17]

Table 1 The 12 Principles of Green Chemistry[11]

Green Chemistry Principle	**Meaning**
1. Waste Prevention	It is better to prevent waste than to treat or clean up waste after it is formed
2. Atom Economy	Synthetic methods should be designed to maximize the incorporation of all materials used in the process into the final product
3. Avoid hazardous substances	Wherever practicable, synthetic methodologies should be designed to use and generate substances that possess little or no toxicity to human health and the environment
4. Designing Safer Chemicals	Chemical products should be designed to preserve efficacy of function while reducing toxicity
5. Safer Solvents	The use of auxiliary substances should be made unnecessary wherever possible and innocuous when used
6. Energy Efficiency	Energy requirements should be recognised for their environmental and economic impacts and should be minimised. Synthetic methods should be conducted at ambient temperature and pressure
7. Use of renewable feedstocks	A raw material of feedstock should be renewable rather than depleting wherever technically and economically practicable

8. Avoid Derivatives	Unnecessary derivatisation should be avoided whenever possible
9. Catalysis	Catalytic reagents are superior to stoichiometric reagents
10. Biodegradation	Chemicals products should be designed so that at the end of their function they do not persist in the environment and break down into innocuous degradation products
11. Analysis for Pollution Prevention	Analytical methodologies need to be further developed to allow for real-time, in-process monitoring and control prior to the formation of hazardous substances
12. Accident Prevention	Substances and the form of a substance used in a chemicals process should be chosen so as to minimise the potential for chemicals accidents, including releases, explosions and fires.

Thus, transitioning from petroleum refineries (oil reliant) to biorefineries (biomass reliant) that operate within green chemistry principles is an interesting concept.

1.3 The Biorefinery Concept

The biorefinery concept utilises biomass as a feedstock, which is then processed into chemicals, materials, and bioenergy. This process is called valorisation as chemical value is added to the components resulting from the refinery stream. Potentially, any form of renewable biomass, for example, wood, crops, algae, crab shells, food waste etc can be utilised.[1,18,19] Figure 1-1 displays the schematic of a closed biorefinery cycle based on microalgae. A biorefinery operates on a carbon neutral circular principle, *i.e.*, release of CO_2 from its products are counterbalanced by the photosynthetic uptake potential of the initial biomass feedstock. This has a significant advantage over a petrochemical refinery which has a negative environmental footprint both during extraction, fractionation and manufacturing processes.[20,19]

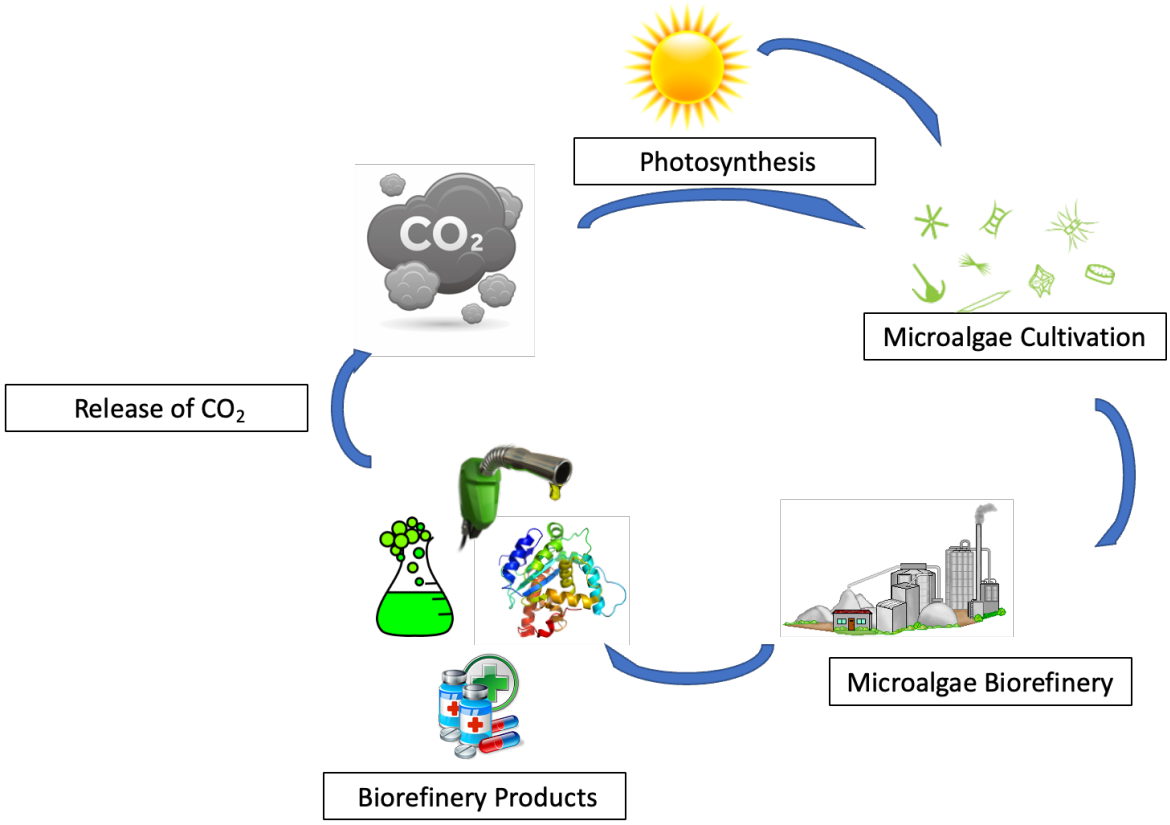

Figure 1-1 Schematic of a microalgae-based biorefinery

There are four generations of biorefineries based on the type of feedstock used and outputs delivered. First generation biorefineries commonly used feedstock that was in direct competition with food production, for example, corn and sugarcane to produce biofuels (bioalcohol in this case). This prompted a significant societal and ethical food versus fuel debate.[21] Second generation biorefineries are based on non-food competing feedstock: predominantly lignocellulosic biomass emanating from, for example, agricultural residues, forestry residues, unavoidable food supply chain wastes, etc, that deliver chemicals, materials and bioenergy.[22,23] Third generation biorefineries focus on aquatic biomass such as micro- and macro-algae as feedstocks to deliver chemicals, materials and bioenergy.[24,25] Unlike terrestrial biomass, aquatic biomass does not compete with land usage and thus may have better societal acceptance. In this thesis, microalgae are used as feedstock and the research may be considered as leading to the development of a third generation biorefinery. Figure 1-3 shows a conceptual microalgal biorefinery. A fourth generation biorefinery utilises genetically modified second or third generation biomass, typically algae, as a feedstock.[26] Although fifth generation (5G) biorefineries do not exist as an accepted term, Remón *et al.* recently reported the concept of non-seasonal

5G biorefineries based on microwave-assisted, synergistic, co-depolymerisation of wheat straw (a second generation feedstock) and *Laminaria saccharina* (a third generation feedstock) to afford sugar-rich aqueous carriers for further downstream processing.[27]

1.4 Microalgae as a Potential Biorefinery Feedstock

Microalgae as a feedstock for multiple individual outputs has been well explored. Recently, Madadi *et al.*[28] conducted an analysis of the literature on microalgae with respect to outputs (see Figure 1-2).

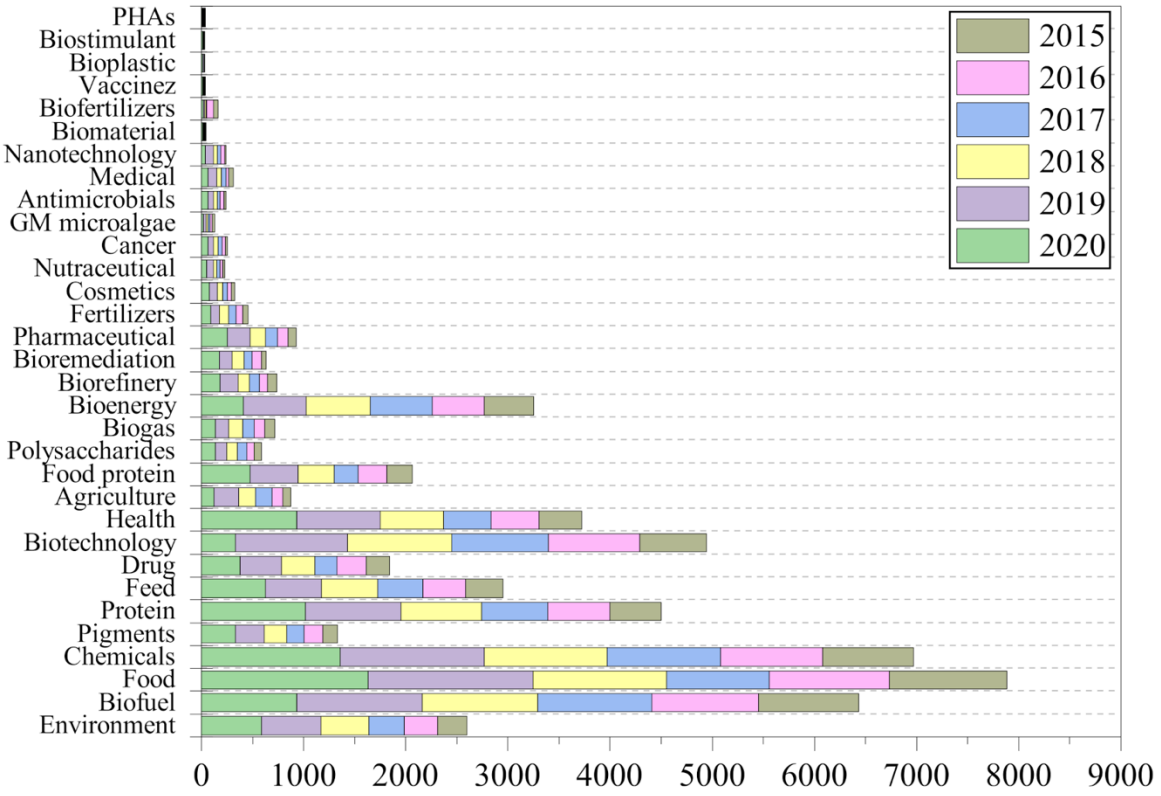

Figure 1-2 *Global research domains of microalgal research (from Web of Science, 2021), taken from Madadi et al.*[28]

While some of the more general domains such as 'Food' and 'Chemicals' seem to generate large responses, more niche topics such as 'Pharmaceuticals' or 'Cosmetics' seem to appear less-researched, as fewer direct publications correlate to them. Interestingly, the domain 'biorefinery' considerably falls behind other domains, which are researched in far greater intensity, thus highlighting again the urgent need to tie together individual areas of research (such as 'chemicals', 'proteins', 'food' or 'biotechnology') into a biorefinery

scheme focussing on multiple streams of products extracted from microalgae at the same time.

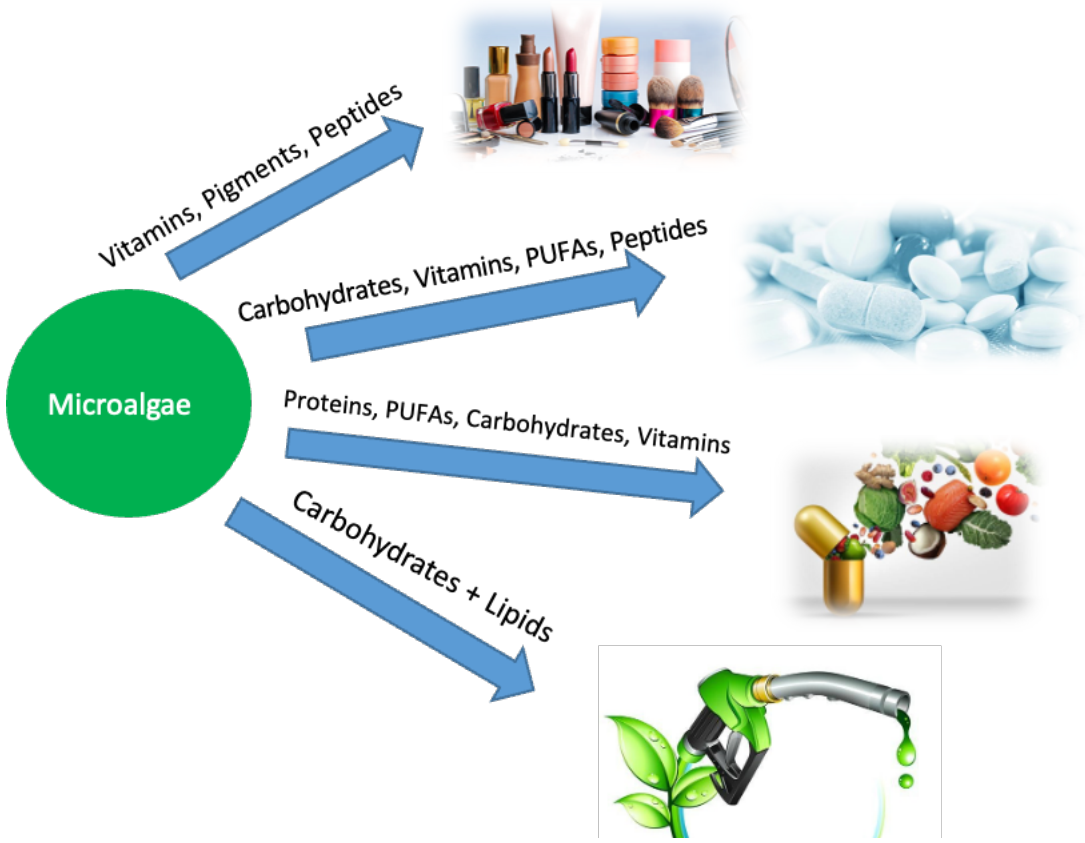

Figure 1-3 Possible microalgal biorefinery products and applications

Lipids are amongst the earliest researched biorefinery products for conversion into biofuels or nutritional applications. Microalgal species such as *Chlorella sp.* and *Nannochloropsis sp.* are rich (approx. up to 50% in dry matter)[29] in lipids and hydrocarbons, which can then be converted into bio-fuels through liquefaction, transesterification or even through pyrolysis.[25,29–31]

Biofuels alone from microalgae are currently economically unviable and thus, a full range of products needs to be considered and/ or low volume, high value niche products within the context of multi-output biorefineries need to be explored.[32] For example, microalgae-derived ingredients for cosmetics, vitamins, lipids, pigments, bioactive peptides or

polyunsaturated fatty acids (PUFAs, e.g. eicosapentaenoic acid (EPA) or docosahexaenoic acid (DHA), Figure 1-5) are all part of a more 'modern' microalgal biorefinery.

In cosmetics, consumer trends pointing towards more natural and sustainable ingredients have resulted in microalgae-derived carotenoids such as *beta*-carotene being widely used due to their anti-inflammatory, moisturising and surfactant properties.[33,34] Astaxanthin or fucoxanthin (Figure 1-5) have been reported for their anti-inflammatory, anti-obesity and potentially even anti-cancer properties.[29,35–38]

The isolation and use of bioactive peptides is not as well established as for pigments in medicinal applications but pose an equally great potential for future growth. Bioactive peptides in particular can possess excellent medicinal properties, with promising uses as therapeutic peptides in anti-inflammatory, antimicrobial or even anti-cancer fields.[35,39,40]

A few start-up microalgal biorefineries already exist.[41] For example, in the USA, ASF Bio-oil co. use sequestered CO_2 from industrial plants and nutrients from wastewater plants to generate cost-competitive biofuels as well as food additives. In Chile, Aeon Biogroup use CO_2 captured from wine growth to generate oil, nutraceuticals, food additives and biochemical compounds. The Israeli company, Seambiotic Ltd. captures flue gas from coal power stations to generate food additives and biofuel while IGV Biotech in Germany produce food, pharmaceuticals and biochemical compounds from various microalgae. AlgaeCytes Ltd. based in Kent, UK produce algal oil consisting of mainly the omega-3 fatty acid EPA (see Figure 1-5) from their proprietary freshwater strain of algae ALG01. Their main objective is to diversify their production of valuable compounds beyond EPA and tie in their current waste into a biorefinery cycle.

1.4.1 Introduction to Microalgae

Microalgae are typically unicellular species that grow via photosynthetic processes in aquatic environments utilising sunlight and CO_2.[21,42–44] Their importance both in nature as well as human development is immense as microalgae regulate the global atmosphere by generating 80% of oxygen from their photosynthetic growth process whilst capturing and fixing a large amount of carbon dioxide.[45] It is estimated that theoretically, microalgae can utilise around 9% of solar energy in order to generate 280 tons of dry biomass per ha^{-1} y^{-1} whilst consuming around 513 tons of CO_2.[46,47] Historically, *spirulina* microalgae were used in the Aztek culture until the 16th century as a direct food source.[48,45]

Microalgae can be grown in any type of water, not just freshwater, without requiring any arable land, therefore making them an ideal candidate for solving the food versus fuel debate by avoiding any potential issue arising from the use of land that could otherwise be used for food crops.[49] Microalgae can be grown in either open ponds or closed systems. Open ponds pose the risk of contamination and increase the difficulty of harvesting and efficient growth, with the more industrially preferred growth contraptions involving tubular, flat-plate or hybrid photobioreactors, which can efficiently be irradiated via LED-lighting, fed with nutrients as well as easily be harvested by draining the tubes through a tap.[41,50]

A full growth cycle lasts for 24 hours to around a few days depending on the species and the growth temperature at full and constant irradiation.[51,52] Thus, microalgae can be harvested on a weekly basis making them an ideal and quickly renewable feedstock as they show much higher growth potential than conventional lignocellulosic biomass as well as requiring far less land than their terrestrial counterparts. Mata *et al.* reported that growing and harvesting microalgae used around 49 or 132 times less time compared to rapeseed or soybean feedstocks.[53] Also, animals traditionally farmed for their nutritional compounds, such as fish (mainly salmon) for omega-3-acids, are only rich in these compounds as they consume microalgae, which are themselves rich in omega-3-acids.[54–56] Rather than depleting the fish levels it is a wiser approach to 'cut out the middle fish' and focus on the species at the bottom of the food chain i.e. microalgae instead.[54]

Figure 1-4 displays a typical and averaged composition profile of microalgae of which there are more than 200 000 to several million species.[45] However, out of this vast selection of microalgal species only very few are fully characterised and explored, yielding a huge pool of potential for selecting the most appropriate species for tailored applications or even genetically modifying them in order to meet certain needs.[53]

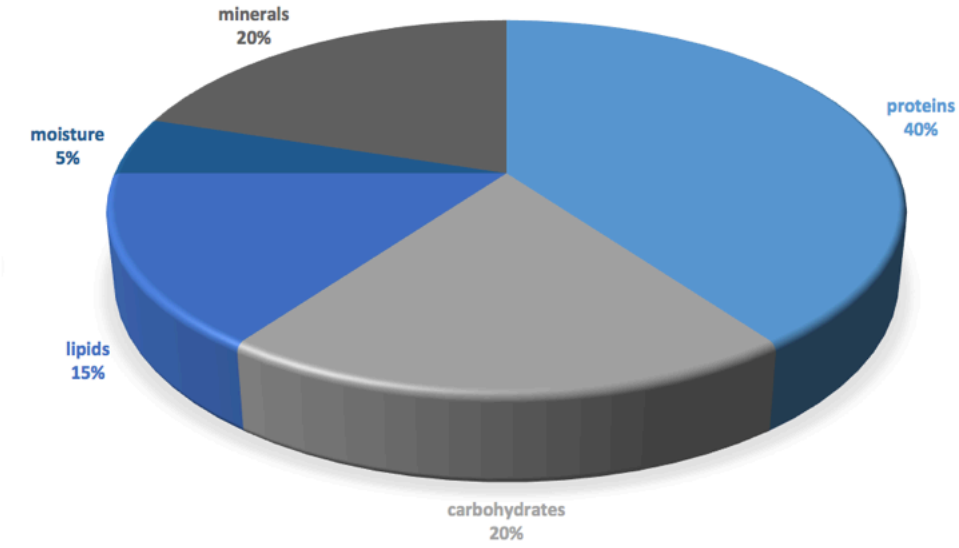

Figure 1-4 Typical averaged composition profile of microalgae

1.4.2 Eustigmatophyceae

The microalgal strain used in this thesis (ALG01) belongs to the Eustigmatophyceae class. This sub-class of microalgae was formed from the group of *Xanthophyceae* (yellow-green algae), and was classed as a group of its own in 1970.[57,58] It is a relatively rare group with their main differences to *Xanthophyceae* to be found in the pigment composition and ultrastructure. Originally, only 30 species were attributed to Eustigmatophyceae, but further extensive research has shown that its diversity might well extend beyond that number due to the large amount of microalgal species at present remaining unidentified and extensively researched.[59] Eustigmatophyceae comprises at least 47 different pigments, with most of them being carotenoids, amongst which the most commonly found are beta-carotene, lutein, luteoxanthin and astaxanthin, shown below in Figure 1-5.[60]

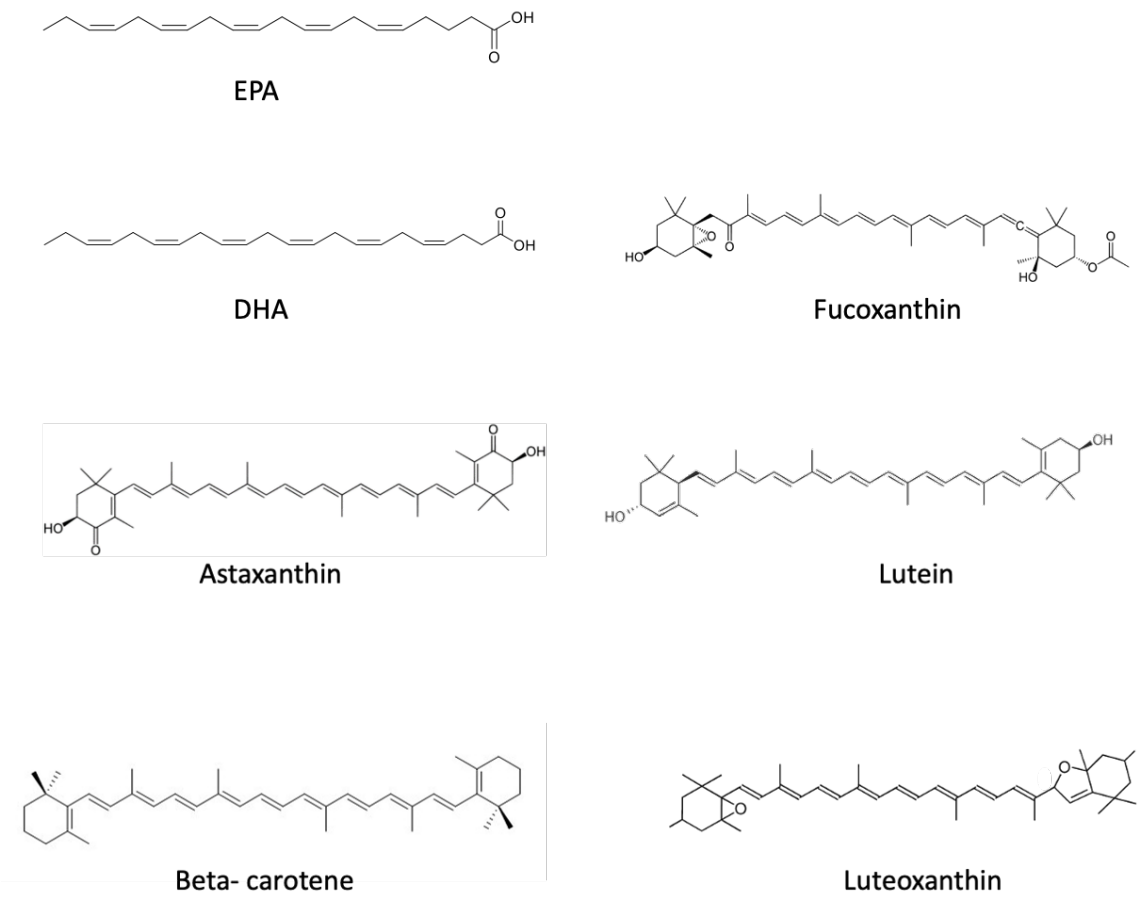

Figure 1-5 Molecular structures of EPA, DHA, fucoxanthin and main pigments found in Eustigmatophyceae microalgae

Interestingly, *Nannochloropsis* is a prominent member of the Eustigmatophyceae family and bears a lot of resemblance to ALG01.[61–67] The general composition of *Nannochloropsis* is summarised in Table 2 and can be used as a proxy for ALG01.

Table 2 General composition of Nannochloropsis species[68]

Carbohydrate content	5.2% (*N.oculta*) – 8.9% (*N. salina*)
Polysaccharide sugar composition	Glucose, fucose, galactose, mannose, rhamnose, ribose and xylose
Protein content	17.8% (*N. occulta*) – 43% (*Nannochloropsis sp.*)
Amino Acid profile	Arginine, glutamic acid, aspartic acid, leucine, methionine, cystine, histidine, tryptophan
Lipid content	8.2% (*N.oculta*) – 16.9% (*N. salina*)
Lipid profile	Palmitic acid, palmitoleic acid, EPA

1.4.3 Microalgal cell wall structure and the algaenan layer

The biggest structural difference between cell walls of terrestrial plants and microalgae is the lack of lignin found in microalgae. Microalgal cell walls, however, consist of a very complex structural system, which varies not just in its three-dimensional structure but also in its monomer composition depending on the algal species (see Figure 1-7). Some papers report monomers such as glucose, mannose, galactose and rhamnose, galacturonic acid and glucuronic acid as consistently reoccurring sugars and acids in various different cell walls of different species.[69,70]

Most microalgal cell walls can be described as consisting of a fibrillar layer of rigid components that are embedded in a matrix consisting of rather plastic polymers.[69] While some species lack rigidity, most microalgae possess a highly rigid, robust cell wall, which is extremely resistant to external stresses occurring naturally as well as during pre-treatment methods trying to disrupt the cell walls for extraction. This rigidity is thought to be of varied origin again depending on the species. Some researchers have proposed encompassing microfibrillar cellulose or chitin-like polysaccharides.[71–73] Most interestingly, however, is the presence of so-called algaenan, which has attracted some high level research recently due to its unique nature and extreme rigidity which makes it resistant to harsh, non-oxidative, acidic or alkaline treatments.[69,70,73–75] Algaenans are often described as

hydrocarbonaceaous, aliphatic macromolecules. Algaenan consists of hydrocarbon backbones of up to 30-40 carbon atoms with varying degrees of unsaturation (mono – and di-unsaturated) linked by ester, ether or glycosidic bonds.[75] Some studies on algaenan from *Botryococcus braunii* have yielded indications towards its structure and its elemental composition obtained from CHN analysis (Figure 1-6).

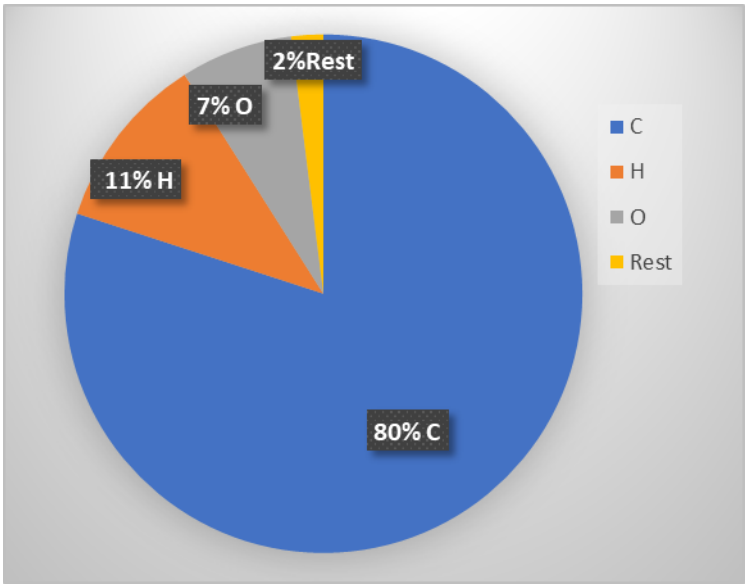

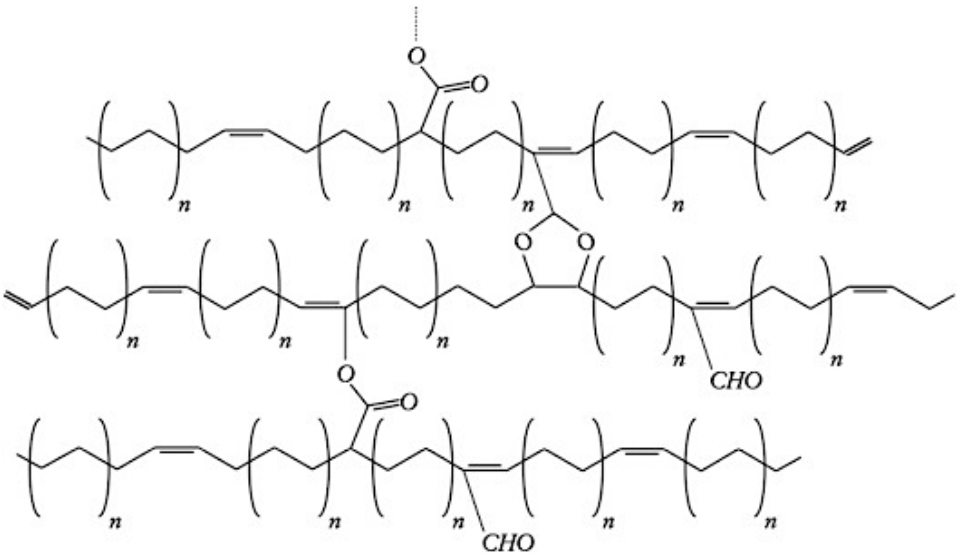

Figure 1-6 Botryal structural model of Botryococcus braunii A-Race algaenan[73]

It is known, however, that algaenan forms the outer layer of microalgal cells thus providing an effective shield against environmental stresses. It forms a trilaminar structure within the

cell wall but the presence of a trilaminar structure not necessarily requires the presence of algaenan. Figure 1-7 displays various cell wall structures of different species with and without algaenan.

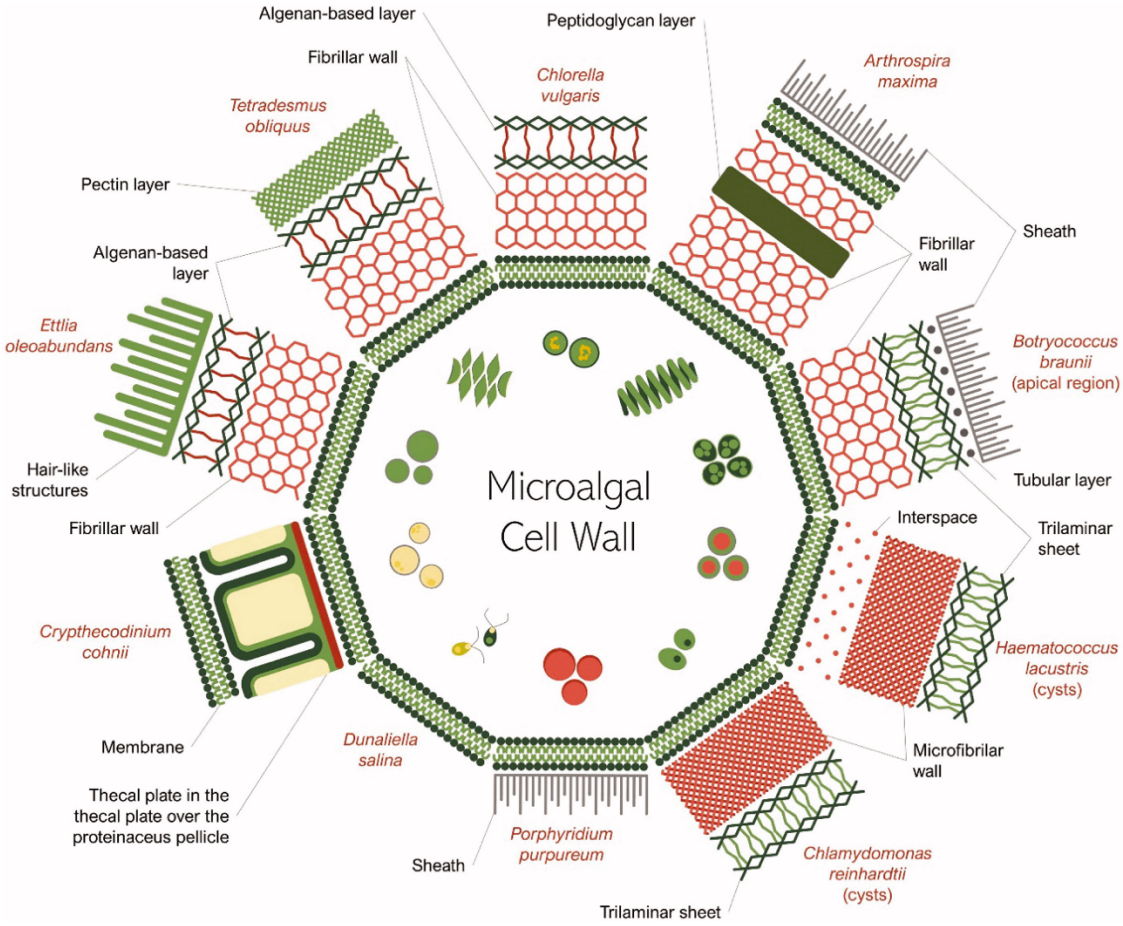

Figure 1-7 Cell wall structures of several important microalgae species

Amongst the species which are known to contain algaenan within their cell walls is *Nannochloropsis*, a close relative of the in this PhD thesis used ALG01 strain, both belong to the family of Eustigmatophyceae.[76]

Due to algaenan's tough properties in terms of resistance to outer influences and pre-treatments, it is very difficult to extract and isolate for analysis. Many of the methods reported in literature for the isolation of algaenan either involve many steps or reagents and solvents which have by now long been deemed as being environmentally toxic or hazardous for humans.[77] For example, some methods utilise benzene as a solvent.[77] The crux in attempting algaenan isolation is the prior removal of any impurities which might

persist, such as lipids, proteins and carbohydrates. This makes a method very complex and involves the use of many chemicals and solvents, which are not necessarily in the best interest of the 12 principles of green chemistry. Multiple groups reported algaenan yields upon prior removal of the aforementioned compounds ranging from 4.4% to 11.9%.[77–79] However, methodologies for algaenan extraction mainly come from the 80s and 90s, with much fewer publications to be found in recent years focusing on algaenan extraction. There remains a vast amount of research to be conducted into the optimal extraction of algaenan, the cell wall composition of many species as well as the compositional nature of different types of algaenan themselves.

1.4.4 Cellulose and carbohydrates in microalgae

1.4.4.1 Cellulose

Cellulose in microalgae plays an important role in the cell wall composition. However, the exact cellulose content varies from species to species with a general range from 14 - 40%.[28] Within the cell wall carbohydrate system, cellulose can make up around 85% of the polysaccharides in *Nannochloropsis gaditana*, which belongs to the same algal family as ALG01.[80] Cellulose comprises glucose monomer building blocks which are linked together with β-(1-4)-glycosidic linkages to form a linear polymer.[81] The cellulose strands bundle together binding to each other via hydrogen bonding of the hydroxyl-groups and thus form microfibrils (Figure 1-8).[82] Each of the microfibrils can contain between 5000 and 14 000 glucose monomers which are ordered (crystalline) and dis-ordered (amorphous).[83] This renders cellulose as hydrophobic and water insoluble and makes it difficult to process. [82,84]

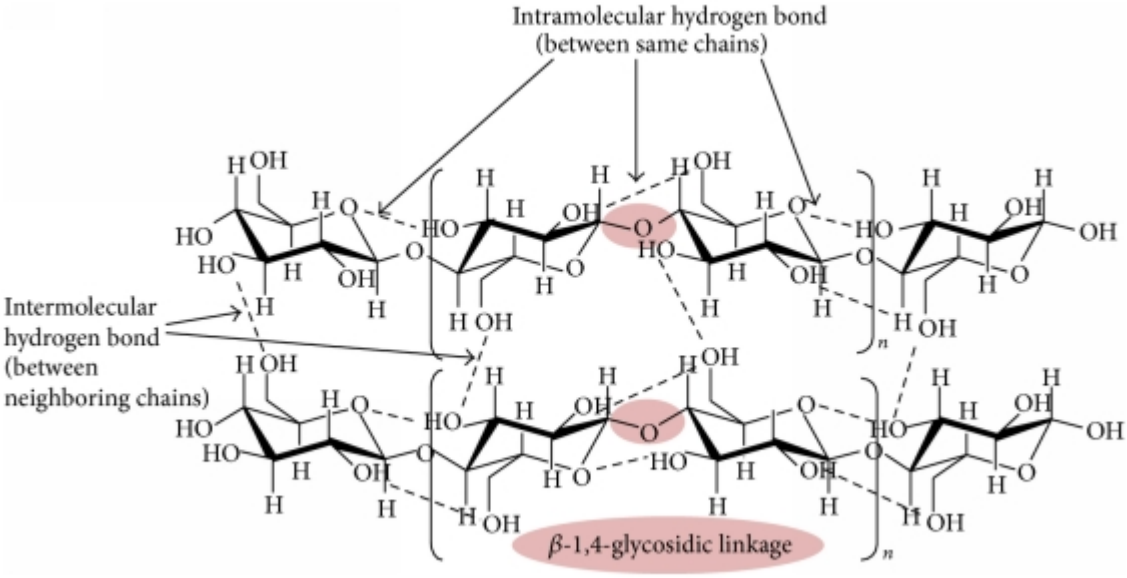

Figure 1-8 Structure of cellulose with intermolecular hydrogen bonding[82]

Madadi *et al.* reported the isolation of highly crystalline cellulose (95% crystalline) from *Valonia* and *Chladophora sp*.[28] Mihranyan *et al.* reported, that this highly crystalline cellulose from *Chladophora sp.* can be used to reinforce bioplastics as well as form composite, paper-like materials with polyaniline with conducting abilities.[85]

1.4.4.2 Carbohydrates

Most carbohydrates in the algal cells are present in the cell wall as building blocks (e.g., cellulose as discussed earlier in section 1.4.4.1), while some are also present within the cell itself in the form of starch or glycogen granules serving as energy storing molecules for the cells.[69] The location of these depend on the type of storage carbohydrate with starch mostly being present in the chloroplasts and glycogen in the cytosol.[69]

Carbohydrate sugars in microalgae mainly consist of xylose, mannose, glucose, rhamnose and galactose. For example, *spirulain platensis* contains 54.4% glucose and *Chlamydomonas reinhardtii* 74.9% glucose (both as a percentage of total carbohydrate content). Other species such as *Phaeodactylum tnicornutum* only contain carbohydrates consisting of 21% glucose while mannose makes up 45.9% of their total carbohydrates. *Spirulina platensis* carbohydrates consist of rhamnose (22.3%) whilst *Chloroccum sp.* contains 0% rhamnose.[86] Furthermore, total carbohydrate content can change depending

external factors applied.[87] For example, the increase of light intensity, CO_2 concentration as well as the nitrogen content can increase carbohydrate content up to maximum levels of 77% in *Chlorella sp.*[88,89] Furthermore, the carbohydrate composition in *Neochloris oleabundans* changes whether it is grown in freshwater (rhamnose, galactose, glucuronic acid) or saltwater (rhamnose, galactose, glucose).[88]

1.4.5 Lipids from Microalgae

Microalgae are a promising source of lipids, specifically for the biofuel sector but also concerning human nutrition and health as their lipid content can be comparably high (30-68% dry weight)[44,90] but can be even increased by starving the microalgae of nutrition, in particular nitrogen sources.[91–93] In turn, deprivation of nitrogen will impact the protein composition and most likely reduce the percentage of protein present, therefore a careful balance has to be struck depending on the desired components that the extraction is aimed at.[92]

In general, two types of lipids can be found in microalgae: non-polar storage lipids and more polar structural lipids.[62,91–96] The former mainly comprises triacylglycerides (TAGs) which are a precursor for biofuels while the second category includes polyunsaturated fatty acids (PUFAs) such as EPA or DHA which are most commonly found in microalgae and can be used for various health applications.[62,91–96]

TAGs are present in large quantities in the cell walls of microalgae (>44% of total lipids)[96], which can be readily transesterified with methanol into biodiesel (fatty acid methyl ester FAME) [91,93,94] in the presence of either inorganic acid catalysts or alkaline catalysts (Figure 1-9). The former are preferred as latter lead to saponification due to the high level of free fatty acids present. [62,97]

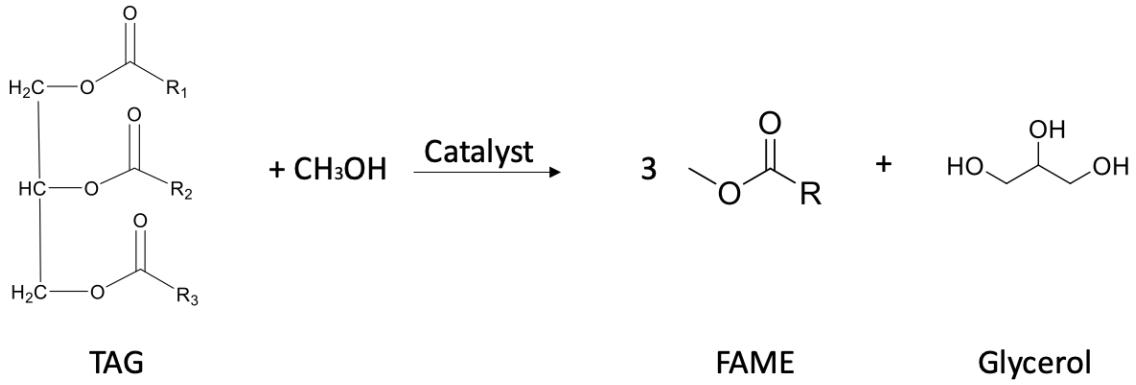

Figure 1-9 General scheme of transesterification reaction used to produce biodiesel (FAME)

Polyunsaturated fatty acids, in particular EPA and DHA are valuable compounds for the nutritional industry as they possess various health benefits such as anti-inflammatory properties and protective properties concerning the human heart.[98–103] In microalgal cells they are found to improve fluidity of the cell membranes.[99–103]

Lipids are often extracted using conventional solvents such as ethanol and hexane depending on their polarity. Lipid yields of around 80-90% can be achieved using conventional solvents. [99,103] However, hexane is a potential carcinogenic solvent and a substance of very high concern (SVHC). Thus, supercritical CO_2 extraction has proven to be an alternative extraction process to using hexane. Supercritical CO_2 is a safe, non-flammable solvent. Carbon dioxide pushed beyond its critical point by high pressure (350 bar) and temperatures (usually 40-60°C) is called supercritical.[104] A co-solvent such as ethanol can be used, usually in low concentrations of around 10%-20% v/v to increase polarity and extract more polar lipids.[105] One of the main advantages is the recyclability of the carbon dioxide, as upon finished extraction the pressure is released, thus converting the supercritical CO_2 back to its gaseous form, which leaves the extract behind and allows the CO_2 to be recycled.[105,106] However, lipid yields of only 30-40% can be significantly lower than for traditional 'wet' solvent extractions (80-90%). [101,102] On the other hand, selective DHA extraction purity could be increased from around 30% to 60% if $scCO_2$ was employed.[100] Despite the lower yields, higher selectivity towards PUFAs can be seen with supercritical CO_2 as a solvent resulting in a PUFA content of the overall extracted lipids of 20.68% with only 3.48% after Soxhlet extraction.[106]

1.4.6 Proteins from Microalgae

In 2016 it is estimated that 815 million people were directly influenced by malnutrition with the global population rising to 8.3-10.9 billion in 2050 according to estimations resulting in ever increasing demand for food putting pressure on our established economy of food production and agriculture.[107,108] The planetary boundaries for agricultural land will be exceeded by a factor of 2 in 2050 based on estimations by Conijn *et al.*[109] requiring urgent action regarding our food safety. Of the nutrition required each day around 13% are recommended to be proteins, which help to build bones, muscles, hormones as well as playing an important factor in the regulation of the immune system.[107,110] These proteins are mainly sourced from traditional agriculture, which is under threat due to arable land becoming more and more scarce and at risk of decreasing due to land use change and armed conflicts.[107,108] It is estimated that a billion people suffer from inadequate protein intake with the prime global sources of proteins being plants, whereas European consumption mainly relies on animal proteins.[111] Furthermore, global trends towards a more protein-rich diet as well as a shift away from animal proteins (the main animal protein sources currently are eggs, milk, seafood and meat)[110] towards vegan sources of protein open up a wide area of both research interest as well as new sectors with huge growth potential.[110] Animal protein sources are predicted to face a decline of around 50% over the next decades with vegan protein gaining rapid significance, with the number of vegans globally estimated at around 79 million with an increase of 580% registered between 2014 and 2019, and even more drastic increases expected over the coming years.[112,113]

A possible solution to this issue might be the utilisation of microalgal biomass as a source of protein, which has been discussed as a potential route by various different researchers suggesting that microalgae might be able to contribute 18% to global protein production in the future[114,115] or even 50% together with insects by 2054.[116]

However, microalgae face competition as a potential source of vegan protein. Traditionally, both soy (35% protein) as well as chickpea (18% protein) have widely been utilised for their non-animal source of protein, with the disadvantage that generally not all essential amino acids are present within them, which complicates matters as typically a vegan protein-rich diet would have to be comprised from multiple protein sources.[117] However, microalgae contain a more complete amino acid profile (see Figure 3-8 and Figure 3-9) as well as

composition profiles which includes other essential components of the human diet such as vitamins, antioxidants or omega-3-acids.[117] Depending on the species, amongst the most prominent essential amino acids present in microalgae are lysine, methionine, threonine, tryptophan, histidine, leucine, isoleucine, valine, and phenylalanine.[110] Figure 1-10 shows the protein content of many conventional microalgal species compared to animal and other vegetable sources of protein.

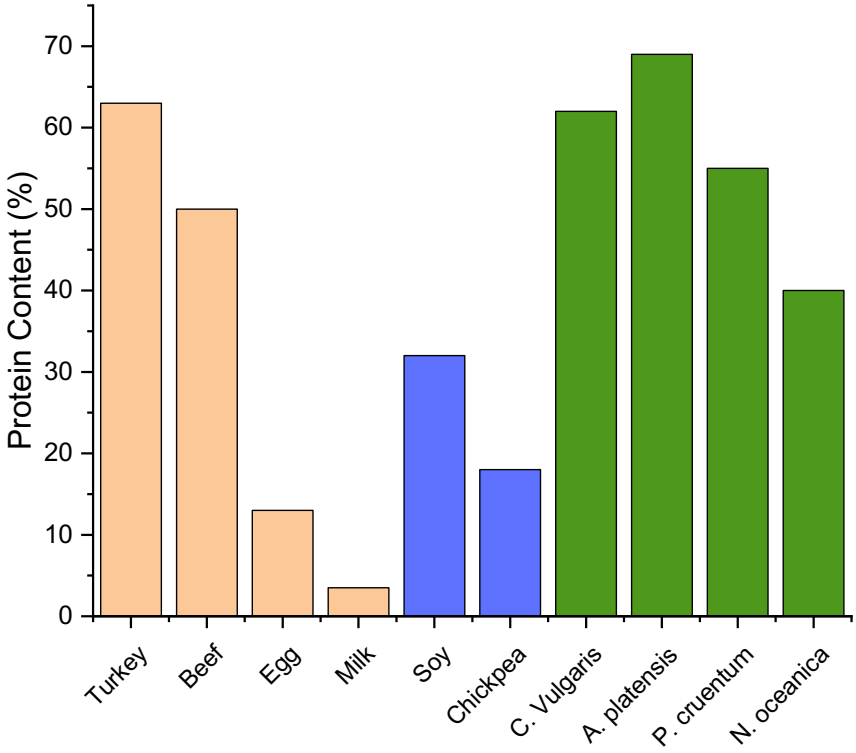

Figure 1-10 Protein Content of animal, vegetable and microalgal protein sources[117]

1.4.6.1 Protein Extraction

Proteins in microalgae comprise both water-soluble and water-insoluble protein. However, proteins are amongst the hardest components to extract from microalgae due to the mild conditions required to maintain their functionality if they are to be applied in the nutritional industry.[118]

In terms of food grade proteins, they can either be extracted in their intact folded structure or as hydrolysates which consist of proteins enzymatically cleaved into peptides.[119] These can improve the biological value and be of importance for the food and drinks industry,

depending on the target market as they can be directly mixed with additional ingredients to create various ranges of products such as sports drinks, fortified foods or food supplements.[120,121] However, protein purity is vital and is expected to be at least 70% for nutritional applications.[120]

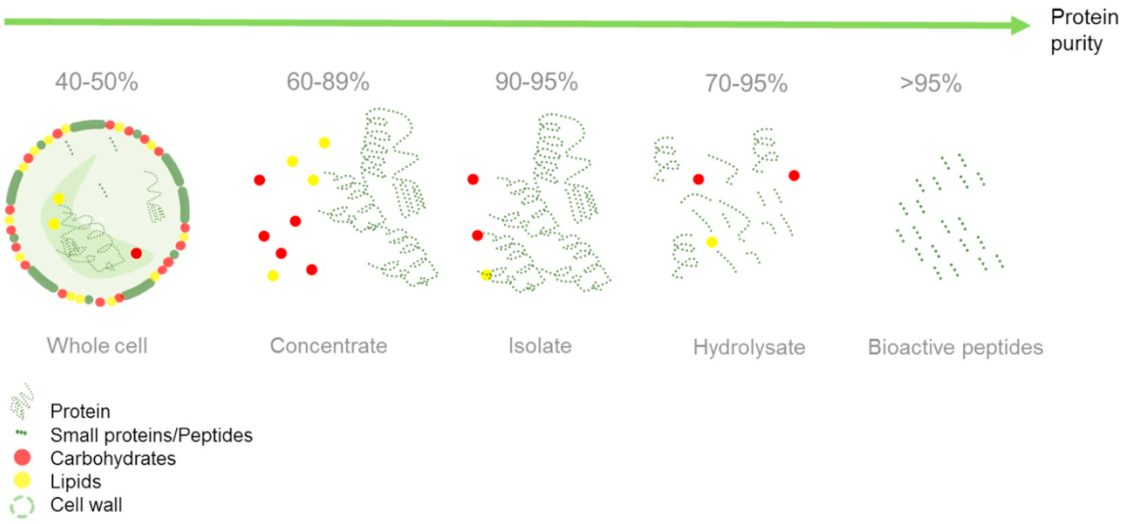

Figure 1-11 Protein purity at various stages of the purification process

Figure 1-11 shows protein purity at various stages of the purification process with the protein concentrate still retaining a lot of impurities such as carbohydrates and lipids while the proteins are being present in their functional and folded structure, which changes with the hydrolysate and the bioactive peptides which yield the highest purities.

Protein extraction is made even harder due to the rigidity in microalgal cell walls making an extraction without any cell lysis or pre-treatment difficult.[120,122] Furthermore, many proteins are non-water-soluble due to their hydrophobic nature or disulphide bonds between proteins that impact the solubility negatively. A compromise has therefore to be found between efficient extraction and mild conditions to maintain protein functionality and stability.[122]

1.4.6.2 Overview of cell disruption methods

Cell disruption or pre-treatment of microalgae is commonly required to increase protein yields. In addition to the chemically induced cell disruption methods there are three further categories to be considered which are summarised in Figure 1-12: thermal cell lysis by microwaving, freezing or to an extent spray drying; mechanical disruption including bead

milling, ultrasonication or high-pressure homogenisation, and; biological pre-treatment utilising enzymes or microbial organisms.[123–129]

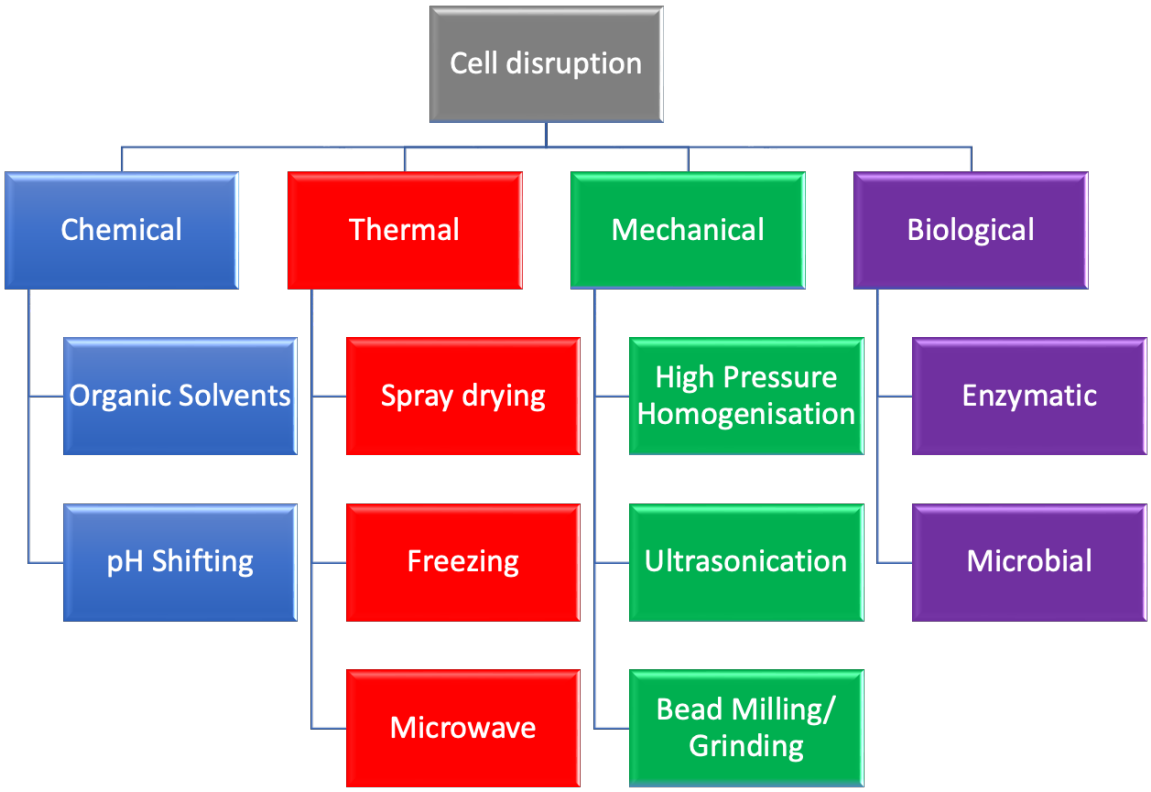

Figure 1-12 Overview of cell disruption methods

Chemical cell disruption:

Traditionally proteins have been extracted using chemical treatment by changing the pH of the supernatant obtained upon centrifugation of microalgal biomass that has been immersed in water to acidic conditions (mostly from alkaline 12 to around 4) precipitating out the proteins and collecting the solid.[122,130] However, acid and alkali treatment has their downside such as denaturing the proteins at high pH-values as well as inefficient and heterogeneous cell disruption which decreases the efficiency.[131] Moreover, from a green chemistry perspective solvent use and varying the pH are not the greenest methods as they generate a lot of waste as well as using potentially hazardous solvents in the process. More recently, ultrafiltration as an extraction method for proteins has gained popularity but still yields low protein purity, mostly around 20%.[66,123,132,133]

Biological Cell Disruption:

Of recently increasing importance is the biological pre-treatment method of using enzymes to generate bioactive peptides and hydrolysates. Enzymatic hydrolysis of proteins as a means of both cell disruption as well as tailored protein extraction to meet industrial needs has been a prime focus of research in recent years. Proteins hydrolysed through proteolytic enzymes (pepsin, pancreatic proteases or bacterial proteases) appear in many applications in the clinical or nutritional sector due to their high bioactivity and anti-inflammatory or antioxidant properties.[134–136] However, potential applications and bioactivities extend even further into the areas of being anti-diabetic, anti-cancer as well as anti-hypertensive, thus covering a broad spectrum in terms of medicinal applications.[119,137] Mainly responsible for these activities are peptides which are being formed in their low-molecular state through enzymatic hydrolysis of proteins and often possess weights of 3kDa – 5kDa or even below 1kDa.[119,138] Enzymatic hydrolysis reactions can range from very complex methods replicating and mimicking gastric fluid to simple setups requiring a mix of microalgae with the desired enzyme at the optimal pH, followed by the reaction at elevated temperatures to guarantee maximum enzyme efficiency, inactivation of the enzyme and separation through centrifugation.[139,140] The choices of enzymes can be very widespread with gastric enzymes being most popular, among which is pepsin, which is not only a part of human gastric fluid, but has also been used in conjunction with tangential ultrafiltration yielding successfully generated peptides, which proved to exhibit anti-bacterial properties against *E.Coli* and *S. aureus*.[138] Most literature findings have reported a successful enzymatic hydrolysis resulting in the desired low molecular weight peptides, which are responsible for the bioactivity.[141–143]

Mechanical Cell Disruption:

In terms of non-biological cell disruption amongst the most popular methods are ultrasonication as well as manual or mechanical cell disruption treatments. Ultrasonication works on the principal of acoustic cavitation, where the ultrasonic waves generate large pressure differentials within the liquid, which in turn can form vapour-filled bubbles, which burst to release large amounts of energy, which is then rupturing the microalgal cell walls to ease any subsequent extraction (Figure 1-13).[144–146]

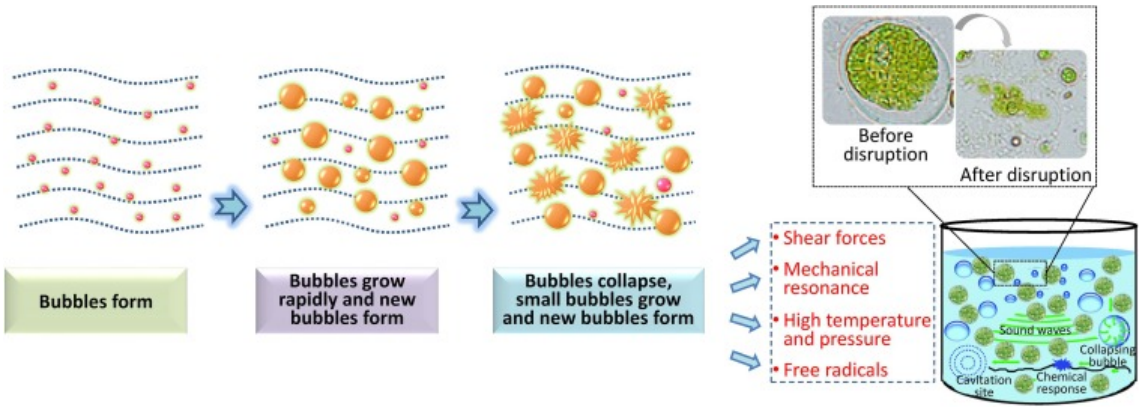

Figure 1-13 Schematic representation of ultrasonication cell disruption of microalgae[145]

Manual treatment on the other hand relies on the energy build-up during mechanical shearing forces which act on the microalgal cell walls and can consist of various different technologies, ranging from simple household coffee grinders to industrial bead-milling machines.[144]

Mechanical cell disruption benefits from its relative ease of extraction, the potential of scalability as well as high efficiency in extraction of proteins and other compounds without being too harsh to impact the integrity of extracted compounds. However, for algal species containing very rigid cell walls and small diameters such as *Nannochloropsis*, mechanical treatment can pose problems.[144,147] Protein yields obtained from literature differ greatly even within the same method employed due to differences in algal species and their protein content, cell wall structure and resistance towards cell disruption and extraction. However, protein yields can vary from 4% up to 67% for ultrasonication, with bead milling resulting in protein yields from 21% up to releasing 95% of water-soluble proteins into solution.[144,146,148] It was also found that ultrasonication yielded protein contents of the extracted fractions of 20%-50% for *Nannochloropsis sp*. and 40% for *Nannochloropsis gaditana*, while bead milling resulted in protein contents of 23%-51% for *Nannochloropsis gaditana*.[144]

Thermal Cell Disruption:

Microwave-assisted-extraction (MAE) has shifted more and more into focus as a cell disruption technique due to it not requiring dewatering of microalgae, but also due to its efficacy in disrupting even the toughest microalgal cell walls.[144,149,150] Microwaves possess wavelengths of around 1m – 1mm and usually frequencies of 30 MHz – 300 GHz, with the

mechanism of microwave heating in order to disrupt cells explained in more detail in section 1.5.3.[151] The effect of MAE causes many compounds within the microalgae to react and change their original shape due to the high temperatures that can be reached which is of utmost significance especially for proteins. MAE is commonly used to generate hydrolysed peptides as the harsh conditions break down the proteins into peptides or even individual amino acids.[152] Protein yields can reach up to 63.2%, however the large differences in different method setups, conditions, heating times, powers and temperatures as well as additional solvents (let alone different species of microalgae used in each experiment) make results extremely hard to compare and replicate.[144,153]

Moreover, scalability and energy efficiency are key in addition to protein yields and contents, as future success of incorporation of microalgal products into the global markets requires competitive scale-up of not only harvesting but also the cell disruption. Table 3 therefore summarises advantages and challenges for each cell disruption method, adapted from Timira *et al*.[144] In addition to these more traditional cell disruption methods, some novel methods have also been trialled which can involve high-technology methods such as ozonation, switchable solvents, high voltage electrical discharge or explosive decompression.[154]

Table 3 Summary of advantages and challenges of common cell disruption methods[144]

Method	Advantages	Challenges
Bead Milling	High disruption efficiency and high yields. Easily operated and scaled up	High energy consumption at large scale Can lead to overheating Can pose difficulties with small cells
Ultrasonication	Easily scaled up Low cost involved High yields and purities	Ultrasounds can lead to overheating – cooling necessary
Microwaves	Very thorough process also for tough cell walls Easy to scale up Low operating costs	High maintenance costs Can heavily impact structure of extracted compounds
Enzymatic digestion	Mild conditions Highly selective Very low energy input Easily combined with other methods	Enzyme costs are high Long reaction time Upon scale-up enzyme availability can become problematic
Acid and Alkali treatment	Effective and easy method	Quality of extract often low Use of highly concentrated acids and bases -> not green

N.B. The quantification of proteinaceous matter present in microalgae is difficult due to limitations regarding the nitrogen-% to protein conversion factor which is most commonly assumed to be 6.25 as an average of all amino acid weights assuming an equal composition.[155] In most cases this leads to an overestimation of proteins present as marine microalgae can incorporate high levels of inorganic nitrogen as well as possessing different amino acid compositions therefore resulting in varying conversion factors and effective conversion factors of 5.63 – 5.96.[156,157]

1.5 Research Aims and Green Chemistry Context

The aim of this PhD is to explore the valorisation of a proprietary strain of microalgae (ALG01, provided by AlgaeCytes Ltd.) as a biobased feedstock, into chemicals, materials and (bio)energy towards the development of an integrated zero-waste microalgal biorefinery. Four main areas of research will be explored, namely: i. the preliminary characterisation of proprietary ALG01 feedstock; ii. the isolation, purification, and characterisation of water-soluble microalgal proteins; iii. the production of defibrillated celluloses via acid-free hydrothermal microwave processing and their subsequent characterisation, and iv. the production and characterisation of bio-oils and biochars via microwave processing.

1.5.1 AIM 1: The preliminary characterisation of proprietary ALG01 feedstock

As ALG01 is a proprietary feedstock, it will be characterised by elemental analysis (CHN), ATR-IR, TGA, Solid State CPMAS NMR and HPLC to better ascertain its structure and composition.

1.5.2 AIM 2: The isolation, purification, and characterisation of water-soluble microalgal proteins

As discussed earlier, human consumption of proteins is one of the areas in the food industry that keeps rising. Approximately 40% of all proteins being consumed are estimated to be sourced from animal proteins.[158] The problem with animal-derived proteins lies mainly in the inefficiency of animal farming and the associated concerns regarding climate change and ethic arguments.[158] Microalgae provide an excellent source of proteins that can potentially serve as replacements of protein sources for the food industry. Due to the high protein content in microalgae (58% for *chlorella vulgaris* or 65% for *arthrospira platensis*)[121] depending on the species used they are a promising candidate as an unconventional source of proteins that can be used for human nutrition.[120,131,159]

Protein extraction from ALG01 is set out as one of the main objectives of this thesis in collaboration with industrial support and expertise from AlgaeCytes Ltd. Expanding on their industrial business strategy, potential protein extractions from ALG01, with the outlook of upscaling to pilot scale, will be prioritised. As an important way of adding value to the microalgal biorefinery the protein extraction potential will be evaluated from spray dried, freeze dried and spent biomass to assess potential differences in the resulting product and

its extraction efficiency. A key outcome will be to judge, whether the protein extraction would fit best before industrial EPA removal or afterwards, hence all three different biomass types will be tested.

In order to refrain from using traditional chemical/ organic solvent extraction methods such as salting out, three phase extraction or pH shifting, a method using solely water coupled with physical and thermal pre-treatments (e.g. Manual Grinding, Ultrasound, Microwaves) and biochemical treatment (using enzymes to judge their hydrolysing effect and compare resulting peptides to peptides obtained from microwaving) followed by micro- and ultrafiltration, will be devised.

Membrane filtration technology (microfiltration and ultrafiltration) will be explored to isolate water-soluble proteins from microalgae (ALG01). This technology depends solely on the principle of pore size filtration and spatial separation of protein/ peptides from carbohydrates, lipids and pigments to obtain a purified protein fraction.

Microfiltration and Ultrafiltration both rely on a similar principle but with different aims concerning the desired separation. While microfiltration mainly aims to remove any unwanted cell debris or impurities such as bacteria by setting a pore size (usually in the µm scale) that removes all large components but retains all the desired chemical compounds, ultrafiltration focuses on a more molecular level by separating components based on the molecular mass and yielding a low molecular weight and high molecular weight fraction.[160–164] The separation process takes place by introducing a range of pores into a membrane which possess an averaged cut-off molecular weight (usually around 10 kDa, but 300 kDa or any value in between are also possible). The feed is being pushed through the membrane through force generated by a pump as well as a backpressure which is applied to achieve more efficient separation in case of more concentrated mixtures.[160–166] All compounds that are smaller than the pores (in this case 10 kDa) get washed out into a permeate while all bigger compounds are being retained and concentrated in the retentate. Due to no uniform pore size, there is some 'cross-contamination' resulting in some low molecular weight species ending up in the retentate. This problem can be overcome by introducing another additional process called Diafiltration. Here, the impure liquid in the retentate is being replaced with an equal volume of either water or a salt buffer

to wash out the undesired components and purify the protein retentate.[160–166] Figure 1-14 displays a schematic of membrane filtration technology.

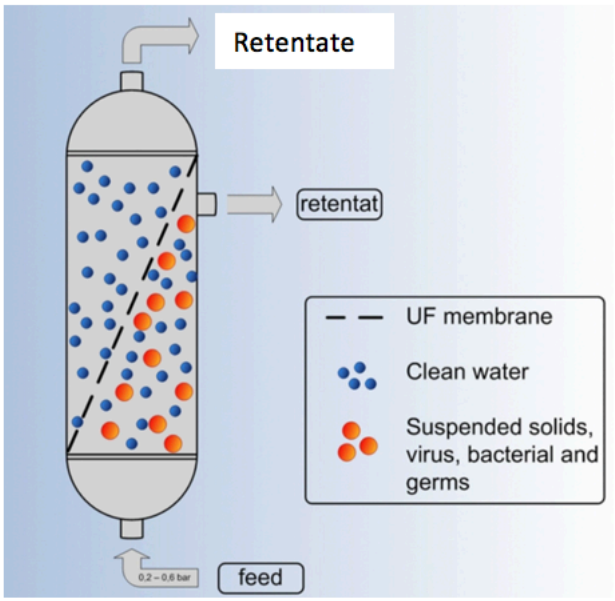

Figure 1-14 Schematic of membrane filtration unit[167]

One of the major problems concerning membrane filtration is membrane fouling through microalgae cells or macromolecules clogging up the membrane pores which results in a lower separation efficiency and impacts the purity of the protein retentate negatively.[168,169] Certain cleaning strategies such as flushing the membrane with 0.1M NaOH solution can be employed to overcome this problem by defouling the membrane (which is mostly composed of polymers such as polysulfone or polypropylene), however it is something to be considered when it comes to using membrane filtration as a protein purification method.

Due to the absence of solvents or high energy consuming equipment required for ultrafiltration (applying backpressure and operating a pump and the software on the controlling tablet are the only energy consuming parts of the process) it is a green and efficient alternative to purify and concentrate proteins from microalgal biomass.

In terms of utilisation of ultrafiltration for protein extraction and purification from microalgae, the literature is still scarce with most publications dealing with this specific topic only surfacing in the last two to three years, thus making the scope of this thesis very

much cutting-edge research.[66,132,170] The use of membrane filtration for protein purification is particularly suitable to its green nature not using any chemicals apart from water as well as its ability to preserve the integrity and functional properties of the proteins.[132] It is therefore preferable and of high research interest to extract proteins from microalgae using different types of pre-treatment in aqueous conditions, followed by fractionation and purification using membrane filtration. The focus on the desired proteins can be set very widely, with high molecular weight proteins or hydrolysed peptides at both ends of the molecular weight spectrum of proteins both possible goals using ultrafiltration. While various groups have tried to isolate as many proteins as possible by setting a very high molecular weight cut-off point of the filtration membrane (300 kDa up to 1000 kDa) and thus collecting the proteins in the permeate, others have tried to isolate hydrolysed peptides by pre-treating the microalgal biomass with enzymes such as pepsin and subsequently filtering with a very low cut-off point (less than 10 kDa) to collect the peptides in the retentate.[66,132,133,170] Protein yields therefore vary heavily depending on the selected focus upon choosing the ultrafiltration membrane. Some groups have shown the highest protein yields upon opting for a lower cut-off point (amongst 1000 kDa, 500 kDa and 300 kDa) with the lowest of the three resulting in 25% of protein yield.[132] When employing low cut-off points of 5 kDa a protein yield of 11.7% has been reported, and despite the seemingly low yield the functional properties of the proteins were better upon purification than compared to the initial crude, unfiltered protein extract.[132] Low protein yields can also be a sign of membrane fouling, which impacts the purity of the extracts upon extended use and improper cleaning.[66] However, the advantages of ultrafiltration fractionation still outweigh the negatives (especially compared to traditional pH-shifting) by a long shot, with the improved protein recovery (up to 100%), high selectivity, sole use of water and low energy consumption, thus making it a promising tool for protein purification of microalgae in the future, with endless combination possibilities in terms of pre-treatment and different algal species opening up a large amount of research to be conducted.

In this thesis, microalgae (ALG01, 10 g) will be mixed with deionised water (350 mL) and then centrifuged without pre-treatment or with pre-treatment (manual grinding, ultrasonication, microwaving and enzymatic treatment) to enhance protein extractability.

The extracted proteins will be characterised by CHN to judge their nitrogen content, Bradford Assay and SDS PAGE.

Some of the extracted proteins will then be subjected to bioactivity testing to judge their potential for industrial applications such as cosmetics, food supplements or other more targeted applications.

As the protein extraction process from microalgae will leave behind residual biomass and as the overarching aim of this body of work is to establish a zero-waste biorefinery, the utilisation of this residual biomass (pellet) is highly important and is discussed in Aim 4.

1.5.3 AIM 3: Generation and characterisation of Defibrillated Celluloses (DFC)

As a form of processed cellulose, the term Defibrillated cellulose (DFC) describes a mimic of micro- or nanocellulose fibres, while at the same time not being as purified due to the presence of residual algaenan or other contaminants.[171,172] Microcellulose aggregates of cellulose fibrils consist typically of around 10-50 microfibrils which are several micrometres in length and possess a width of around 20 – 60 nm.[173] While pure micro- or nanocellulose can be processed from lignocellulosic biomass such as pea, ginger or orange waste,[174,175] the additional complexity of microalgal cell composition with the presence of algaenan results in a less pure product, the defibrillated cellulose. This resulting DFC is a very desirable natural product as its properties include high surface area, high colloidal and thermal stability as well as tough mechanical strength.[171,176–178] They can be used in a wide range of applications, such as coatings, optically transparent materials, aerogels, rheology modifiers, electronics, filters, packaging, or molecular scaffolding.[179] Traditionally, defibrillated cellulose is produced via intensive chemical and mechanical processing of high cellulosic content biomass such as wood pulp.[179,180] Microwave hydrothermal treatment is considered a fast and less energy intensive method than traditional approaches, enabling the production of defibrillated celluloses without the use of any chemical or biological additives.

Microwave heating has gained popularity as a viable alternative to conventional heating. It utilises electromagnetic radiation in the frequency range of 0.3 to 300 GHz.[181] The emitted radiation interacts with the medium and heats it up via so called dielectric heating effects. Essentially, a dipolar molecule will interact with the electromagnetic radiation and try to align itself in the oscillating field. The enhanced rotation due to population of rotational

levels leads to increased collisions resulting in induced molecular motion distributing kinetic energy to its environment via friction, which heats up the sample.[181–185] Some materials are better at absorbing microwaves than others due to the nature of their dipoles, thus depending on the absorbing capacity, microwave heating is less effective for certain materials.

The advantage over conventional heating is due to the fact that microwave heating creates no temperature differential which occurs for example when using a hot plate (which heats up the sample from the bottom inducing a temperature gradient as well as local hot spots due to stirring inefficiency). A sample is being heated up uniformly thus allowing for a quicker, more efficient heating but also impacting chemical reactions which proceed more homogeneously and show increased reaction rates.[181,182]

In addition to heating, microwaves can also be employed as a method for cell disruption as the electromagnetic radiation and its induced heating causes lysis of the cell wall. The heating of water under a pressurised microwave vessel causes cell wall components to disintegrate as well as decomposing them to various organic acids, which in turn facilitate the breakdown of less mobile cell wall components even further[182–185]

The removal of hemicellulose, pectin, and amorphous cellulose is facilitated through microwave energy, resulting in defibrillated cellulose fibres with a high degree of crystallinity. This process has been successfully achieved in a range of biomass types including orange peel[175], spent ginger waste[174]and spent pea biomass[179] but never with microalgae. According to literature, the microwave-assisted hydrolysis of hemicellulose, entangling the cellulose microfibrils, should be achieved below 180°C, whereas beyond 180 °C, the hydrolysis of amorphous cellulose and the dispersion of cellulosic fibres should be witnessed.[174,175,179]

Considering the structural differences between lignocellulosic biomass and microalgae, the latter contain little to no lignin. Thus, the production of defibrillated cellulose should be theoretically less challenging. However, there are only a few reports in the literature that discuss the formation of defibrillated cellulose from microalgae—but with the use of chemicals and/or biological additives. For example, Lee *et al*. report the production of nanocellulose from microalgae using 2,2,6,6-tetramethylpiperidine-1-oxyl (TEMPO) as a free-radical chemical reagent.[178] TEMPO is corrosive and toxic to aquatic life and, in line

with the 12 principles of green chemistry, the use of auxiliaries, especially those that are toxic, should be minimized or eliminated. In addition, the presence of algaenan in the microalgal cell wall could pose a significant hurdle in producing pure DFC, as the algaenan is even more resistant towards destructive treatments than cellulose.

The 'water-soluble-protein-free' pellet from AIM 2 will be subjected to hydrothermal microwave processing as outlined in Table 4.

Table 4 Microwave hydrothermal process parameters

Biomass type	Ramp time/ min	Holding time/ min	Final temperature/ °C
Spray or Spent[a)]	15	15	160
Spray or Spent	15	15	180
Spray or Spent	15	15	200
Spray or Spent	15	15	220

a) Spray = untreated ALG01; spent = ALG01 after industrial EPA extraction

The then generated defibrillated cellulose will be characterised (X-Ray Diffraction, solid state NMR, TGA, TEM) but will also be subjected to a very novel technology involving the use of a fluorescent optotracer, which specifically binds to cellulose and can be visualised via Confocal Laser Spectroscopy. This is the first documented use of this Carbotrace 480 with defibrillated cellulose obtained from microalgae.[172]

1.5.4 AIM 4: The production and characterisation of bio-oils and bio-chars via microwave pyrolysis

Microwave pyrolysis is a technique for converting biomass into biofuels (bio-char, bio-oil and bio-gas) [186–191] Pyrolysis describes the process of heating and thermally decomposing the microalgal biomass under a nitrogen atmosphere reaching temperatures ranging between 300°C to 800°C depending on the method used.[187] The resulting char is an energy dense material consisting of around 62% C, 8% H and 10% N with higher heating values of around 29-45.9 MJ/kg making it less energy dense than fossil fuels (higher heating value of 41 MJ/kg) but higher than wood (21 MJ/kg).[190] The oil contains a wide range of compounds such as complex hydrocarbons, nitrogen compounds (due to the high amount of proteins present), aliphatic compounds and alcohols.[186–190] Its higher heating values range from 30-42 MJ/kg with yields of 18-59 wt% according to Chen *et al* [187]. The formation of bio-oil depends on the temperatures used as higher temperatures towards 800°C can favour oil

and gas formation and decrease char yields. Bio-oil yields can be optimised at around 500°C with a yield of 40%.[190,191] The gaseous fraction mostly contains hydrogen, CO, CO_2 and gaseous hydrocarbons which can be used for burning, thus completing the biorefinery circle by valorising the biomass fully in terms of valuable compounds and energy.[187]

Microwave pyrolysis (see Table 5) will be applied to the ALG01 biomass at a fixed safe temperature (280°C) and varying power (50W, 100W and 150W) in order to generate bio-chars and bio-oil and judge the effect of the varied parameters on the resulting products.

Table 5 Microwave Pyrolysis process parameters

Biomass type	**Microwave power/ W**	**Target temperature/ °C**	**Number of pyrolysis runs**	**Sample Code**
Spray dried	50	280	Single	Spray 50W
Spray dried	100	280	Single	Spray 100W
Spray dried	150	280	Single	Spray 150W
Spray dried	50	280	Double	Spray 50W D.P.
Spray dried	100	280	Double	Spray 100W D.P.
Spray dried	150	280	Double	Spray 150W D.P.
Spent	50	280	Single	Spent 50W
Spent	100	280	Single	Spent 100W
Spent	150	280	Single	Spent 150W
Spent	50	280	Double	Spent 50W D.P.
Spent	100	280	Double	Spent 100W D.P.
Spent	150	280	Double	Spent 150W D.P.

The resulting bio-char and bio-oils will be analysed (ATR-IR, TGA, CHN and GC-MS where applicable) and compared to their counterparts produced from both microalgal and terrestrial biomass.

1.5.5 Green Chemistry and SDG Context

The aims of this research connect with the following 12 Principles of Green Chemistry and SDGs. The latter has been mentioned previously in relation to SDG12: Responsible Production and Consumption, which tackles waste reduction and resource efficiency.

Principle 1 – Waste Prevention: It is better to prevent wate than to treat or clean up waste after it is formed

Although this principle strictly relates to the chemical waste associated with a particular reaction or process, it is now commonly extended to all types of waste, for example, household waste, biological waste, electronic waste etc. The valorisation of industrial spent microalgal waste for which AlgaeCytes Ltd. have limited use, avoids waste.

Principle 3 – Avoid hazardous substances: Wherever practicable, synthetic methodologies should be designed to use and generate substances that possess little or no toxicity to human health and the environment, and

Principle 5 – Safer Solvents: The use of auxiliary substances should be made unnecessary wherever possible and innocuous when used

Whenever dealing with any extraction methodology throughout this body of work it will be of utmost importance to avoid any use of hazardous chemicals and substitute them with more harmless alternatives. This research primarily focusses on the use of water for the isolation of proteins and defibrillation of cellulose. Conventionally, the defibrillation of cellulose to form nanocellulose uses bleaching agents and harsh oxidants. Where organic extraction solvents are used, they have been limited to ethanol, acetone and ethyl acetate.

Principle 6 – Energy Efficiency: Energy requirements should be recognised for their environmental and economic impacts and should be minimised. Synthetic methods should be conducted at ambient temperature and pressure.

Wherever possible, it has been attempted to design new methods during the establishing of a microalgal biorefinery which use more energy efficient heating technologies compared to conventional heating. Microwaves will be used to defibrillate celluloses and to pyrolyze ‘protein-free’ algal pellets.

Principle 7 – Use of renewable feedstocks: A raw material of feedstock should be renewable rather than depleting wherever technically and economically practicable

This principle is already fulfilled and of great importance by using microalgae as a feedstock. Microalgae have fast growing cycles (typically a few days).

Principle 12 – Accident Prevention: Substances and the form of a substance used in a chemical process should be chosen so as to minimise the potential for chemical accidents, including releases, explosions and fires.

Throughout this body of work, all methods will be carefully adapted to pose as little risk to the researcher as well as the environment. The use of mostly water as well as little hazardous solvents promotes the fulfilment of this principle. Microwave systems are in addition less accident-prone than conventional heating as the stopping of microwave radiation in an emergency situation results in an immediate halt of heating and with the contents of the vessel hotter than the vessel leading to instant cooling.

Chapter 2

Experimental

All chemicals and reagents were purchased as either analytical grade or HPLC-grade quality and sourced from either Merck Ltd. (formerly Sigma-Aldrich) or Fisher Scientific Ltd. In-house, laboratory supplied, de-ionised water was used throughout.

Different types of ALG01, a proprietary strain of microalgae belonging to the class of Eustigmatophyceae, were provided by AlgaeCytes Ltd., Kent, UK. The ALG01 was grown and harvested at AlgaeCytes Ltd. as follows:
The ALG01 proprietary strain was up-scaled from a petri dish to 100 L in AlgaeCytes' proprietary upstream pyramid process and inoculated into the 1000 L Industrial Plankton seeding tank at their industrial facility at the Discovery Park in Sandwich, UK. Upon reaching the late exponential phase the culture was then transferred into the pilot plant production module (VacrionAqua 12000L Phyco-Flow^{TM}, see Figure A1 in Appendix). After reaching an appropriate density, it underwent semi-continuous harvesting to provide material for spray drying. Each day of harvest, 1000 L of cell culture was dewatered with an Alfa Laval Clara 20 model disc-stack centrifuge to produce an algal slurry of around 15% +/- 5% solids. Subsequently, the slurry was dried using a Büchi mini spray dryer B-290 to yield a dried algal powder of less than 1% moisture content.

Different ALG01 feedstocks were used in this project depending on the drying method as well as prior treatment undertaken by the supplier, i.e., ALG01 spray dried biomass (native algae with no EPA extraction), ALG01 spent biomass (residual matter after EPA extraction using ethanol and base followed by acid neutralisation) and ALG01 freeze dried biomass (native algae with no EPA extraction)

2.1 Protein Extraction

2.1.1 General Extraction Methodology

The generic extraction protocol for the isolation of water-soluble proteins from the various types of microalgal biomass is depicted in Figure 2-1, with the membrane separation module shown in Figure 2-2.

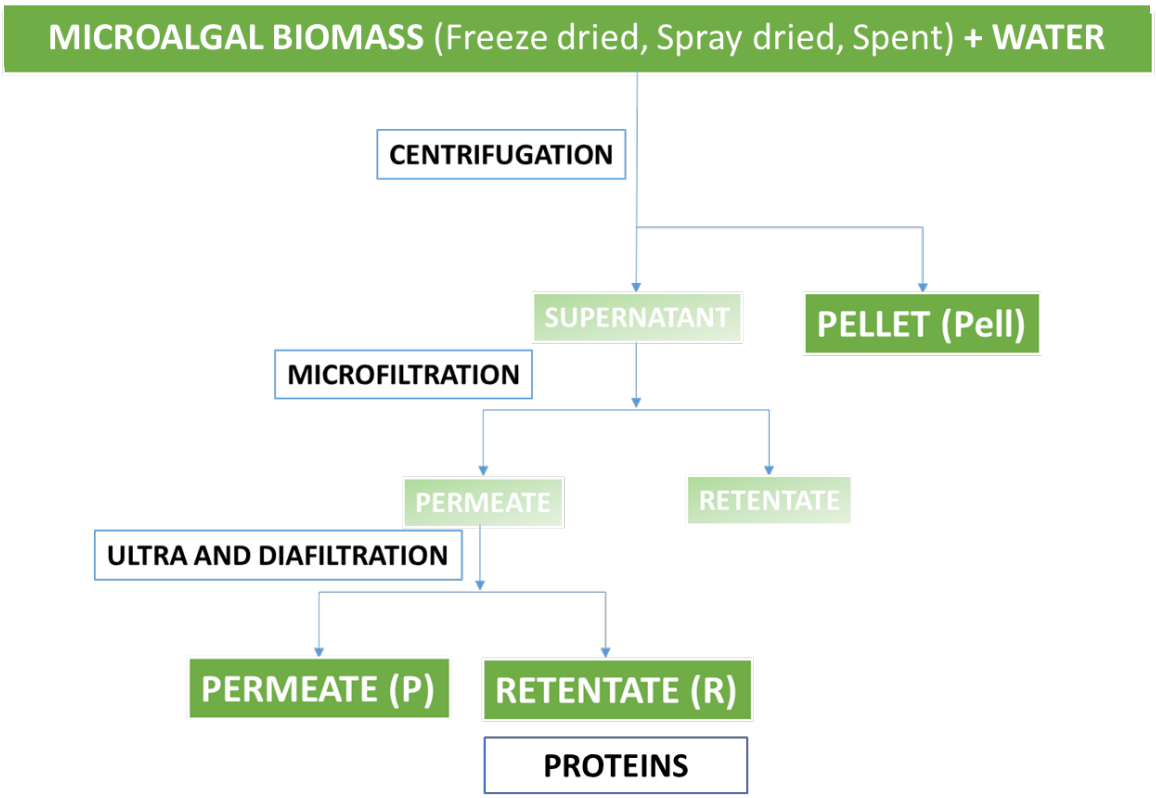

Figure 2-1 Schematic for extraction of water-soluble proteins

A mixture of the desired microalgal biomass (ALG01, 10 g) and de-ionised water (350 mL) was stirred for 15 min and either subjected to pre-treatment methods (see section 2.1.2) to break up the microalgal cell walls to increase protein yields or directly centrifuged without any pre-treatment for 20 minutes at 3500 rpm at 5°C. The obtained pellet (Pell) from centrifugation was isolated, freeze dried and stored for later use (either microwave pyrolysis or generation of defibrillated celluloses). The supernatant was subjected to microfiltration in a KrosFlo Research Iii Tangential Flow Filtration System (Figure 2-2) using a mPES MidiKros filter module (pore size: 10 μm) in order to remove any solid particles and general impurities from the drying process or transport. The retentate from microfiltration (usually consisting of 1-3 mL of cell debris and contaminants) was discarded whilst the ensuing permeate was further subjected to ultrafiltration and diafiltration to separate high molecular weight from low molecular weight species (pore size: 10 kDa) using a backpressure of 15 psi.

The retentate was concentrated 10-fold during ultrafiltration (from 350 mL to 35 mL) after which diafiltration (DF) was performed with pure deionised water to wash out any remaining impurities. The DF volume was set at five times the volume of the concentrated retentate, i.e., 35 mL x 5 = 175 mL. The resultant permeate (P) containing low molecular

weight species such as carbohydrates as well as the retentate (R) which contained the desired proteinaceous matter were freeze dried on a Lablyo Freeze Drier in 50 mL centrifuge vials with a pierced aluminium foil on top to prevent cross-contamination. The samples were pre-frozen in a conventional freezer and deep-frozen using liquid nitrogen right before loading onto the freeze drier. The samples were taken off after three days of drying. In case of residual moisture within them, the samples were frozen again with liquid nitrogen and loaded onto the freeze dried for another one or two days depending on the wetness of the samples. All samples were analysed by CHN, ATR-IR and SDS-PAGE, as appropriate.

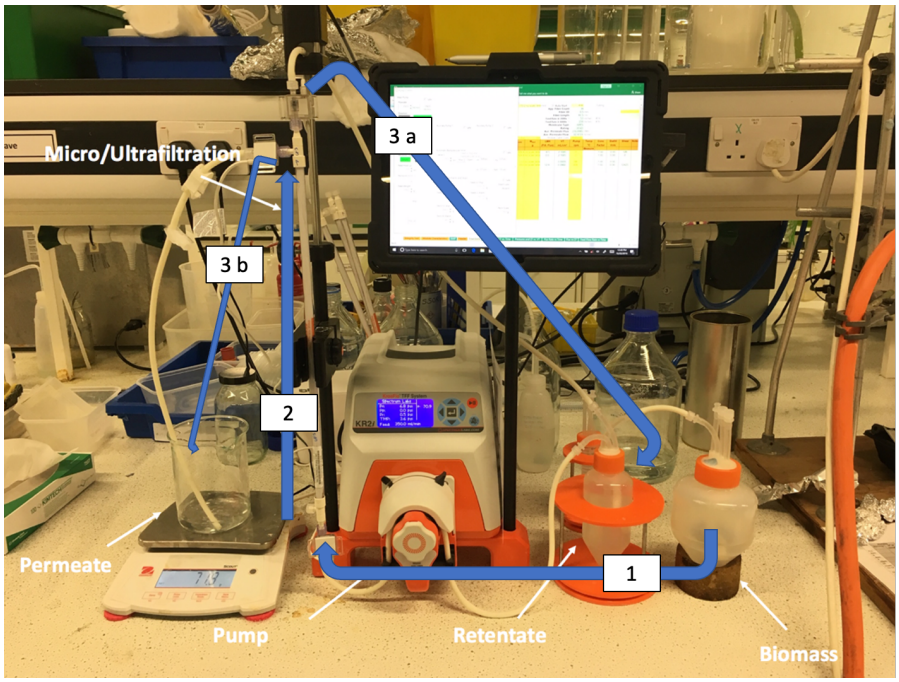

Figure 2-2 *KrosFlo Research Iii Tangential Flow Filtration System using a mPES MidiKros filter module with the blue arrows indicating the direction of flow: 1- flow of biomass through pump towards membrane. 2- flow through filtration membrane. 3a – flow back towards retentate/ restart the cycle. 3b – flow of permeate*

2.1.2 Pre-treatment Methods

2.1.2.1 Ultrasound probe pre-treatment

An ultrasonic probe (Sonics vibra cell) was used to investigate the effect of cell wall disruption. The ALG01/water mixture (10 g ALG01 in 350 mL deionised water) was split into 50 mL aliquots in centrifuge tubes, which were then subjected to ultrasonic treatment by

placing the tubes in an ice bath, submersing the probe into the sample and sonicating for 10 min with a 4 s pulse followed by 2 s relaxation time to allow the sample to cool. The amplitude was set at 60%. The resulting pre-treated samples were combined, centrifuged and the generic extraction method was followed as described in section 2.1.1.

2.1.2.2 Physical Grinding

The crude, dry, ALG01 biomass was physically ground with a pestle and mortar for 2 minutes and subsequently further ground in a commercial 'Kitchen Perfected' spice/coffee grinder for around 1 min until a consistent fine powder was obtained. The exact treatment time varied due to the sometimes non-homogeneous nature of the dried biomass allowing for a uniform texture of the resulting treated biomass. The treated biomass was collected, dispersed in water at the aforementioned ratio and centrifuged and the generic extraction method was followed as described in section 2.1.1.

2.1.2.3 Microwave pre-treatment

Initial trials were performed to test the behaviour of the microalgae upon microwave treatment as microwave heating of microalgae can lead to rapid, uncontrollable, spontaneous overheating leading to possible shattering of microwave tubes. A CEM Discover microwave reactor using a 10 mL vial was used at fixed power and safe temperature settings.

Spray dried ALG01 biomass (0.4 g) was dispersed in deionised water (4 mL) and subjected to microwave irradiation at varying power (100 W; 200 W; 300 W) with a holding time of 2 min as trial reactions.

Thereafter, a full run with a larger amount of microalgal biomass (ALG01, 10 g) in deionised water (350 mL)) was performed using a Milestone Synthwave reactor as follows:

The biomass/water mixture was irradiated at five different temperatures (80°C, 160°C, 180°C, 200°C and 220°C) with a ramp time of 15 min followed by a 15-min holding time at the desired temperature with a subsequent cooling at a rate of 10K / min. The resulting biomass was centrifuged, and the general extraction method was followed as described in section 2.1.1.

2.1.3 Protein Characterisation and Analysis

2.1.3.1 SDS – PAGE

Sodium Dodecyl Sulfate-Polyacrylamide Gel Electrophoresis (SDS-PAGE) analysis was performed on all protein samples in order to qualitatively visualise the molecular weight distribution of the proteins present in the retentates. Samples were run by measuring an accurate amount of protein sample (10 mg) into a small vial upon which 8 mg of loading buffer was added along with deionised water (24 µL). The resultant mixture was vortexed, heated (heating block, 70°C for 10 min), re-vortexed and centrifuged for one min. The supernatant was loaded onto a NuPAGE-Bis-Tris Mini Gel and immersed in a 1:20 solution of buffer : water in an SDS-PAGE container. The initial voltage was set at 60 V and increased to 120 V once the dye front had started separating and running along the gel. After the run was complete, the gel was stained with NBS SafeBlue protein stain overnight and subsequently de-stained with deionised water.

2.1.3.2 Bradford Assay Protein Concentration Determination

A calibration curve was constructed using an albumin standard stock solution (2000 µg/mL), from which the following concentrations were prepared: 2000 µg/mL, 1500 µg/mL, 1000 µg/mL, 750 µg/mL, 500 µg/mL, 250 µg/mL, 125 µg/mL, 25 µg/mL, 0 µg/mL.

Each concentration (0.05 mL) was added to Coomassie Plus Reagent (1.5 mL), shaken, incubated for 10 min and the absorbance was determined on a Jasco 550 UV-vis spectrophotometer at a fixed wavelength of 595 nm. A calibration curve was plotted for determining the protein concentration of the retentate samples and is shown in the Appendix (Figure A2).

To determine the protein concentration in the various protein samples, 1.0 mg was placed in a vial, deionised water (2 mL) was added and shaken slightly to allow for full solubilisation of the proteins. Of each of these solubilised protein samples, an aliquot (0.05 mL) was added to Coomassie Plus Reagent (1.5 mL), incubated for 10 min and the UV-vis absorbance was determined at 595 nm. The protein concentration of the sample was calculated from the calibration curve.

The residue containing the back-extracted proteins using K_3PO_4 salt was analysed via Bradford Assay by dissolving the salt / protein mixture (2 g) in deionised water (2 mL) of

which 0.05 mL were mixed with Coomassie Reagent (1.5 mL) and run as the previous samples on the UV-vis machine for analysis.

2.1.3.3 Foaming capability and stability of proteins

A 0.5 % (wt/v) mixture of protein samples and deionised water was shaken vigorously in a sample vial (12 mm radius) for one minute to allow for foam formation. Immediately upon shaking the total height (mm) of the sample was recorded followed by another measurement after 10 minutes as well as two hours. The volume v_x was calculated from the height h_x using Equation 2.1; foaming capability was calculated according to Equation 2.2 and foaming stability as per Equation 2.3:

$$\text{Volume } (v_x) = \pi r^2 h_x \qquad \textit{Equation 2.1}$$

$$\text{Foaming capability } (\%) = (v_2 - v_1)/ v_1 \qquad \textit{Equation 2.2}$$

$$\text{Foaming stability } (\%) = (v_4/ v_3) \times 100 \qquad \textit{Equation 2.3}$$

h_x= height recorded (mm)

r = radius of sample vial (12 mm)

v_1 = initial volume (µL)

v_2 = volume after foaming (µL)

v_3 = volume of foam (µL)

v_4 = volume of foam after X min (µL)

2.1.3.4 Emulsion stability of proteins

The aqueous protein solution from the foaming capacity (2% (w/ v) was shaken for 1 min with an equal volume of avocado oil in a sample vial (12 mm radius) and left to stand sealed for 24h with measurements taken immediately, after 2 h and 24 h.

The emulsion capability was calculated according to Equation 2.4 and the emulsion stability according to Equation 2.5. The same conditions applied with regards to the radius of the sample vial, and the calculation of the volume from the height as in section 2.1.3.3.

Emulsion Capability (%) = $(v_2 - v_1)/ v_1$ *Equation 2.4*

Emulsion stability (%) = $(v_4/ v_3) \times 100$ *Equation 2.5*

v_1 = initial volume (µL)

v_2 = volume after emulsifying (µL)

v_3 = volume of emulsion layer (µL)

v_4 = volume of emulsion layer after X min (µL)

2.1.4 Enzymatic Hydrolysis of Protein Retentates

Protein retentates (0.05 g) were mixed with deionised water (3.0 mL) and adjusted to pH2 using 1M aqueous HCl solution. Commercial pepsin was added (0.001 g = 2%) and the mixture was incubated at 37°C for 4 h under constant shaking. Heat treatment (100°C) was used to deactivate the enzyme and stop the hydrolysis reaction. The samples were subsequently centrifuged at 3500 rpm for 20 min, the supernatant was freeze dried and analysed by CHN, Bradford Assay and SDS-PAGE.

2.1.5 Liquid Chromatography- Mass Spectrometry (LC-MS)

Samples submitted for LC-MS were prepared on an SDS PAGE gel by loading a generous amount of protein retentate (around 20 mg) into a small sample vial to which 8 mg of loading buffer and 24 µL of deionised water were added. The mixture was vortexed, heated (heating block, 70°C for 10 min) re-vortexed and centrifuged for one min. The supernatants were loaded on to NuPAGE-Bis-Tris Mini Gel and immersed in a 1:20 solution of buffer : water in an SDS-PAGE container. The samples were run around 2 cm into the gel at 60V and then stained with NBS SafeBlue stain overnight.

The samples were cut out and in-gel digested prior after reduction and alkylation (reduction: preparation of a 1.5 mg/mL (10 mM) solution of dithioerythriol in 100 mM ammonium bicarbonate. 200 mL were added to the gel and incubated at 56^{o}C for 1 h; alkylation: gel pieces returned to room temperature. Solution of 9.5 mg/mL (50 mM) iodoacetamide in 100 mM ammonium bicarbonate (alkylating solution) was prepared. Supernatant was removed from the gel and 200 mL of the alkylating solution was added and incubated in the dark at room temperature for 30 min), followed by resuspension in 0.1% trifluoroacetic acid (TFA). LC-MS analysis was undertaken on a 50 cm PepMap column

on a Waters mClass HPLC coupled to a Thermo Fusion Trybrid mass spectrometer. The acquired data was searched against 'National Centre for Biotechnology Information' (NCBI) entries for Nannochloropsis sp. in addition to the 'The common Repository of Adventitious Proteins' (cRAP) database of common contaminants using the Mascot search engine. The Mascot output was then read into the Scaffold software suite for processing with the XTandem engine and the generation of a results summary. False discovery rates were adjusted to 1% at the protein and peptide level and a filter of a minimum of two peptides required for protein identification was applied. LC-MS was performed by Dr. Chris Taylor, Department of Biology, University of York.

2.1.6 Klason digestion for sugar content

To determine the sugar profile of the initial biomass, ALG01 (100 mg) was placed in a serum bottle and a 72% aqueous-H_2SO_4 solution was added (1 mL). The mixture was placed at 40°C for 2 hours and stirred every half an hour. Thereafter, deionised water (28 mL) was added and the mixture was placed in an autoclave (121^{o}C for 1h) and 2 mL were passed through a regenerated cellulose syringe filter with 0.2 µm pore size. The resultant clear solution was subjected to HPLC analysis to determine its sugar profile.

2.2. Defibrillated Cellulose (DFC) Generation from Microalgal Biomass

2.2.1 Hydrothermal Microwave treatment and DFC generation

Microalgal biomass (ALG01, 10 g) was mixed with deionised water (350 mL) and microwaved in a Milestone Synthwave (1500 W, 2.45 GHz) in a PTFE vessel with 60% stirring at various temperatures (160°C, 180°C, 200°C and 220°C) for 30 min with a 15-min ramp and 15-min holding time. The samples were subsequently centrifuged for 20 min at 3500 rpm. The supernatant was separated from the pellet and saved for ultrafiltration to yield purified proteins. The pellet was washed with hot water (350 mL, 15 min), hot ethanol (2 x 350 mL, 15 min), cold ethanol (350 mL, 15 min) and cold acetone (350 mL, 15 min) to afford the desired DFC. Two types of biomass were used for this method: spray dried biomass and spent biomass. The yield of the DFC was calculated as according to Equation 2.6.

DFC Yield (%) = (Weight of DFC/ Weight of dried raw biomass) x 100

Equation 2.6

2.2.2 Hydrogel formation

DFC samples were prepared for the formation trials of hydrogels by preparing solutions of different concentrations (0.5% - 3%, w/v) by mixing an appropriate amount of DFC with deionised water. The samples were subsequently homogenised at 10000 rpm for 3 min to afford the hydrogels, which were then refrigerated. The inversion test was used to test the success of hydrogel formation. A successful hydrogel formed if, upon inversion of the vial, the sample did not flow down but self-supported itself.

2.2.3 Water Holding Capacity (WHC)

The water holding capacity (WHC) was determined by dispersing the appropriate dry DFC (2 g) in water (38 mL) in a weighted centrifuge tube and shaking it for 10 min. The resultant mixture was centrifuged (30 min at 3000 rpm), and the supernatant was carefully removed from the wet pellet. The weight of wet pellet was determined and the WHC was calculated according to Equation 2.7.

WHC (gH_2O/g sample) = (mass of wet sample + mass of tube and dry sample)
mass of dried sample *Equation 2.7*

2.2.4 Algaenan Isolation

The following samples (Spray DFC 160, Spray DFC 220, Spent DFC 160 and Spent DFC 220) were mixed with concentrated phosphoric acid at a ratio of 1:10 (w/v) and left in the fumehood for two weeks (according to Zych *et al*.)[192], after which the samples were filtered and washed three times with deionised water. The residual matter was assumed to be mainly algaenan and its yield was calculated according to Equation 2.8:

Algaenan Yield (%) = (Weight of algaenan/ Weight of DFC sample) x 100
Equation 2.8

2.3 Pyrolysis of Pellet

2.3.1 Microwave Pyrolysis

The pellet obtained from centrifugation upon protein extraction was used for microwave pyrolysis on a CEM Discover microwave.

The appropriate pellet (0.5 g or 1.0 g) was placed in a quartz glass tube in the microwave. Reactions were conducted with a safe temperature of 280°C, a 20 min overall run time and fixed power settings. The power was varied from 50 W, 100 W to 150 W to judge the effect on the pyrolysis process. According to the power, the amount of microalgal biomass placed in the pyrolysis tube was varied to avoid over pressurisation resulting in explosions of the vessel: 50W – 1.0 g; 100W – 0.5 g; 150W – 0.5 g.

For the double pyrolysis the same procedure was used but after completion of the first run the biomass was stirred around and rearranged with a spatula before subjecting it to another pyrolysis run under identical conditions.

Upon completion of microwave irradiation, ethyl acetate (10 mL) was added to the microwave tube to dissolve the bio-oil. The latter was separated from the biochar by filtration and biochar was allowed to air dry whilst the bio-oil was subjected to rotary evaporation to remove any residual ethyl acetate. The yields of the bio-char and the bio-oil were calculated according to Equations 2.9 and 2.10:

Char yield (%) = (Weight of char/ Weight of raw dried biomass) x 100 *Equation 2.9*

Bio-oil yield (%) = (Weigh of bio-oil/ Weight of raw dried biomass) x 100 *Equation 2.10*

2.3.2 Estimation of the Higher Heating Value (HHV)

The HHV of the chars was estimated using their CHN data and applying a modified version of Channiwala's equation shown in Equation 2.11.[193]

HHV (MJ/ kg) = 0.3491C (wt.%) + 1.1783H (wt.%) – 0.1034O (wt.%) – 0.015N (wt.%)
Equation 2.11

While the values of C, H and N were obtained directly from CHN analysis, the value for O was derived and approximated using the following equation 2.12:

O (wt.%) = 100% - C (wt.%) – H (wt.%) – N (wt.%) *Equation 2.12*

2.4 Instrumentation

2.4.1 Attenuated Total Reflection Infrared Spectroscopy (ATR-IR)

Attenuated Total Reflection Infrared Spectroscopy was performed using a Perkin Elmer FTIR/FTNIR Spectrum 400 Spectrophotometer. Prior to loading the sample on the sapphire window, the latter was pre-cleaned with ethanol and tissue wipes. Thereafter, enough sample was placed on the sapphire window and a light amount of pressure applied to trap and compress the sample between the sapphire window and the anvil. Spectra were recorded between 650-4000 cm^{-1} (32 scans) at a resolution of 4.00 cm^{-1}. The raw data was saved as a txt. file and processed using Origin 2018™ software.

2.4.2 Elemental Analysis (CHN)

The samples were analysed using an Exeter Analytical Inc CE440 analyser. Analyses were performed in-house by Dr. Graeme McAllister, Department of Chemistry, University of York, UK. Samples (1.6 mg-1.8 mg) were weighed on a Sartorius SE2 analytical balance and subsequently placed in a high-temperature furnace (975°C) and burnt under oxygen. Two measurements were conducted for each sample and the average is reported in the results and discussion section.

2.4.3 Thermogravimetric Analysis (TGA)

Samples (around 30 mg) for TGA were run on a Netzsch STA 409 under a nitrogen atmosphere at a flow rate of 100 mL/min with a temperature range from 25°C to 650°C at a heating ramp of 10°C/min. The data was collected as a txt. file and processed using Origin 2018™ software.

2.4.4 Scanning Electron Microscopy (SEM)

Samples for SEM were prepared by loading the slightest amount possible on SEM stubs with a sticky surface and coated with gold/palladium (around 7 nm thickness). The samples were run on a Jeol JSM-6490LV by Dr. Meg Stark, Department of Biology, University of York.

2.4.5 Solid state ^{13}C CPMAS NMR

Solid State ^{13}C cross polarization magic angle spinning (CPMAS) spectroscopy was performed on a 400 MHz Bruker Avance III HD spectrometer using a Bruker 4 mm H(F)/X/Y triple-resonance probe and 9.4T Ascend superconducting magnet. Solid State NMR experiments were run with a spin rate of 10,000 +/- 2 Hz, recycle delays of 5 s, a total

number of 512 scans and a linearly ramped contacted pulse of 1 ms. Chemical shifts were referenced using adamantane (29.5 ppm) as an external secondary reference and reporting of the chemical shifts was performed with respect to tetramethylsilane (TMS). The spectra were processed and analysed using MestReNova software.

2.4.6 X-Ray Powder Diffraction

X-Ray powder diffraction (XRD) studies were run on a Bruker AXS D8 Advance Diffractrometer equipped with a Cu source and PSD Lynx eye detector. The resulting monochromatic K- α radiation was at a wavelength of 1.54184 Å. The samples were finely ground prior to analysis and loaded onto a 0.75 mm thick sample holder. The samples were run using a locked-coupled scan type, with a scan speed of 0.1 s per step, voltage of 40 kV, and current of 40 mA. Data was collected in its raw form and processed in Origin 2018^{TM} software.

The crystallinity index (CrI) was calculated from Segal's method according to Equation 2.13:

$$CrI = (I_t - I_a)/ I_t \times 100 \qquad \textit{Equation 2.13}$$

I_t = intensity at 22.7^o

I_a = Intensity at 18^o

2.4.7 Transmission Electron Microscopy (TEM)

Samples for TEM were conducted on a TEM Tecnai 12 BioTWIN instrument with a SIS Megaview 3 camera at a 76-acceleration voltage of 120 kV. A 2% mass ratio of the finely ground samples were dispersed in water and ultrasonicated in an ultrasound bath at 1500 W for 20 min to improve the image clarity. TEM was performed by Joanne Marrison, Department of Biology, University of York.

2.4.8 Gas Chromatography FID and Gas Chromatography-Mass Spectrometry (GC-MS)

Gas chromatographic measurements were made with an Agilent Technologies HP 6890 gas chromatograph (or Agilent Technologies 7890B gas chromatograph), with a flame ionisation detector (GC-FID), fitted with a Rxi-5HT capillary column (30 m, 250 mm x 0.25 mm nominal, max temperature 400°C). Helium was used as the carrier gas at a flow rate of 10 mL/min with a split ratio of 5:1 and a 1 µl injection. The initial oven temperature was 50°C and was increased instantly at a rate of 30°C/min to 300°C and held at this temperature for 5 min, with a total run time of 13.3 min. Injection temperature was 250°C

and the detector temperature was 250°C. Electron Ionisation took place on a Clarus 560 MS. Scans were run over 40 m/z to 500 m/z, with a solvent delay of 2 min. The total run time was 13.33 minutes. The MS data was analysed using NIST library version 2.2.

2.4.9 High Performance Liquid Chromatography (HPLC)

HPLC was run on an Agilent 1260 HPLC instrument to determine the sugars extracted upon the different extraction methods employed. The samples (3-6 mg) were dissolved in deionised water (3 mL), passed through a regenerate cellulose syringe filter with 0.2 µm pore size and submitted for HPLC analysis. A reverse-phase Hi PLEX H (300 x 7.7 mm, 8 µm particle size) column maintained at 60°C with a 0.005M H_2SO_4 mobile phase was used for analysis with a run of 30 min at a flow rate of 0.4 mL/min and a 5 µL injection volume. Samples were detected using a refractive index detector. HPLC was run by Dr Richard Gammons at the GCCE, University of York.

2.4.10 Confocal Laser Microscopy (CLSM)

Carbotrace 480 was obtained from Ebba Biotech (Stockholm, Sweden) and was mixed with phosphate-buffered saline (PBS) in a ratio of 1:1000 (pH 7.4) and subsequently the defibrillated cellulose samples were mixed with aliquots of this stock solution and left to incubate for 30 minutes at room temperature. Carbotrace images were captured using a Zeiss LSM980 confocal microscope, AxioObserver Z1 using ZEN 3.4 (blue edition) software and either a EC Plan-Neofluar 10x/0.3 or a Plan Apochromat 20x/0.8 objective. All samples were excited with a 405nm laser using a 405nm main beam splitter and emission collected from 411-694nm in bins of 8.9nm. The pixel size was 1.657um2 or 0.829um2 for the 10x or 20x objectives respectively. The pinhole was 1AU and the images were taken in16 bit.

Reference spectra of cellulose stained with Carbotrace 480 and autofluorescence from unstained samples were collected independently to permit spectral unmixing. Samples were typically averaged x8 to reduce noise and increase the precision of the spectral unmixing which was performed using the in-built application within ZEN 3.4 on a pixel-to-pixel basis. The images were unmixed as follows:

SY_temperature samples using SY160 unstained autofluorescence spectra and the cellulose CT480 spectra

ST_temperature samples using ST160 unstained autofluorescence spectra and the cellulose CT480 spectra

Confocal Laser Spectroscopy (CLSM) was performed by Joanne Marrison and Grant Calder at the Department of Biology, University of York

Chapter 3

Results and Discussion

This chapter is sub-divided into 4 sections, which are commensurate with the aims of the research as outlined previously in Chapter 1, section 1.5, namely:

i. Preliminary characterisation of microalgal biomass (ALG01)
ii. the isolation, purification and characterisation of water-based microalgal proteins;
iii. the tandem production of defibrillated celluloses (DFC) and protein isolation from hydrolysates via acid-free hydrothermal microwave processing and their subsequent characterisation, and;
iv. the production and characterisation of bio-oils and biochars via microwave processing.

3.1 Preliminary Characterisation of Microalgal Biomass (ALG01)

The microalgae used in this research belong to the class of Eustigmatophyceae, which also contains *Nannochloropsis*, hence some tentative comparisons will be drawn between the two species. However, ALG01 is proprietary to AlgaeCytes Ltd. so no further information is available regarding its exact speciation. ALG01 naturally produces EPA, which is extracted using an ethanol-base mixture followed by acid neutralisation, with the residual biomass termed 'spent' biomass. 'Spray-Dried' ALG01 refers to spray dried (by AlgaeCytes Ltd) and freshly harvested ALG01 which has not undergone EPA extraction. Similarly, 'Freeze-dried' ALG01 refers to freeze-dried (by AlgaeCytes Ltd) freshly harvested ALG01, which has not undergone EPA extraction.

3.1.1 Visual and Microscopic Appearance

The visual (naked eye) and microscopic images of the different samples of microalgal biomass (freeze dried, spray dried and spent) received from AlgaeCytes Ltd. are depicted in Figure 3-1 and Figure 3-2.

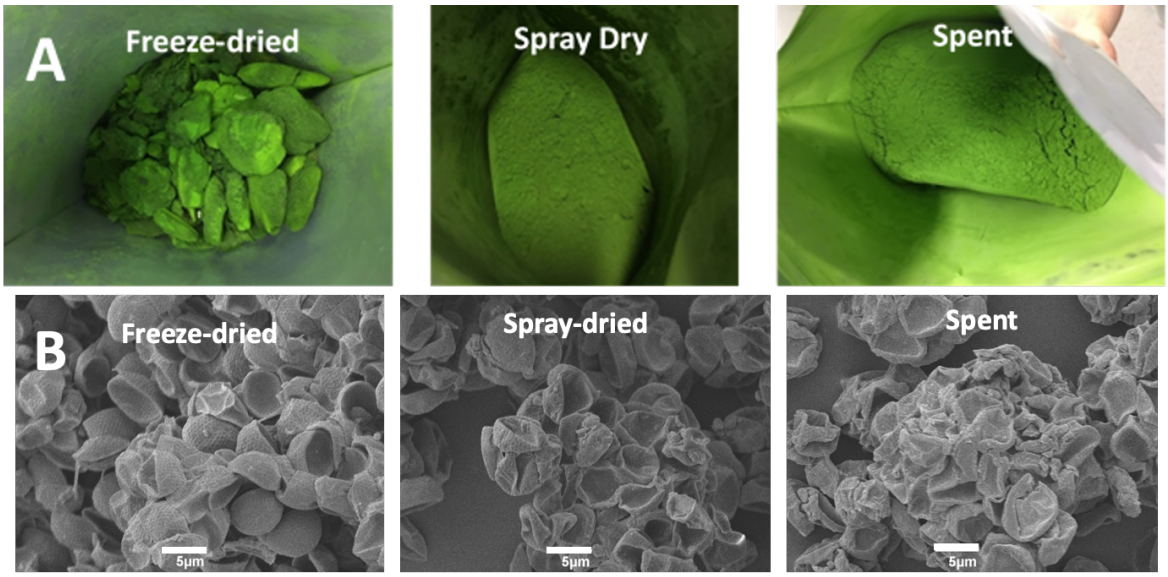

Figure 3-1 Appearance of as received algal biomass samples: A: naked eye; B: SEM

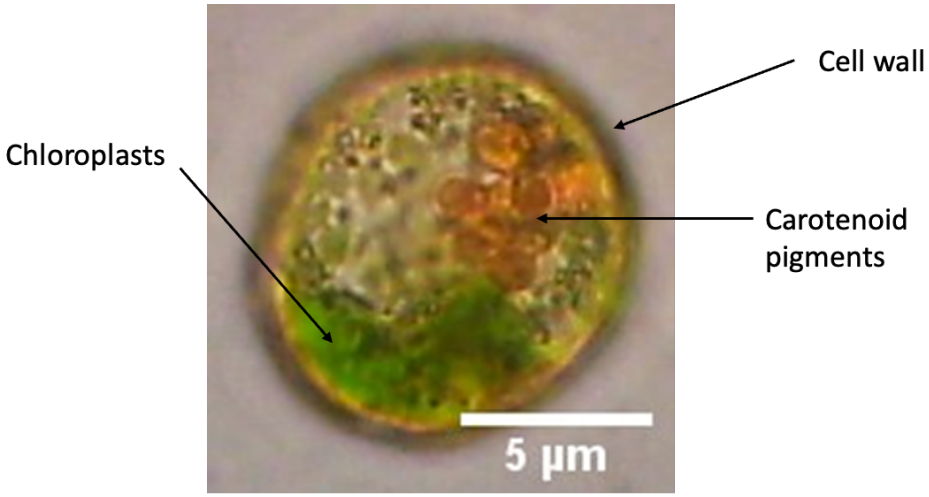

Figure 3-2 Light-microscopic images of ALG01 strain used in this project – image provided by AlgaeCytes

As expected, all ALG01 microalgal types appear as differing shades of green. Spent ALG01 possesses a slightly lighter and more intense colour profile than its freeze and spray dried counterparts. However, this colour difference could also be due to differences in particle size. The cell dimensions were estimated to be around 7-10 µm, which is consistent with the observations from the light microscopic image in Figure 3-2. The latter shows the congregation of cell components, specifically the grouping of green and red pigments present in the cell suggesting that in addition to proteins, carbohydrates and fats, highly valuable red pigments (carotenoids) can also be exploited.

SEM imaging (Figure 3-1 B) has produced interesting results which are helpful in judging the effect that the different drying methods have had on the cellular structure of the microalgae. All methods of drying seem to have had an impact on the overall appearance of the cells. All produce cell structures with a hexagonal, honeycomb surface texture (akin to golf balls) which are in almost all cases collapsed due to dehydration and form aggregates due to loss of water during the harsh drying process. The spent biomass shows a slightly more collapsed cell structure.

3.1.2 Composition Summary of ALG01 Microalgal Types

The elemental (CHN) analysis, protein content and carbohydrate content of the three ALG01 microalgal types are summarised in Table 6.

Table 6 Composition summary of ALG01 microalgal types

	Composition (%)		
	Freeze dried	Spray dried	Spent
C	46.24	45.34	38.61
H	6.52	6.36	5.28
N	6.75	6.21	6.94
Protein	42.19	38.81	43.38
Carbohydrate	39.20	43.12	30.24

The protein content was estimated using a traditional 6.25 multiplication factor and carbohydrate content is derived from the HPLC results of the Klason digestion with in-depth results displayed in Figure 3-3.[194] As expected, the composition of the native spray and freeze-dried ALG01 microalgal types are relatively similar. It must be noted that the exact nitrogen-to-protein conversion factor differs from species to species which makes all protein values an estimate. The assumed protein content varied from 38.81% (freeze dried) to 43.38% (spray dried) with spent biomass containing the most protein as well as the lowest carbohydrate content, carbon percentage and hydrogen percentage. This can be traced back to the industrial lipid (EPA) extraction process, during which the spent biomass has already undergone removal of many of the oils and lipids. The higher protein content is a result of less overall lipid content thus increasing the contribution of proteins towards the overall composition. The lower carbohydrate content, however, can be attributed to

some of it having been co-extracted during the industrial process which has disrupted the cell walls during the process and resulted in losses of cell wall structures.

In order to determine the type of carbohydrates (sugars) present in the initial biomass, samples were prepared using the Klason digestion method and subsequently analysed via HPLC. The results are displayed in Figure 3-3. The resulting molecules from the acid digestion are mainly water-soluble carbohydrates (sugars) as well as organic acids and furans. The monosaccharides are a result of the decomposition of larger cell wall components within the microalgal biomass while the organic acids are a result of the subsequent degradation of these monosaccharides.[195]

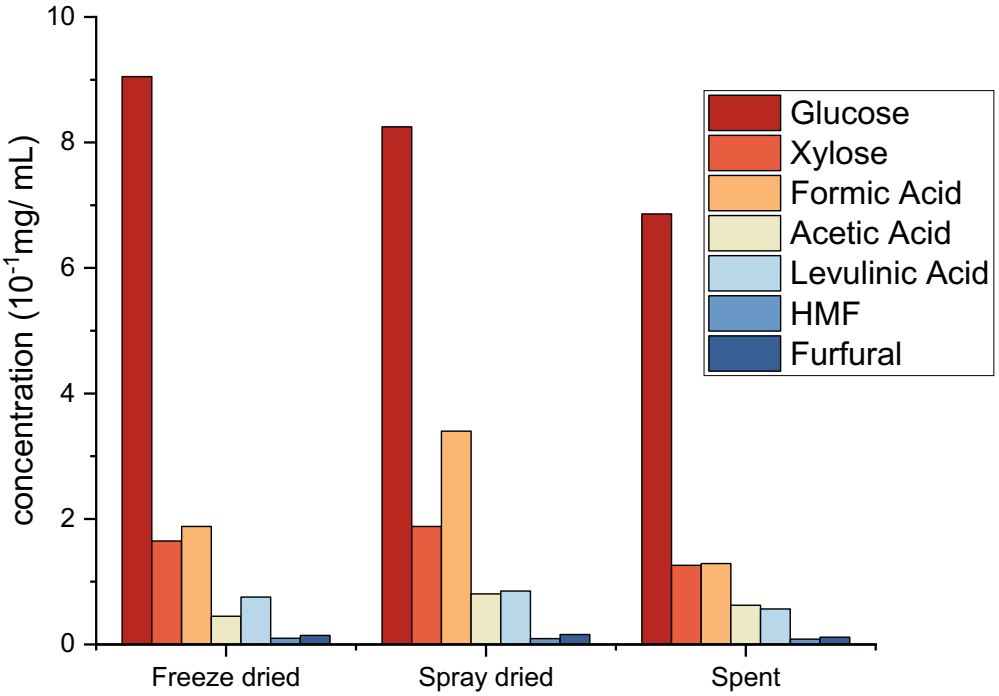

Figure 3-3 HPLC results obtained from Klason digestion of initial biomass samples

All initial samples show a very similar carbohydrate (sugar) and organic acid profile with glucose being by far the most prominent compound detected by HPLC. Glucose is most likely formed from the acid induced digestion of cellulose present in the microalgal cell wall

and is therefore most abundant. 5-Hydroxymethyl furfural (HMF), levulinic acid and furfural are subsequently formed through further glucose breakdown.[196] The presence of formic acid is attributed to the secondary degradation pathway in which glucose degrades to formic acid via HMF (Figure 3-4).[197]

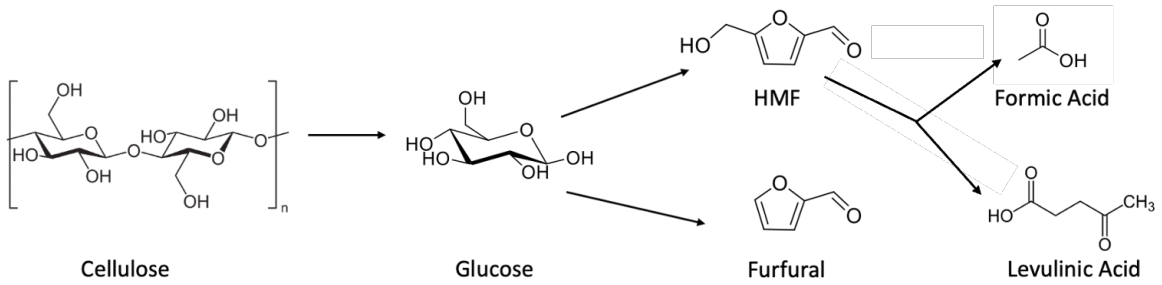

Figure 3-4 Cellulose and Glucose decomposition pathways

Formic acid and xylose are the two other most prominent compounds. Xylose is formed from the degradation of hemicellulose, however its low presence points towards a low hemicellulose content in ALG01. The spent ALG01 shows a very similar profile to the other algae indicating that the lipid extraction process had no significant impact on the carbohydrate profile of the microalgae apart from a reduction in quantity for each sugar.

As there are many hundreds of thousands of microalgal species, their composition profiles also vary greatly. In order to better contextualise the composition of ALG01, Table 7 displays the averaged composition profile of several of the most common microalgal species such as *Nannochloropsis sp., Chlorella vulgaris* and *Spirulina*. It has to be noted that the listed values are either averaged or display the control value for microalgae which have been grown in standard conditions. As the composition profile of microalgae can be greatly varied depending on different environmental stresses or changes in their nutrition profile such as nitrogen starvation, the listed composition profile can vary greatly depending on the growth setting.

Table 7 Composition profile of different microalgal species

	Composition (%)		
	Protein	Carbohydrates	Lipids
ALG01	41[a]	41[a]	12[b]
Nannochloropsis sp.	43[61]	35[61]	33-60[198,199]
Spirulina	50-60[200]	15-25[201]	14.3[202]
Chlorella vulgaris	42-58[203]	12-54[204]	5-40[203]

[a] average of spray dried and freeze-dried

[b] supplied by AlgaeCytes Ltd.

When comparing ALG01 to the other listed species the nearest similarities prevail with *Nannochloropsis sp*, which belongs to the same class of microalgae as ALG01. While the protein content is similar to the average of the other species, its carbohydrate content tops the list with lipids being on the lower side. However, as noted in the previous paragraph, microalgae composition can be adapted by introducing stresses or limiting certain sources of nutrition. With the ALG01 strain not only high EPA levels but also a high protein content can be observed, which makes ALG01 a very useful candidate for subsequent protein extraction.

3.1.3 Attenuated Total Reflectance IR Spectroscopy (ATR-IR)

The ATR-IR spectra of the three as received algal biomass samples are overlaid for ease of clarity in Figure 3-5.

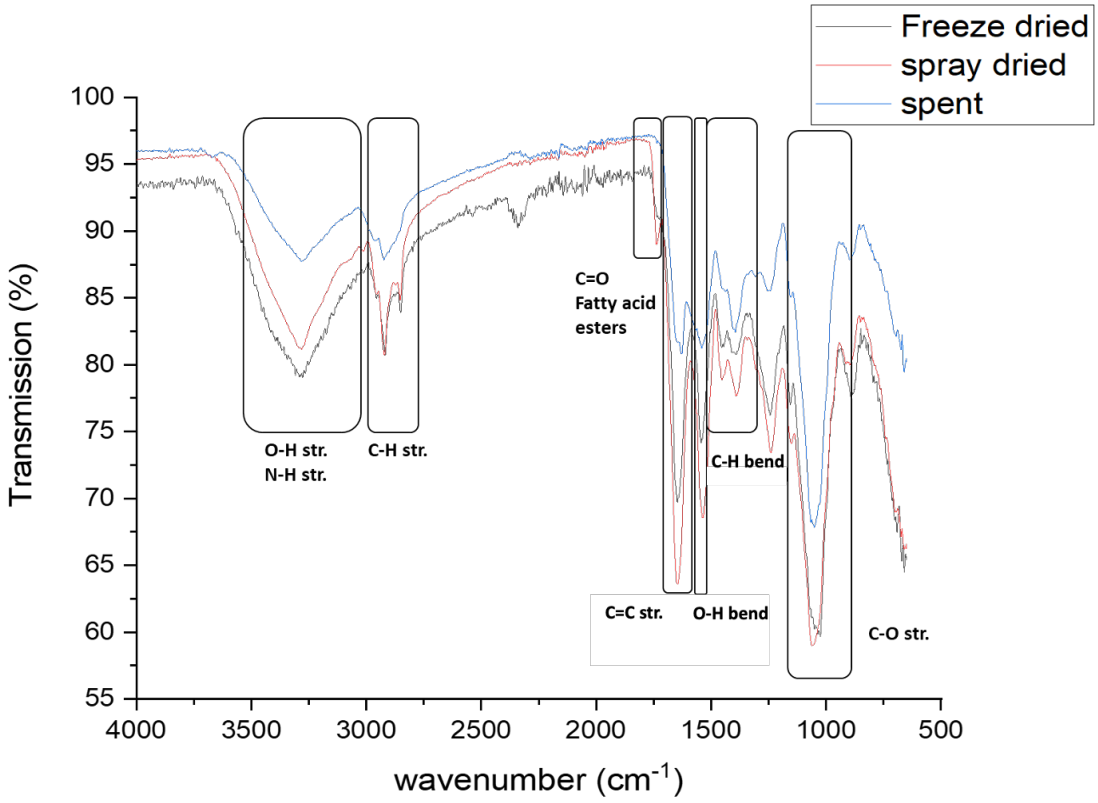

Figure 3-5 ATR-IR spectra for freeze dried, spray dried and spent biomass as indicated in the legend

All three IR spectra showcase similar absorbance bands. Most notably, spent ALG01 does not display a prominent carbonyl stretching band at 1730 cm^{-1}, which corresponds to fatty acids and esters, because it has already undergone industrial EPA extraction. Freeze dried and Spray dried samples show the presence of carbonyl bands that can be attributed to EPA (including the C=O str. at 1730 cm^{-1}, C=C str. at 1640 cm^{-1} and C-H bend at 1380 cm^{-1}). Characteristic for cellulose-containing hydroxyl groups is the O-H stretching band appearing at 3300 cm^{-1} while the C-H stretch at 2920 cm^{-1} corresponds also to both cellulose and hemicellulose but can also be attributed to the long aliphatic chains of the EPA, as mentioned above. The C-H str., C=C str. and C-O str. may also be attributed to algaenan. A detailed analysis of algaenan is given later in section 3.3.2.

3.1.4 Thermogravimetric Analysis (TGA)

Thermogravimetric analysis (TGA) measures mass loss (decomposition) with respect to temperature. The results of the TGA analysis are summarised in Table 8 and Figure 3-6.

Table 8 Mass loss (%) data extrapolated from TGA traces results for algal biomass samples

Algal biomass	**Mass loss (%)**		
	Moisture and Volatiles	**Hemicellulose, cellulose**	**Residual matter at 650°C**
Freeze dried	9.5	59.5	31.0
Spray dried	4.5	64.5	31.0
Spent	10.5	50.3	39.2

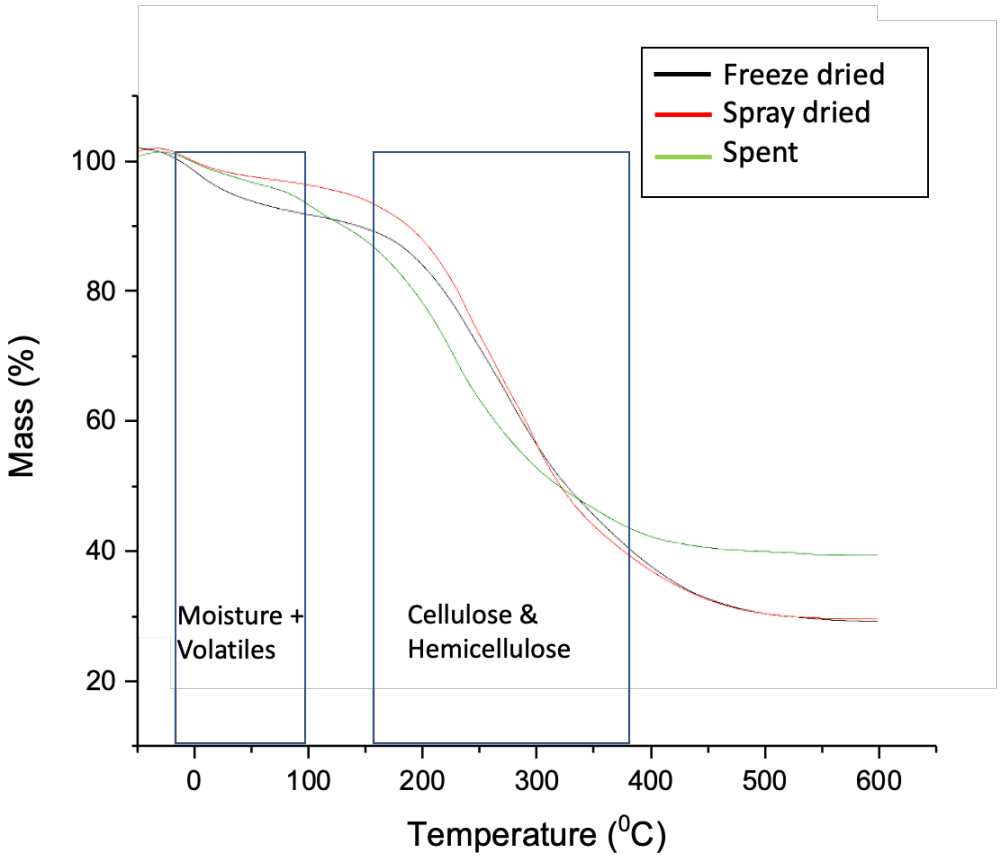

Figure 3-6 TGA traces of initial ALG01 biomass types

As the first mass loss is connected to moisture and volatile losses, it can be seen that spray drying is the most effective drying method with residual moisture of about half of that present in both freeze dried and spent biomass. Interestingly, while both freeze dried and spray dried biomass show a very similar decomposition profile, the TG profile of spent algal

biomass is significantly different to its counterparts. Spent algal biomass has the highest residue content at 650°C (85ranula. 39%) compared with its counterparts (85ranula. 31%). This, as well as the much lower hemicellulose/cellulose content may be correlated to the aforementioned industrial EPA extraction process.

3.1.5 ^{13}C -Cross-polarisation-magic-angle spinning (CPMAS) solid state NMR

CPMAS Solid state NMR was performed on all three initial biomass types in order to extend the information gained through ATR-IR spectroscopy and to be able to judge the cell wall composition of ALG01. Cell wall compositions of microalgae are hugely dependent on the species with a myriad of potential cell wall structures existing and not being fully understood and researched yet, thus making a clear analysis very difficult. The 13 C CPMAS spectra are displayed in Figure 3-7.

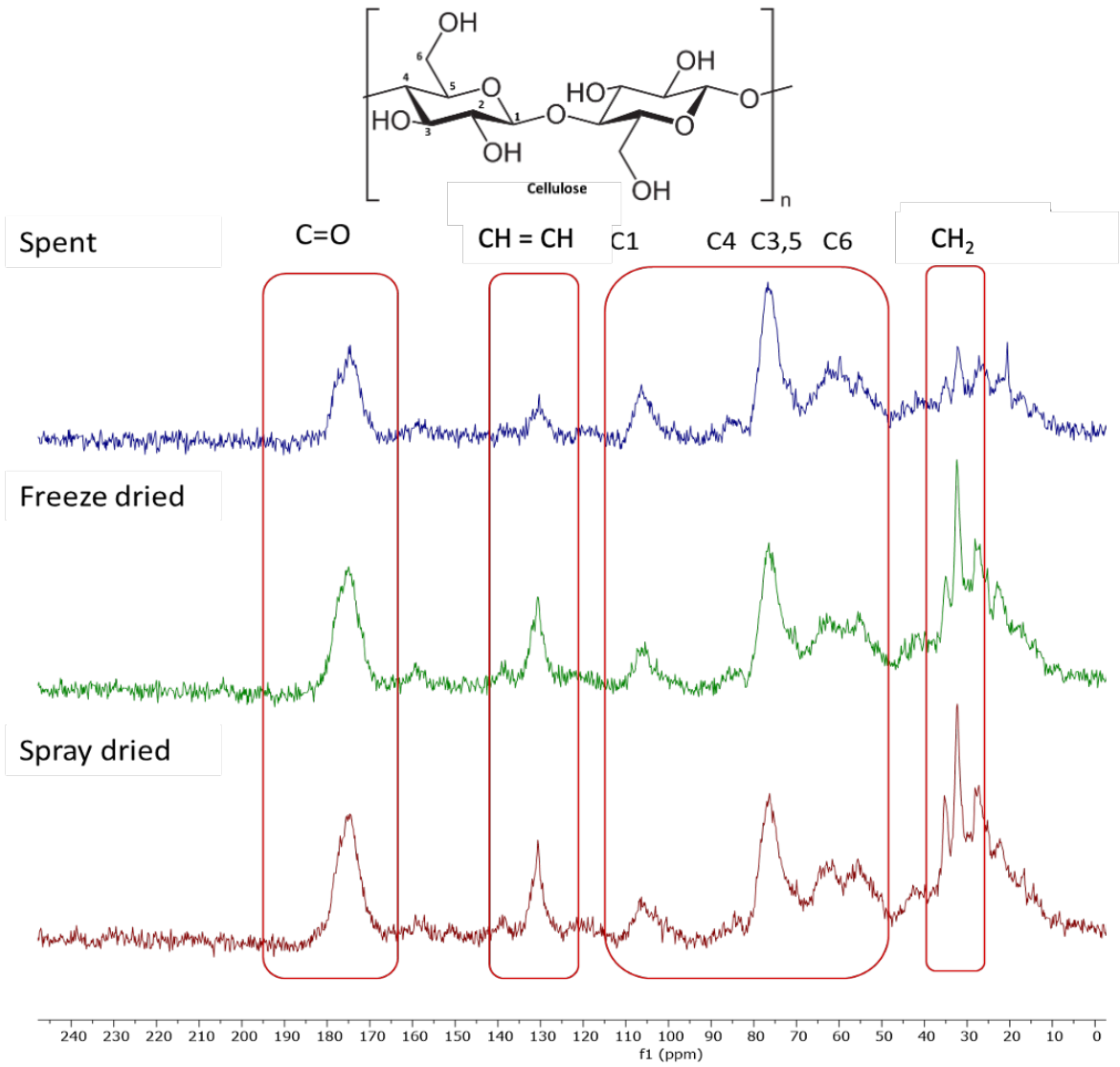

Figure 3-7 CPMAS Solid state 13C NMR spectra of the initial biomass types

The CPMAS spectra for all three biomass types look very similar except for the intensity of signals at 130 ppm (-C=C-) and between 25 – 35 ppm (-CH_2-), which is much less in spent ALG01. The diminished intensity of these signals correlates well with the removal of EPA. However, the continued presence of these signals in spent ALG01 may be due to algaenan, which also gives signals in these regions (see later).[74,205–208] For spray dried and freeze dried biomass, the intensity of the signals around 25 – 35 ppm appear to give the strongest response indicating a high presence of EPA within the microalgal cell. In addition, the unsaturation found within the EPA backbone results in the sharp signal appearing at around 130 ppm. The collection of signals in the 50 – 110 ppm area correspond to cellulose and the signal at around 175 ppm can be assigned to a carbonyl carbon most likely associated with EPA and/or hemicellulosic matter or proteinaceous matter.

3.1.6 Amino Acid Analysis

The freeze-dried algae were analysed for their amino acid content, which totalled to 35.819 g/100 g of amino acids (Aas) found in this specific batch of microalgae. As there are natural variations from batch to batch the values obtained from this analysis are slightly different to values of the batches that were used for this project. The amino acid analysis was performed by AlgaeCytes prior to this project and is shown in Figure 3-8.

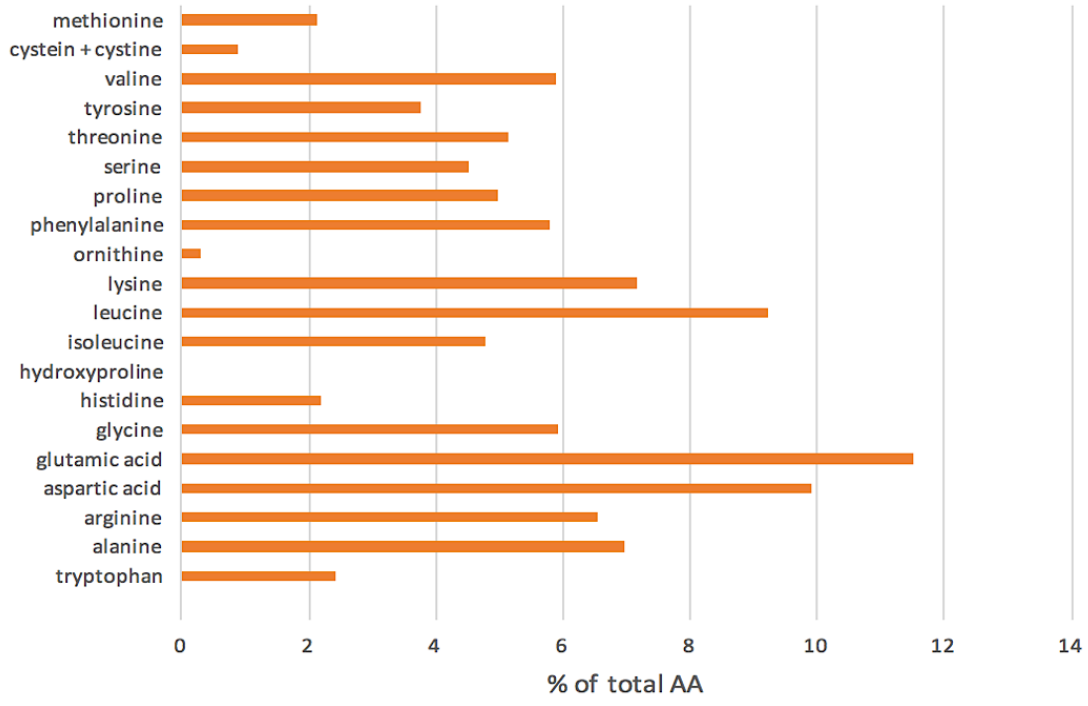

Figure 3-8 Individual contributions of amino acids to total amino acid content

Glutamic and aspartic acid as well as leucine and lysine are the most prominent Aas in this strain of microalgae. Compared to other microalgal species as reported by Olsen *et al*.[194] and Tibbets *et al.*[209], ALG01 overlaps with their analyses of *Scenedesmus sp.* and *Nannochloropsis 87ranulate,* which both showed the same three amino acids (Glutamic and aspartic acid and leucine) as the most prominent ones present in their algal biomass. 20 out of 21 amino acids are present in ALG01 apart from hydroxyproline. Furthermore and very importantly, all nine essential amino acids are also found in ALG01, which fits well with any potential nutritional applications of the extracted proteins and is in line with findings of other algal species.[194]

Amongst the essential amino acids, leucine, isoleucine, lysine and valine are present in ALG01 in significant amounts. This profile matches very well with the amino acids most abundant in eggs, which consists of high doses of glutamic acid, aspartic acid, leucine, serine, valine and lysine suggesting high suitability with potential nutritional applications of algal proteins replacing their animal-derived counterparts.[210]

With recent global trends of protein sources steering towards vegan protein, one of the main competitors of microalgal protein are those obtained from soybeans. Adapted from Olsen *et al.*[194] and Zarkadas *et al.,*[211] Figure 3-9 compares the composition profile of essential amino acids of ALG01 and the mean of 14 different soy cultivars.

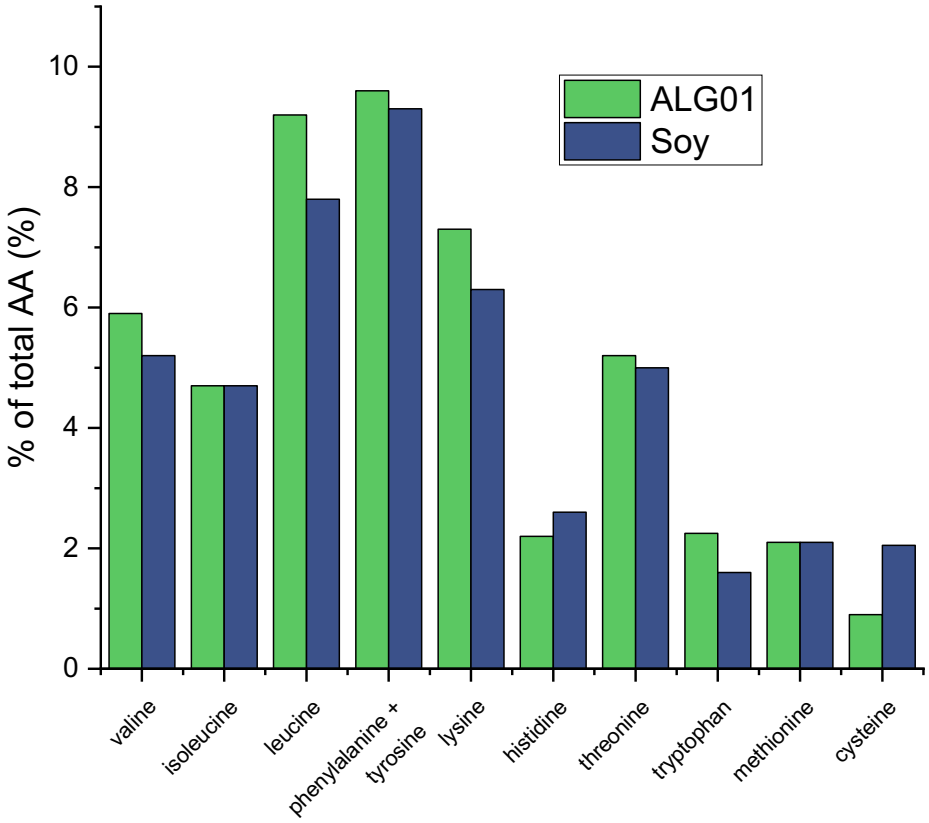

Figure 3-9 Comparison of essential amino acid content between ALG01 and the mean of 14 commercial soybean cultivars[194]

In direct comparison of the essential amino acid profile of ALG01 against soybean protein, it is notable that apart from histidine and cysteine all other essential amino acids are present in a higher proportion in ALG01, although apart from leucine there are no major discrepancies between the two. This strongly highlights the nutritional potential of microalgal proteins and its competitiveness, not just in comparison to egg protein but also to direct vegan competitors.

In conclusion, the composition profile of the microalgal feedstock has shown that it is very suitable for subsequent protein extractions both due to their abundant nature within the algal cells as well as their amino acid profile which holds many benefits to later industrial applications.

3.2 The Isolation, Purification and Characterisation of Water-Based Microalgal Proteins

The main objective throughout the protein extraction was to assess the protein potential of the different algal types and judge the resulting yields and compositions. Thereafter, the process was optimised through various pre-treatments aimed at both rupturing the tough cell wall and to change protein composition within to fit different potential applications. Although freeze dried algae were initially tested, for many later experiments they were dropped due to the very strong similarities to spray dried biomass and AlgaeCytes Ltd. industrially having opted for spray drying over freeze-drying as a stabilisation method.

As a reminder, in order to refrain from using traditional chemical/ organic solvent extraction methods such as, salting out or three phase extraction, a method using solely water coupled with physical pre-treatments, e.g., manual grinding, ultrasound, microwaves and biochemical pre-treatment (enzymes), followed by micro- and ultrafiltration, was devised.

3.2.1 Initial Protein Extraction without pre-treatment

3.2.1.1 Appearance, Protein Content and Yields

Protein extraction using deionised water alone, centrifugation and subsequent micro- and ultrafiltration – and without any pre-treatment – was successfully performed on the three biomass types available (spray dried, freeze dried and spent). The yield, appearance and protein content evaluated from CHN is summarised in Figure 3-10 with full CHN data shown in Figure 3-11.

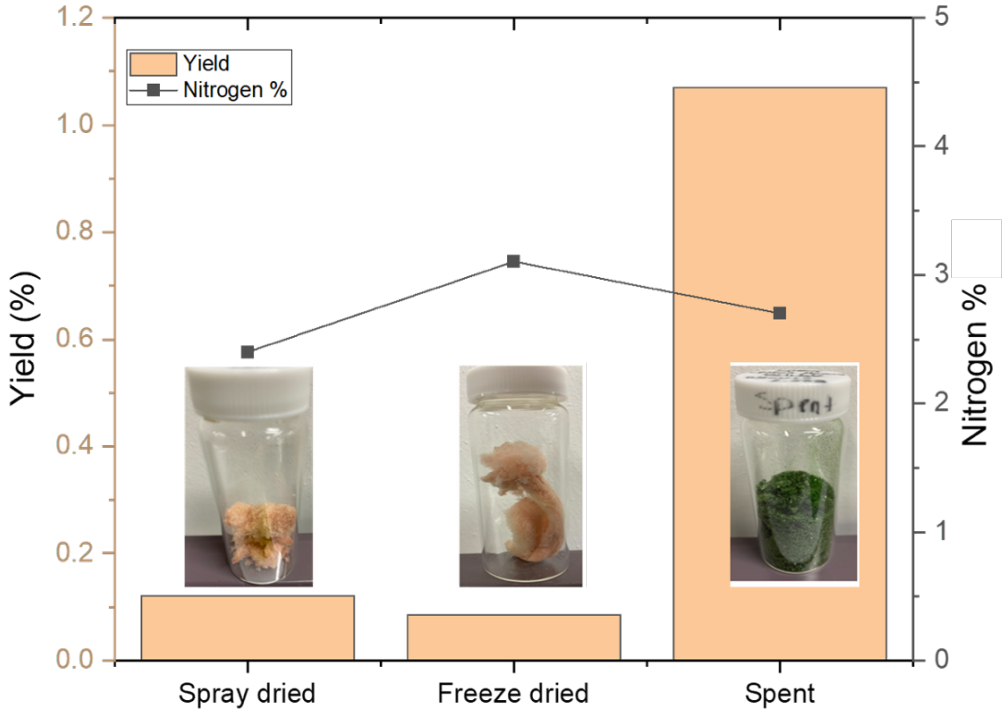

Figure 3-10 Yields and protein content of microalgal retentates without pre-treatment

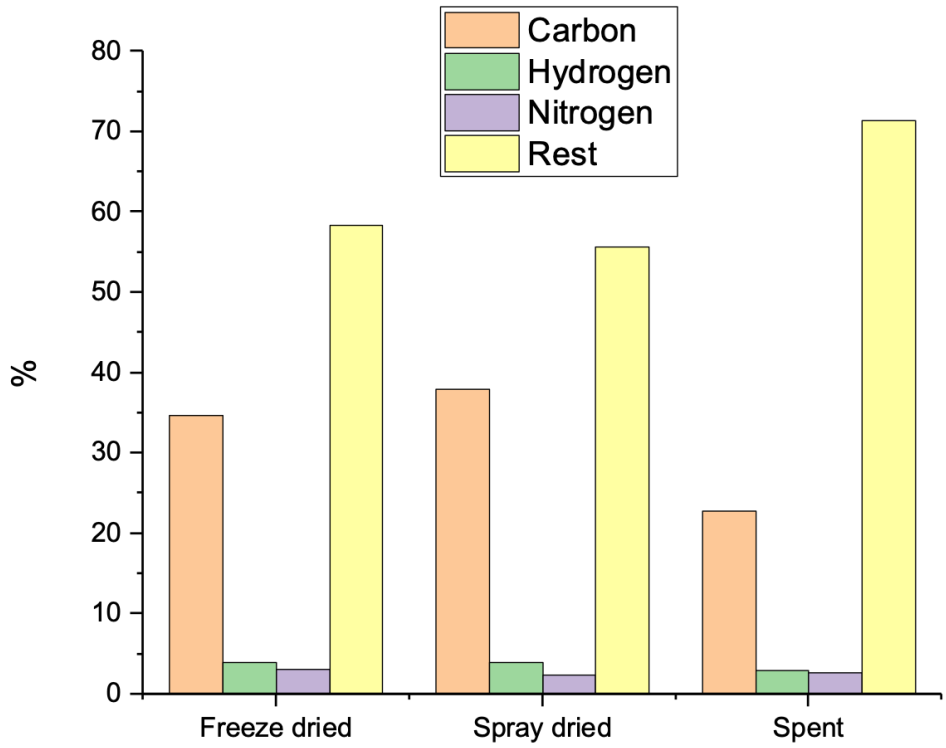

Figure 3-11 CHN data of untreated protein retentates obtained from all 3 ALG01 biomass types

Although the protein yields are quite low (compared to the total amount of protein present in ALG01 (around 41%)) it is interesting to note that the yield of spent ALG01 protein (1.08%) is approximately 10 times higher than for spray dried ALG01 (0.12%) and freeze dried ALG01 (0.08%). This may be due to significant cell disruption as a result of the ethanol-base industrial EPA extraction process, which facilitates the ease of extraction resulting in higher yield. The SEM images confirm cell rupturing (Figure *3-1*).

The influence of the EPA extraction can also be seen in the colour of the samples, as spray dried and freeze dried retentates appear light pink with the spent retentate being intensely green. The pink colour suggests residual carotenoid pigments in the retentates, while the intense green refers to additional chlorophyll and chloroplasts in the retentate, which have been extracted due to the fragmented cell structure of spent biomass.

The elemental analysis of the retentates shows that the nitrogen content seems to be comparable between all three retentates with only a difference of around 0.5% by wt. between the samples (freeze dried 3.1% N, spray dried 2.4% N, spent 2.8% N). This suggests

that although the overall yield has increased upon industrial lipid removal in the spent retentate, the purity of proteins seems to be limited by the extraction process. The 'rest' which was assumed to be oxygen varies significantly: spray dried retentate (56%), spent retentate (72%). This discrepancy may be due to the spent retentate containing more impurities, which have been washed out of the disrupted cells, such as carbohydrates, and which have not been fully removed by the ultrafiltration membrane. However, the very high 'rest' content may also be due to improper drying of the sample prior to analysis resulting in residual water. The surface structure of the retentates was explored by SEM (Figure 3-12).

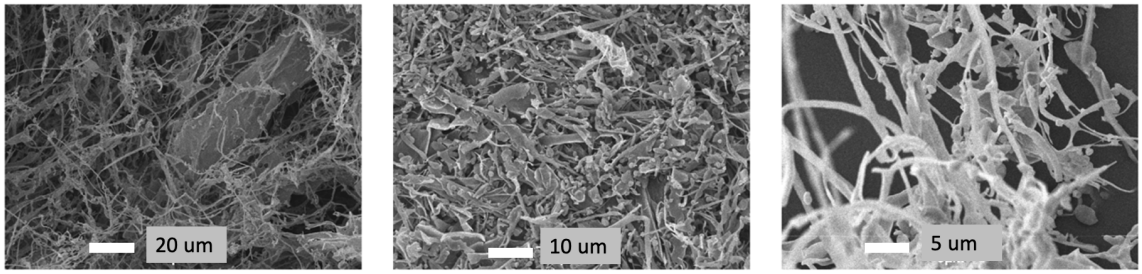

Figure 3-12 SEM images of protein retentate from spray dried biomass

SEM produced insightful images into the nature of the protein retentate showing an interlinked web of strands that can congregate to bigger lumps or appear as more spider web-like structures.

The protein/ peptide composition of each of the samples were further explored via the Bradford Assay and SDS- PAGE as the CHN data merely reflects the total amount of nitrogen but does not give further indications on the molecular weight distribution of proteins in the samples.

3.2.1.2 Bradford Assay and SDS-PAGE analysis

The Bradford Assay is a UV-vis spectrophotometric technique based on monitoring the absorption of the Coomassie Brilliant Blue G250 dye (CBBG, Figure 3-13) as it interacts with proteins in an acidic environment.[155,212–214]

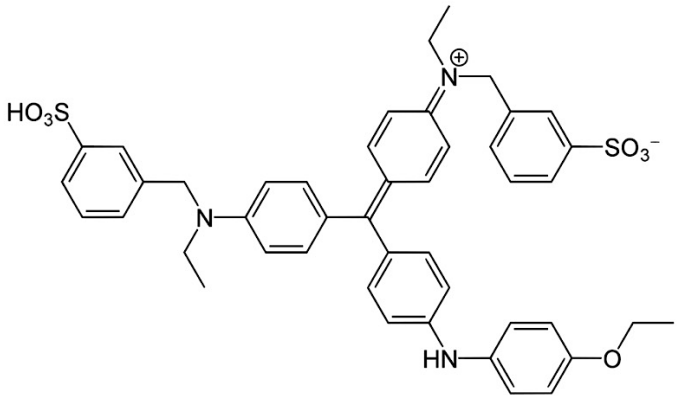

Figure 3-13 Chemical structure of CBBG dye (neutral form)

The Bradford dye exists in three forms: the cationic form (doubly protonated, red), the neutral form (green) and unprotonated anionic form (blue). In the acidic Bradford Assay medium, the CBBG dye exists primarily in its unstable cationic form, which has a distinctive red-brown colour and absorbs at 420 nm, while the anionic form is presumed to not exist under these conditions.[215] The protein then binds to the dye through electrostatic, van der Waals and hydrophobic interactions to produce the stable protein-bound anionic form of the CBBG dye through a metachromic shift, which has a wavelength of maximum absorption of 595 nm (brilliant blue colour).[216,217] The dye exhibits a preference of binding to arginine and basic and aromatic amino acid groups (Figure 3-14).[155,213] The exact mechanism of the binding, however, is not fully understood yet, with some sources suggesting the anionic (blue) form does not exist under acidic conditions[215], while others suggest that only the neutral (green) and anionic (blue) forms of the dye can bind to proteins and that they exist in minimal quantities under acidic pH.[218]

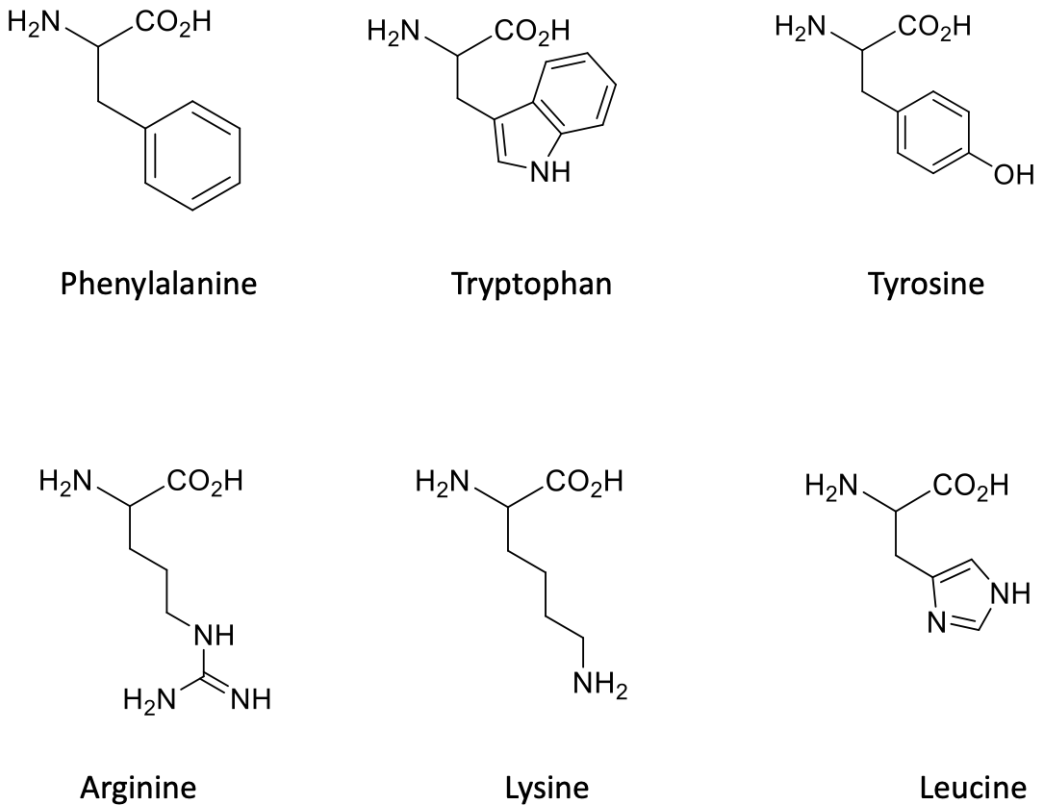

Figure 3-14 Structures amino acids binding to CBBG dye

The absorption at 595 nm can be read and compared to the calibration curve constructed using Bovine Serum Albumin (BSA).[155] The Bradford Assay results of the initial extracted proteins are summarised in Figure 3-15.

The CBBG dye does not complex with other nitrogen-containing compounds, free amino acids or short-chain peptides (less than 5 kDa) and detects only those proteins that are water soluble. Thus, the Bradford Assay has limitations and furthermore, does not give information about the molecular weight distribution of the protein sample. Therefore, SDS-PAGE analysis (Figure 3-16) was performed on the protein samples to better understand their molecular weight distribution.

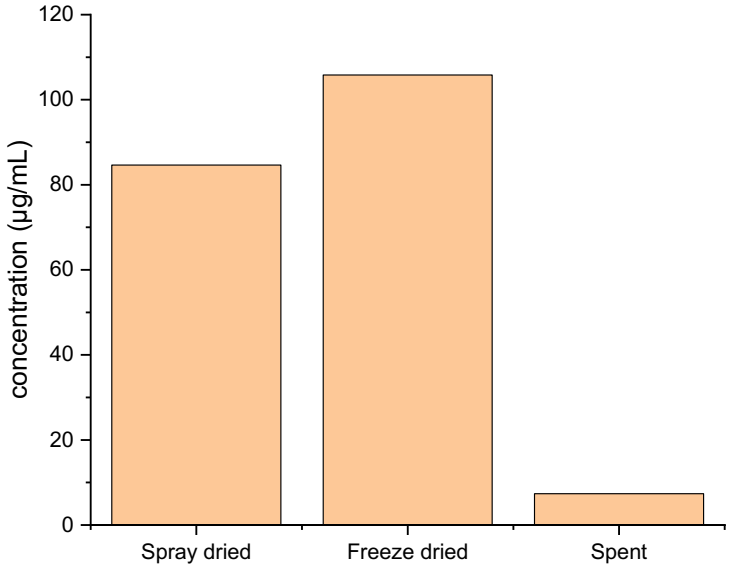

Figure 3-15 Bradford Assay results of protein retentates of different microalgal types

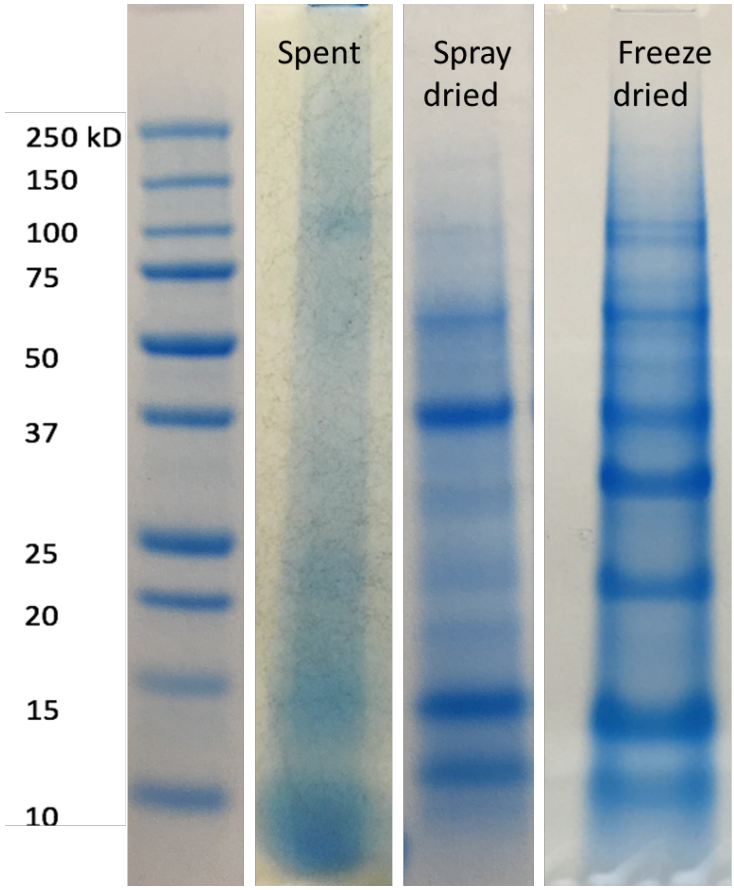

Figure 3-16 SDS-PAGE gel of protein retentates of different microalgal types

While the freeze-dried ALG01 protein retentate has the highest overall nitrogen percentage (3.05%, Figure 3-10), it also has the highest water-soluble protein concentration (107 ug/mL, Figure 3-15), closely followed by the proteins obtained from spray dried ALG01 (83 ug/mL). Proteins from spent ALG01, however, show a high nitrogen percentage (2.64%, Figure 3-10) but a very low Bradford Assay response for water soluble proteins (8 mg/mL). This discrepancy may be explained by consulting the SDS- PAGE results (Figure 3-16), which qualitatively show a vast difference in the molecular weight distribution between the samples. There are no discernible clear protein bands for spent ALG01 above approximately 15 kDa. The SDS-PAGE exists primarily in the state of low-molecular weight peptides which do not generate the same response on a Bradford Assay.[219] The response which can be seen of the spent retentate, however, is caused by peptides above 5 kDa as well as the low amount of residual higher molecular weight proteins with a faint band to be made out at around 75 kDa as well as some other minor ones at lower weights which appear more smudged and less clear. The industrial EPA extraction process (ethanol-base treatment followed by acid neutralisation) has significantly hydrolysed the proteins to short-chain peptides.

The proteins from freeze and spray dried ALG01 that have not undergone the previous industrial extraction process, still show a distribution of higher molecular weight proteins with the most prominent bands at around 100 kDa, 55 kDa, 37 kDa, 22 kDa, 14 kDa and 12 kDa. Most importantly, freeze dried proteins show more intense bands at 30 kDa and 22 kDa compared to the spray dried biomass which could be due to the spray drying process involving temperatures as high as 180^{o}C which could have degraded some of the lesser heat resistant proteins and caused the band intensity to weaken.

3.2.2. Protein extraction using pre-treatment

As only water-soluble proteins are being extracted, which can make up around 20% of the salt-free dry weight of *Nannochloropsis sp.* microalgae, a strain very similar to ALG01[66], three different pre-treatments were explored: ultrasonic probe treatment (US), manual grinding (MG) and microwave treatment (160^{o}C, in order to ensure complete cell lysis). The pre-treatment methods aimed to increase the water-soluble protein yield by breaking the rigid cell wall, which is further strengthened by an algaenan layer.

3.2.2.1 Visual Appearance

The effect of the three different pre-treatments (ultrasonic probe treatment (US), manual grinding (MG) and microwave treatment (MW 160°C)) on the visual appearance of the starting ALG01 (spray dried, MW 160°C, MG and US) and their subsequent retentates following micro- and ultrafiltration are depicted in Figure 3-17.

SEM images of pre-treated ALG01 show that microwave treatment at 160°C (MW 160°C) significantly alters the physical structure compared to the native or initial spray-dried microalgae. The physical structure of manually ground (MG) and ultrasound-treated (US) appears to be intermediate with respect to spray dried and MW160°C, *i.e.*, the untreated looks like pasta shells with a relatively regular diameter. US and MG look like 'thinner, rougher and more distorted', slightly closed pasta shells with an irregular diameter, whilst MW 160°C shows near-closed closed pasta shells comprising a very narrow diameter or slit.

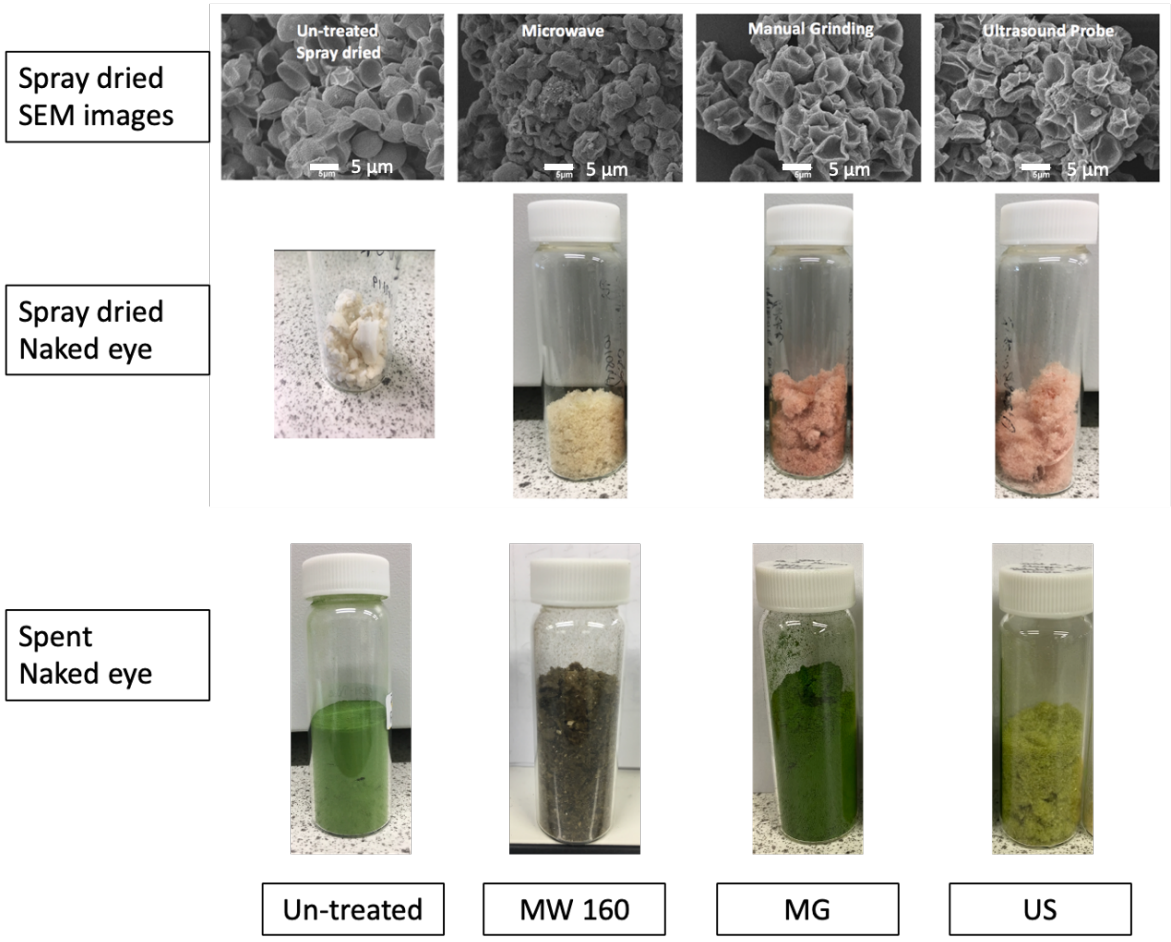

Figure 3-17 Naked eye appearance of protein retentates and SEM images of microalgal biomass upon different pre-treatment methods

The difference in the visual (naked eye) appearance of the retentates derived from the corresponding pre-treated ALG01 is striking. The retentate from manually treated spray dried ALG01 (MG) appears as an intense red-pink colour whilst the retentate from microwave-treated spray dried ALG01 (MW160^{o}C) appears creamish, off-white. The retentate from ultrasound treated spray dried ALG01 (US) affords a lighter red-pink colour. The red-pink colour suggests the release of pigments (carotenoids) into the sample during the cell disruption via manual grinding and ultrasound treatment. The pigments could be further separated from the retentate thus adding value to the extraction process, i.e., two value products, proteins and pigments. Similarly, Chew *et al.*[22] reported, that the red colour corresponds to carotenoid pigments that are preferentially released upon milling and ultrasonication. Pigments may also be released during microwave treatment but as the retentate appears creamy, off-white, they are most likely degraded at 160^{o}C under microwave processing. Retentates from freeze dried ALG01 appear identical to those obtained from spray dried ALG01.

With respect to the retentates derived from spent ALG01, the prominent green colour is present in all samples, as already seen previously (Figure 3-10). The green colour is further intensified upon manual grinding, while the ultrasonicated samples show a more pastel shade of green, suggesting a lower presence of chlorophyll/ chloroplasts in the retentates. Similar to the microwaved retentate from spray dried ALG01, the microwave spent sample also shows a less intense colour, but rather a smudgy brown interspersed with specks of cream, a result of the 160^{o}C achieved during the microwave processing.

3.2.2.2 Retentate Yield and Protein Yield (Nitrogen Basis)

The protein retentate yields and nitrogen percentages for all pre-treatment methods on both spray dried, freeze dried and spent algae are summarised in Figure 3-18.

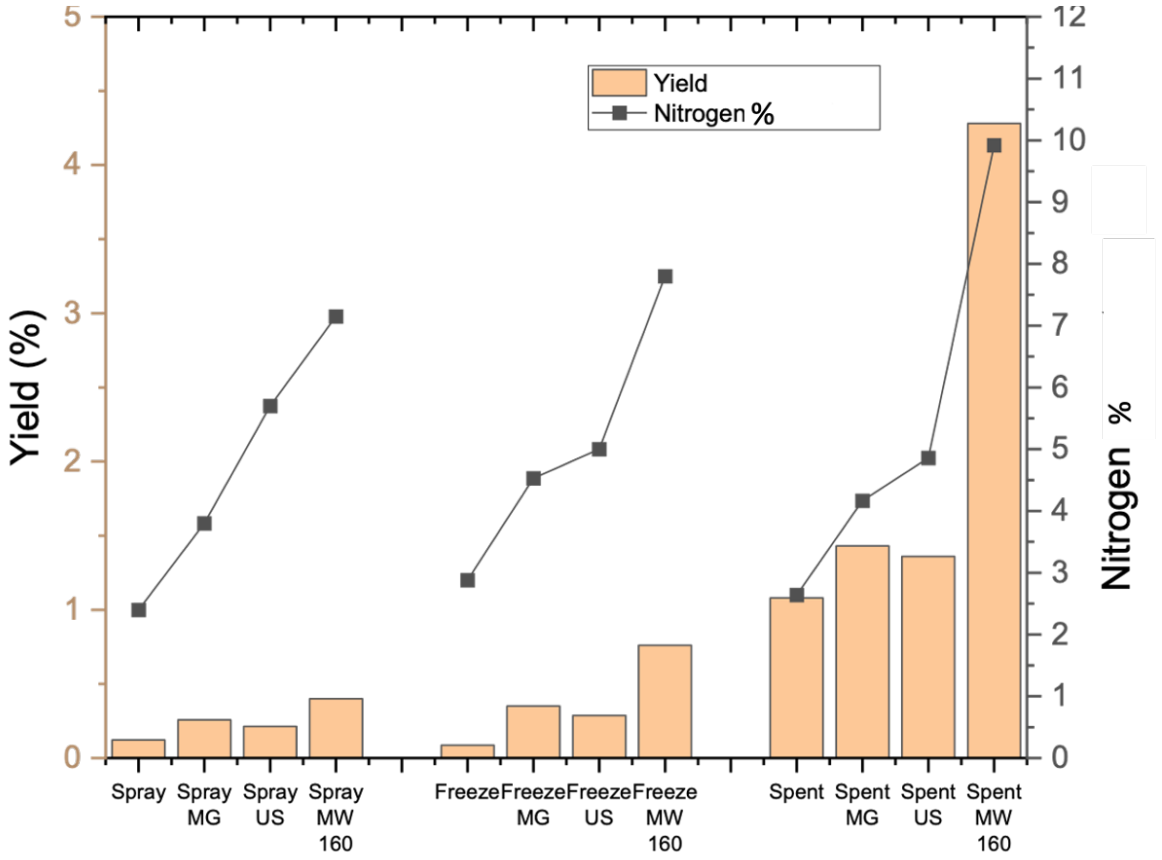

Figure 3-18 Retentate yields (%, bars) and nitrogen content (%, lines) from spray dried, freeze dried and spent ALG01 with and without pre-treatment methods

As Figure 3-18 evidences, pre-treatment (MG, US, MW160) has a positive impact on the extraction yield (%) and nitrogen content (%) of proteins with respect to no pre-treatment (native ALG01). Microwave treatment for spent retentates (Spent MW160) gave the highest retentate yield (4.35%), around ten times higher than for spray dried MW160 (0.4%) and freeze dried MW160 (0.75%) and approximately three-fold higher than spent MG (1.5%), the second-highest yield. The nitrogen percentage reached levels of 8-10% for the microwaved proteins, being almost double that of the next highest pre-treatment (US) for both freeze dried (5%) and spent biomass (4.9%). The difference in N% between the highest value (MW160) and the second highest (US) is largest for spent retentates (5%) and freeze dried retentates (3%), while the same difference is only around 1.5% for spray dried retentates. A clear increasing trend can be seen regarding the nitrogen content following the pre-treatment methods in the order of untreated < MG < US < MW 160. This trend seems to also replicate itself in the yield albeit not as evenly increasing, and with ultrasonication yields being slightly below their manually ground counterparts (around

0.1% for all samples), while the increase in yield towards the microwaved samples is very large (0.25% for spray dried, 0.25% for freeze dried and 2.85% for spent).

Interestingly, spent biomass shows considerably higher yields for all different types of protein samples with even the highest yield of freeze-dried protein retentates (MW 160, 0.85%) not reaching the lowest value of the spent protein retentates (untreated, 1.06%). As previously discussed, the industrial lipid extraction has already served as an initial pre-treatment method, which has caused the cells to disrupt and ease the protein extraction, which is even further aided by subsequent pre-treatments.

Literature findings also attribute the use of different pre-treatment methods to a significantly higher protein yield as well as protein content.[123,125,144] Safi *et al*[125] found nitrogen content in their protein samples to increase along the order of untreated < manual grinding < ultrasound with nitrogen percentages ranging between 0.5-4.5% for manual grinding and 0.6-6.1% for ultrasound between different microalgal species (*Haematococcus pluvialis*, *Nannochloropsis oculate*, *Chlorella vulgaris*, *Porphyridium cruentum*, *Arthrospira platensis)*.[125] A nitrogen content for ALG01 proteins with an average of around 4% (manually ground) and 5% (ultrasound) correlates well with the highest values found by Safi *et al*. thus placing ALG01 pre-treated proteins on the top end in terms of protein content. Zocher *et al.* have shown that microwave pre-treatment on *Chlorella vulgaris* has been proven to be the most effective pre-treatment method at generating high protein yields and nitrogen content, similar to the results from ALG01.[220,221]

3.2.2.3 Protein Content (Bradford Assay) and Molecular Weight Distribution (SDS-PAGE)

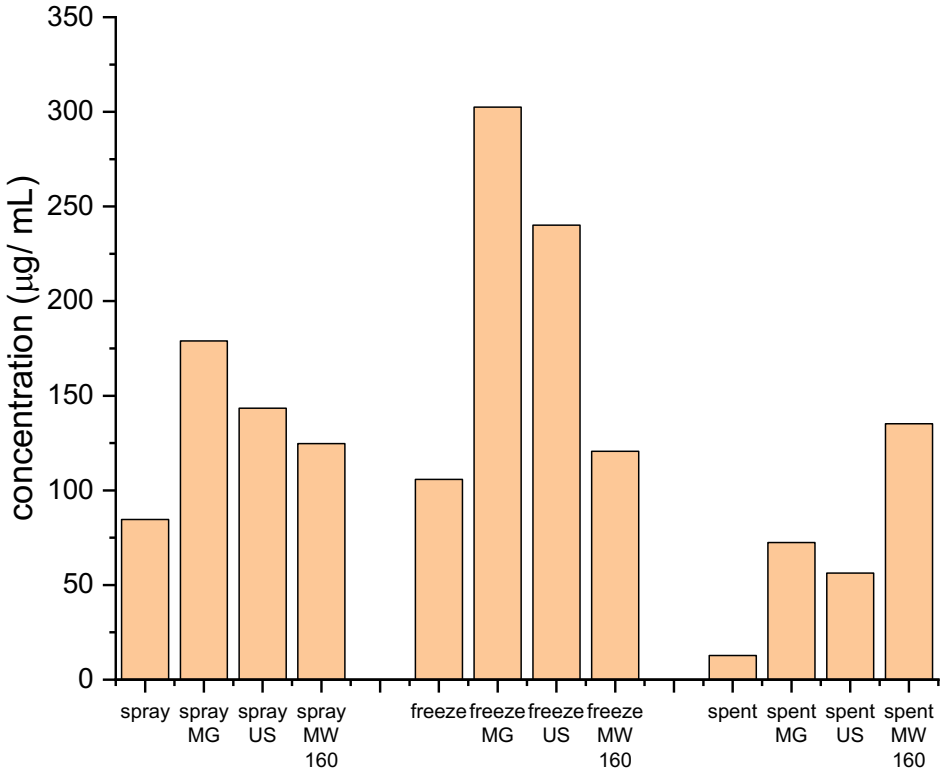

Figure 3-19 Bradford Assay responses of protein retentates from spray dried, freeze dried and spent biomass with different pre-treatment methods

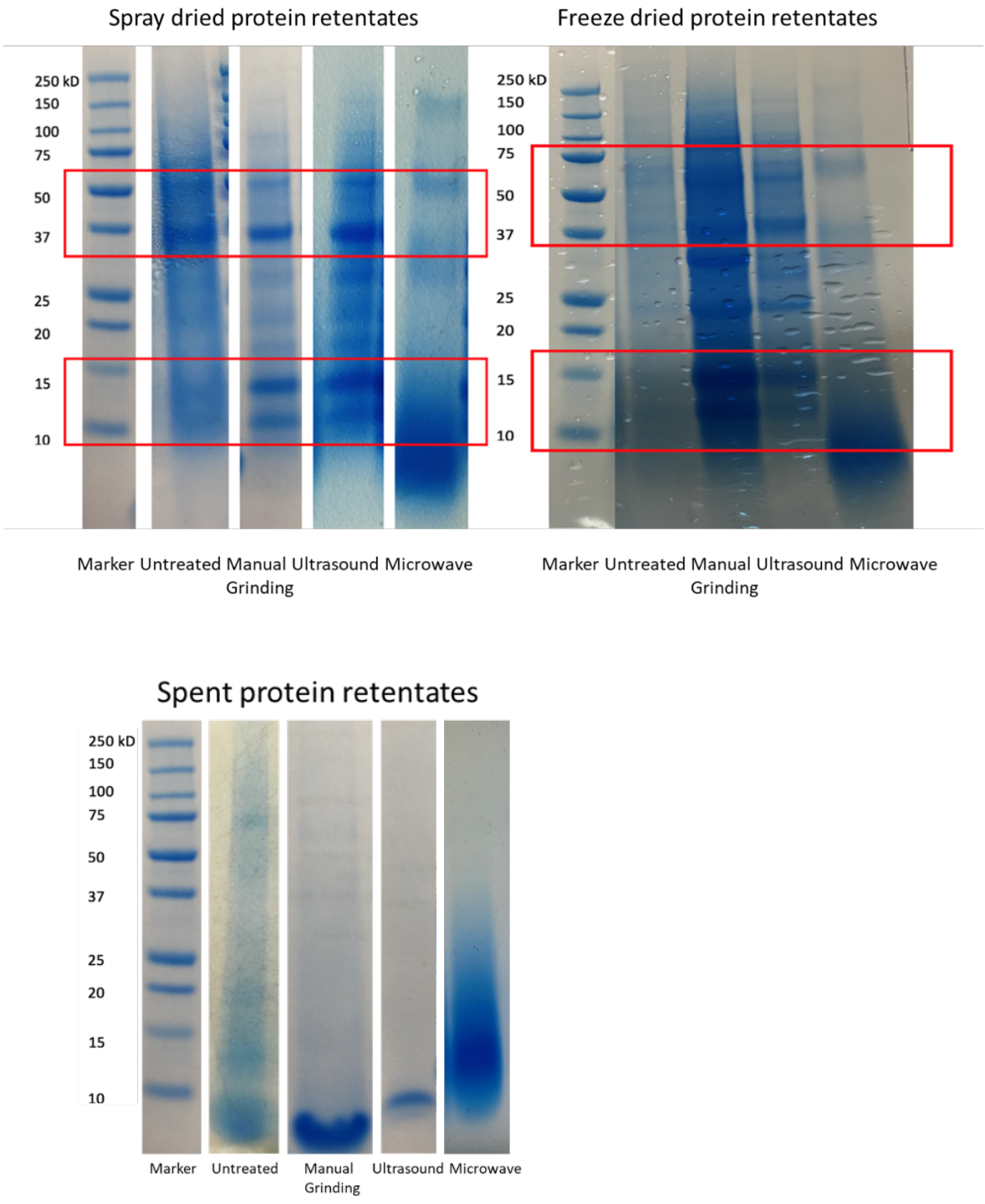

Figure 3-20 SDS- PAGE gels of protein retentates from spray dried, freeze dried and spent biomass with different pre-treatment methods

Results from Bradford Assay (Figure 3-19) as well as SDS- PAGE (Figure 3-20) show the influence of the different pre-treatment methods on the nature (content and molecular weight distribution) of the proteins in the retentates. Results from the Bradford Assay mirror previous results (Figure 3-18), i.e., there is an increase in water soluble protein

content upon pre-treatment. In terms of Bradford Assay responses for each biomass type (Spray, Freeze, Spent), Manual grinding resulted in the highest Bradford Assay responses for spray dried retentates (180 ug/mL) and freeze dried retentates (310 ug/mL). The second highest Bradford Assay response for each biomass type was ultrasonic treatment (145 ug/mL for spray dried and 240 ug/mL for freeze dried). The initial untreated retentate protein contents are considerably lower for all three biomass types (60 ug/mL for spray dried, 110 ug/mL for freeze dried and 20 ug/mL for spent), whilst the total nitrogen content is highest for all three retentates with microwave pre-treatment (7.1% for spray dried, 7.9% for freeze dried and 10% for spent). Their apparently low Bradford Assay response (125 ug/mL for spray dried, 120 ug/mL for freeze dried and 140 ug/mL for spent) may be explained by the SDS-PAGE gels (see Figure 3-20), which show a predominance of aggregated bands around 10 kDa and lower, a range which makes it difficult to detect using Bradford Assay.

Microwave treatment (in this case at 160^{o}C) has a destructive effect on large proteins and generates mostly peptides by breaking down (hydrolysing) the proteins, in contrast to ultrasound and manual grinding, which appear to be non-destructive but are yield- and protein content- enhancing. This is also evidenced within the SDS-PAGE gels (Figure 3-20), with the increased intensity of bands at 37 kDa, 12 kDa and 10 kDa. Spent retentates show a completely different composition to spray dried and freeze-dried protein retentates due to an intense band of peptides congregating around 10 kDa followed by faint bands of heavier proteins around 20 kDa and 75 kDa. These latter bands vanish upon pre-treatment whilst the former, low molecular weight peptides gain in intensity.

The highest Bradford response for spent retentates is recorded for the microwaved proteins (140 ug/mL), which correlates well to the considerably higher yield (4.35%) compared to the untreated spent retentate (1.06%), as well as the fact that the SDS-PAGE gel shows a more continuous smear of various proteins appearing at higher molecular weights, which are picked up by the Bradford Assay more than low molecular weight peptides. Microwave treatment therefore has increased the release of peptides by hydrolysing higher molecular weight proteins, but also introduced a more continuous spectrum of peptide molecular weights.

3.2.2.4 Summary

In summary, employing pre-treatment methods across all microalgal types has proven successful in both disrupting the cell wall to increase protein release yields, but also to increase the purity of the samples by gradually enhancing the nitrogen content. Manual Grinding (MS) compared to Ultrasonication (US) shows very comparable retentate yields (0.25% for spray MG and 0.20% for spray US; 0.30% for freeze MG and 0.25% for freeze US; 1.5% for spent MG, 1.3% for spent US) and nitrogen content (4% on average for MG, 5% on average for US). Manual grinding is probably the best pre-treatment method due to its shorter time (2 minutes compared to 10 minutes for ultrasonication and microwave), ease of application (simple setup for grinding in a coffee grinder compared to more complex setup for ultrasonication including ice bath) and better scalability (manual grinding can easily be scaled up in large containers while ultrasonication requires very strong probes to penetrate larger volumes of biomass). Interestingly, microwave treatment is also quick and convenient but denatures and hydrolyses the protein into low molecular weight peptides (<10 kDa). However, the type of product required can influence the desired pre-treatment method, i.e., manual grinding is best for high molecular weight proteins whilst, if low molecular weight peptides are desired, microwave pre-treatment is preferential. There is strong commercial interest in low molecular weight peptides for their biological activity.

3.2.3 LC-MS analysis of spray and spent protein retentates

LC-MS was performed on the protein retentates of both spray dried ALG01 and spent ALG01 (Figure 3-21). The data shows qualitatively an overall protein count of 116 identified proteins. However, false discovery rates are still very large indicating that there is still a large number of proteins that remains unidentified due to the algae strand ALG01 being proprietary to AlgaeCytes Ltd. and therefore not having been previously analysed and fed into a database. The close relation to *Nannochloropsis sp.* was exploited and used for the literature search. The data shows a closely equal split concerning molecular weight as there are proteins identified in the whole range from 9 kDa to 145 kDa, which confirms the ultrafiltration cut-off point of 10 kDa as well as being in line with SDS-PAGE gels that show a similar molecular weight profile (Figure 3-22).

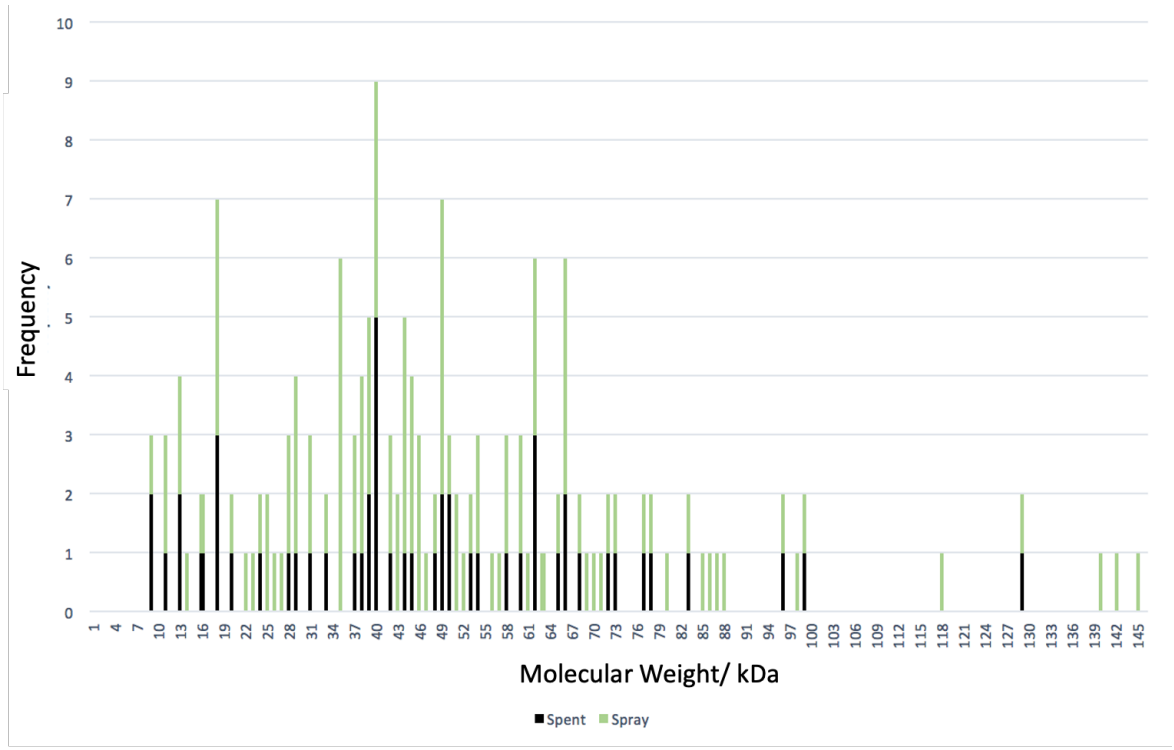

Figure 3-21 Protein molecular weight distribution of ultrafiltration retentates from spray dried and spent ALG01 biomass, data obtained from LC-MS

The data (Figure 3-21) shows that protein retentates from spray biomass contain more proteins than from spent biomass, which is in line with spent biomass mostly consisting of peptides. Moreover, both retentates show a large grouping of proteins in the mid to low kDa region around 34 kDa – 50 kDa while proteins above 75 kDa are present less frequently with proteins from spent biomass almost exclusively appear in the low – mid region.

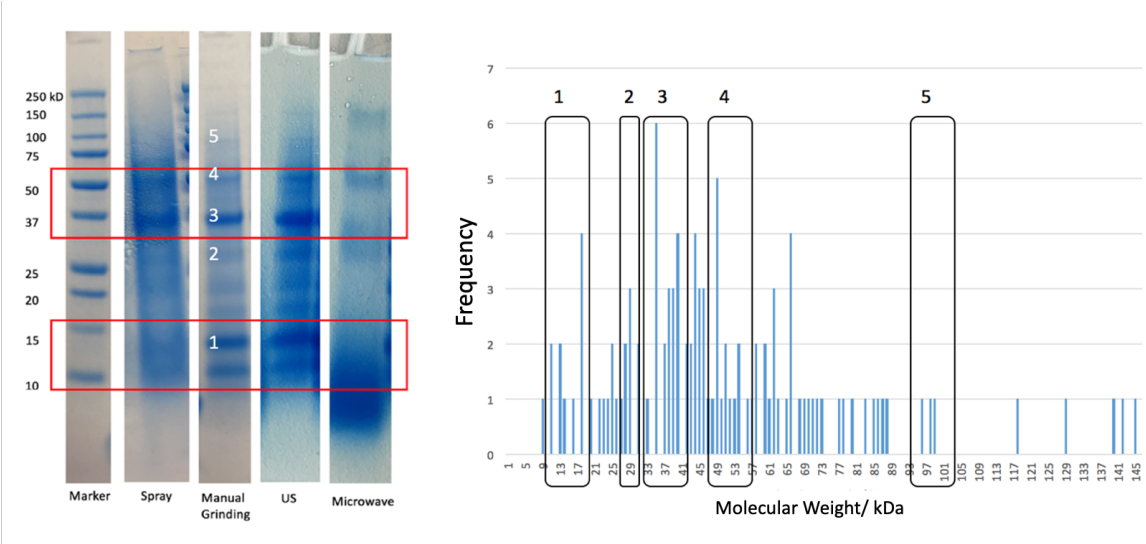

Figure 3-22 Corresponding protein bands in LC-MS and SDS-PAGE for spray dry manual grinding protein retentate

From Figure 3-22 it can be seen that the SDS-PAGE results correlate well with the results obtained from LC-MS analysis. Although the LC-MS has been performed qualitatively, it allows some conclusions concerning the quantitative nature of the data as the frequency of protein hits from protein identification relate well to the intensity of protein bands on the SDS PAGE gel confirming the proteins around 18 kDa, 35 kDa, 40 kDa, 49 kDa and 66 kDa to be the most present in the protein retentates. However, more analysis needs to be performed to be able to identify single protein or peptide sequences from the data and correlate them with potential bioactivity, preliminary results of which are detailed in later sections (3.2.6).

3.2.4 Enzymatic Hydrolysis of Proteins

Due to various industries such as cosmetics, medicinal and therapeutics emphasizing the high value of peptide mixtures due to their increased biological activity[222,223] compared to fully folded proteins, the freeze dried retentates were subjected to enzymatic hydrolysis to judge the effectiveness of forming hydrolysed peptides.[135] As the spent biomass already produces peptides due to the prior industrial extraction process impacting the cell integrity and structure, these two formed peptides (spent peptides and enzymatically hydrolysed from freeze dried ALG01) can be compared against each other to judge the most effective

way of producing them. Commercial Pepsin was chosen as the preferred enzyme due to its ready availability and occurrence in human gastric fluid, as well its well-documented use in several literature publications.[137–139] Pepsin mainly attacks hydrophobic aromatic amino acid residues, phenylalanine, leucine and tyrosine, of which there are many present in ALG01 biomass according to Figure 3-8.[137]

The effect of pepsin hydrolysis on differently pre-treated freeze dried microalgal protein retentates on %N and recovery yield (%) is summarised in Figure 3-23.

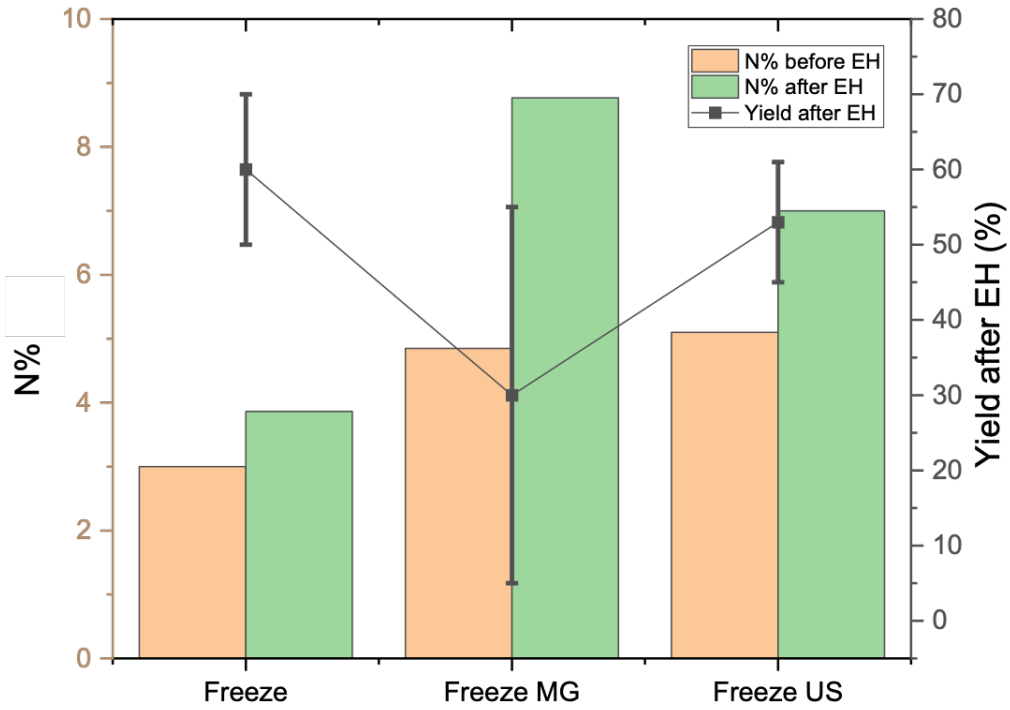

Figure 3-23 Enzymatic hydrolysis (EH) with Pepsin on different protein retentates, n=3

Upon enzymatic hydrolysis the recovery yields vary quite considerably with freeze dried samples ranging between 31% for Freeze MG and 60% for untreated freeze-dried proteins. However, the quantity of protein retentates used in the MG sample were quite low, which resulted in losses in accuracy of measuring out the exact enzyme and the final yield resulting in high uncertainties associated with the run. The nitrogen content in all the samples was found to have increased slightly which in turn indicates a rise in purity, with

maximum purities of around 9% for Freeze MG. Nitrogen content has increased by 0.8% for un-treated freeze dried samples, 3.6% for Freeze MG and 1.8% for Freeze US.

Compared to literature findings the recovery yields using pepsin in this instance (ranging between 31% and 60%) seem to sit firmly in the middle-ground with groups reporting recovery yields as low as 6.6% (using Celluclast), 32.4% for Alcalase, but also values as high as 80.3% for *Nannochloropsis* biomass and equally using Alcalase.[143,224]

The SDS-PAGE gel (Figure 3-24) confirms the effectiveness of the enzyme treatment as most high molecular weight protein bands have disappeared with a larger congregation of peptides collecting around the 10 kDa mark. The most intense protein bands that could be made out in the hydrolysed samples are around 35 kDa and 17 kDa. The 35 kDa band also appears in the original non-hydrolysed protein sample while the 17 kDa band only appears in the hydrolysed protein samples, suggesting it has been formed through enzymatic treatment. The SDS-PAGE appearance therefore starts to show more similarities to the one obtained from spent biomass, which almost exclusively shows hydrolysed peptides, suggesting a similar nature in terms of overall composition and potentially also in activity.

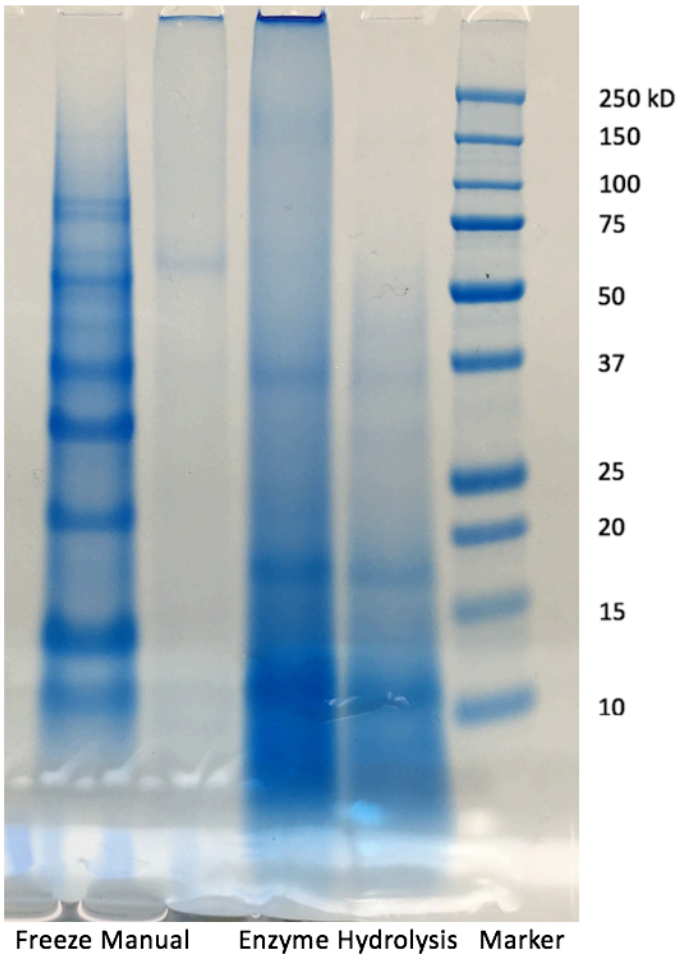

Figure 3-24 SDS-PAGE gel of protein samples before and after enzyme hydrolysis

The decrease of higher molecular weight proteins with subsequent rises in low molecular weight peptides upon enzymatic treatment has been found in multiple studies which sometimes even saw more drastic reduction of proteins to peptides than in this case with no higher molecular weight protein bands present anymore at all.[135,141,142] Furthermore, the decrease in protein and increase in peptides was also confirmed by employing the Bradford Assay method which monitors concentration of water-soluble proteins (Figure 3-25).

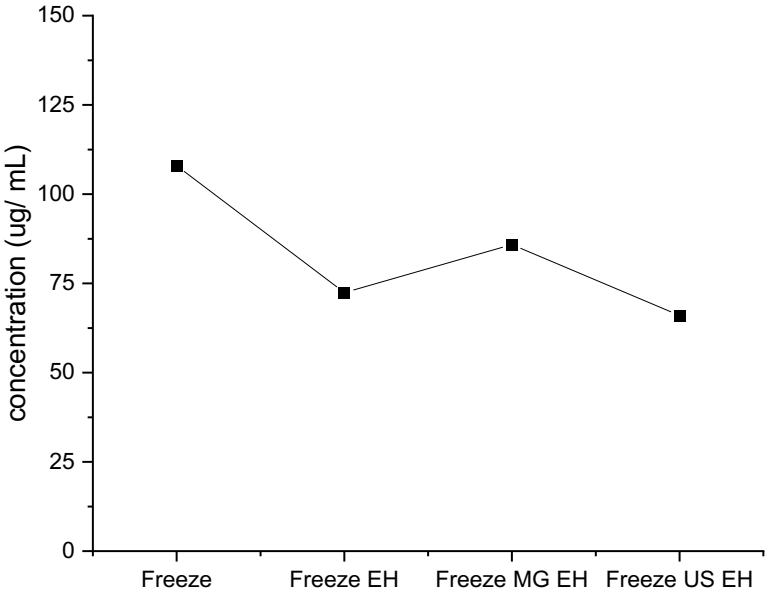

Figure 3-25 Water soluble protein concentration of enzymatically hydrolysed proteins of freeze-dried biomass determined via Bradford Assay compared to the unhydrolyzed freeze dried protein retentate

In comparison to the untreated sample (110 ug/mL) the enzymatically hydrolysed samples (82 ug/mL for Freeze MG EH and 68 ug/mL for Freeze US EH) show a slightly lower response to water soluble proteins. This correlates with the SDS-PAGE results, which show mainly low molecular weight peptides that are not detected by the Bradford assay well or at all. The Freeze MG EH sample, like the high nitrogen percentage (8.8%), shows the highest Bradford response (82 ug/mL) of all the hydrolysed samples. Enzymatically hydrolysed peptides, therefore, have been successfully generated with protein recoveries within the literature standards and generating peptides, which can be explored in various applications.

3.2.5 Foaming and emulsion capabilities of proteins

Foaming and emulsion properties of proteins are of vital importance in selecting potential fields of applications as the properties dictate the usability of the peptides. Foaming and emulsion formation are particularly important for the nutritional industry, where proteins are often added to processed foods as they can stabilise foams and emulsions.[225–227]

3.2.5.1 Foaming stability and capability of proteins

Proteins and peptides are able to thermodynamically stabilise foams by stabilising the air-water interface through formation of an elastic network around the air bubbles.[226,227] The foaming capabilities of all the extracted microalgal proteins were tested and their stability after 10 mins and 2 h were examined (Figure 3-26).

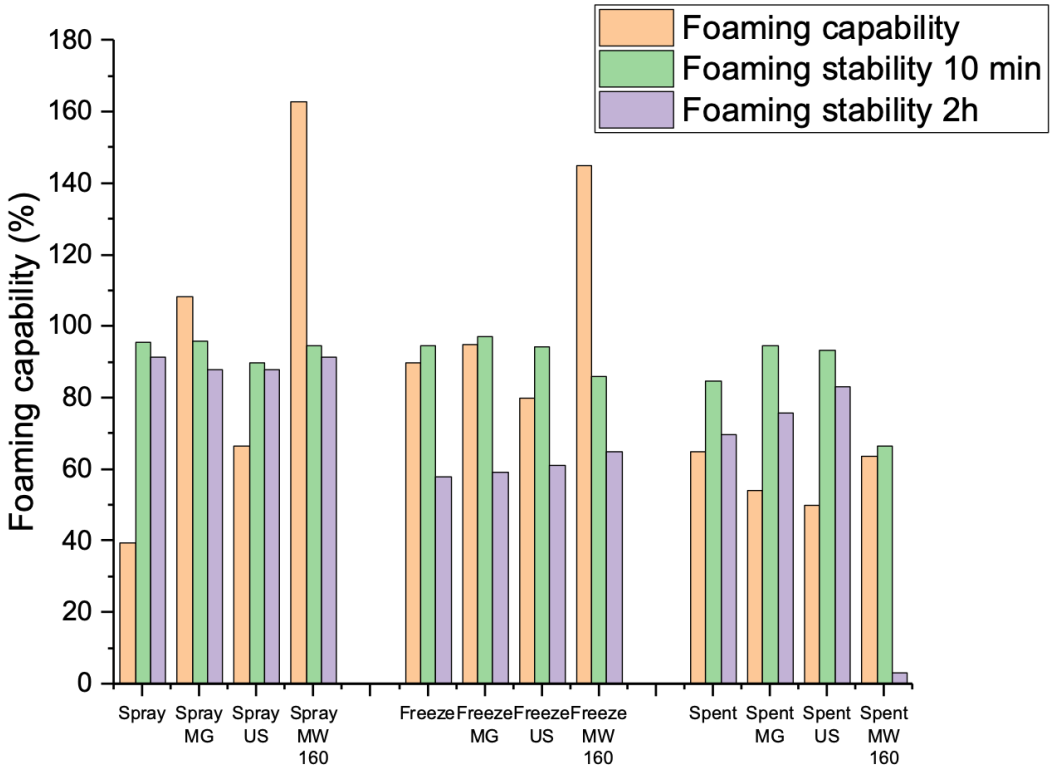

Figure 3-26 Foaming capabilities and stabilities of untreated and pre-treated proteins

Foaming capabilities of the untreated proteins of the three biomass types are the highest for freeze dried microalgae (91%). For freeze dried proteins, values range from 80% for ultrasonicated proteins to 98% for manually treated proteins and even 145% for microwaved proteins. Spent untreated proteins lag slightly while all the spray dried proteins show a very varied response to foaming depending on their pre-treatment with manually ground peptides generally generating the best response when microwaving is not considered. This is in accordance with literature, which also reports hydrolysed peptides able to further stabilise foams and emulsions beyond the capabilities of globular proteins.[225,228,229]

Spray dried proteins generate the most stable foams with foam heights after 2 hours not dropping significantly. It can be noted that the foaming stabilities within spray/ freeze/ spent proteins are very comparable. An exception is the foaming stability of the spent MW160, which drops significantly to 3%, and thus differing drastically from the trends seen with spray dried and freeze dried samples. Similarly, the spray MW160 and freeze MW160 also show considerably higher foaming capabilities (165% for spray MW160, 145% for freeze MW160), while the stability after 10 mins approximately equals the stabilities of the other pre-treated samples from the same ALG01 type.

3.2.5.2 Emulsion stability and capability of proteins

The emulsion capability and stability of the proteins (Figure 3-27) have been determined similarly to the foaming properties however with measurements taken after 2 h and 24 h.

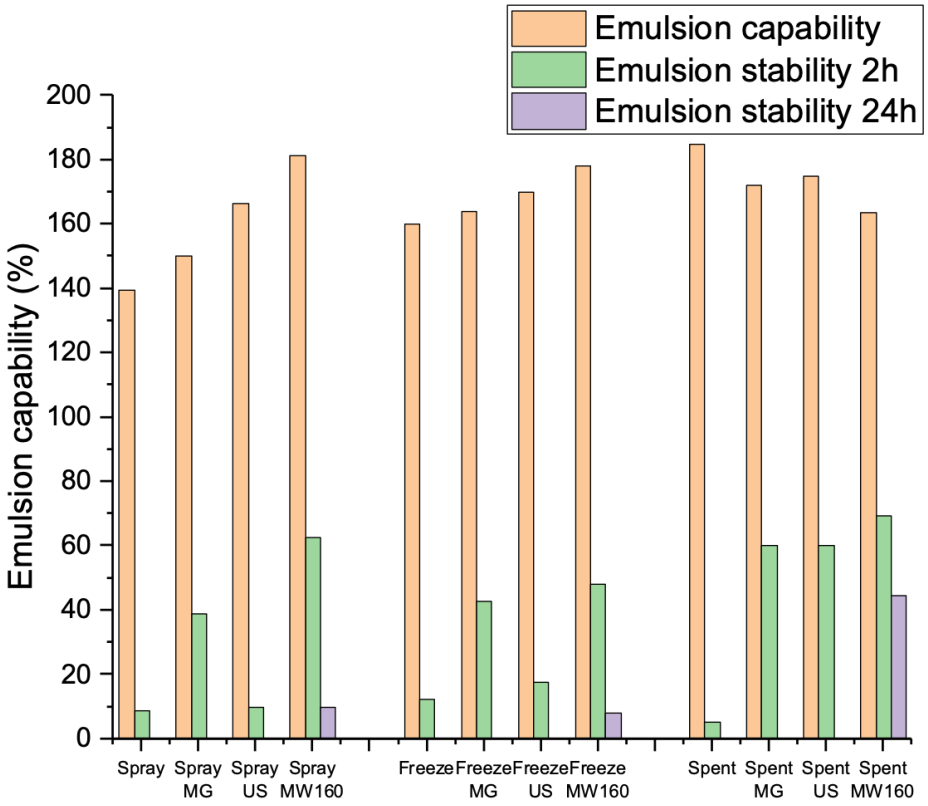

Figure 3-27 Emulsion Capability and stabilities of untreated and pre-treated proteins measured after 2 h and 24 h

Similar to the role of proteins and peptides in improving foaming, their unique properties also lead to them reducing interfacial surface tension between oil and water droplets during an emulsion. The hydrophobic and hydrophilic parts of amino acid side chains aid this phenomenon making peptides and proteins potential emulsifiers.[229,230]

Emulsion capabilities throughout appear to be very similar without any significant discrepancies arising between peptides from different initial biomass types or pre-treatment. Minimum stability values of 140% for spray dried untreated peptides and a maximum of 188% for spent untreated peptides were recorded. Whilst the spray dried (140% to 182%) and freeze dried (160% to 175%) samples showed an increase in emulsion capability in the order: untreated -> MG -> US -> MW160, the spent peptides gave an inverted or reverse trend by decreasing slightly (from 188% to 162%). However, the emulsions did not appear very stable, with a considerable drop of emulsion stability after

only 2 h. After 2 h a peak emulsion stability response for spent MW160 at 70% could be observed, with un-treated spent only recording a 2 h emulsion stability of 5%. After 24 h, most samples did not show any emulsion anymore, apart from the microwaved samples: spray MW160 (9%), freeze MW160 (7%) and spent MW160 (43%). This suggests that short chain peptides generated through microwave treatment produce more stable emulsions after both 10 mins and 24 h than non-microwaved proteins/ peptides. The literature suggests that protein hydrolysates possess higher emulsification properties than fully folded proteins.[229]

3.2.6 Bioactivity testing of peptides

The bioactivity of the different peptides was tested externally by Aelius Biotech (Newcastle, UK). The peptide samples were coded as follows: Enzymatically hydrolysed peptides – EHP; Peptides from spent biomass extracted using microwave-assisted extraction – Spent MW160; Peptides from spent biomass – Spent Un-treated. A summary of the protocols is given in the Appendix in Section A3-1.

The results summarized by Aelius Biotech showed no statistically significant change in cell viability, suggesting that the extracted peptides do not negatively influence the viability of cells, thus making them safe from a toxicological point of view with regards to their impact on cells.[231] Furthermore, experiments on pepsin and trypsin inhibition after raw data analysis revealed, that the Enzymatically Hydrolysed Peptides (EHP) group was the only group significantly different from the control ($P<0.05$) with inhibition of pepsin activity at 53.8%. Similarly, following statistical analysis (ANOVA), the enzymatically hydrolysed peptides group (EHP) was found to be significantly different to the control ($p<0.05$), indicating an inhibition of trypsin of 52%. All other peptides did not show any significant deviation from the control. The results are summarized in Figure 3-28 and Figure 3-29.

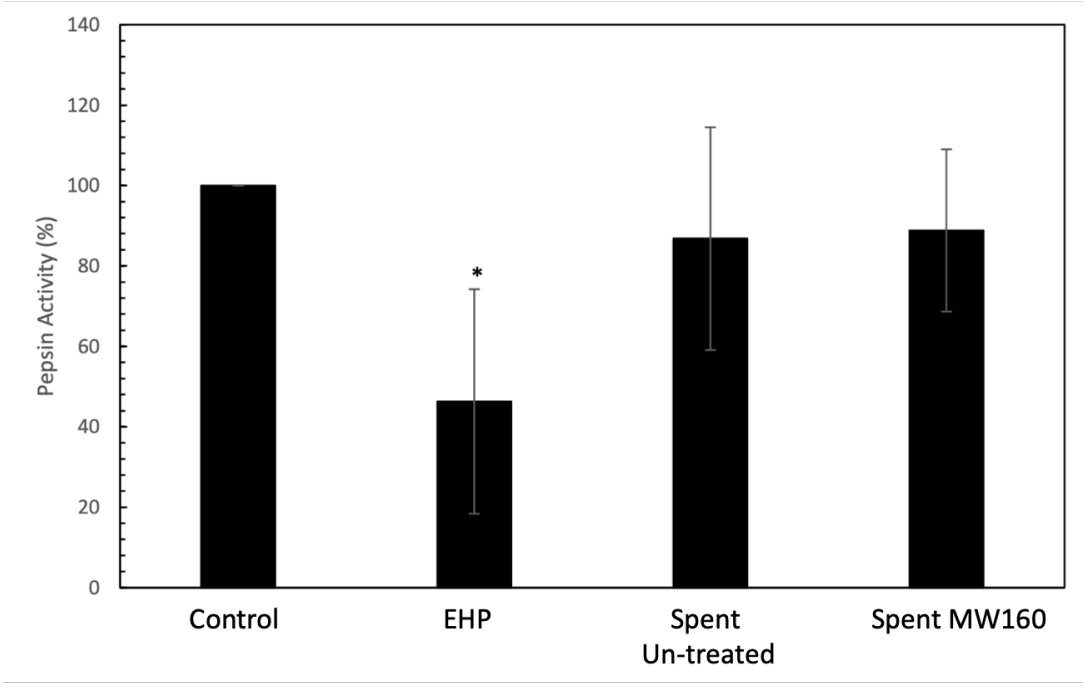

Figure 3-28 *Modulation of pepsin activity (300 µg/ml) in the trinitrobenzenesulfonic acid, n-terminal assay. All samples (control and peptides) were tested at a concentration of 1 mg/ml. Data is shown as average and standard deviation of n=3.*

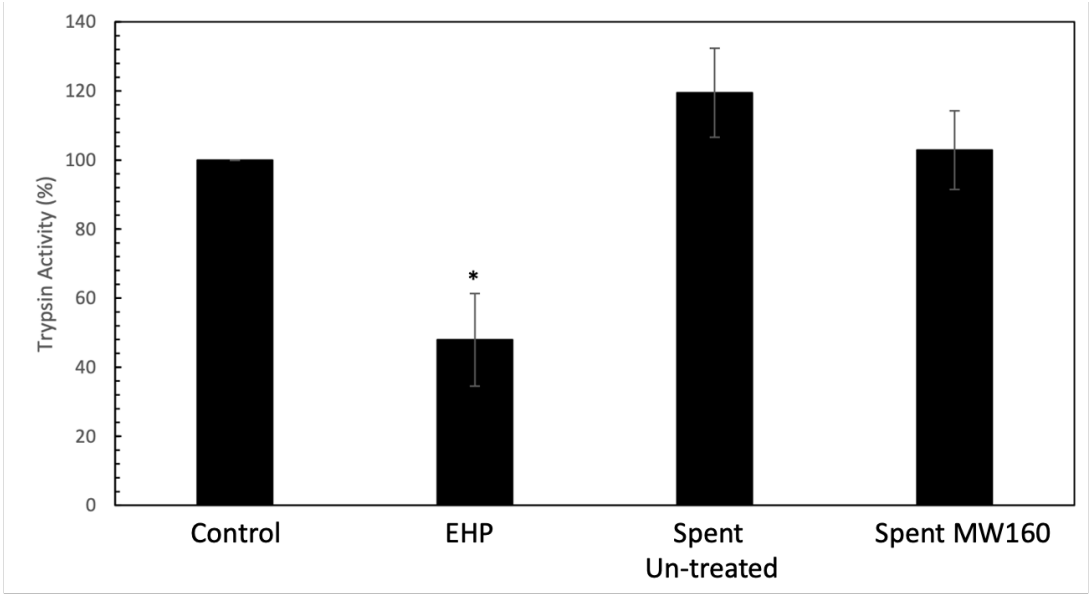

Figure 3-29 *Modulation of trypsin activity (20 µg/ml) in the trinitrobenzenesulfonic acid, n-terminal assay. All samples (control and peptides) were tested at a concentration of 1 mg/ml. Data is shown as average and standard deviation of n=3.*

Results indicate a stark difference between the enzymatically hydrolysed peptides and the other two peptides (Spent MW160 and Spent un-treated) as the EHP is the only peptide sample that inhibits both pepsin and trypsin. Pepsin and trypsin inhibition are classified as reflux aggressors, which can both cause Gastro- Oesphagul Reflux Disease (GORD). Pepsin and trypsin inhibition properties therefore show that the concerning sample can potentially be used to treat this condition and thus be used in a bio-medicinal context.[232] The EHP with pepsin inhibition of 53.8% is of comparable strength to the strongest alginate candidate, which has been shown to inhibit pepsin by 46.1%.[232]

Subsequent analyses on the peptides showed an increase in the levels of anti-inflammatory cytokine IL-10 (with EHP and Spent MW160, Figure 3-30).

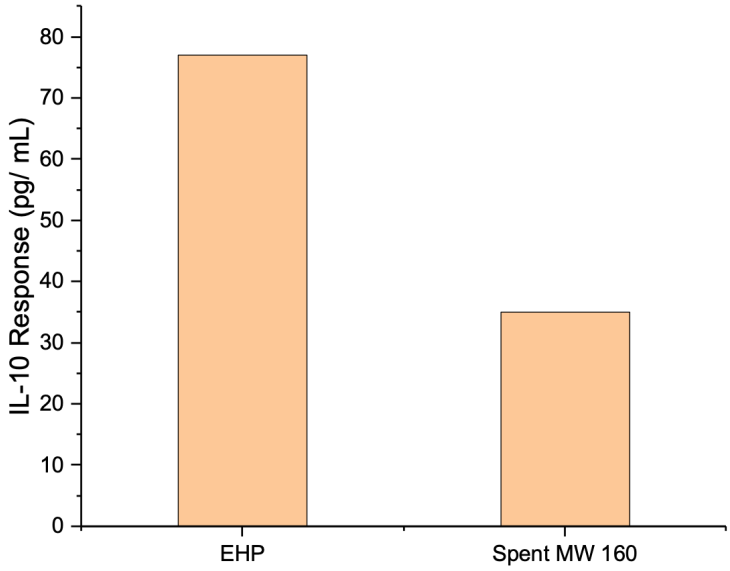

Figure 3-30 Positive response results for both EHP and MAE peptides using IL-10 ELISA

In this set of analysis, the spent un-treated peptides did not show any response. Again, the EHP showed the highest response at 77 pg/ mL with MAE at around half of the response at 35 pg/ mL. Both peptides therefore exhibit anti-inflammatory properties, which can make them suitable candidates to be used in a wide range of applications based on their bioactivity.

3.3 Tandem Production of Defibrillated Celluloses (DFC) and Protein Isolation from Hydrolysates via Acid-free Hydrothermal Microwave Processing and Their Subsequent Characterisation

This section details both the generation of defibrillated cellulose and the protein isolation from hydrolysates via acid-free hydrothermal microwave processing (Figure 3-31) from spray dried and spent ALG01. Parts of this section have been published in peer reviewed journals:

Zitzmann, F.L.; Ward, E.; Meng, X.; Matharu, A.S. Microwave-Assisted Defibrillation of Microalgae. *Molecules* **2021**, *26*, 4972. https://doi.org/10.3390/molecules26164972

Zitzmann, F.L.; Ward, E.; Matharu, A.S. Use of Carbotrace 480 as a Probe for Cellulose and Hydrogel Formation from Defibrillated Microalgae. *Gels* **2022**, *8*, 383.

https://doi.org/10.3390/gels8060383

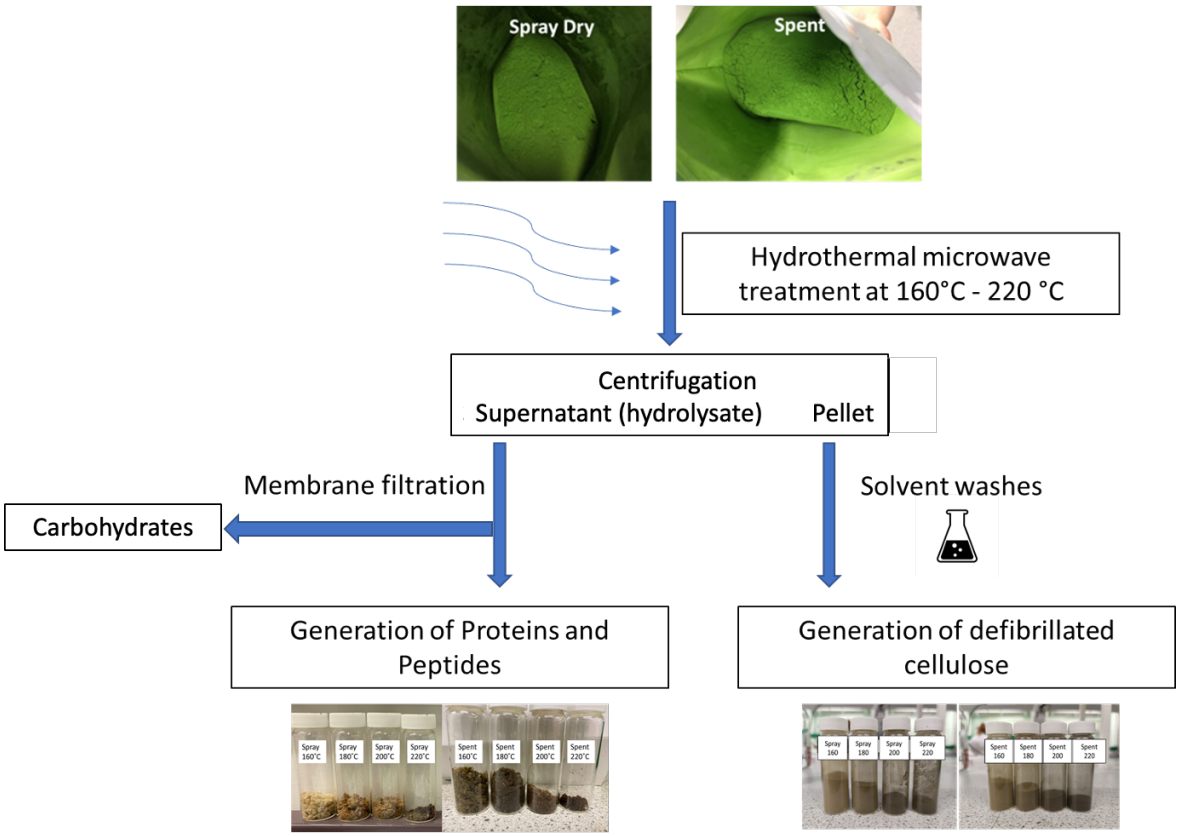

Figure 3-31 Flowchart of Hydrothermal Microwave Process to generate both proteins and defibrillated cellulose

3.3.1 Production of Defibrillated Celluloses via hydrothermal Microwave Processing

3.3.1.1 Defibrillated cellulose yields and carbohydrate analysis

Defibrillated cellulose from both untreated spray dried microalgal biomass as well as spent biomass was successfully produced via hydrothermal microwave processing at various temperatures (160 – 220°C). As shown in Figure 3-32, an increased brown colourisation was observed with increasing temperature which stems from the Maillard reaction (Figure 3-33) between carbohydrates and residual proteins at high temperatures. [233,234]

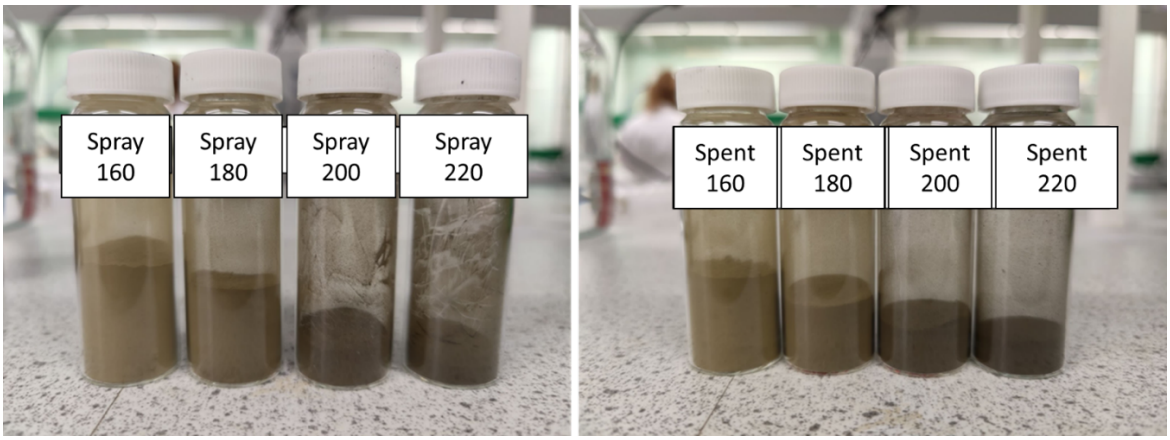

Figure 3-32 Appearance of defibrillated celluloses at various temperatures. Left: spray dried biomass. Right: spent biomass

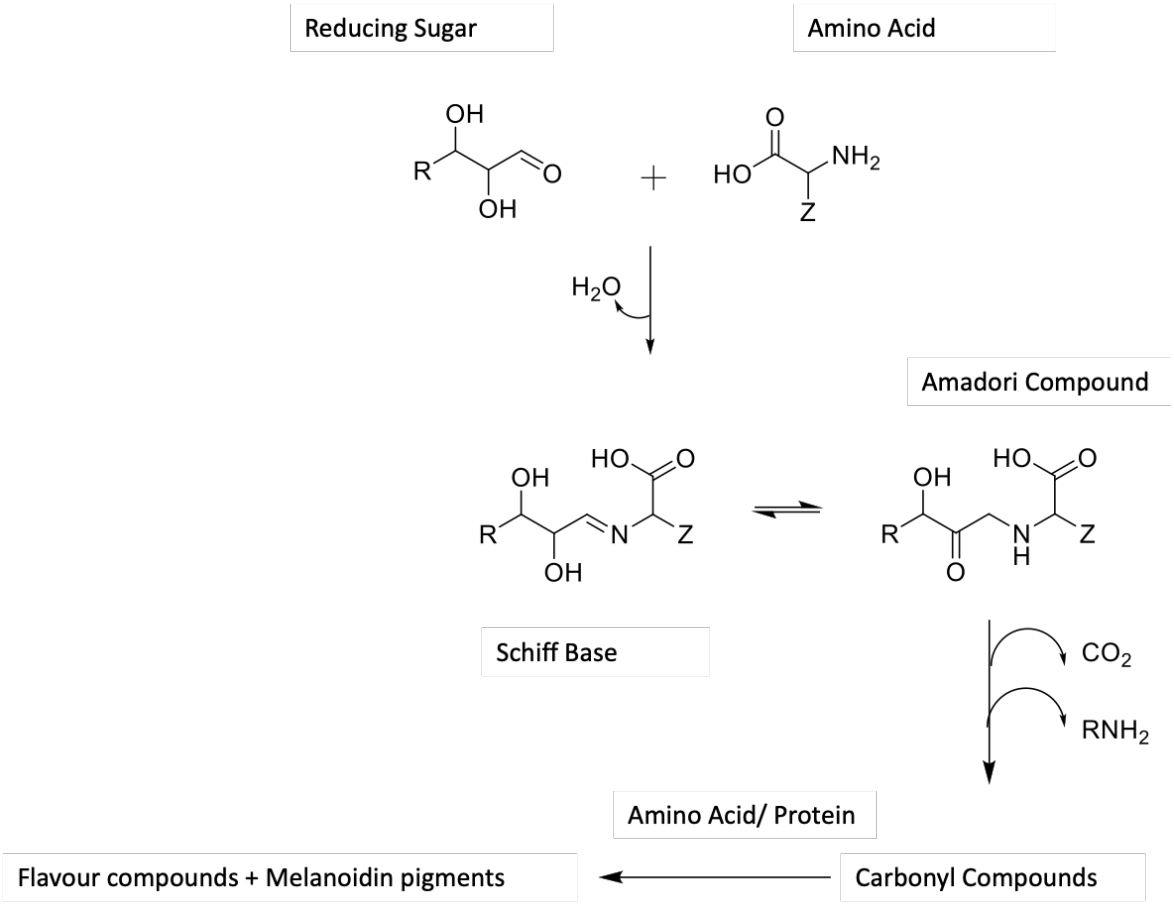

Figure 3-33 Maillard reaction

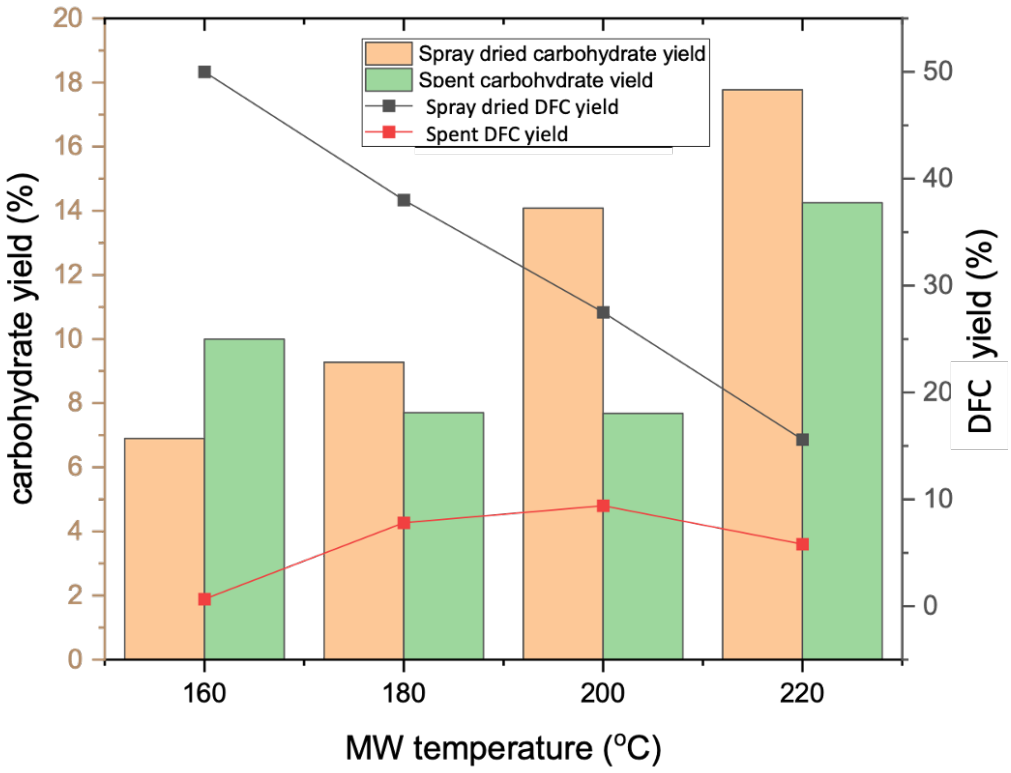

Figure 3-34 DFC yield and carbohydrate yields of spray dried and spent microalgal biomass at different microwave temperatures

Figure 3-34 depicts the trends in yields of both DFC and carbohydrates (isolated by tangential ultrafiltration along with proteins). The yields for spray dried DFCs constantly decrease by approximately 1 g (or 10%) per every 20 K increase, *i.e.*, 51% to 15%, reflecting the effect of microwave-induced degradation and removal of labile microalgal cell components such as lipids, pigments, hemicellulose and proteins. Due to the rigidity of the cell wall caused by the algaenan layer (see later, Section 3.3.2) considerable energy input is required in order to achieve the desired formation of DFC. [182,184,235]

Analogous with the degradation and defibrillation of cellulose, the carbohydrate yield for the spray dried biomass similarly increases as expected in linear fashion from 7% to 18%.[174,175,179] Figure 3-35 shows the individual carbohydrate profile obtained from HPLC analysis.

The DFC generated from spent ALG01, however, behaves very differently with respect to DFC from spray dried ALG01. Spent ALG01 yields are considerably lower than for spray dried ALG01 and even the highest spent DFC yield (9.4% for Spent DFC 200) does not reach the levels of the lowest spray dried ALG01 yields, *i.e*., 15.5% for Spray DFC 220. In addition, the trend of spray dried DFC (lower yield with increasing temperature) seems to be reversed for the spent DFC as the highest yields have been recorded for 200°C (9.4%) with the lowest yields at the lowest (0.64% at 160°C) and highest temperature (5.8% at 220°C). This could be because the spent ALG01 has already undergone industrial lipid extraction and this pre-treatment has changed the carbohydrate structure in such a way that most carbohydrates have already been released earlier. This is in connection with findings in Figure 3-3 which showed a slightly lower carbohydrate content of spent ALG01 compared to spray dried ALG01. The spray dried ALG01 also releases more carbohydrates than the spent ALG01 at the higher temperatures suggesting that the latter releases most of its carbohydrates at lower temperatures due to the already ruptured and altered cell walls.

The carbohydrate profile obtained upon ultrafiltration that was analysed by HPLC is shown in Figure 3-35. Glucose is the most concentrated sugar in the hydrolysate, which is an integral building block of the algal cell wall, along xylose and mannitol which both appear in the hydrolysate but at lower concentrations and with xylose only appearing in the spray dried hydrolysate.[236–238] These cell wall polysaccharides are subsequently broken down increasingly with higher microwave temperatures as evidenced in Figure 3-34. In contrast to glucose and mannitol, xylose seems to remain fairly constant and even increases up to 200°C which makes its formation plausible through the conversion of hemicellulose into xylose which results in this increase. The aforementioned apparent lack of xylose in the spent biomass can be explained through the industrial lipid extraction having already impacted hemicellulose composition in spent biomass thus reducing the amount of xylose in the spectrum, which would also account for the much lower carbohydrate yields that spent hydrolysates show.

The concentration of lactic acid and acetic acid (for spent biomass) keeps increasing with increasing microwave temperature, indicating increased further degradation of carbohydrates. Small organic acids, in this case mainly lactic acid and acetic acid, indicate the breakdown of mainly amorphous cellulose and hemicellulose as crystalline cellulose

does not tend to participate in this breakdown at temperatures used in this study.[171,174,175,179] The high value seen for acetic acid from spent biomass at 220°C is surprising, as the carbohydrates from spray dried ALG01 do not show acetic acid at all (apart from Spray DFC 160) and indicates very accelerated decomposition reactions at this temperature. Its lack in spray dried hydrolysates might be related to the cell wall components in spent biomass being much more labile and more prone to decomposition due to having already been primed during the industrial extraction. Interestingly, the breakdown of glucose seems to steadily decrease or remain stable with increasing temperatures indicating that the structure of the cellulosic matter must have changed in a way that slowed down the conventional amorphous cellulose breakdown.

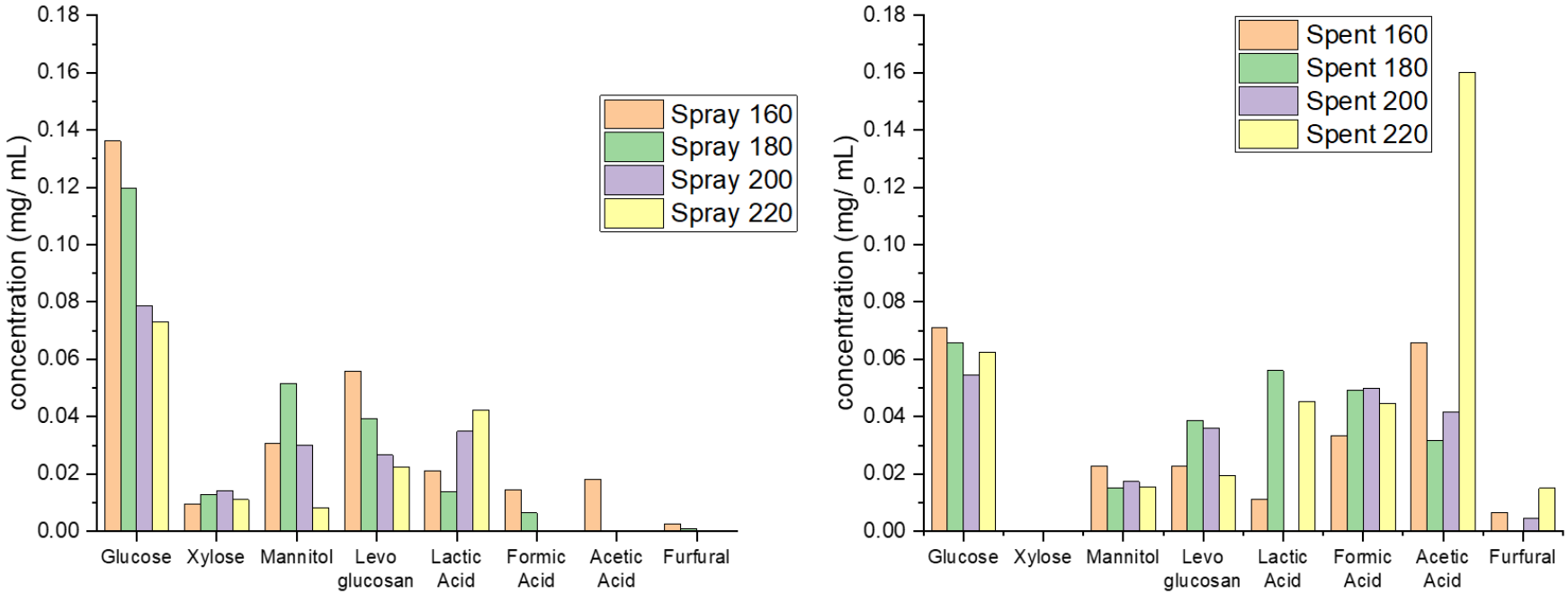

Figure 3-35 Carbohydrate profile obtained from HPLC for spray dried biomass (left) and spent biomass (right)

3.3.1.2 TGA and DTG analysis

Thermogravimetric analysis results for both the spray dried and spent DFC are shown as the first derivative (differential thermogravimetry, DTG) in Figure 3-36. From the DTG traces more information about the nature of the DFC with increasing microwave temperatures can be extracted. There are two major decomposition events: i) volatiles and moisture loss accounting for 4%-8% of mass with a decomposition temperature Td = 60°C. ii) cellulose decomposition accounting for 55%-65% of mass with Td = 310°C. There is a noticeable shift to be made out for the highest microwave temperature run at 220°C for both methods with maximum cellulose decomposition shifted approximately 30°C higher than for the other samples as indicated by the black arrow. The heat-treatment induced restructuration of cellulose towards more crystalline structures is being reflected in this shift. As only the highest temperatures appear to show this behaviour it is assumed that microalgal cellulose requires very high temperatures for this structural change to occur.

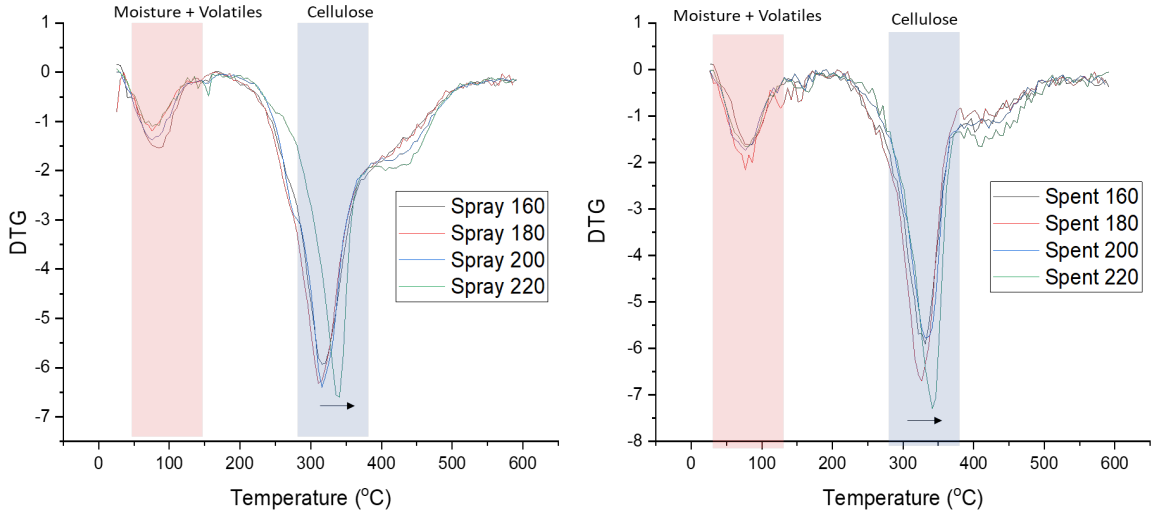

Figure 3-36 DTG thermograms of spray dried and spent DFC

3.3.1.3 X-Ray Powder Diffraction Analysis and Crystallinity Index

The XRD patterns of both the spray dried and spent biomass are shown in Figure 3-37. The diffraction patterns of crystalline cellulose are marked in black numbers arising at 2θ = 16.5° and 22.5°.[239–241] With higher microwave temperatures, the intensity of the peak at 2θ = 16.5° increases indicating a higher crystallinity which is confirmed by the crystallinity index derived from the XRD patterns shown in Figure 3-39. Interestingly, the traces for the spray dried biomass at 200°C and 220°C and the spent biomass at 220°C follow a slightly

different pattern than the lower temperatures indicating a perceivable shift in cellulosic structure towards a more crystalline structure which is in line with DTG findings portrayed in Figure 3-36.

The XRD traces of the spent biomass DFC interestingly are much more similar to each other than the spray dried spectra and also show a high resemblance to the high temperature spray dried traces. This suggests that the nature of the cellulose in the spent DFC correlates very closely with the spray dried DFC at high temperatures, again explained through the fact that the previous industrial treatment has made it easier for carbohydrates to be defibrillated. The 110 cellulose plane in the spent DFC spectra is also much more prominent than in the spray dried DFC spectra.

Additional peaks that can be found at 2θ = 15.1°, 24.4°, and 30° might indicate the presence of insoluble calcium salts, most notably calcium oxalate (CaC_2O_4) which can be present in microalgal cell structures, especially the vacuole and the cell wall.[242,243] There does not seem to be any noticeable change in intensity for these calcium salt peaks, suggesting they are a constant component of microalgal DFC regardless of the temperature of the microwave treatment.

Compared to the spectra of pure cellulose and xylan (Figure 3-38), it can be seen that the DFCs comprise biopolymers that are neither xylan nor cellulose-like. The algaenan layer may be contributing to the diffraction patterns (see later, for example, Figure 3-40).

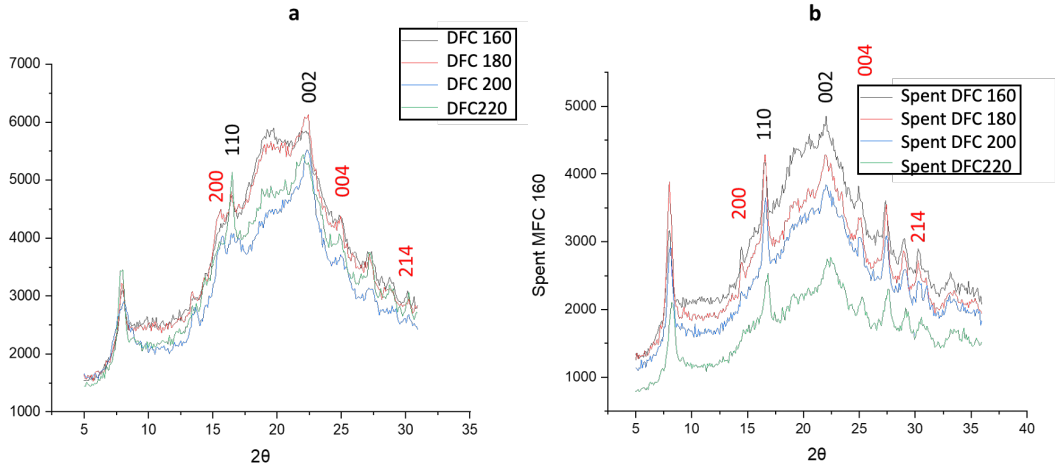

Figure 3-37 X-Ray diffractograms of (a) spray dried DFC and (b) spent DFC. Black numbers indicate cellulose planes, red numbers indicate CaC_2O_4 planes

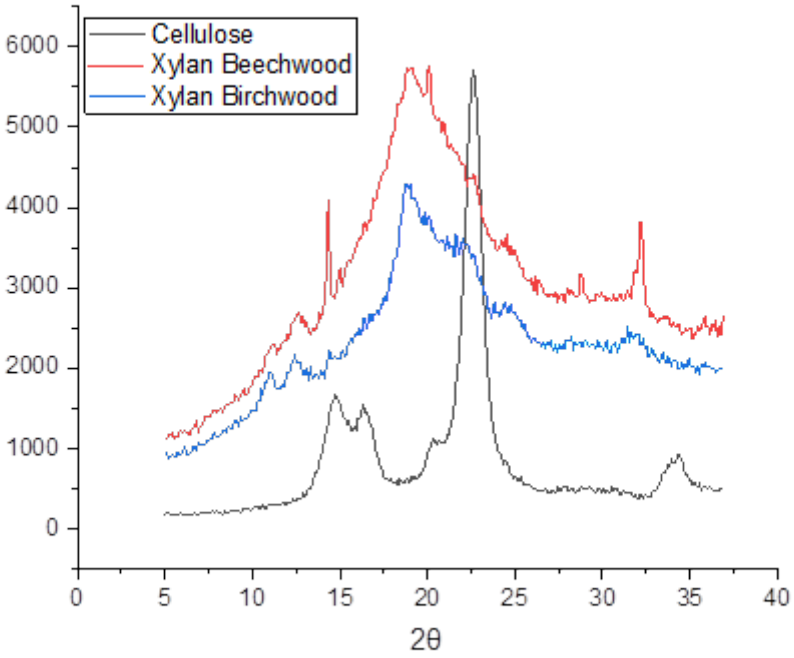

Figure 3-38 XRD spectra of pure cellulose as well as Xylan obtained from two different sources

The crystallinity index (CrI) derived from the XRD traces according to the Segal method reveals a steady increase in the crystallinity index up to 200°C peaking at this temperature for spray dried DFC (27.3% for spray dried DFC 200). Crystallinity values increase with temperature due to the gradual removal of amorphous impurities from the biomass such as starch and hemicellulose which will be released from the cellulose matrix.

While the CrI for spray dried DFC drops at the highest temperature (22% for Spray DFC 220) the spent CrI keep increasing with increasing temperature to a maximum of 32% for Spent DFC 220. In addition to this, defibrillated cellulose derived from spent biomass shows consistently higher crystallinities than the cellulose samples obtained from spray dried biomass (values of the 200 samples being almost identical). The overall difference between CrI of spray and spent samples can be attributed to the fact that the previous industrial extraction process has left the spent biomass fewer labile cell wall components which are still present in the spray dried biomass, thus lowering the yield while at the same time increasing the overall crystallinity as the 'contaminants' are more fully removed. The largest difference in CrI at the same temperatures reaches its largest value at 160°C with

Δ = 11.2%. The role of residual algaenan within the samples also could influence the crystallinity differences, as spent biomass contains fewer algaenan than spray dried biomass which in turn could lead to a higher crystallinity index. The analysis and isolation of residual algaenan from the defibrillated cellulose samples is detailed in section 3.3.2.

Compared to previous studies on pea waste, almond hull and cassava peel, which also contain lignin in addition to cellulose and hemicellulose, the CrI values of pea waste defibrillated celluloses seem to be comparable to those of spray dried defibrillated cellulose with pea waste crystallinities ranging from around 22% to 26%.[174,179,244] Cassava peel defibrillated celluloses, however, show crystallinities of 41.3% at 170°C and up to 63.1% at 220°C, considerably higher even than the spent samples. Almond hull shows lower but still high CrI of 42.7% at 170°C and 54.4% at 220°C. All these lignocellulosic biomass types therefore contain very highly crystalline cellulose which in the microalgal samples does not seem to be the case to as such a high degree.

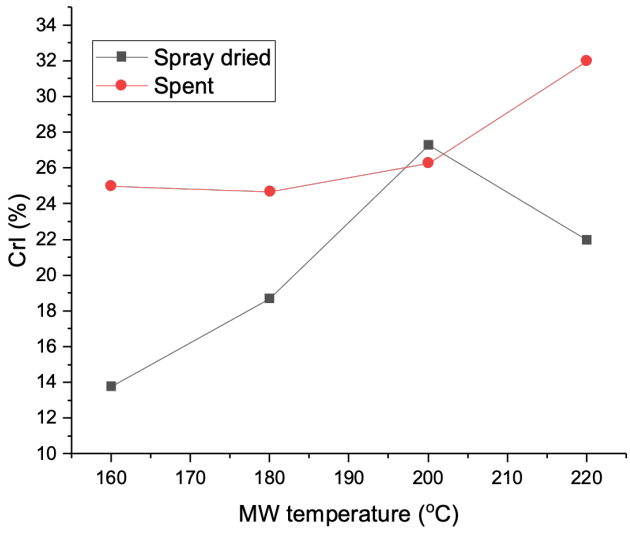

Figure 3-39 *Crystallinity index of DFC from spray dried and spent biomass at different MW temperatures calculated from XRD traces in Figure 3-37 via Segal's method*

3.3.1.4 13C CPMAS solid state NMR and TEM imaging

The stacked 13C CPMAS spectra for both spray and spent DFC are shown in Figure 3-40. The signal appearing at 175 ppm corresponds to the carbonyl carbon of carbonyl and carboxylic acid groups cognisant of hemicellulosic matter and/or polyunsaturated fatty acids in microalgal cell walls.[245,246] The signal at 130 ppm indicates the possible presence of double-bonded carbons, which may correspond to residual EPA or other polyunsaturated fatty acids. It could also indicate double bonds within the algaenan structure, which is detailed further in section 3.3.2. The intensity of this signal decreases with increasing microwave temperature suggesting the breakdown/removal of these lipids in the final DFC. Furthermore, potentially related to lipids is the strong methylene (-CH_2-) signal appearing at 32 ppm which also consistently decreases in intensity with increasing microwave temperature. Similar to the 130 ppm signal, it is more likely its assignment tends towards algaenan. The carbon signals for cellulose appear in the region 120 – 60 ppm and are assigned in the spectrum to their corresponding position in the cellulose chain (C2 – C6).[245,246] It is seen that these distinct cellulose resonances are more intense in the DFCs obtained from spent biomass suggesting a higher percentage of cellulose in the final DFC compared to the DFC from spray dried biomass due to reasons discussed previously. These signals are confirmed in Figure 3-40 where the NMR spectra of both pure cellulose and xylan are displayed on top. Due to the NMR spectra of both cellulose and xylan showing peaks in similar regions it is very difficult to differentiate between the two in the DFC spectra as they are much less clean and sharp than their pure counterparts.

Definite assignment and changes in the amorphous/crystalline structure are harder to observe due to the broad signals found in this region arising from residual amorphous regions (84 ppm and 62 ppm for surface/ amorphous cellulose respectively) and crystalline cellulose (89 ppm and 65 ppm respectively).[247,248] However, similarly to previous findings the increasing microwave temperature results in increased crystallinity evidenced by the presence of peaks at 65 ppm which gain sharpness as the temperature increases. Characteristic amorphous signals at 84 ppm and 62 ppm decrease slightly which is mirroring the CrI displayed in Figure 3-39 (displayed by the arrows in the solid-state NMR spectrum). Moreover, the sharpness of the double signal at 77-74 ppm reaches its maximum at 200^{o}C before becoming broader and less defined again at the maximum temperature which again mirrors the drop in CrI and loss of crystalline structures.

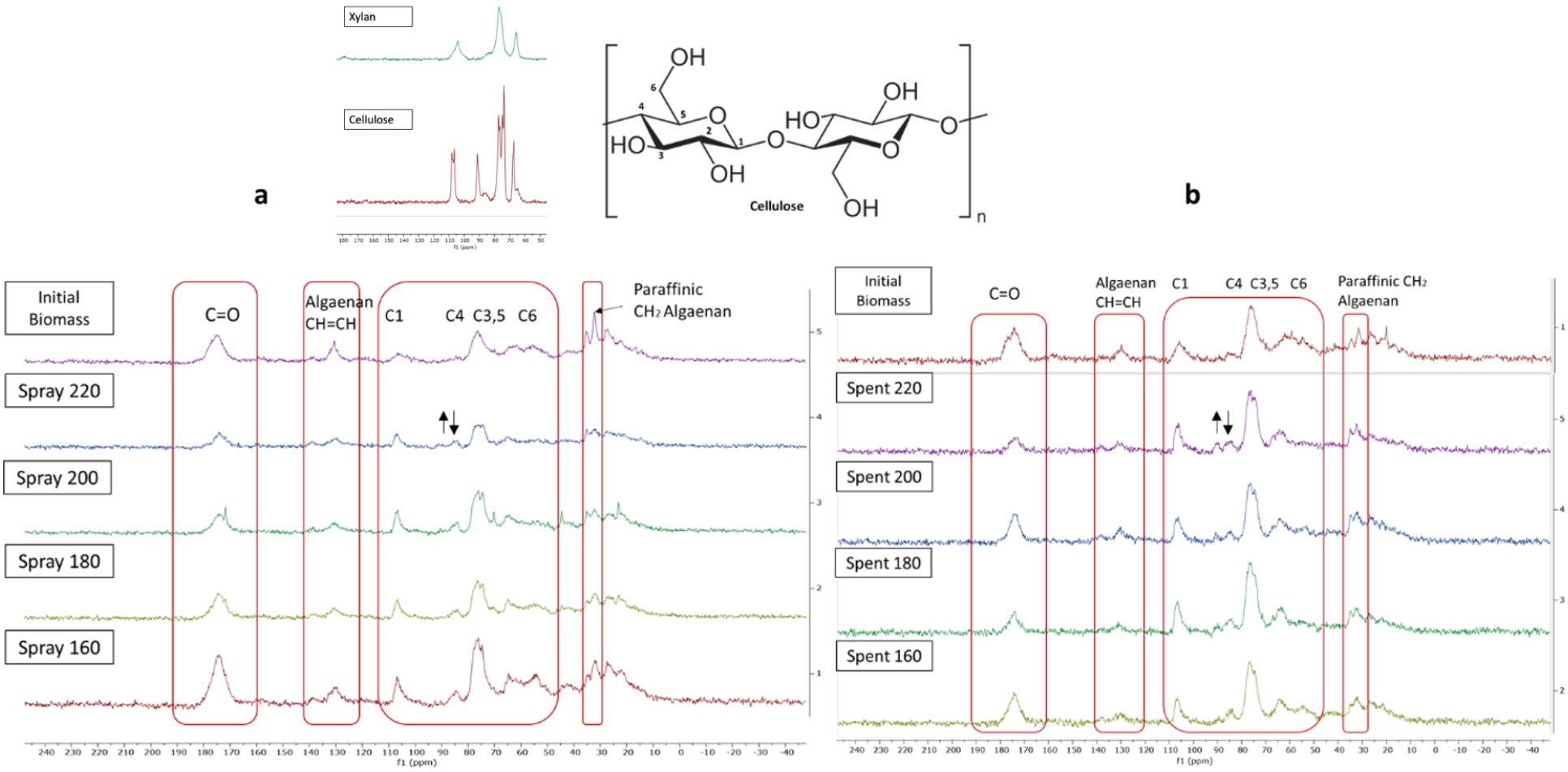

Figure 3-40 Solid state 13C CPMAS NMR spectra of (a) spray dried defibrillated cellulose and (b) spent defibrillated cellulose

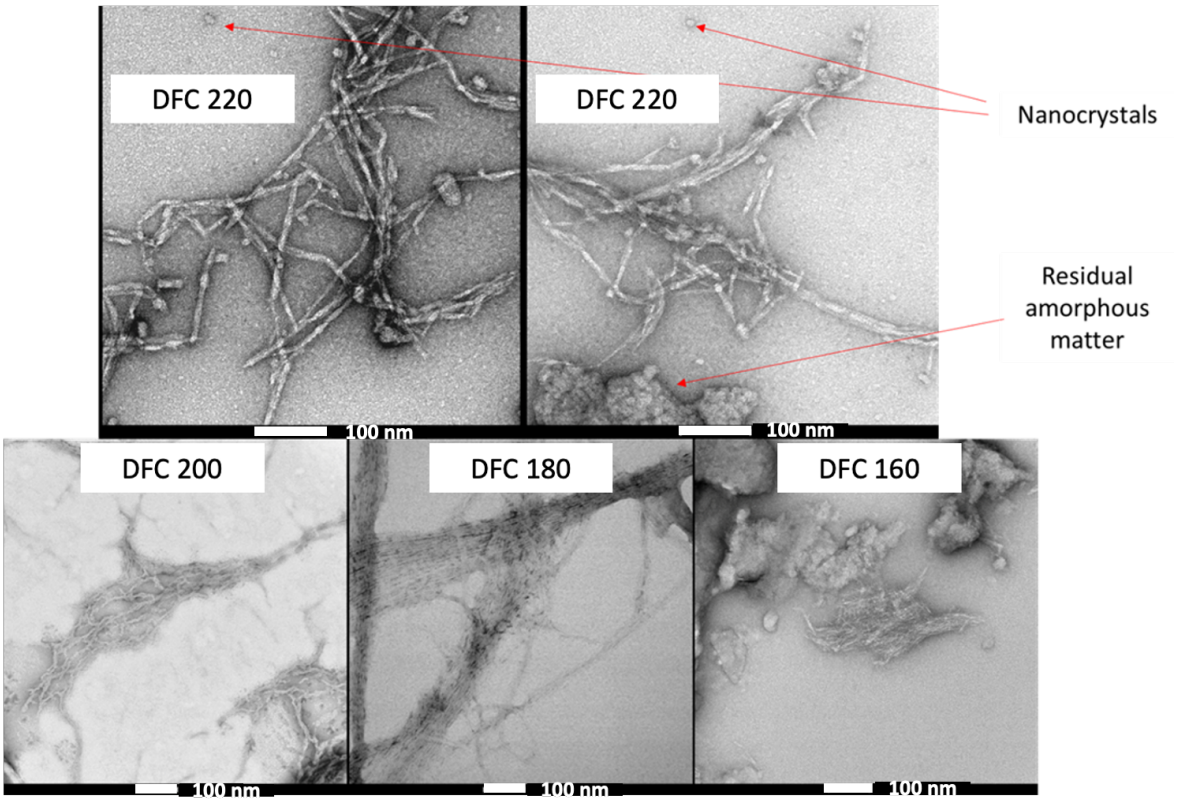

Figure 3-41 TEM images of DFC samples at different temperatures as labelled

TEM (Figure 3-41) gave clear indication of the defibrillation of cellulose to afford fibres and potential crystals. The width of the cellulose fibrils decreased from around 20–25 nm for the 160°C and 180°C samples to 7–8 nm for 200 °C, reaching a minimum width of 6 nm width at 220 °C, putting the fibrils into micro-fibrillated territory. Furthermore, the very linear strand arrangement of the cellulose fibres, which can be seen very well in the 180 °C sample, is noticeably broken and defibrillated at the highest microwave temperature (220 °C). At the highest temperature (220 °C), fraying of the fibres was noticed to reveal the onset of nanocrystals. The TEM images correlate well with the CrI discussed earlier. The 180°C sample is highly ordered whilst the 220 °C sample is highly disordered. The dark grey areas which can be seen around the cellulose fibres particularly at 160°C but also still at 220°C could either refer to residual amorphous matter or the presence of algaenan.

3.3.1.5 Analysis of DFC samples by using Carbotrace 480

The Carbotrace molecules are commercial fluorescent optotracers, which specifically bind to the glycosidic linkages in cellulose, and thus, are able to visually map cellulose content using confocal laser microscopy.[249–251] Carbotrace optotracer molecules have previously been used to identify cellulose in plant cells for mapping cellulosic nanofibrils in microfluidic devices and anatomical mapping in plant cells.[249,250,252,253] However, this thesis reports the first use of Carbotrace to analyse defibrillated cellulose obtained from microalgae, which were used for the formation of hydrogels.

Carbotrace 480 (CT 480) was chosen to be the ideal CT molecule because its emission maxima do not interfere with the autofluorescence of the DFC samples. This allows for good resolution of the images and a clear designation of cellulose with respect to other parts of the DFC that do not bind to Carbotrace 480.

Reference spectra were generated of ALG01 autofluorescence, only CT480 as well as CT480 mixed with pure cellulose. These were applied to all later samples for unmixing and clear peak referencing. The resulting spectra were compared to Ebba Biotech's literature reference spectra (Figure 3-42).

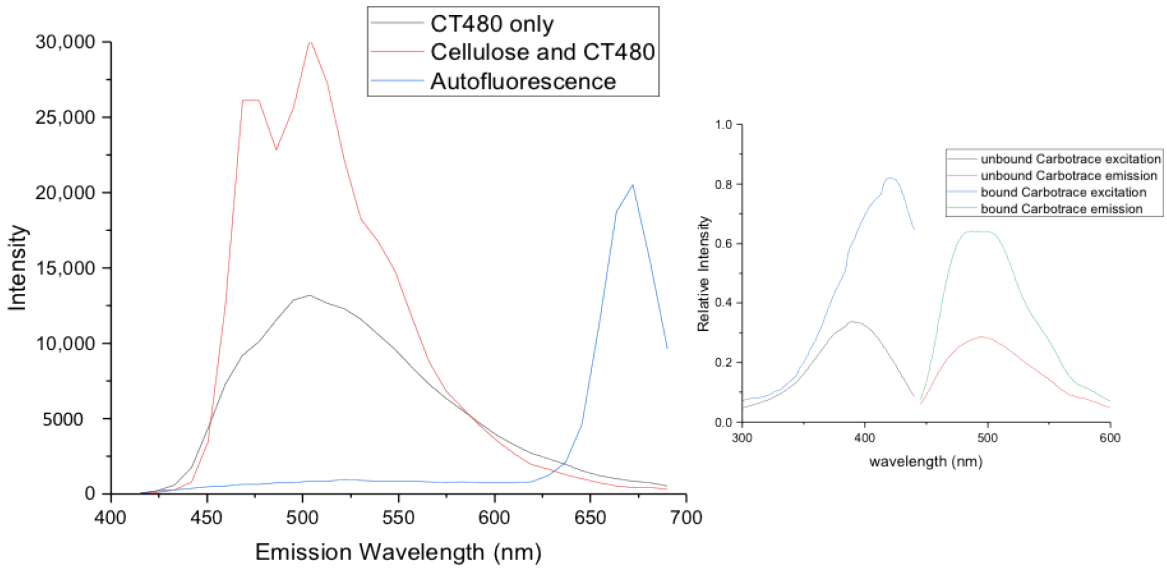

Figure 3-42 Confocal Laser Microscopy emission spectra of unbound CT480, bound CT480 to pure cellulose, DFC autofluorescence and their comparison to the literature reference spectra (dotted line – unbound Carbotrace, straight line – bound Carbotrace)

The obtained emission spectra correlated well with the literature spectra with emission maxima in the region of 480 nm as well as the perceived shift to the left upon Carbotrace binding to cellulose. Also, with the autofluorescence peaking at around 670 nm and no emission appearing in the region where Carbotrace emits, there is a very nice separation between the two allowing for confident de-mixing of the channels of the subsequent DFC samples.

In order to confirm that the CT480 binds to cellulose preferentially and not xylan, both carbohydrates were mixed in their pure form with CT480. Figure 3-43 shows that pure cellulose manifests a very bright response to the CT binding, whereas the xylan stays almost exclusively black (dark), confirming that the Carbotrace indeed binds to cellulose only and not to xylan.

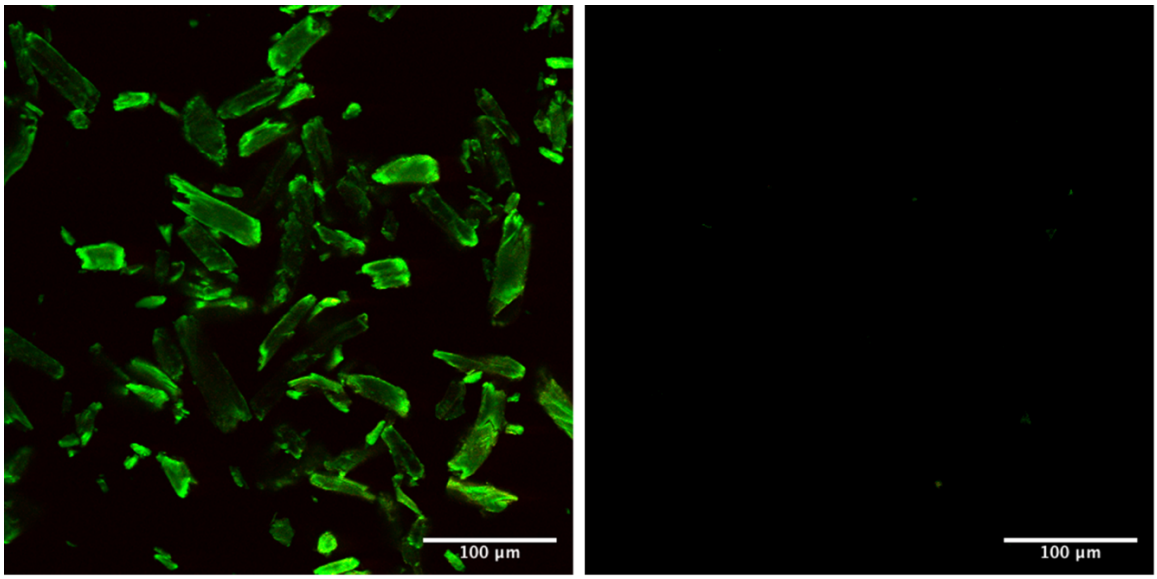

Figure 3-43 Laser Confocal Microscopy images of CT480 mixed with pure cellulose (left) and pure xylan (right) with the exact same instrument settings

Furthermore, the individual crystals of cellulose can be made out very well under this magnification and with this level of Carbotrace applied to the sample.

In order to further ensure that the emission reference giving rise to the green colour only refers to the CT480 bound to cellulose, the spray dried DFC 160 was run without any Carbotrace to confirm the autofluorescence as the only component picked up by the microscope (Figure 3-44).

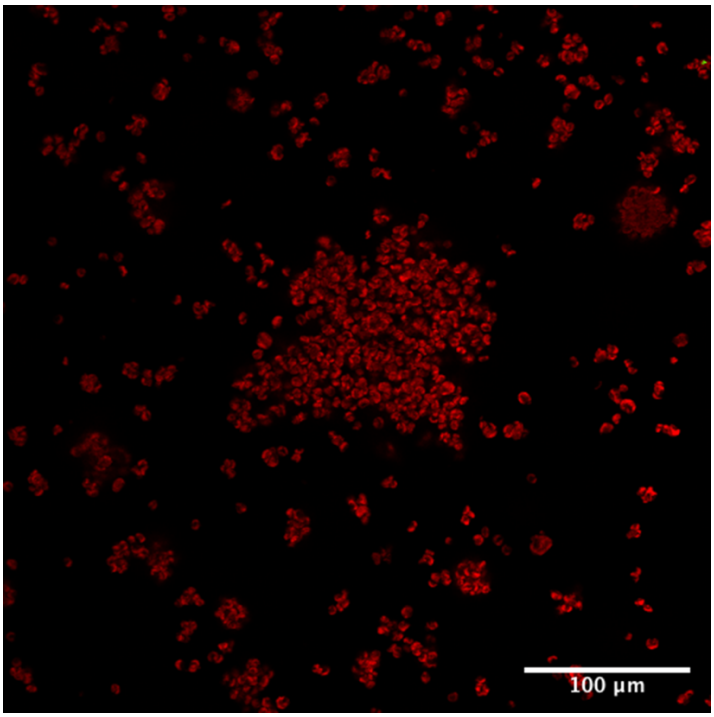

Figure 3-44 Laser Confocal Microscopy Image of unstained Spray DFC 160

The pure red colour channel obtained from this picture was used to generate the autofluorescence emission spectrum used as a reference for all later DFC samples to de-mix cellulose bound to Carbotrace and autofluorescence of all the rest of the samples.

In order to look at the initial untreated biomass and their differences in cellulose distribution across the microalgae, Figure 3-45 shows both the spray dried and spent biomass mixed with CT480.

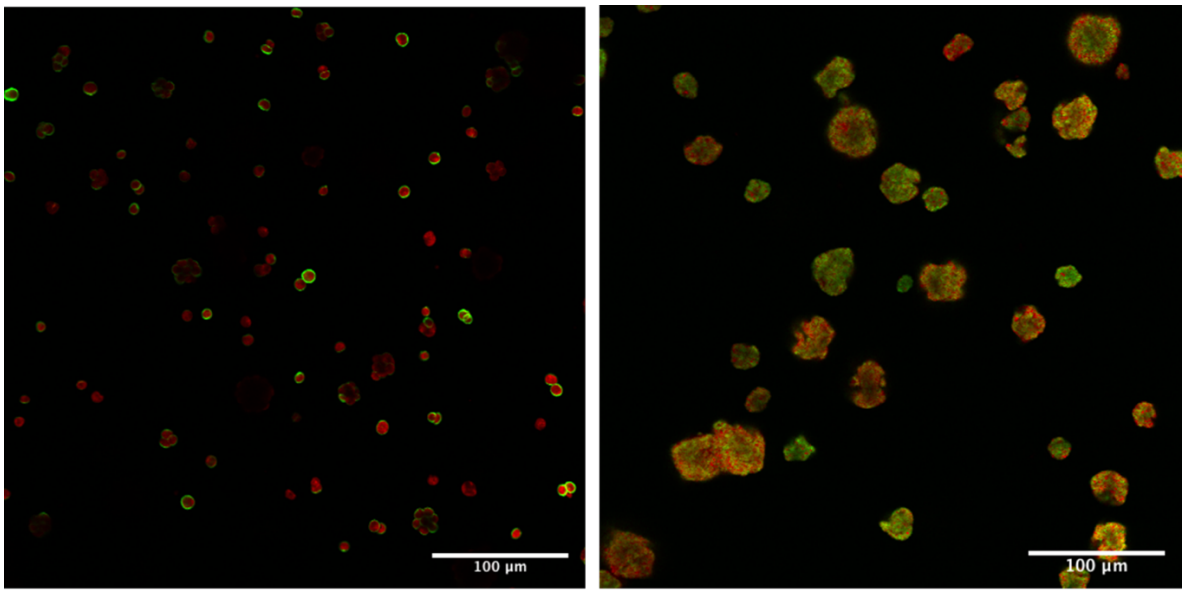

Figure 3-45 Confocal Laser Microscopy image of initial spray and spent biomass mixed with Carbotrace 480

The differences between the initial spray dried and spent biomass can be seen very clearly in these images with the spray dried biomass showing an array of single microalgal cells each with a ring of cellulose encapsulating the cells, which is in line with the basic structure of microalgal cells which sees a cell wall containing cellulose wrapped around the inner cell. Furthermore, the Carbotrace very nicely binds to the cells and shows the cell wall in each of them; for better clarity the cellulose-only channel is displayed in Figure 3-46.

On the other hand, the spent biomass shows a much more disrupted profile with no individual circular cells that can be made out anymore but rather an array of smudged and smashed cells with irregular shapes and a more even distribution of cellulose across the whole cell, indicating that the industrial process has indeed destroyed and ruptured the cells and thus distributing cellulose and cell wall material across the whole profile. This is in line with previous findings that suggest an ease of extraction from spent biomass precisely due to the factors that the image shows with a completely disrupted cell.

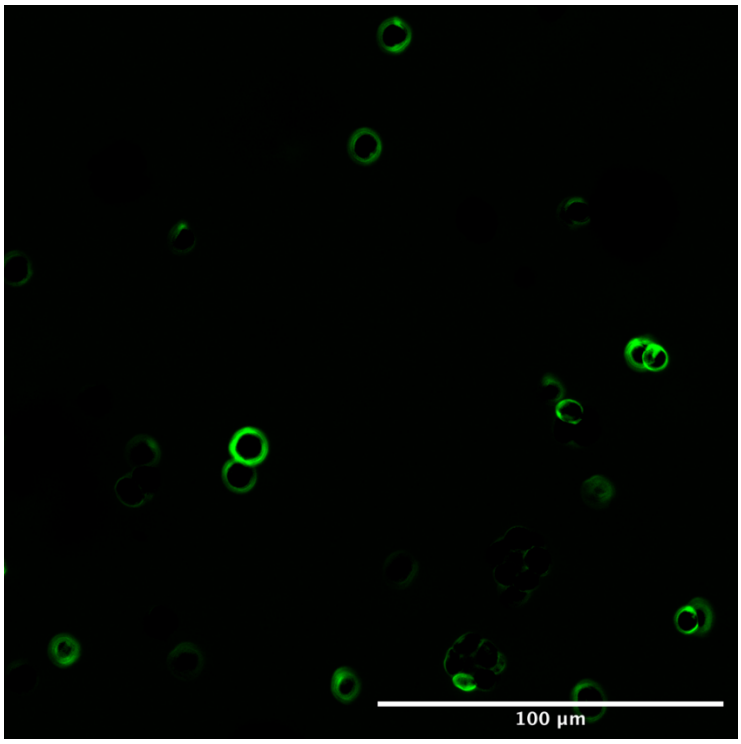

Figure 3-46 Laser Confocal Microscopy Image of the cellulose-only channel with CT480 of initial spray dried biomass

In order to apply the Carbotrace technology to the DFC samples and to use a visual tool that can directly identify and spatially show the distribution of cellulose, all the eight DFC samples were mixed with the Carbotrace 480 with the results displayed in Figure 3-47.

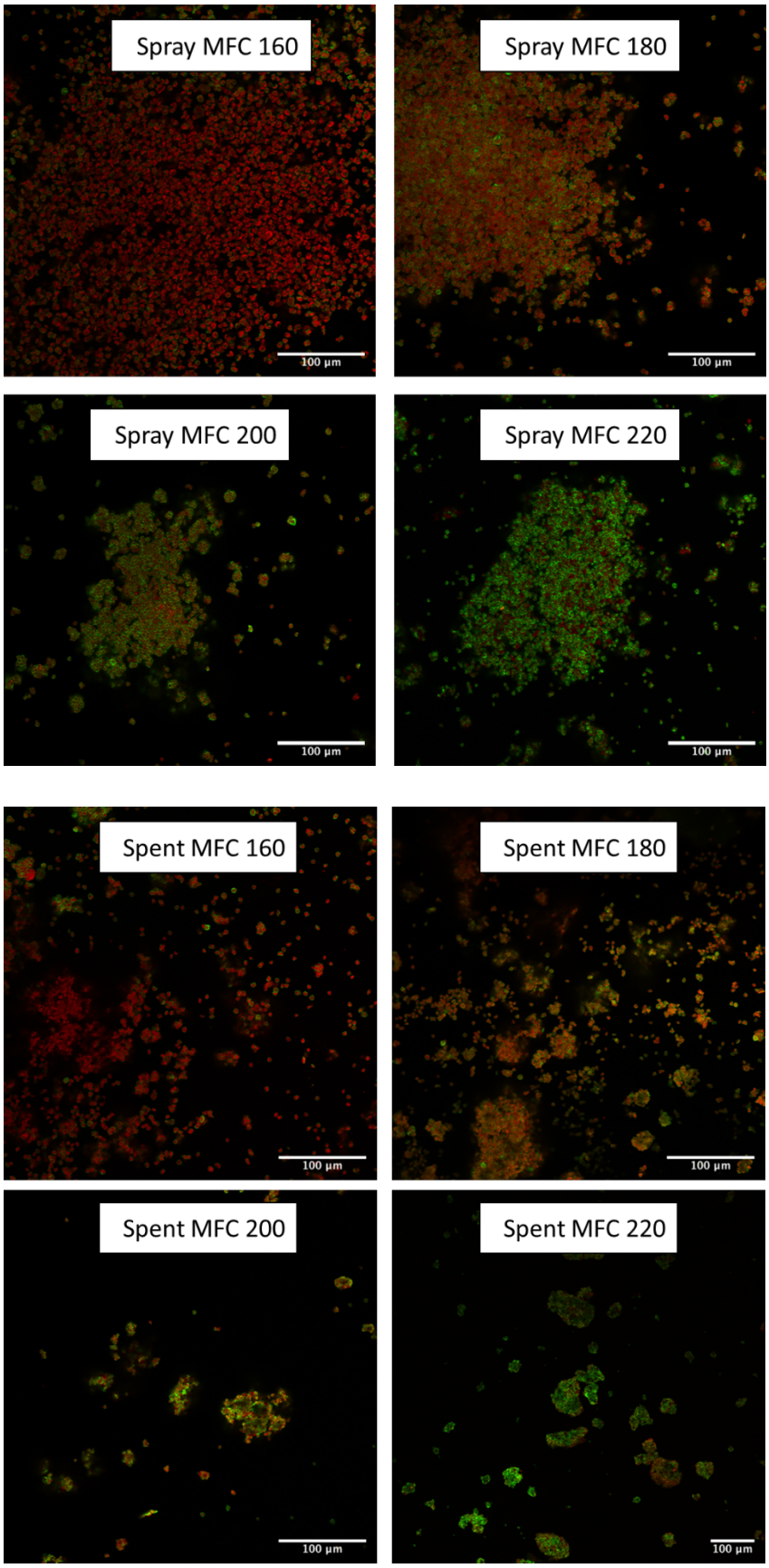

Figure 3-47 Laser Confocal Microscopy Images of all spray dried and spent DFC samples

The results show very clearly that both types of DFC form very small grains which then lump together into larger aggregates. This grain formation is shown in more detail in Figure 3-48.

Both types of DFC clearly show that with increasing microwave temperature an increasing amount of cellulose can be observed in the samples (green colour) which is in line with previous findings that suggested that the highest temperatures of microwave processing show the highest correlation with pure cellulose. However, it is interesting that at the lowest temperature (160^{o}C) there is still very little sign of cellulose as the red autofluorescence is much more prominent than any green specks indicating the presence of cellulose. At the highest temperatures, this ratio is reversed with mostly cellulose being present in the samples. Interestingly, the spent biomass, which has shown much more resemblance of its spectra with pure cellulose at all temperatures seems to show no difference in its trend compared to the spray dried DFC when using CT480 as the analytical tool.

It must be noted that this type of analysis is suitable only for qualitative analysis and cannot be used to quantitatively calculate the exact percentages of cellulose present in the samples. It still confirms visually what the previous analyses (XRD, NMR) hinted at, namely that cellulose content increases with higher microwave temperatures.

Figure 3-48 shows the nucleus/grain formation of the DFC with spray 200 DFC as a very clear example image next to the initial spray dried biomass. The nucleus formation and aggregate formation can be seen very clearly which bears some resemblance to the initial microalgal cells, however there is a size difference of 4-5 times that can be made out when comparing them to the initial spray dried biomass on the left. Also, the shape of the grains is less perfectly circular but slightly off-shape. Interestingly, it can be seen that there is again encapsulation of the core by the cellulose, which is flagged up green by the Carbotrace. This might be due to the core of the grains being so dense that the Carbotrace molecules are not able to penetrate to the inside and therefore forming a circular layer around them.

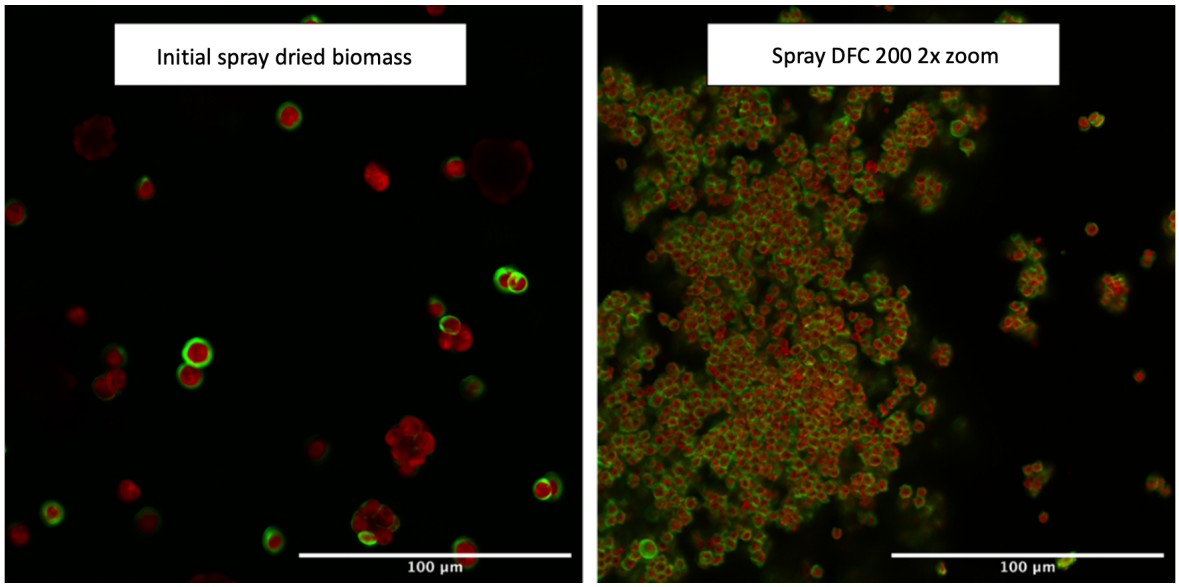

Figure 3-48 Laser Confocal Microscopy Images of initial spray dried biomass and Spray DFC 200 at 2x zoom

3.3.2 Isolation and Analysis of Algaenan

3.3.2.1 Algaenan Yields

Algaenan has been isolated from four different defibrillated cellulose samples to judge their algaenan content as well as to isolate algaenan and analyse it more in-depth.[192] Figure 3-49 and Table 9 display algaenan yields in context with DFC.

The algaenan contents vary greatly with the algaenan derived from Spray dried 160 defibrillated cellulose showing the lowest content (13.5%) while the one isolated from spent 220 shows the highest (52.9%), being four times higher. However, from the calculated amounts of algaenan present in the DFC samples it becomes apparent that the lower DFC yield but higher algaenan content in the spray dried 220 sample cancel out and in both 160 and 220 samples roughly the same amount of algaenan can be found. This allows the conclusion that the increase in microwave processing temperature has not influenced the algaenan in the sample but has washed out a lot of other components which have made up most of the yield of the lower temperature Spray dried 160.

In general, algaenan generated from spray dried samples shows lower yields for both temperatures with a difference between them of 35% while algaenan yields from spent biomass are higher with a difference between the 160 and 220 samples of 28%. It also can be noted that the defibrillated cellulose samples of both spray dried and spent at 220°C

both consist of around 50% of algaenan. For the spent DFC it can be seen that the higher microwave processing temperature seems to have increased the algaenan overall.

Table 9 *Summary of algaenan yields, DFC yields and algaenan content within the DFC samples*

	DFC yield/ g	**Algaenan content/ %**	**Algaenan weight in DFC/ g**
Spray 160	5.00	13.50	0.675
Spray 220	1.56	48.35	0.754
Spent 160	0.07	24.80	0.017
Spent 220	0.58	52.94	0.301

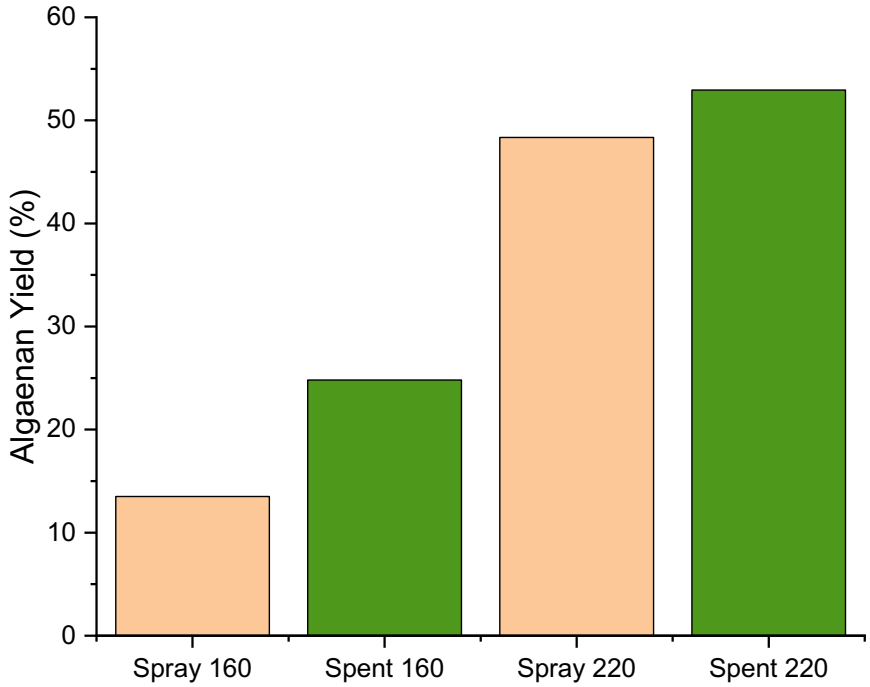

Figure 3-49 *Yield of algaenan generated from different defibrillated cellulose sample*

3.3.2.2 ATR-IR analysis of algaenan

The ATR-IR analysis of the algaenan is displayed in Figure 3-50.

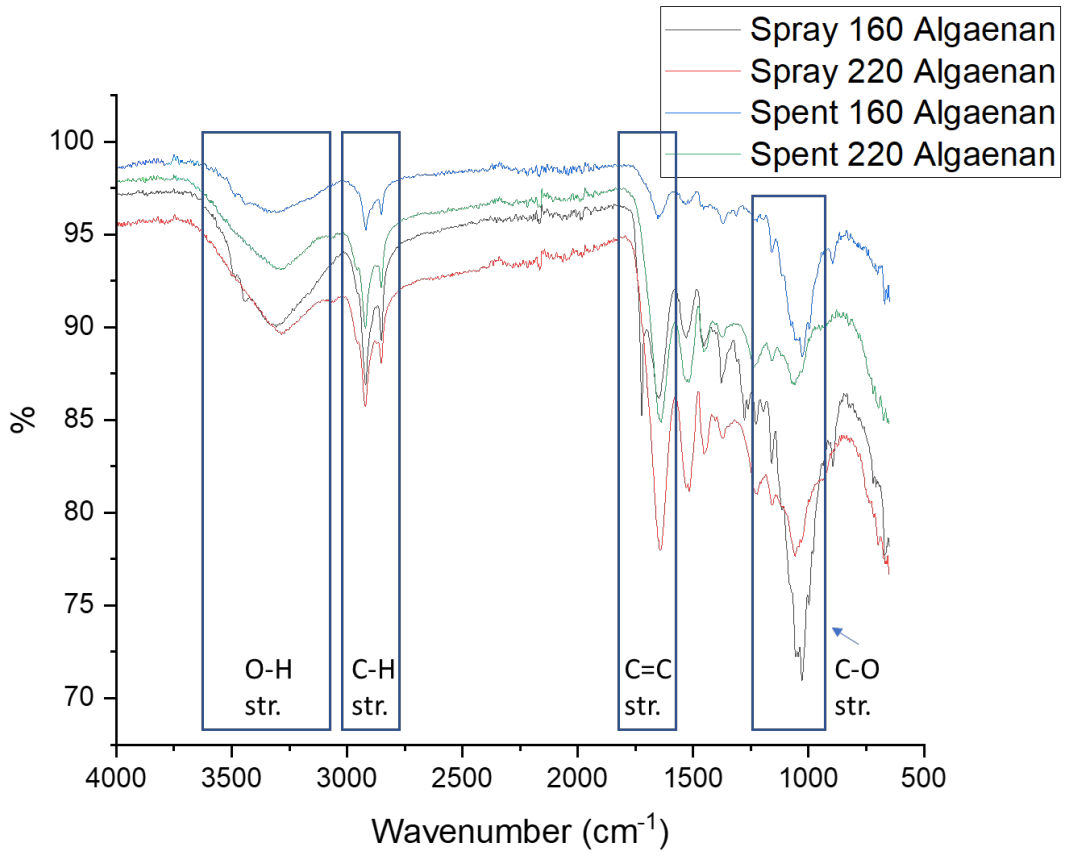

Figure 3-50 ATR-IR of different isolated algaenan samples

In line with the general structure of algaenan which is displayed in Figure 1-6, the IR spectra correlate closely with the functional groups present in the algaenan as reported in the literature.[254] The C-H stretch (2850 cm^{-1}) as well as the C=C stretch (1650 cm^{-1}) both correspond well to the long aliphatic chains found in algaenans while the C-O stretch (1100 cm^{-1}) points towards ethers or esters which serve as the linkages between the aliphatic chains and build up the highly crosslinked network which makes the algaenan so stable against environmental influences. There are no major differences between the four samples of extracted algaenan.

3.3.2.3 Solid State NMR analysis of Algaenan

The results of CPMAS solid state NMR analysis of the isolated algaenan samples are shown in Figure 3-51. It is noted that although the Spent 160 algaenan sample has been generated, it has not been enough to generate a meaningful and interpretable signal on the NMR machine despite all efforts to increase its response. It is, however, attached in the Appendix Figure A3 and also shows a strong signal appearing around 30 ppm – 40 ppm, which again points towards the sample containing a considerable amount of algaenan.

The resonances shown in Figure 3-51 all correlate well with literature.[77,205–207] For example, the resonances in the range 30 ppm – 40 ppm correspond to the aliphatic chains within algaenan. However, although these resonances are also evident in the spent 220 algaenan sample, they are not the most intense as this particular sample still shows very strong responses associated with signals attributable to cellulose. Especially the resonances at approximately 65 ppm and 90 ppm are indicative of interior/crystalline cellulose while the resonances at 84 ppm and 62 ppm attributable to surface/amorphous cellulose are almost non-existent. Thus, this algaenan contains a considerable amount of residual crystalline cellulose. The crystalline cellulose responses for the spray algaenan samples are noticeable in both samples, however the spray 220 algaenan shows very little clear response in this region suggesting a much lower cellulose content. Overall, it can be concluded from the NMR spectra to contain the least amount of cellulose of the three samples. Spray 160 shows peaks 22 ppm and 44 ppm which could be due to small molecule impurities or allylic carbons at 40 – 45 ppm.

The resonance centred at 175 ppm is synonymous for the carbon of a carbonyl group, which may be carboxylic acid groups present within algaenan or residual hemicellulosic matter, albeit unlikely. In addition to the paraffinic CH_2 resonances, the other characteristic algaenan resonance corresponding to unsaturated carbons (-C=C-) is evident but not as intense. Overall, the presence of algaenan in ALG01 brings up many similarities again between ALG01 and *Nannochloropsis sp.* which also contains a bilayer cell wall structure with an outer algaenan layer followed by an inner cellulose layer.[75,255,256]

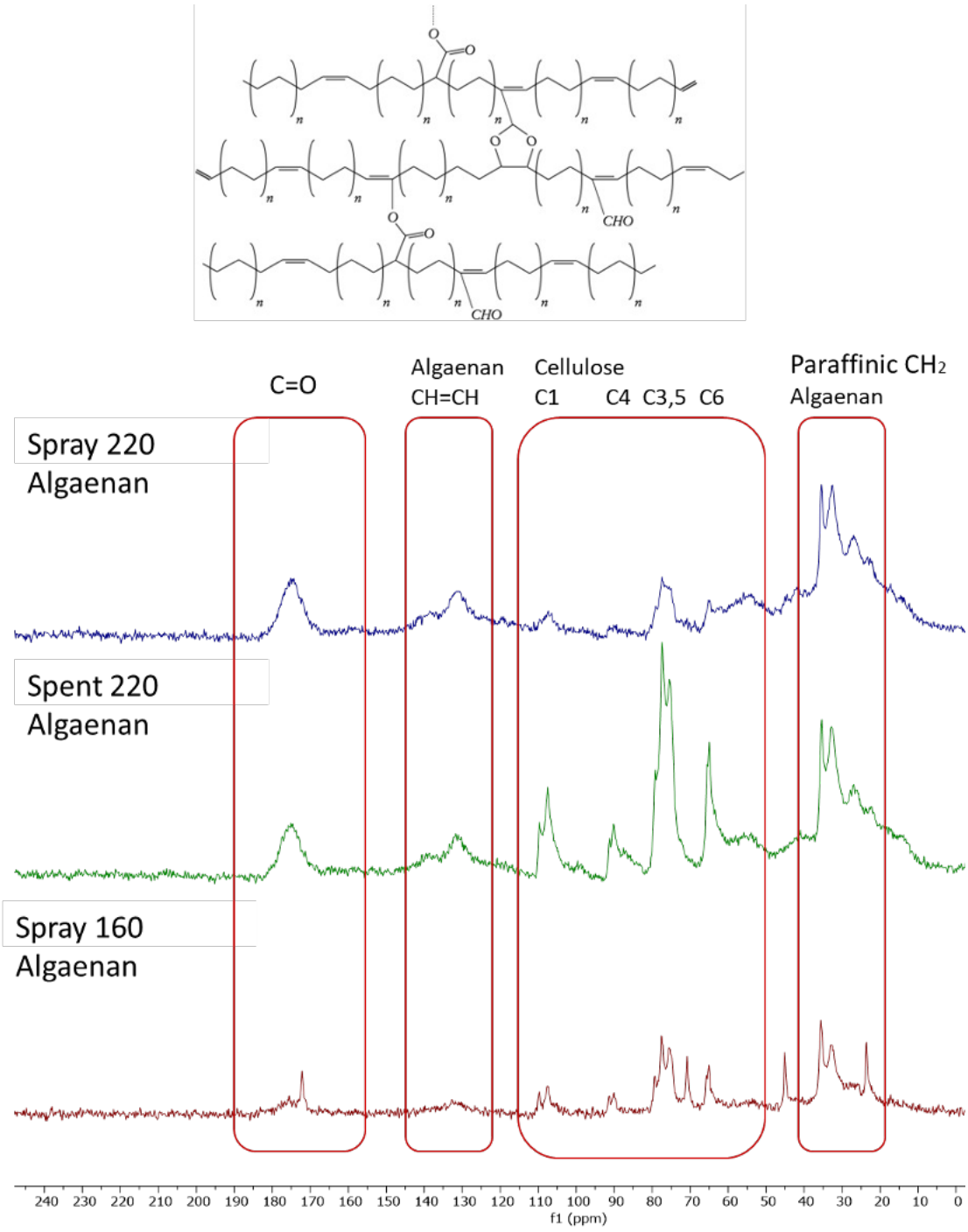

Figure 3-51 CPMAS solid state NMR spectra of isolated algaenan samples

3.3.2.4 Carbotrace analysis of Algaenan

Confocal laser microscopy studies (Figure 3-52) using Carbotrace CT480 as an optotracer molecule were conducted on the algaenan samples in addition to the defibrillated cellulose samples detailed earlier in this chapter in order to differentiate between cellulosic and non-cellulosic matter.

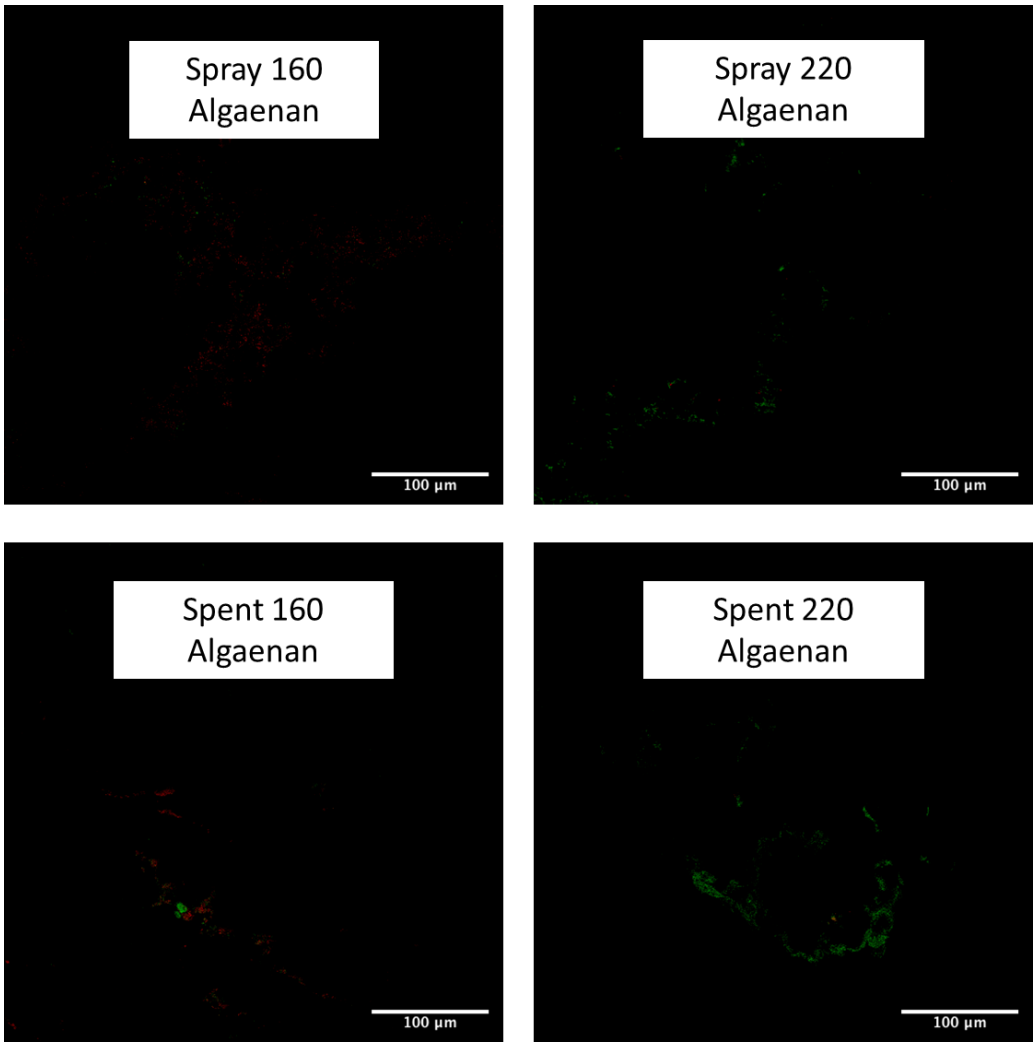

Figure 3-52 Carbotrace 480 images of isolated algaenan samples analysed via confocal laser spectroscopy

The Carbotrace images show major differences to the previous images taken of the defibrillated celluloses (Figure 3-47). All images taken of the algaenan stained with CT480 were almost exclusively black (dark). On very close inspection, some specks of red and green may be seen, however they are very dim and only appear in selected places of the sample. This suggests a considerably lower presence of cellulose in the algaenan samples, in line with the lower cellulose peaks and higher algaenan peaks in the solid-state NMR spectra (Figure 3-51). The bright red response for the 160 samples as well as the green

response stemming from cellulose in the 220 samples have almost faded to a consistent black interspersed with residual cellulose signals, which is in line with the previous analytical results suggesting that the algaenan has been isolated and partly purified from cellulose and other cell wall components. Considerable impurities, however, remain as evidenced by not completely black pictures as well as impurity resonances appearing in the solid-state NMR (Figure 3-51). This is particularly the case for the Spent 220 algaenan sample, which not only shows the most residual green response stemming from cellulose, but also shows the largest correlation to crystalline cellulose within the solid-state NMR.

3.3.3 Properties of DFC

3.3.3.1 Water holding capacity

The water holding capacities of the different DFC samples are summarized in Figure 3-53. WHC values fluctuate around 4.5 g H_2O/g for spray dried defibrillated cellulose and around 5.1 g H_2O/g for spent samples without any perceivable trend. Cellulose can incorporate water into its fibrillar network resulting in fibre swelling properties. These properties are enhanced upon increasing the surface area via particle size reduction and defibrillation, which has been achieved through the hydrothermal microwave process.[174,175] The values obtained for the microalgal samples are similar to values of WHC obtained for defibrillated cellulose samples of spent ginger waste (4 g H_2O/g).[174]

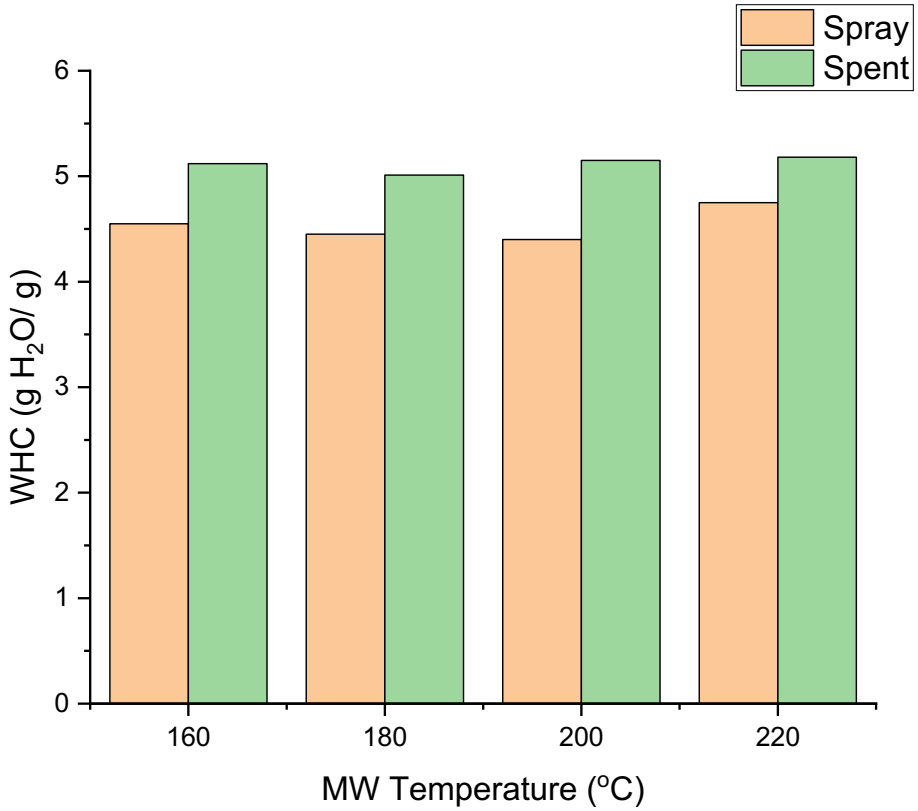

Figure 3-53 Water holding capacities (WHC) of DFC of both spray dried and spent biomass

3.3.3.2 Hydrogel Formation

Hydrogels derived from biomass are becoming increasingly sought after in various fields of application, such as hygiene products, contact lenses, wound healing products, or lubricants.[257] Due to cellulose-based hydrogels being both biodegradable as well as low-cost and highly abundant, they pose a very promising and green candidate for future innovations. The abundant hydroxyl groups in cellulose possess the capability to capture and trap water in the wider cellulosic structure through hydrogen bonding to form a three-dimensional hydrogel.[257–260] However, in most cases additional chemical or physical stimuli are require to increase the amount of trapped water.

In this case, the DFCs were formed using acid-free hydrothermal microwave processing and in order to enhance gelation the samples have undergone homogenisation. The hydrogel formation ability at various concentrations of DFC in deionized water (0.5%, 0.75%, 1%, 1.5%, 2% and 3%) is depicted in Figure 3-54 and Table 10. Hydrogel formation proved to

be a challenging task with only two of the eight samples being capable of forming a short-lived hydrogel. The two cellulose samples generated at the highest microwave temperature (220°C) formed hydrogels after intense homogenisation which were stable upon inversion of the vial. However, after around 30 seconds the gels started to descend the vial and lose their stability. Compared with previous findings on defibrillated celluloses from almond hull and cassava peel, the microalgal cellulose samples are less able at hydrogel formation which may be due to the residual hydrophobic algaenan layer.[244] This assumption correlates well with atypical observations for DFC samples reported in the XRD pattern (Figure 3-37) and in the solid state NMR spectrum (Figure 3-40). The latter evidences resonances for algaenan.

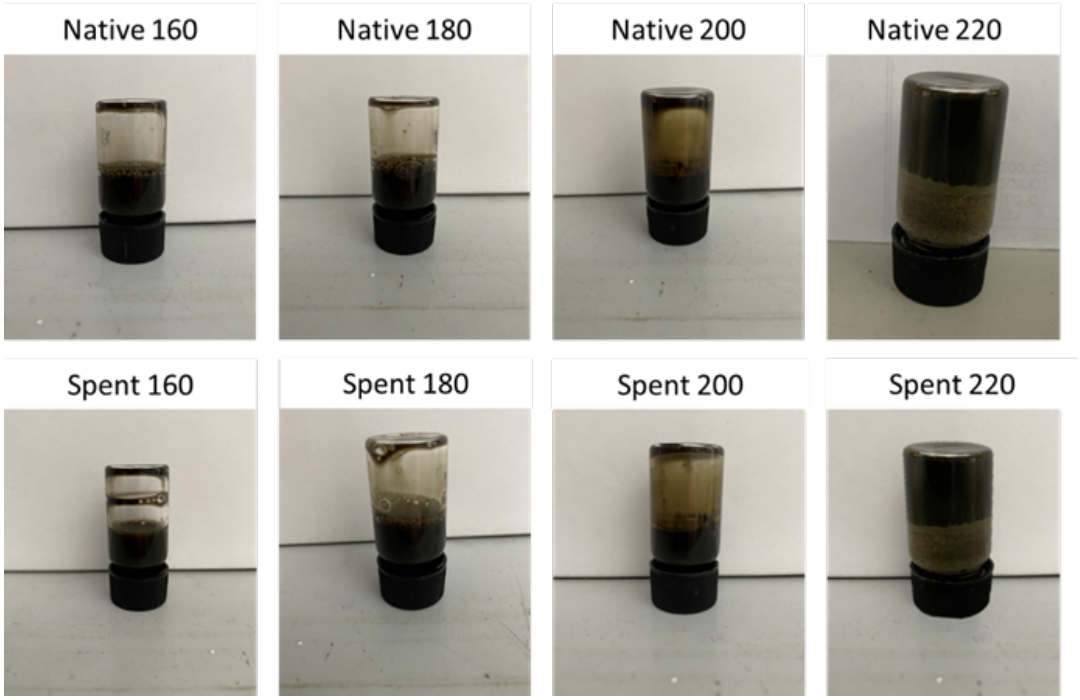

Figure 3-54 Hydrogels formed from defibrillated cellulose samples obtained from spray dried biomass and spent biomass. Numbers refer to the temperature of the microwave process used for production of the defibrillated celluloses

Table 10 *Hydrogel formation capabilities of different defibrillated cellulose samples generated from both spray dried and spent biomass*

Sample type	Hydrogel formation
Spray 160	x
Spray 180	x
Spray 200	x
Spray 220	Reasonably stable gel
Spent 160	x
Spent 180	x
Spent 200	x
Spent 220	Reasonably stable gel

3.3.4 Protein Extraction upon hydrothermal microwave treatment

As part of a zero-waste biorefinery concept, the production of DFC also produces a hydrolysate, which contains carbohydrates/sugars (see earlier, Section 3.3.1) and possibly additional water-soluble proteins that have been removed as a result of microwave processing (see earlier Figure 3-31). Proteins were successfully extracted from both spray dried algae as well as spent algae.

3.3.4.1 Visual Appearance and Yields

The visual appearance of the protein retentates are shown in Figure 3-55.

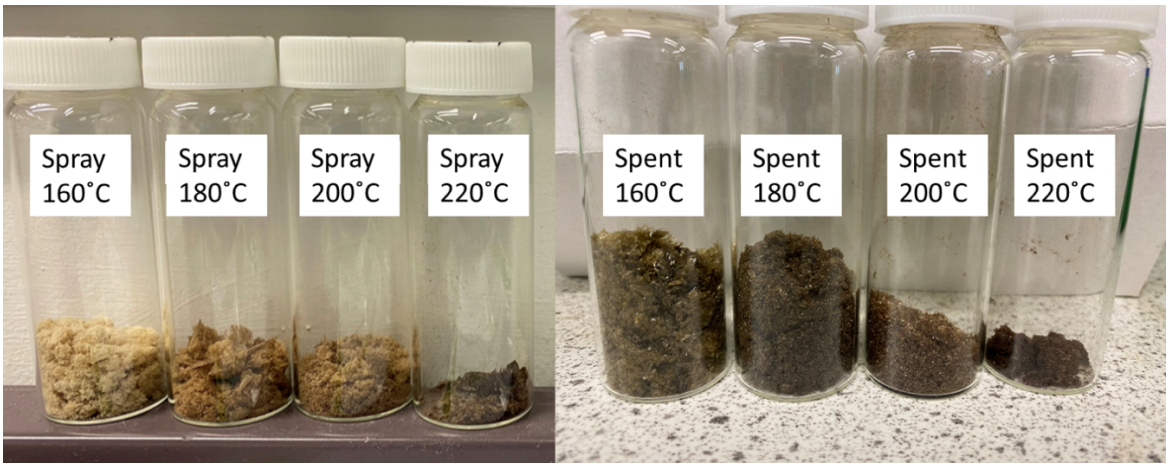

Figure 3-55 *Visual appearance of protein retentates of both spray dried and spent microalgae upon different microwave temperature treatments*

Like for like, the protein retentates derived from spray dried ALG01 with respect to spent ALG01 were lighter in appearance. The former darkened in colour with increasing temperature. The latter were dark green/brown in colour with a shimmer akin to crystals.

The protein yields isolated from the hydrolysate of spray and spent ALG01 are shown in Figure 3-56. The yields from both biomass types follow a similar trend regarding the yield with a maximum occurring at 180°C (2.75% for spray dried biomass and 4.8% for spent biomass).

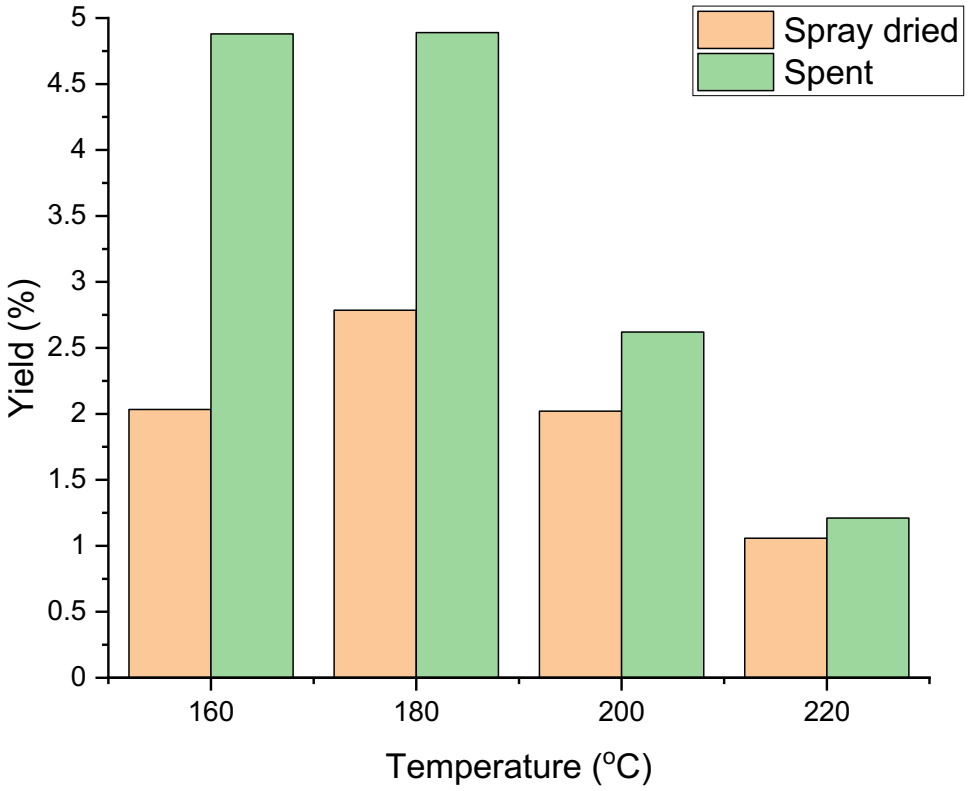

Figure 3-56 Protein retentate yields from both spray dried microalgae and spent microalgae

The decreasing yield with higher temperatures can be explained by considering the destructive force of the microwave at these temperatures which results in residual short-chain peptides which can fall below the 10 kDa cut-off point of the ultrafiltration membrane thus leeching into the permeate. Interestingly, the protein yield for the spent biomass is consistently higher than that of the spray dried biomass; for the lower temperatures even

50%-65% higher. At the highest microwave temperatures these differences gradually decrease with yields at 220°C almost identical. The generally higher yield of spent biomass has been observed in previous protein extraction experiments (see Figure 3-18) and is a result of the industrial extraction process that the spent biomass has undergone which has already severely ruptured the tough algal cell wall thus making any component extraction considerably easier and more efficient.

3.3.4.2 CHN, Bradford Assay and SDS-PAGE

In order to judge the actual protein content of the protein retentates, Figure 3-57 combines the CHN and Bradford Assay results.

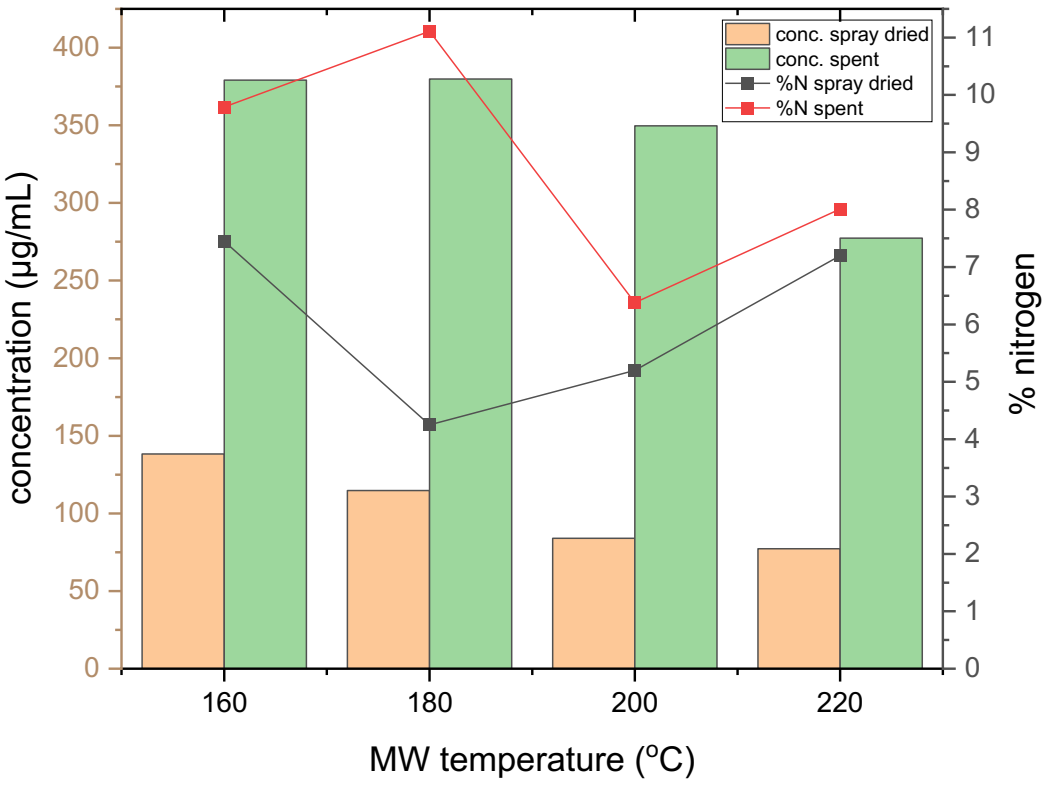

Figure 3-57 Combined protein content from CHN as well as soluble protein concentration obtained from Bradford Assay of the protein retentates from spray dried and spent biomass

CHN results show that using a nitrogen to protein conversion factor of 6.25 the maximum protein content is 69% (or 11% nitrogen) for spent biomass protein retentates obtained at

180°C. [261] This value is the highest protein content of any protein sample that has been generated throughout the work presented in this thesis, which can be attributed to the already disrupted cell wall of the spent biomass coupled with the optimal microwave temperature for generating protein yield and content. There seems to be a large variation in individual protein content with 180°C surprisingly also showing the lowest nitrogen content for spray dried protein retentates (4.3%). While the spray dried samples have a considerably lower protein content at lower temperatures than the spent samples the gap is closing at the highest temperatures where the protein contents become more similar. When compared to the Bradford Assay results it can be seen that the general trends are different, with water soluble protein content showing a gradual decrease in concentration with increasing microwave temperature as well as very large discrepancies between spray and spent proteins, spent proteins giving a considerably higher response. This is in contrast to previous results where spent proteins generally generated a lower Bradford response than spray dried proteins. This could be attributed to the fact that spent biomass yields much higher yields and also possesses a higher protein content which results in the large discrepancy in water soluble protein response. Furthermore, it has to be noted that Bradford Assay does not pick up certain proteins which fall below the 3 – 5 kDa range, of which there certainly are still some present in the retentates, especially at high temperatures.[212,213] Moreover, compared to the microwave pre-treatment results shown in Figure 3-19, the microwave method in this case involved a holding time of 10 minutes while the microwave treatment previously did not involve any holding time. The additional 10 minutes at constant high temperature therefore had not only an impact on the higher yields but also on the much higher Bradford Assay response.

As shown in Figure 3-58, a significant amount of proteins present in the retentates falls within that 3-5 kDa range, which has not been filtered through into the permeate as might be expected due to the 10 kDa cut-off point. Due to the pore size in the filtration membrane being an average rather than an absolute value, this can happen frequently. This inability to pick up low molecular proteins and peptides makes the Bradford Assay unsuitable in this case for a quantitative analysis and merely qualitatively represents the discrepancies between the samples.

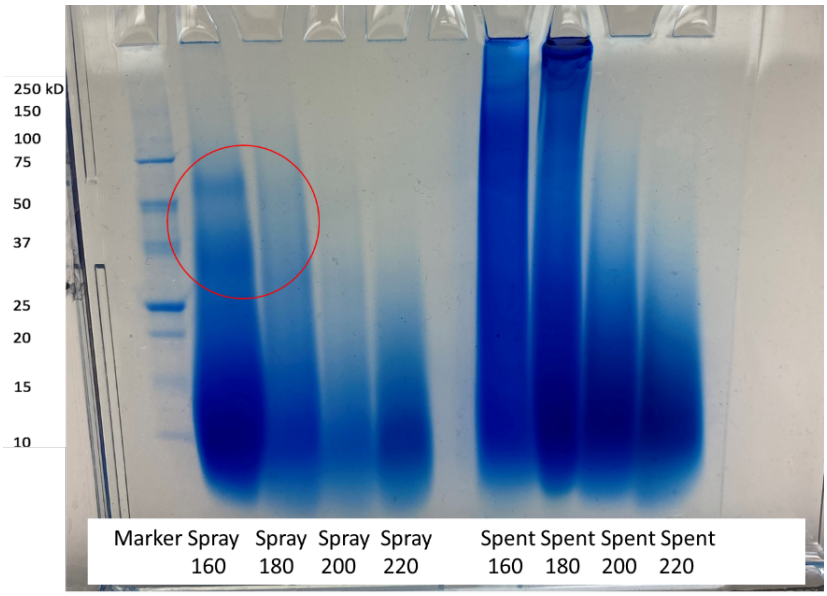

Figure 3-58 SDS PAGE gels of microwaved proteins from both spray dried and spent microalgae

The SDS PAGE gels confirm that most proteins found in the retentates across all temperatures are low molecular weight proteins and peptides as a result of the harsh microwave treatment having hydrolysed the proteins. This is particularly intense at the highest temperature which coincides with the full breakdown of proteins which has been reported to start above around 200°C. [262,263]

Furthermore, some protein bands at higher molecular weights can still be made out in the lower temperatures for spray dried proteins, especially at 160°C and 180°C. These are in the region of around 35 kDa and 55-60 kDa and are circled in red. Their degradation with higher temperatures is in line with previous findings.

The spent peptides, however, do not show the remaining protein bands visible in the spray dried biomass due to their previous industrial lipid extraction. Instead, their overall profile of an extending blue smear indicates the presence of various peptides across all size ranges especially at lower weights. The smears visible towards the top of the gel are due to the concentrated nature of the proteins in the spent samples resulting in a less than ideal running profile. The gel furthermore shows that at higher microwave processing temperatures both the spray dried and spent peptides appear very similar and any previous difference have been eliminated.

3.3.5 Foaming and emulsion capabilities of proteins

3.3.5.1 Foaming capabilities and stabilities

The foaming capabilities and stabilities (Figure 3-60) were determined for the microwaved peptides, similarly to the untreated and pre-treated peptides (Figure 3-26).

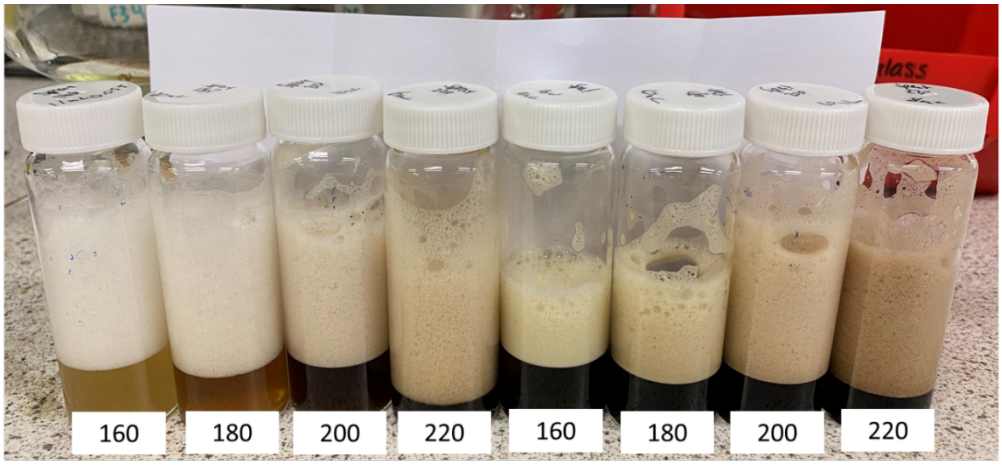

Figure 3-59 Visual appearance of foams from microwaved peptides

Visually (Figure 3-59), the foams appear to consist of fine bubbles, with colours matching the intensity of the peptides dispersed in water.

Foaming capabilities can be seen to be dependent on microwave temperature with increasing foaming capabilities with increasing temperature, which also corresponds to a higher presence of hydrolysed peptides. For spray dried peptides, values ranged from 150% (Spray 200) to 275% (Spray 220). For spent peptides, values increased from 70% (Spent 160) to 182% (Spent 220). Interestingly, the lower two samples generated from spent biomass (Spent 160 and Spent 180) did not hold up well altogether to foaming stability, both of which dropped significantly after 2 h to almost 0%. This could be attributed to the fact that excessive hydrolysis of peptides can in turn lead to a drop in foaming capabilities.[229]

Overall, the highest foaming capacity was seen for Spray 220 (275%). However, it is significantly lower in comparison to egg white protein (358%) and egg white protein mixed with: soy protein (470%); corn protein (419%), and; fish skin protein (423).[225,264]

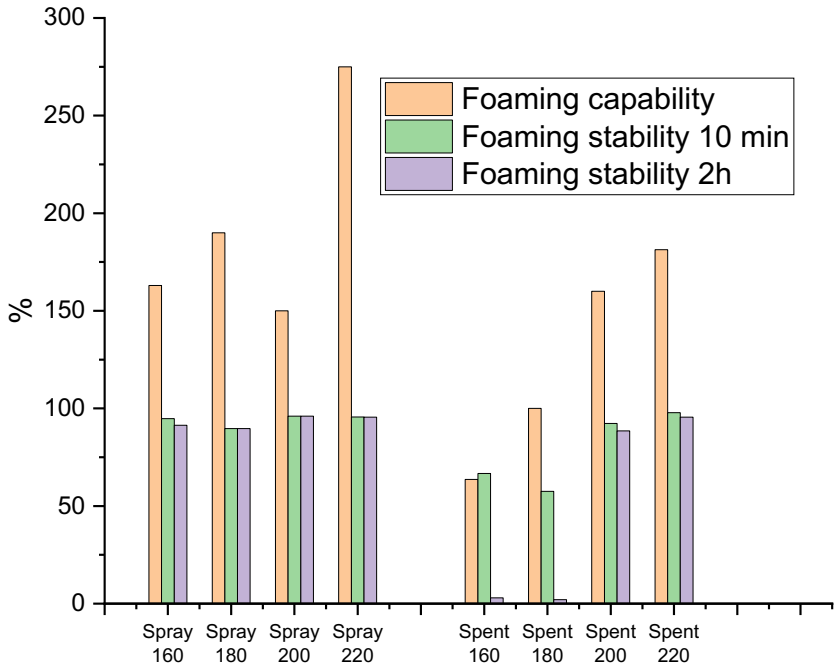

Figure 3-60 Foaming capabilities and stabilities of microwaved proteins from both spray dried and spent ALG01

3.3.5.2 Emulsion capability and stability

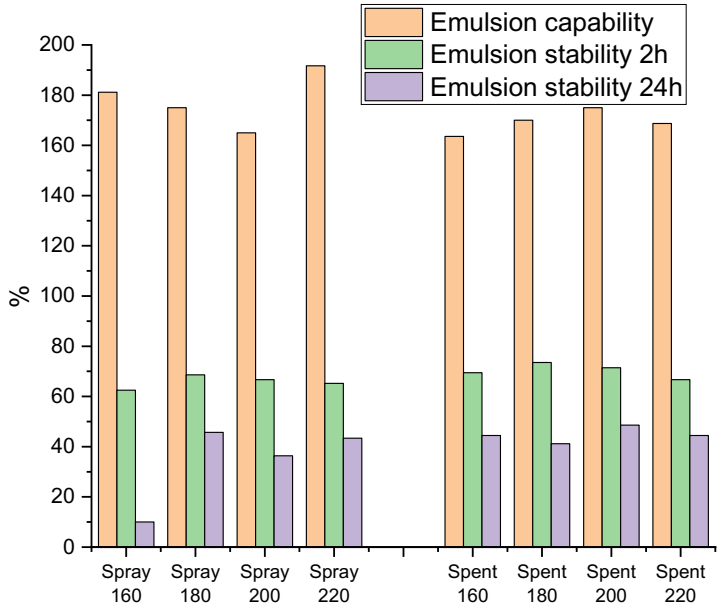

Figure 3-61 Emulsion capabilities and stabilities of microwaved proteins from both spray dried and spent ALG01

Emulsion capabilities (Figure 3-61) showed very similar values for all samples, regardless of either spray dried or spent, with values ranging between 165% (Spent 160) and 192% (Spray 220). Similarly, the stabilities after 2h and 24h also were almost identical at approximately 65% - 70% and 40% -50%, respectively. The only outlier was Spray 160, where the emulsion stability after 24h dropped down to 10%.

Emulsion stabilities reported in the literature of proteins obtained from *C.vulgaris* showed stabilities ranging from 61% to 79%, albeit after 24 h.[122] Compared to stabilities of ALG01 microwaved peptides (approx. 60% - 70% after 2 h and approx. 40% after 24 h on average) the microwaved peptides show similar stabilities after 2h as the *C.vulgaris* peptides after 24 h, while the ALG01 peptides further dropped to be comparatively around 40% lower than reported in the literature, potentially due to their very hydrolysed nature.

3.3.6 Bioactivity testing

Bioactivity testing was performed (Aelius Biotech, Newcastle, UK) on the peptides obtained from spent biomass, which have been microwaved at four different temperatures (Spent 160, Spent 180, Spent 200 and Spent 220). The protocol for the test is summarised in the Appendix in Section A3-2.

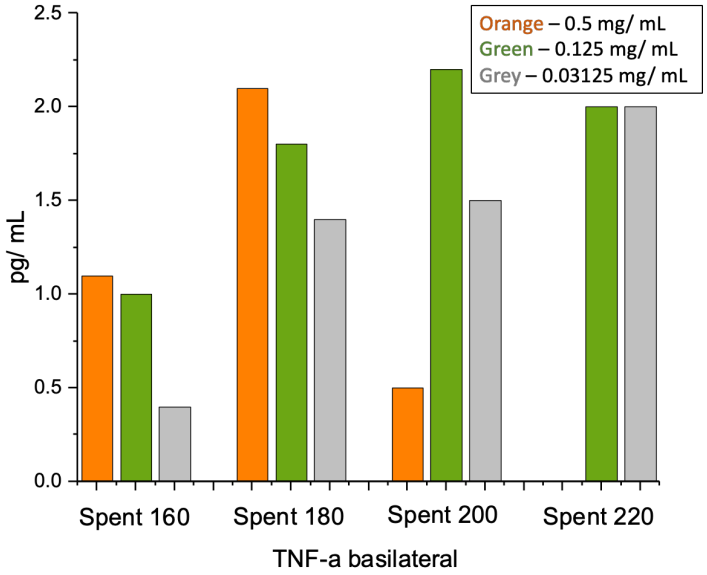

Figure 3-62 Cytokine response data for all samples at concentrations 0.5, 0.125, and 0.03125 mg/ml

Results show that only TNF-α responses were detected with some of the tested samples, however these were all in the range 0-2.5 pg/mL, at the lower end of the detection range. This shows, that despite some upregulation of pro-inflammatory cytokines, the upregulation is so minimal it can be rejected as being not significant.

Either way, positive results prevail for spent peptides, as they all do not influence cell viability, inhibit pepsin and trypsin (especially enzymatically hydrolysed peptides as detailed earlier) and show an anti-inflammatory response. This makes the spent peptides (in particular enzymatically hydrolysed peptides and microwaved peptides) a potential candidate for promising future applications based on their bioactivity.

3.4 Production and Characterisation of Bio-oils and Biochars via Microwave Processing

With a view to achieving a zero waste microalgal biorefinery, the residual biomass (pellet) after non-microwave protein extractions was further valorised into bio-oils and bio-chars via microwave pyrolysis.

3.4.1 Biochar formation and characterisation

Microwave pyrolysis of the pellet from both spray dried ALG01 and spent ALG01 was performed at three different power settings (50 W, 100 W, 150 W) at a maximum (safe) temperature of 280°C. Due to the very rapid heating resulting from good microwave absorption capabilities of the microalgae the amount to be pyrolyzed had to be adjusted according to the power to avoid exceeding the maximum pressure of the microwave vessel resulting in explosions. Furthermore, in order to assess the completion of pyrolysis using microwave technology the results of both a single pyrolysis run, and a double pyrolysis were compared. The yields are summarised in Figure 3-65 and Figure 3-66 with the visual appearance of the chars in Figure 3-63.

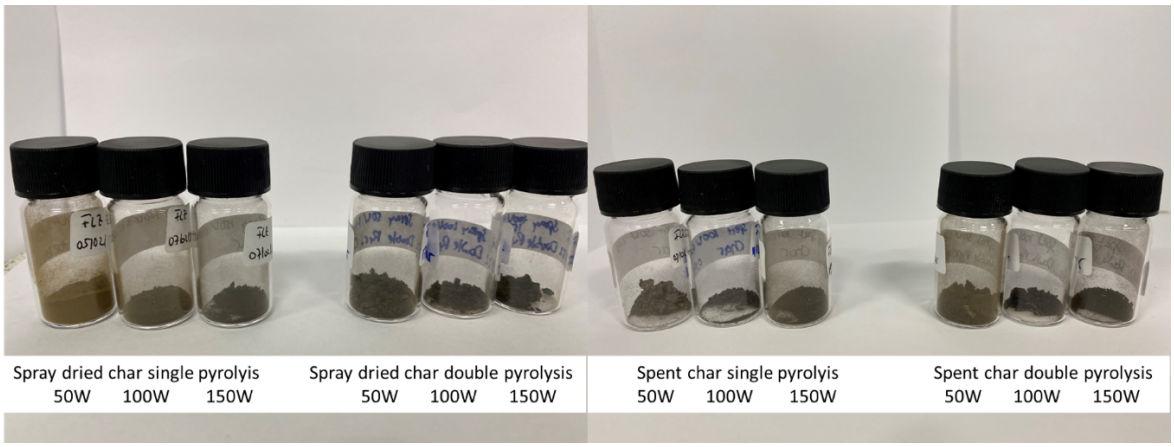

Figure 3-63 Visual appearance of chars from spray dried and spent biomass

Visual appearances of the char changes across the samples depending on the power setting with Spray dried 50W being noticeably different in appearance to the other chars by exhibiting a green/ brown colour resembling the original algal colour more than the black brittle chars for both spent chars as well as all the doubly pyrolyzed chars. This green/ brown colour indicates incomplete pyrolysis and in correlation to the findings in Figure 3-64, detailing the temperature profile of the microwave pyrolysis runs, the higher the achieved temperature the darker and more brittle the resulting char.

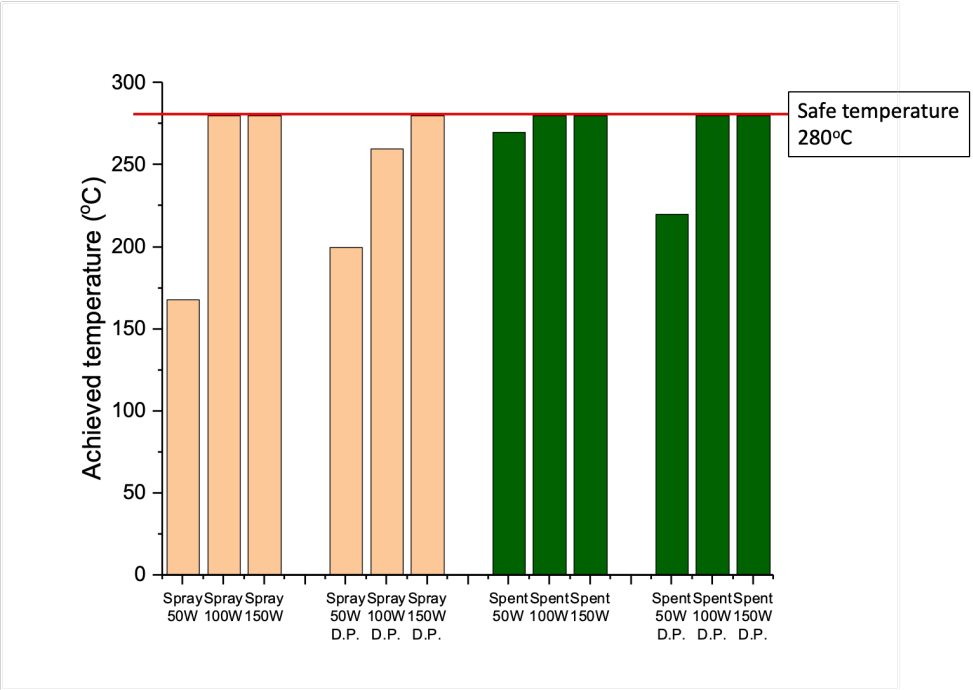

Figure 3-64 Achieved microwave temperatures for spray and spent samples at fixed powers and a safe temperature set at 280°C

Microwave pyrolysis typically occurs over four stages. Stage 1 sees a slow rise in temperature due to the microalgal biomass drying and volatile compounds escaping. During this stage heating mainly is driven due to the excellent microwave absorption properties of water.[265] In stage 2, the temperature rises more slowly as the microwave absorption now relies on biopolymers such as cellulose and hemicellulose.[266] Bio-oils and gases are being formed during this stage. A slight temperature reduction may follow due to net heat losses from the formation of bio-oils and gases, indicating Stage 3. In stage 4, the temperature reaches a plateau during which many reactions have reached equilibrium or ceased.[267]

Following on from the visual appearance the achieved temperatures shed more light on the thoroughness of pyrolysis with Spray 50W only reaching 168°C as a maximum. Similarly, all 50W runs did not reach the maximum temperature with higher power settings being more efficient. Only 150W managed to reach the maximum temperature of 280°C every time. The double pyrolysis has managed to increase the temperatures for the lowest power setting for spray dried biomass although it achieved a lower temperature for spent biomass. The phenomenon of higher microwave powers yielding higher achieved pyrolysis temperatures can be explained through higher powers' more intense heating as well as

enhancing the microwave absorption potential of the microalgae, resulting in a better translation of microwave power into heat.[267]

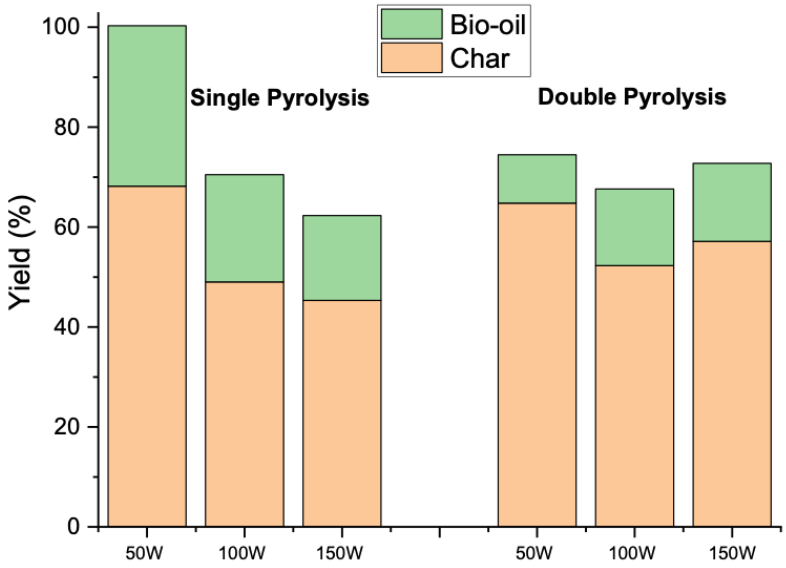

Figure 3-65 Yields of char and bio-oil for single and double pyrolysis of spray dried biomass

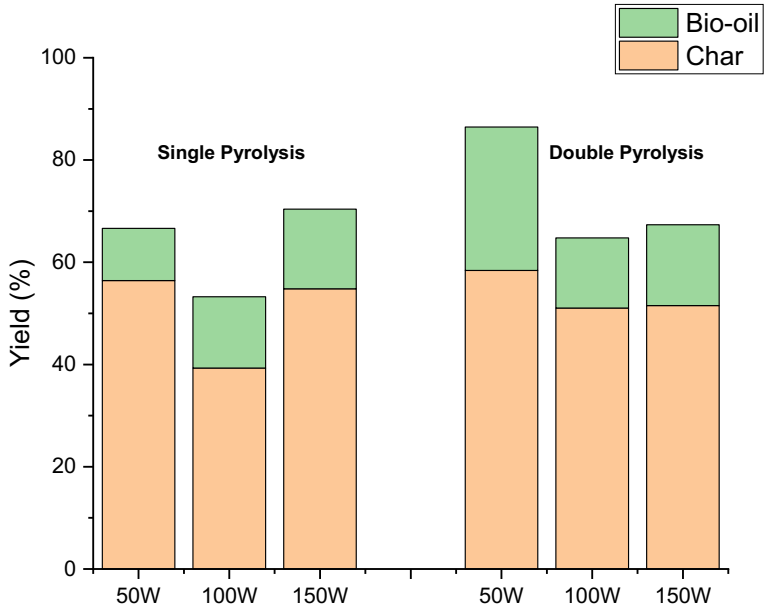

Figure 3-66 Yields of char and bio-oil of single and double pyrolysis of spent biomass

Generally, char yields for both spray and spent biomass fall between 40% and 60% with an overall slight reduction of yield at higher powers due to the increased formation of gases.

There is no discernible difference between char yields of spray dried and spent biomass suggesting a very similar response to pyrolysis in terms of general microwave absorption and reaction to the pyrolysis process. Compared to conventional pyrolysis the yields are still considerably higher as conventional processes typically yield around 30% of char.[268] When comparing char yields of the single and double pyrolysis run there is again no clear trend to be identified with similar yields on both sides.

3.4.2 Analysis of chars: CHN

The chars have been analysed via CHN with the results summarised below in Figure 3-67 and Figure 3-68.

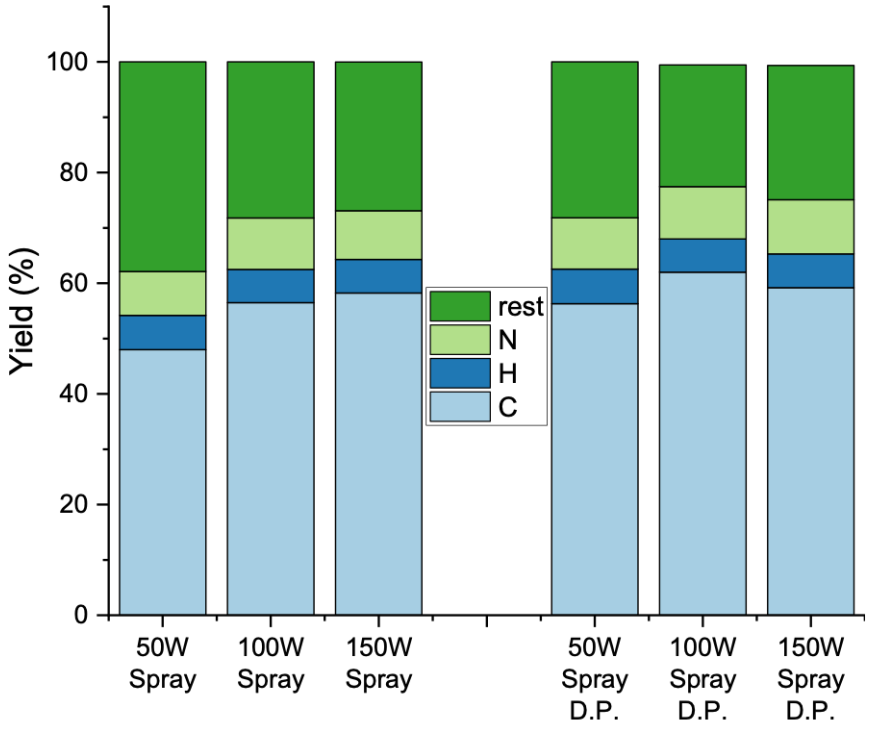

Figure 3-67 CHN results of char from spray dried biomass

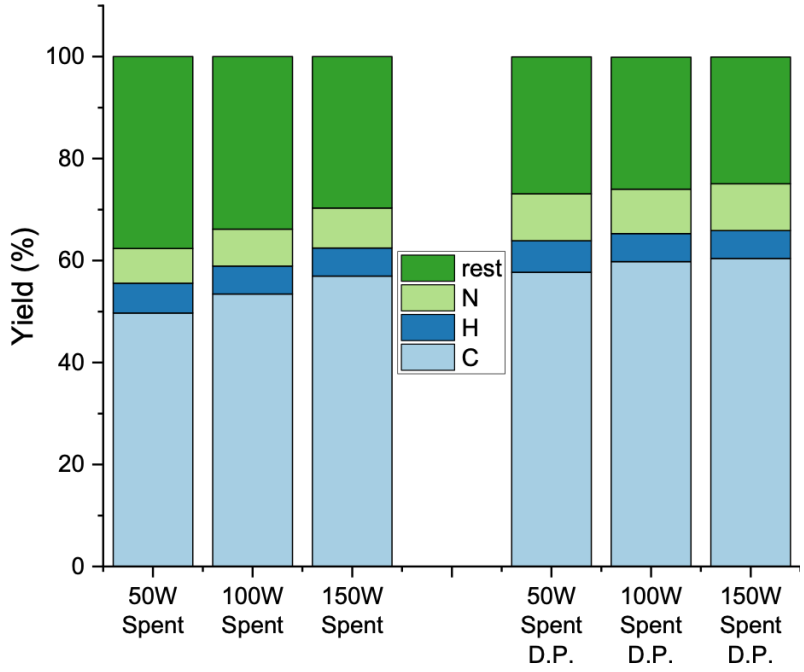

Figure 3-68 CHN results of chars from spent biomass

The results of CHN analysis reveal that the carbon contents of the chars range from 48% up to 60% with a generally increasing trend upon increasing the microwave power, which can be observed for both the single and double pyrolysis. The C% of the doubly pyrolyzed samples can be seen to be slightly higher than for the single pyrolysis suggesting that a double pyrolysis results in a more thorough product.

Nitrogen and Hydrogen percentages remain very stable throughout varying power as well as single and double pyrolysis.

The increasing carbon content upon increasing power suggests a larger rate of carbonisation in the chars as well as reflecting the larger formation of gases such as H_2, H_2O, CH4, C_2H_4, C_2H_6, CO and CO_2.[188,269] These gases all contain a larger proportion of other atoms (H and O) compared to carbon, hence the increasing C% upon higher temperatures.

The calorific values (or higher heating values (HHV)) of the chars and initial biomass have been determined from the CHN results and are displayed in Figure 3-69.

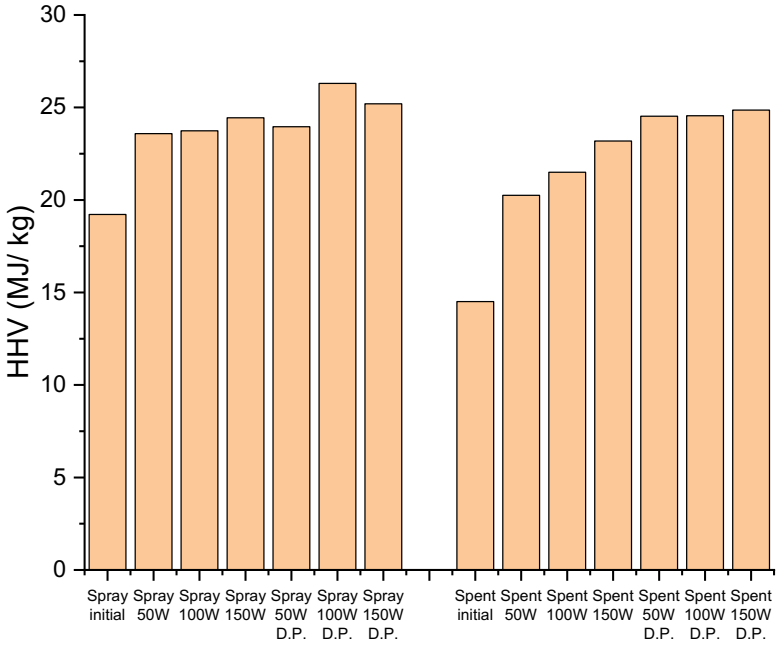

Figure 3-69 Higher Heating Values (HHV) of chars and initial biomass

The HHV of all the chars possess a minimum HHV of 20 MJ/ kg with the maximum obtained value being 26.3 MJ/ kg for Spray 100W D.P. The average value of the spray dried chars is 24.54 MJ/ kg while the spent chars' average is 23.15 MJ/ kg – around 1.5 MJ/ kg less. This can be attributed to the fact that the initial spent biomass only had a HHV of 14.5 MJ/ kg with the spray dried initial biomass recording 19.2 MJ/ kg – almost 5 MJ/ kg less. This can be due to the fact that spent biomass has already had a lot of lipids removed during the industrial extraction process which will impact the higher heating value negatively and which is also the cause of the spray dried chars overall having a higher average HHV.

Compared to other initial HHV of other microalgal species, ALG01 HHV are within the algal average, especially looking at the spray dried algae, while spent biomass is considerably lower but not too far off from some other species despite the previous lipid removal. Higher heating values of other microalgal species are summarised below in Table 11.

Table 11 Higher Heating values of selected microalgal species[269]

Species Name	HHV/ MJ kg^{-1}
Tetraselmis sp.	16.34
Spirulina	21.2
Nannochloropsis occulata	18.25

It can also be noted that with increasing microwave power the HHV rises, which is due to the better energy densification at higher powers. Overall, both biomass types have shown that they are able to increase their HHV through energy densification through a microwave pyrolysis process. However, as the HHV of initial spent biomass was considerably lower than that of spray dried biomass, its chars are merely around 1.5 MJ/ kg lower than their counterparts, suggesting that spent biomass is able to increase its energy density more than spray dried biomass when compared to the initial value.

Gong *et al*.[270] took the pyrolysis maximum temperature even further and produced bio-chars at temperatures up to 800°C. The HHV of their chars at 300°C (22.3 MJ/ kg for Chlorella vulgaris and 25.4 MJ/ kg for D. salina) reflects the achieved values of spray dried and spent bio-chars (around 25 MJ/ kg) that reached 280°C.[270] The higher their achieved temperature, the lower the higher heating value of the chars with the ones produced at 800°C only generating HHV of 16.4 MJ/ kg for *Chlorella vulgaris* and 19.6 MJ/ kg for D. salina.[270]

3.4.3 Analysis of Chars: TGA

The DTG traces resulting from Thermogravimetric Analysis are shown in Figure 3-70 and Figure 3-71.

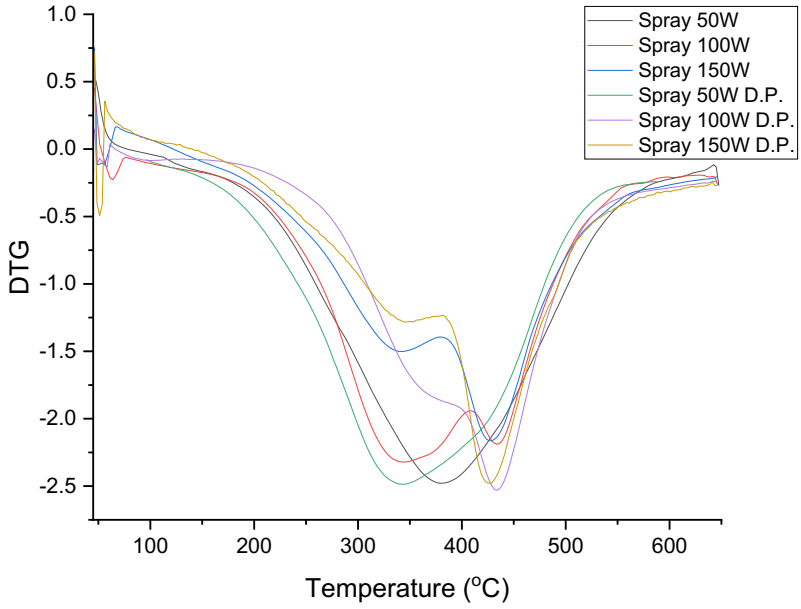

Figure 3-70 DTG traces of chars obtained from spray dried biomass

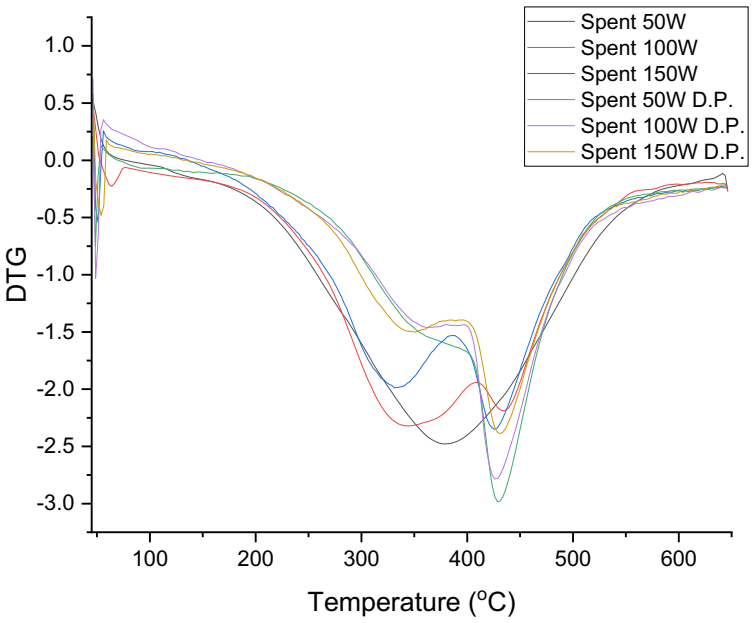

Figure 3-71 DTG traces of chars obtained from spent biomass

The DTG traces show a clear trend with both increasing power and employing double pyrolysis compared to single pyrolysis.

Upon increasing power, the main decomposition peak shifts from lower temperatures around 350°C to 430°C suggesting a more thorough pyrolysis as well as the formation of complex structures which are more heat resistant. Interestingly, at low power (50W) both the single and double pyrolysis chars merely show a broad peak suggesting very incomplete pyrolysis at this stage. Double pyrolysis for both spray dried and spent biomass results in a very prominent decomposition peak centred around 430°C especially at higher powers suggesting this combination as the most successful in terms of pyrolysis.

Spray dried and spent biomass reveal very similar profiles with spent biomass chars hinting at a slightly better response to pyrolysis due to the DTG traces possessing a more prominent 430°C peak and a lesser 350°C peak compared to spray dried traces. The traces show high similarities with literature traces showing microalgal char decomposition profiles.[271]

3.4.4 Analysis of Chars: ATR-IR

The ATR-IR spectra of all bio-chars are displayed in Figure 3-72 and Figure 3-73.

The IR spectra clearly still show strong signals relating to functional groups, indicating that the microwave pyrolysis process has not yielded a completely pyrolyzed char but more of a char still containing functionality. All chars at all powers as well as doubly and singly pyrolyzed chars show very similar IR traces with most bands being identical.

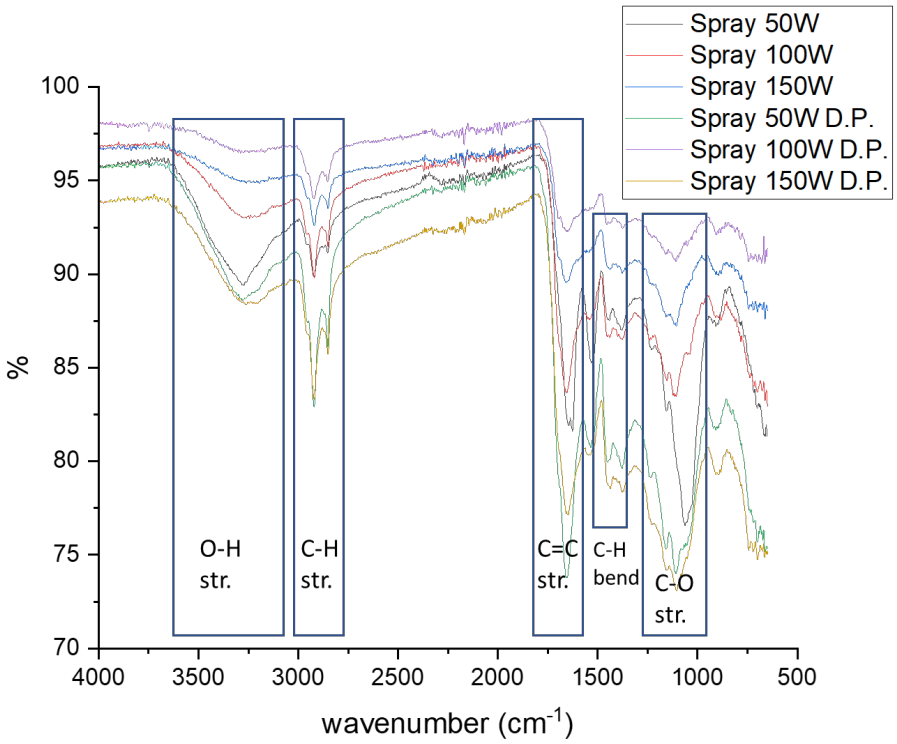

Figure 3-72 ATR-IR spectra of bio-chars derived from spray dried biomass from both single and double pyrolysis

Most prominent are the bands indicating the presence of aliphatic C-H groups (2900 cm^{-1}) as well as unsaturation bands from C=C stretches (1650 cm^{-1} – 1700 cm^{-1}) and C-O stretches (around 1200 cm^{-1}) from ester groups. These functionalities are in line with functionalities and groups found in the Algaenan IR traces reported in Figure 3-50 suggesting that most residual functionality in the bio-chars comes from the presence of algaenan, which is heat resistant up to high temperatures and has therefore survived many of the microwave pyrolysis processes.

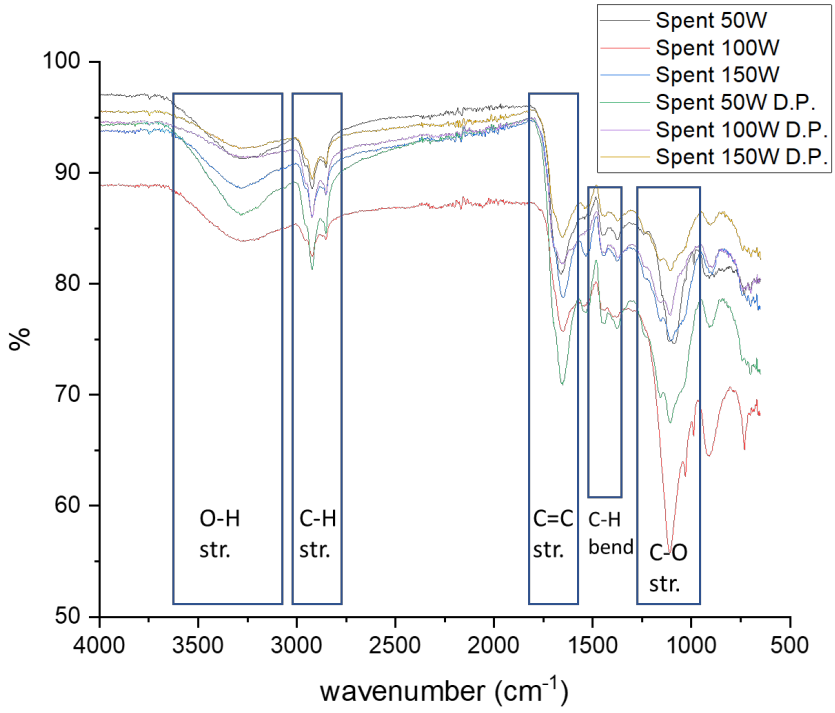

Figure 3-73 ATR-IR spectra of bio-char derived from spent biomass from both single and double pyrolysis

Like the spray dried bio-chars, the spent bio-chars also still show a lot of functionality which can also mainly be attributed to the algaenan, however the intensities of many bands such as the C-H stretches (2900 cm^{-1}) as well as C=C stretches (1650 cm^{-1} – 1700 cm^{-1}) are considerably lower in response. This is once again in line with previous findings, which have suggested a lower overall presence of Algaenan in the spent biomass due to the already undergone industrial lipid extraction process.

3.4.5 Analysis of bio-oil

Bio-oil yields (see earlier, Figure 3-65, Figure 3-66), similarly to the char, do not reveal any major trends apart from fluctuations ranging from around 10% to 32%. Bio-oil yields typically tend to be lower than char yields with the two largest yields obtained both at the lowest power setting of 50 W. Upon higher power an increased gasification of the pyrolysis products occurs which reduces both char and bio-oil yields.[188,267,272] Due to the still low temperatures achieved throughout these experiments the gas yields (difference between 100% and char + oil yields) are still lower compared to pyrolysis products formed at higher temperatures or powers.

For example, with microwave pyrolysis temperatures reaching up to 400°C and 800°C, Beneroso *et al*. have achieved char yields of around 45% and bio-oil yields of around 37.5% at 400°C while the highest temperature of 800°C has drastically reduced char yields (28% on average) as well as bio oil yields to as little as 15%.[188]

Hu *et al.* maximised bio-oil yields achieving maximum values of 35.83% for their bio-oil, which puts the achieved bio-oil values of up to 32% (Spray 50W and Spent 50W D.P.) well within the compared literature findings.

3.4.6 Analysis of bio-oil: GC-MS

GC-MS analysis of the bio-oils allows more insight to be gained into the influence of the pyrolysis process on the nature of the formed bio-oils and allows conclusions to be drawn towards the overall assessment of the completion of the pyrolysis process. GC-MS traces of the individual bio-oils are shown in Figure 3-74 and Figure 3-75. Where possible, the resulting peaks have been subjected to literature search in order to attempt to assign them to identifiable molecules. However, in many cases due to either low confidence values or nonsensical assignment, a general statement has been made to assign a molecule class (such as C16 or C20) rather than a specific compound. In the cases of myristic, palmitic and stearic acid, the retention times and fragmentation patterns have been matched with pure standards, hence the high confidence in their assignments. The results are summarised in Table 12.

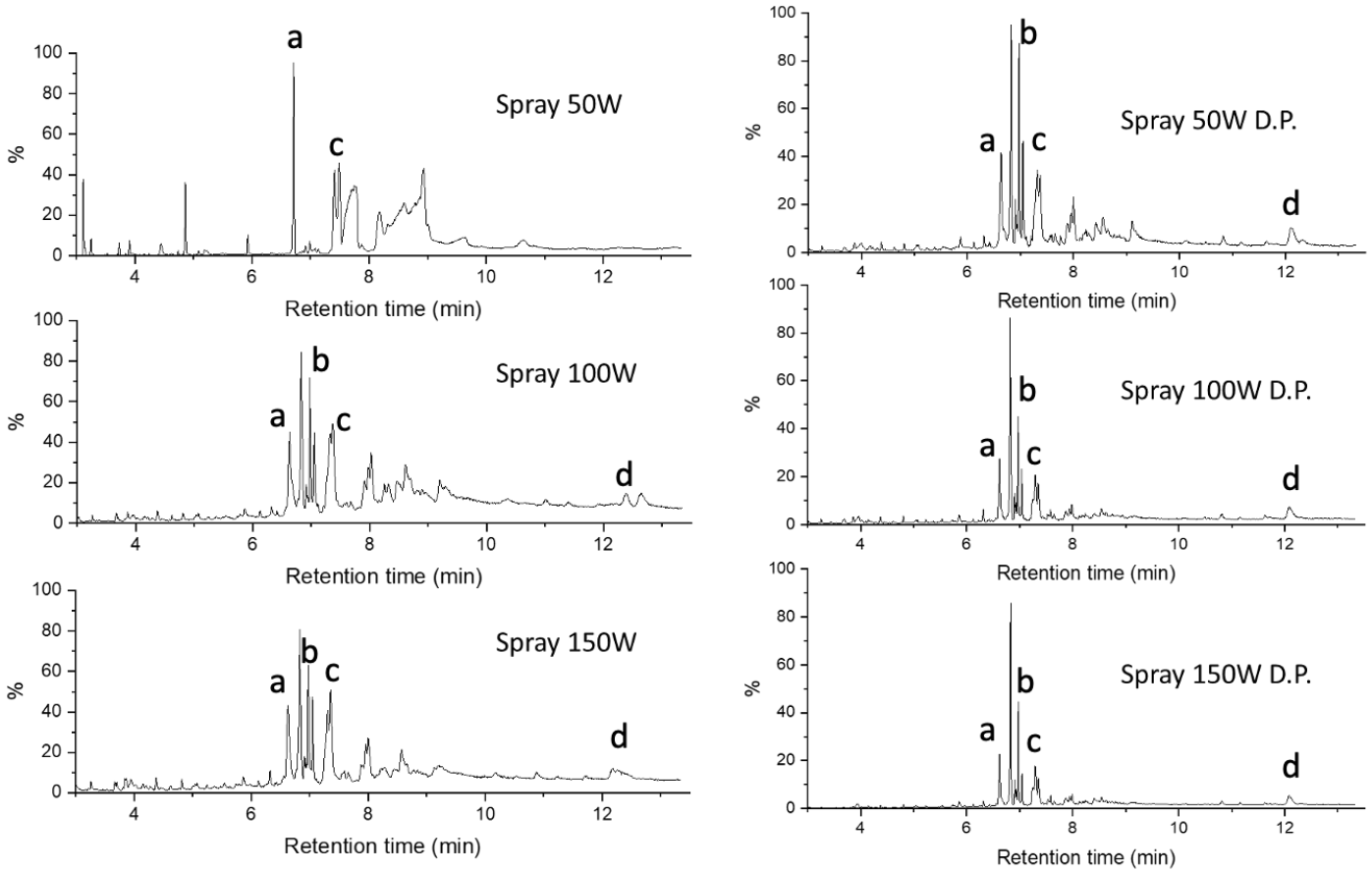

Figure 3-74 GC-MS traces of bio-oils from spray dried ALG01 (a = myristic acid, b = palmitic acid, c = stearic acid, d = vitamin E)

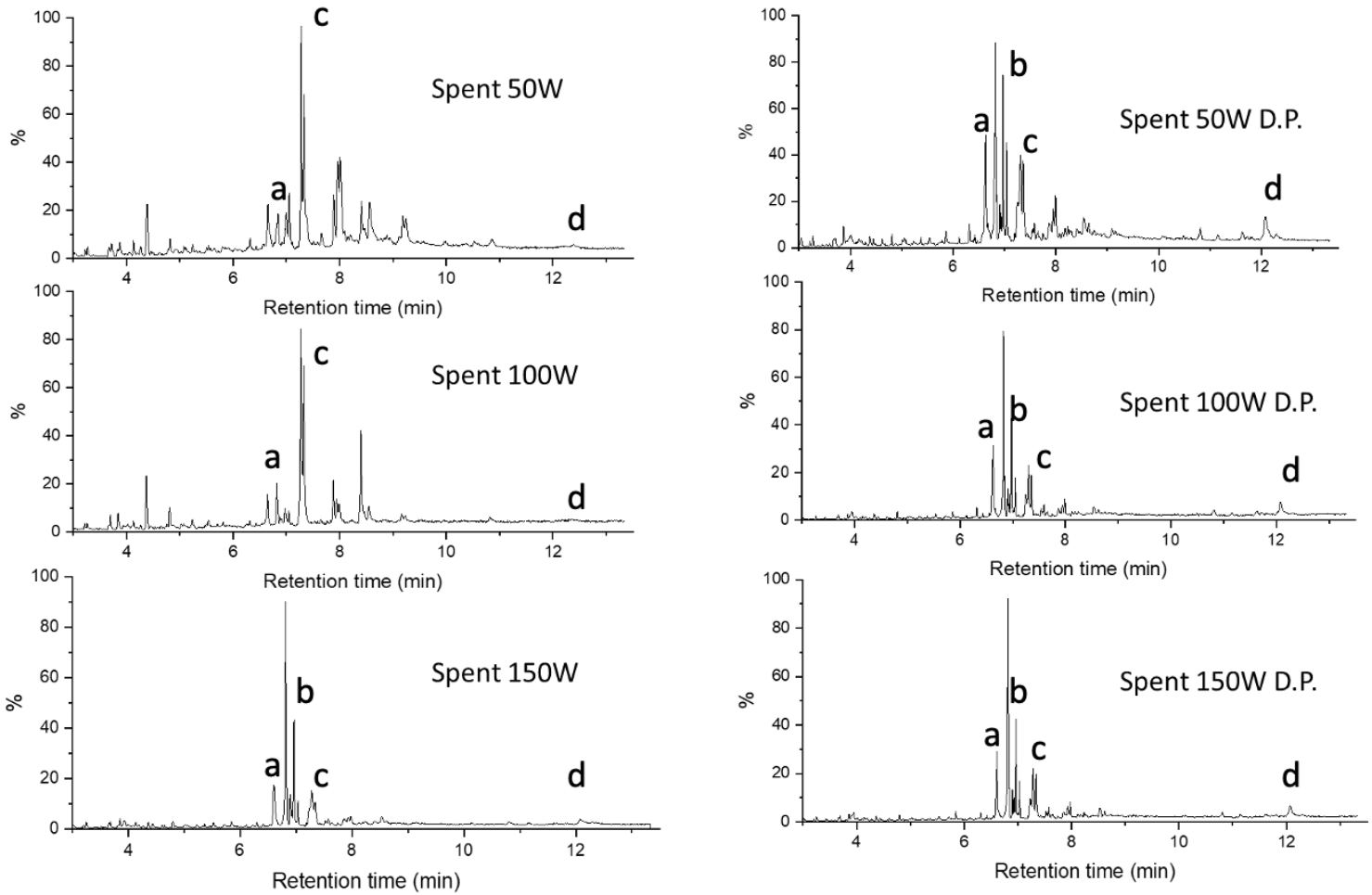

Figure 3-75 GC-MS traces of bio-oils from spent ALG01 (a = myristic acid, b = palmitic acid, c = stearic acid, d = vitamin E

Table 12 Retention times and corresponding compounds from literature search of GC-MS peaks from microwave pyrolysis bio-oils

Compound	Retention time/ min	Number of Carbon
Myristic acid	6.83	C14
Palmitic acid	6.98	C16
Stearic acid	7.33	C18
C20 molecules	~ 8	C20
C22 molecules	~ 9	C20
C24 molecules	~ 10	C24
Vitamin E	12.64	C29

From both the GC-MS traces as well as the identified compounds/ compound classes it can be concluded that higher microwave powers result in a great reduction in short-chain molecules between C2 and C6 that occur at retention times under 6 minutes. This can be attributed to the aforementioned more thorough pyrolysis process at these high powers. Furthermore, a double pyrolysis method shows greatly reduced peaks in the region below 6 mins even at low power, affirming the higher effectivity of the double process.

Apart from the peaks occurring at low retention times, peaks above 8 minutes are also being gradually reduced with increasing microwave power at 150W merely leaving a few intense peaks between 6 mins and 8 mins. This effect is more prominent in the single pyrolysis runs while the double pyrolysis runs appear more similar with fewer deviations amongst the three powers. This once again suggests, that either high powers or a double pyrolysis process achieve the most complete pyrolysis and the most similar results.
The most prominent compounds in all bio-oils have been assigned through matching with standards and literature search as myristic acid, palmitic acid as well as stearic acid which are all contained in every oil but with varying intensity. Most bio-oils contain myristic acid as the most abundant component with palmitic acid following closely after. Stearic acid is most prominent in Spent 50W, Spent 100W, Spray 100W and Spray 150W. All these runs are singly pyrolyzed. Stearic acid appears at much lower concentrations in the doubly pyrolyzed bio-oils, with the lower power samples containing more of it than the higher

power samples. This suggests that at more thorough pyrolysis stearic acid content is greatly reduced while myristic acid is favoured compared to palmitic acid almost by a ratio of 2:1 for the most thorough pyrolysis runs.

Straight-chain alkanes are a direct product of the pyrolysis-induced lipid decomposition and the acids found in the bio-oils are prominent in pyrolysis oils of other microalgal species, too.[270,273]

Notable is also the absence of phenolic compounds, amine containing molecules, pyridine-derivatives or nitriles which are usually produced from proteins during pyrolysis.[269,270,274] However, due to the induced formation reactions of these compounds from proteins beginning at temperatures of around 300°C, the highest temperatures reached in this project (280°C) are still below the decomposition threshold of proteins, thus the absence of nitrogen-containing compounds in the bio-oil.[275] Moreover, as the biomass used for pyrolysis has already undergone protein extraction in the previous step, the absence of these products in the bio-oil can accordingly be explained.

In addition, the very last peak at 12.64 min occurring in low intensities in all samples has been attributed to Vitamin E through both high probability in the literature search as well as cross-checking with a pure Vitamin E standard which eluted at a similar time, see Appendix Figure A4.

3.4.7 Analysis of bio-oil: ATR-IR

The ATR-IR spectra of all bio-oils are summarised in Figure 3-76. Similarly to the ATR-IR spectra of the bio-chars shown in Figure 3-72, all bio-oil traces are also almost identical with the exception of Spray 50W, the lowest power run with single pyrolysis, which as seen in Figure 3-64, only managed to reach a temperature of 168°C, well below the set maximum temperature of 280°C. The most notable difference is the much stronger presence of the C-O stretch centred around 1200 cm^{-1} which is much less intense in all other bio-oils, suggesting a potential functionality which has been degraded upon reaching higher microwave temperatures during the pyrolysis process.

Most prominently, two bands indicating the presence of saturated aliphatic chains (C-H stretch at 2900 cm^{-1}) as well as carboxylic acids (C=O stretch at around 1600 cm^{-1}) point towards the bio-oils mostly consisting of long chain, saturated acids. This supports the results obtained from GC-MS detailed in the previous section, which mainly found palmitic

and myristic acid within the bio-oils. This can not only be seen in the bio-oils from spray dried, but also from spent biomass as well as across the bio-oils, regardless of a single or double pyrolysis process, suggesting at least from the IR a very consistent composition profile.

3.4.8 Analysis of bio-oil: anti-oxidancy

Due to the possible presence of Vitamin E within the bio-oils, the antioxidant activity of the bio-oils was tested using the ABTS radical scavenging assay. All the bio-oils were tested at the same concentration and the results are shown in Figure 3-78.

The ABTS assay relies on the ABTS (2,2'-azinobis-(3-ethylbenzothiazoline-6-sulfonic acid)) molecule, which forms the $ABTS^{\bullet+}$ radical cation upon addition of potassium persulfate. This chromophore shows absorption wavelengths of 645 nm, 734 nm and 815 nm in addition to the 415 nm maximum which is most commonly used.[276] Upon addition of antioxidants to this cation, it is being reduced back to the ABTS form, a pathway which is shown in Figure 3-77. As the reduction reaction depends on many factors such as the antioxidant concentration, the antioxidant capability and the reaction time, the ABTS assay is able to discriminate between different types of antioxidants regarding their strength and is thus widely used for analysis.[276]

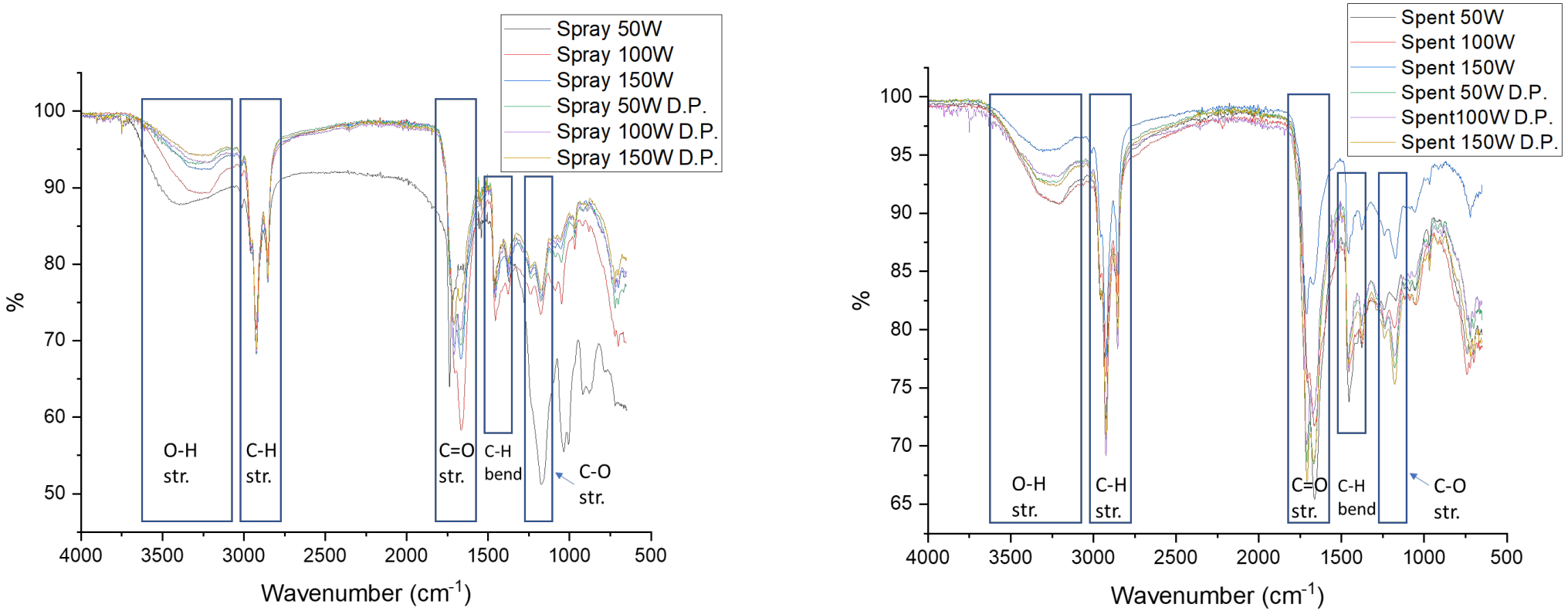

Figure 3-76 ATR-IR spectra of bio-oils obtained from both spray dried and spent biomass through single and double microwave pyrolysis

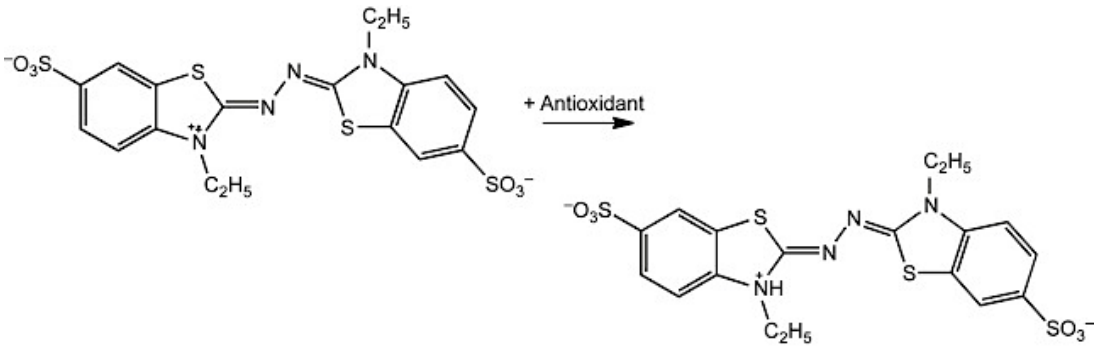

Figure 3-77 Radical scavenging scheme of ABTS radical with antioxidant[277]

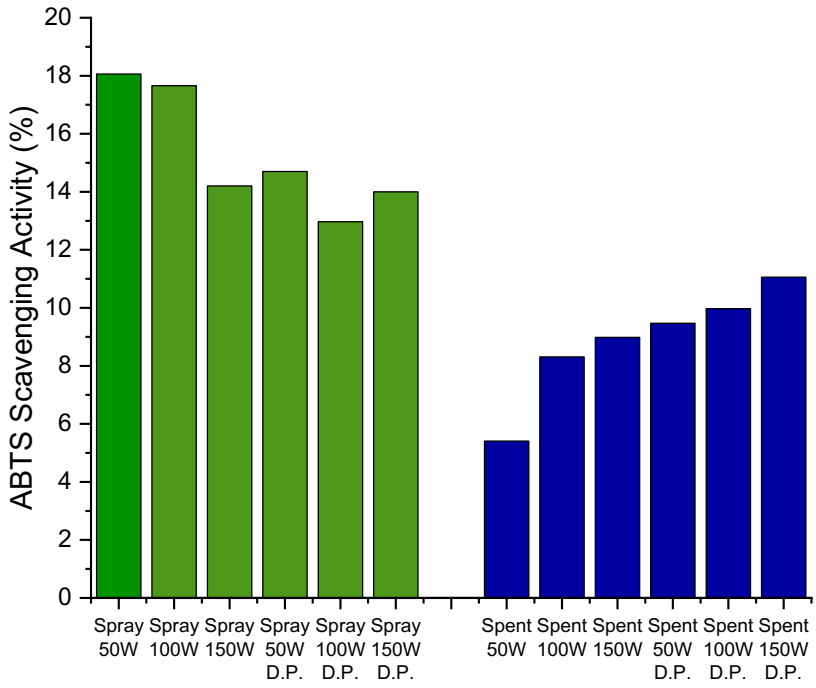

Figure 3-78 ABTS Scavenging Activities of all bio-oils produced from spray dried and spent biomass via single and double microwave pyrolysis

Evidently, the overall scavenging activities of the bio-oils derived from spray-dried biomass appear higher than those of spent bio-oils, with even the highest activity of a spent bio-oil (Spent 150W D.P. with 11%) not reaching the value of the lowest activity of a spray bio-oil (Spray 100W D.P. with 13%). This suggests a higher prevalence of radical scavenging compounds within spray-dried oils, such as Vitamin E, which has been found in all bio-oils,

polyunsaturated fatty acids or phenolics which could be responsible for this activity but have not been able to be confidently identified in this instance. Furthermore, while spray dried bio-oils seem to show a downwards trend in activity, the spent bio-oils show an upwards trend, both of which are difficult to explain in terms of their respective GC-MS chromatograms. Overall activity with a maximum at 18% (Spray 50W) and a minimum at 5.25% (Spent 50W) suggests a lower level of activity for the bio-oils overall, however one which is not negligible and could well be utilised for potential further future applications.

Chapter 4

Conclusions and Future Work

4.1 Conclusions

The work in this thesis has shown that a zero-waste microalgal biorefinery using ALG01 as a feedstock and employing greener, more efficient methods, for example, membrane filtration as protein purification instead of chemical extraction, using an acid- and TEMPO-free method of generating defibrillated cellulose and using microwave heating for hydrothermal treatment and pyrolysis instead of conventional heating, is feasible. There are real possibilities of implementing parts of the work into AlgaeCytes' new pilot plant. The success of combining peptide extractions, waste valorisation (through microwave pyrolysis as well as generation of defibrillated cellulose) and industrial EPA extraction has been proven, which gives industrial companies the flexibility to employ different pathways depending on their specific needs and market opportunities. The general conceptual biorefinery pathway developed within this thesis from initial microalgal feedstock to chemicals, materials and products as well as their respective potential fields of application is shown in Figure 4-1. It has been shown, that microalgal biomass fresh from harvesting (spray dried) behaves differently and yields products with different properties than microalgal biomass, which has already undergone the industrial lipid extraction (spent). This results in two different biorefinery pathways, each with different outcomes. The preferred biorefinery pathway (Figure 4-1), however, has been shown to be the one subjecting the algae to industrial extraction first, followed by using the spent biomass for the rest of the biorefinery process.

The nature of proteins and peptides obtained from both biorefinery approaches depends heavily on the type of biomass used as well as the pre-treatment method. Fully folded proteins are rather obtained from spray dried biomass using 'mild' extraction techniques such as manual grinding and ultrasonication, while all proteins derived from spent biomass, enzymatic treatment as well as microwave treatment occur to various degrees as hydrolysed peptides. Combining both high yields, purities and bioactivity, peptides derived from spent biomass having been pre-treated with powerful microwaves top the charts regarding all three aspects, thus making this method one of the most promising in terms of potential future applications as well as industrial scale-up capabilities. It is also preferred by AlgaeCytes with the aim to potentially market them as additives to the cosmetics market.

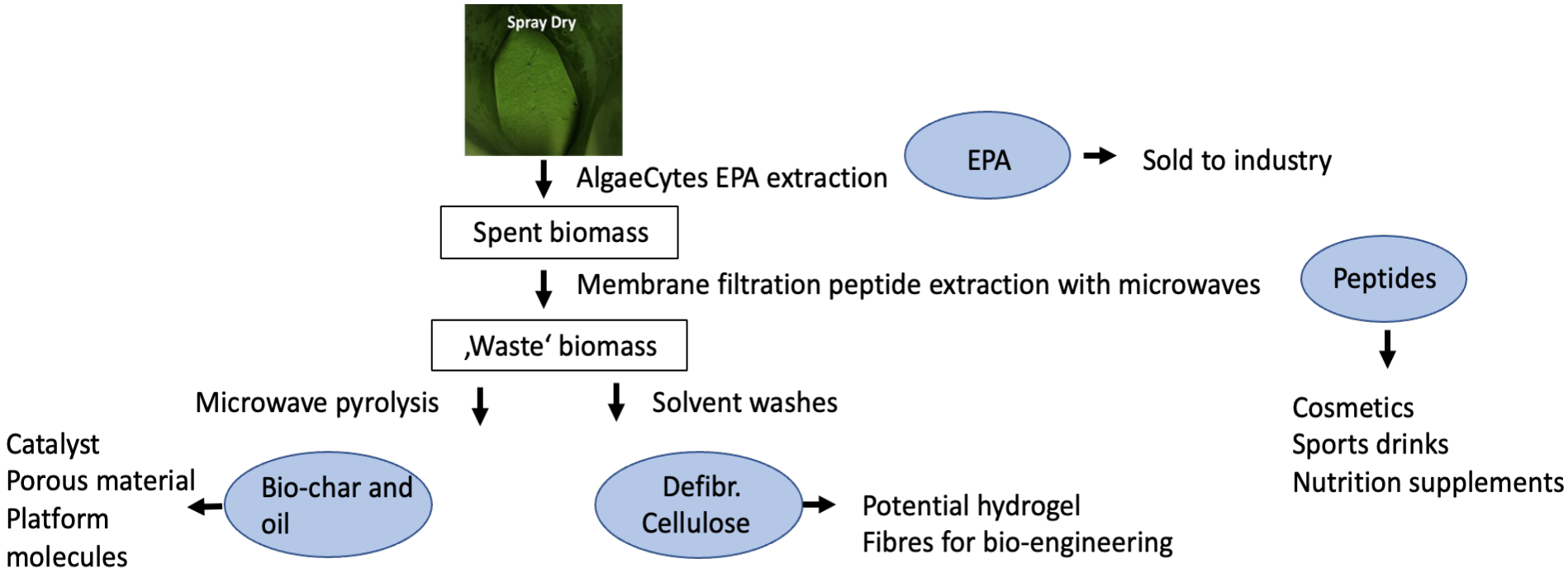

Figure 4-1 Proposed biorefinery schematic including potential applications for all side-products

This cell wall lysis induced through microwaves serves as an additional method to facilitate protein extraction from the tough microalgal cells. At the same time, this opens up an important route which directly can lead to bioactive peptides due to the hydrolysing nature of microwave radiation, which causes proteins to break down into peptides, thus combining both cell wall pre-treatment as well as bioactivity enhancement into a single step. To the best of knowledge, this aspect of the research is the very first to report hydrothermal microwave treatment coupled with membrane filtration to obtain microalgal proteins and peptides.

The resulting residual biomass (pellet) from protein extraction in this case will take a route towards the generation of defibrillated cellulose. This type of cellulose has previously been generated through a novel, acid-free and TEMPO-free water-based method, which also employs a hydrothermal microwave treatment, which in this case has served both as a cell disruption method to facilitate protein extraction, but also as a method to generate defibrillated cellulose for the first time from microalgae.[171,175,179]

The 'waste biomass' after protein extraction has been further valorised to yield bio-char and bio-oil (through microwave pyrolysis) as well as defibrillated celluloses. The bio-char analysis showed that energy densification has been achieved, with the chars serving as potential bio-fuel sources as well as potential chemical adsorbing materials due to their porous structure, which will have to be further investigated in future work on this topic. The bio-oils on the other hand, can serve as sources of platform molecules for various long-chain acids as well as Vitamin E, which has been found within them.

The defibrillated celluloses, which have been formed upon hydrothermal microwave treatment, can be used to form hydrogels for the highest microwave temperature samples from spent biomass, making them a potential application in medicine, wound treatment or cosmetics or thickeners.

4.2 Future Work

4.2.1 Future Work – Peptide Sequencing and Analysis

In addition to the already performed bioactivity testing at Newcastle University, which showed that the spent microwaved as well as the enzymatically hydrolysed peptides exhibited the highest bioactivity, more testing needs to be performed in order to better understand into which exact peptides cause this behaviour.

Mass spectrometry on the proteins with subsequent sequencing would be one way of identifying potential proteins or peptide sequences, which have been shown to exhibit similar properties in terms of bioactivity. Subsequently, potential isolation of these peptides would be performed to try and see, if the isolation results in an increase in bioactivity, or if the peptide mix obtained from ALG01 serves as an overall better product than individual isolated peptides. Upon this research it may be easier to start commercialising the peptides. A potential application in cosmetics would entail the use of bioactive peptides, which would not only provide the necessary stimulation and serve as an active ingredient, but also could open up ways of marketing the product as a vegan, sustainable product, which is in line with current trends favouring plant-based ingredients with algae gaining more and more popularity. Another potential application could be using the proteins as binders replacing egg whites in many industrial nutritional applications.

4.2.2 Protein Extraction using Deep Eutectic Solvents (DES)

A preliminary investigation on the use of Deep Eutectic Solvents (DES) was started but not explored further due to time constraints. DES utilise the concept of the eutectic mixture of two compounds (Figure 4-2), which form a liquid at a certain temperature and composition with the melting point of the mixture being lower than the individual melting points.[278–280]. They are often compared to another solvent class of recent popularity in green and sustainable research, i.e., ionic liquids. Some deep eutectic solvents can consist of ionic species, although in most cases their composition differs from that of ionic liquids and the main force holding the solvent together are hydrogen bonding instead of ionic forces. They have in recent years become the main focus of many research studies as they offer various advantages over conventional solvents as well as ionic liquids: they offer much

higher biodegradability, especially when natural DES are used, higher sustainability as well as better biocompatibility.[278]

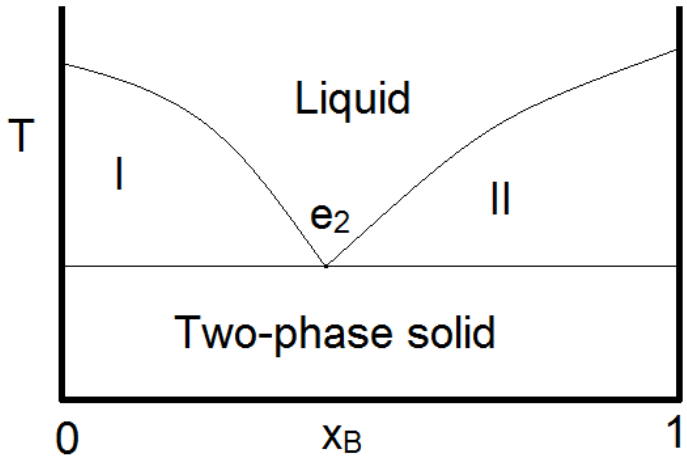

Figure 4-2 Phase diagram highlighting the eutectic composition with the eutectic point at e2

Deep eutectic solvents mostly consist of a hydrogen – bond donor such as urea, citric acid, glycerol or several diols or triols as well as cationic species that are able to accept these hydrogen bonds in order to form a DES. Most commonly, quaternary ammonium salts are used such as choline chloride. [278–280] Choline Chloride specifically occupies such a favoured position in DES synthesis as it is non-toxic, can be readily extracted from biomass and is cheap.[281] DES using choline chloride are furthermore biodegradable and possess 100% atom utilisation.[281] The exciting prospect of DES is that they can be fine-tuned to the compound class to be extracted as well as other factors impacting the effectiveness of the extraction process. By carefully choosing DES components as well as their ratios or the addition of water the overall yields can be maximised which makes their use very versatile for a wide range of reactions. Their non-flammable nature, low vapour pressure, non-toxicity and biodegradability makes them an ideal solvent class to invest more research in in the future. However, their considerable viscosity especially when utilising diols or triols such as glycerol can impact the handling of the solvent in laboratory experiments.

In order to attempt another alternative route towards protein extraction which has not been attempted widely for microalgae, the use of deep eutectic solvents (DES) was studied. Protein extraction using a DES consisting of choline chloride, 1,4-butanediol and water in a 1:3:1 molar ratio did not yield the desired results. Upon extraction using the DES, the resultant supernatant from centrifugation showed a deep green – brown colour

(Figure 4-3) similar to the one seen upon protein extraction using the conventional tangential membrane separation approach.

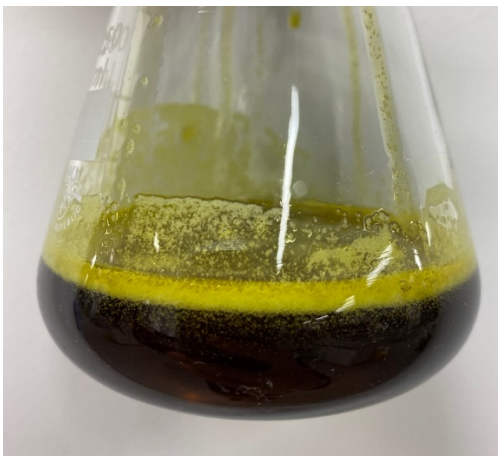

Figure 4-3 Supernatant of microalgae extracted with DES

However, upon addition of deionised water and saturated solution of ammonium sulfate in order to crash out the proteins, no precipitation occurred even after 24 h. However, strong foam formation was noted (see Figure 4-3) suggesting the presence of proteins in the DES.[282,283]

It was therefore decided to analyse the mixture and quantify the amount of proteins present in the DES by using the Bradford Assay. Protein samples were run in duplicates and the spray dried and spent microalgae were used to determine the difference of extraction efficiency with regards to prior lipid extraction. The results are displayed in Figure 4-7. In addition to the analysis of proteins in the mixtures it was also attempted to perform a protein back-extraction in order to further proceed with method development of obtaining a relatively pure protein powder at the end of the process.

In order to back-extract the protein from the DES the formation of a biphasic system was tried using a K_3PO_4 salt solution as the aqueous phase. To find the optimal conditions for formation of a biphasic system, various concentrations were made and mixed with an equal volume of fresh DES (Figure 4-4).

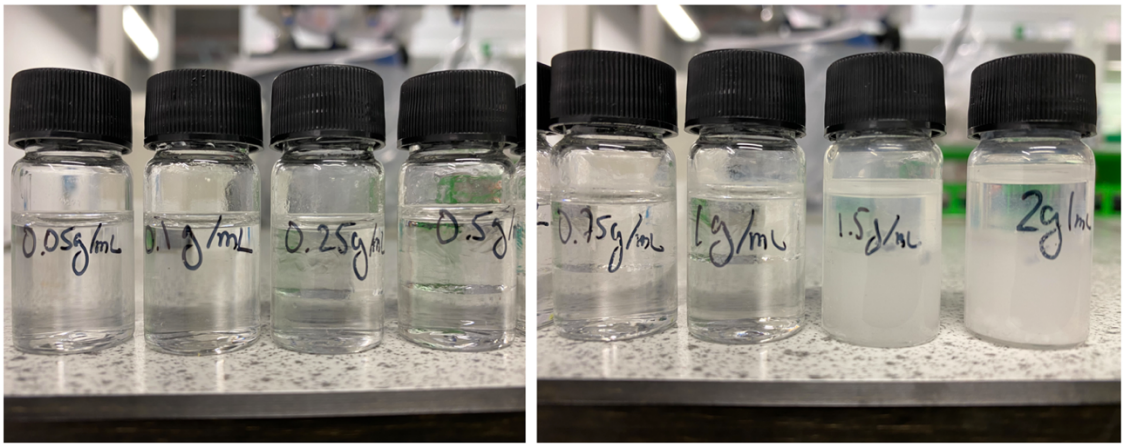

Figure 4-4 Biphasic system formation at different concentrations of K_3PO_4

A biphasic system was not formed for 0.05 g/mL and 0.1 g/mL. The concentrations of 0.25 g/mL, 0.5 mg/mL and 0.75 g/mL all formed biphasic systems although a more equal phase distribution was observed for 0.5 g/mL and 0.75 g/mL only. The 0.25 g/mL showed a larger DES fraction even though an equal volume of both were added. The 1 g/mL solution turned cloudy after half an hour of standing suggesting precipitation of the salt. Both the highest concentrated samples suggested that the concentration of salt was above the maximum solubility of K_3PO_4 in water, as the salt did not fully dissolve.

Due to the similar phase forming properties of both 0.5 g/mL and 0.75 g/mL it was decided to go ahead with the lower concentration of the two samples. However, upon addition of an aqueous solution of K_3PO_4 at a concentration of 0.5 g/mL, a biphasic system could be formed. Upon vigorous shaking and re-formation of the two phases the aqueous layer was dried. Due to the high amount of salt present in the aqueous phase and the low concentration of potential extracted protein, CHN analysis reported nitrogen percentages below the detection limits with 96% of the elemental analysis being flagged up as being 'Rest', confirming the high presence of salt in the dried aqueous fraction.

Figure 4-5 shows the IR spectra of the pure DES as well as the aqueous phase upon extraction.

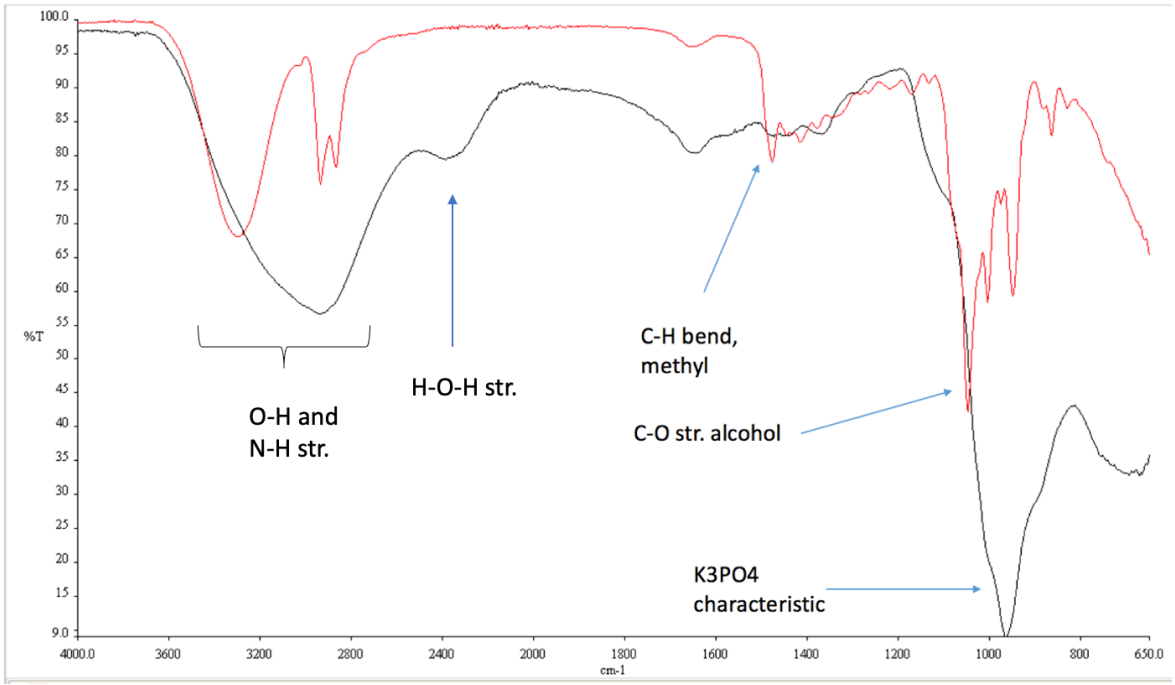

Figure 4-5 IR spectra of pure DES (red) as well as aqueous phase after extraction (black)

From the IR spectra it can be seen that there is not too much similarity between the DES and the aqueous phase suggesting little mixing between the phases or leeching. The IR of the pure DES confirms its components with the amine stretch and the C-H bend referring to the tertiary amide centre and the surrounding three methyl groups found in choline chloride while the C-O and O-H stretches refer to the alcohol functional groups in the 1,4-butanediol. The aqueous phase shows a very strong band around 950 cm^{-1} which is characteristic to K_3PO_4 confirming that most of the dried aqueous phase was indeed the potassium salt.[284] The broad O-H stretch could refer to residual water left in the sample. Furthermore, some amide functionality that might induce vibrations in the characteristic regions around 1640 cm^{-1} is evident, however very weak in appearance which could be due to the excess amount of salt in the sample overpowering any amide functionality in the spectrum. The unusual band at 2400 cm^{-1} could correspond to H-O-H stretching vibration of water crystallisation complexing to the potassium phosphate salt.[285,286]

The compiled results of the Bradford Assay analysis are shown in Figure 4-6 with yields shown in Figure 4-7.

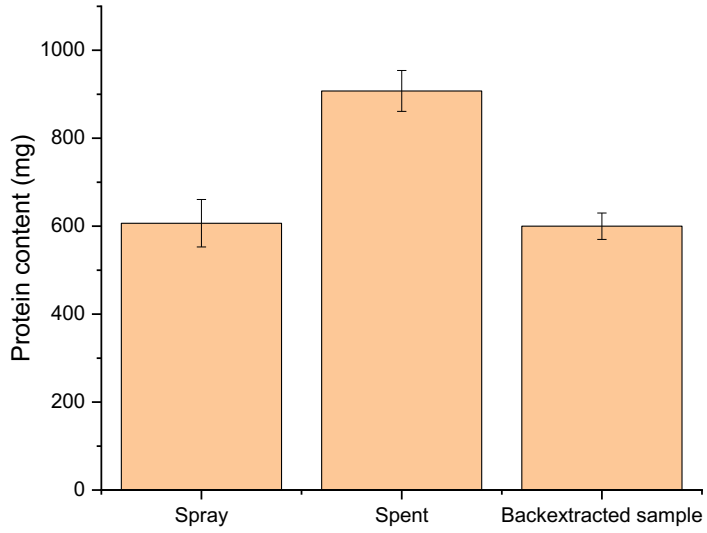

Figure 4-6 Amount of protein extracted from different biomass using DES, analysed via Bradford Assay

The differences between the individual runs are within the boundaries of normal errors happening during the reactions, measuring etc. All Bradford Assay measurements were run in triplets with the average being used for the calculations. Overall, it is clear that the spent biomass results in a higher protein content in the DES mixture, which is in line with previous findings that spent biomass proteins and peptides extract more easily, due to the prior industrial lipid extraction process. Yields have been calculated to be 21.1% for spent biomass and 15.97% for spray dried biomass which amounts to an overall protein recovery of 52% for spent and 39% for spray dried biomass.

Compared to literature, many groups have found protein recoveries of 27% to 95%, with the average around 80%.[287–291] It has to be noted, though, that many methods included an additional ultrasonication step, which in the case of Cicci *et al*, has resulted in only 27% protein recovery compared to the 52% and 39% obtained for ALG01 without additional pre-treatment.[287] The comparatively low values when looking at literature protein recovery of up to 90% could be explained through many non-water soluble proteins or nitrogenous matter being present in ALG01 which cannot be extracted using neither water nor DES.

The back-extracted sample using K_3PO_4 salt also yielded a protein content of 600 mg which accounts for a 98.8% back-extraction efficiency. Compared to literature, the back-

extraction efficiency for this method of 98.8% is significantly higher, with most findings reporting back-extraction efficiencies ranging between 9.47% and 34.35% depending on the salt concentrations used.[281,292,293]

However, the 600mg of proteins were still mixed in with approximately 51 g of salt which has not been successfully separated. In order to compare the efficiency of the DES extraction method with the more conventional water-based extraction using ultrafiltration membranes the extraction yield was calculated and displayed in Figure 4-7.

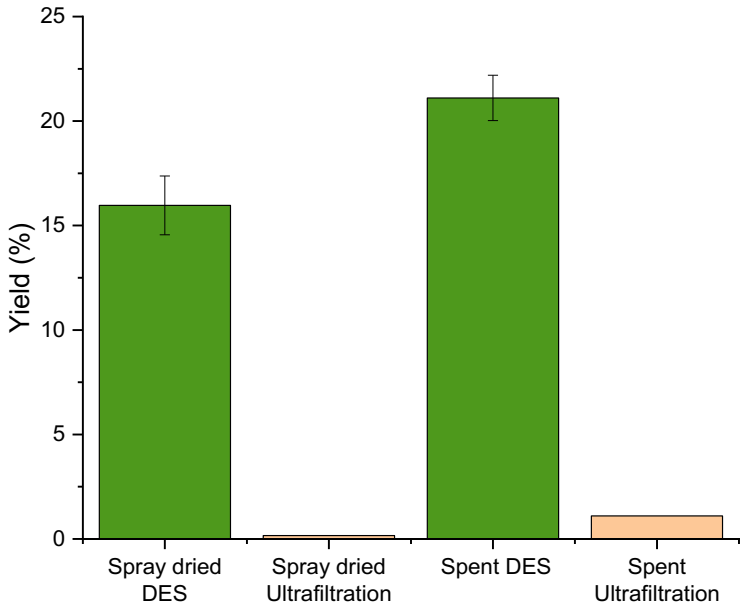

Figure 4-7 Extraction yield of proteins extracted from spray and spent algae compared to protein yields using ultrafiltration

In line with the total content of proteins in the DES, the extraction yield for the spent biomass was higher than the spray biomass with an average 21.1% compared to an average 15.97%. These yields prove to be very high compared to the ultrafiltration method whose yields are considerably lower, approximately by a factor of 100 for the spray dried and a factor of 20 for the spent biomass.

These comparisons on first glance make a strong point towards adopting the DES-based extraction method when extracting proteins due to the significantly higher yields. However, the problem of back-extracting the proteins plays a vital part of the method development and is ultimately the crucial determining factor in the success or failure of the DES-based approach as proteins in form of a relatively pure powder are the desired

outcome which so far can be better realised by aqueous extraction and further purification using ultrafiltration membranes, as shown earlier in this chapter. Unless the back-extraction problem is satisfactorily solved, most DES-based extraction methods found in literature might boast high protein recoveries, which are essentially not practical as the proteins only exist within the DES mixture or upon back-extraction within a heavily salt-rich fraction.

4.2.3 Future Work – Scale-up of protein extraction for pilot plant

This research is in close collaboration with the industrial partner AlgaeCytes Ltd. and aims to establish a sustainable, zero-waste microalgal biorefinery, which not only works in the laboratory and academic sense of being in itself a complete picture, but also focuses on being scalable to pilot plant levels. The appropriate pieces of equipment employed such as membrane filtration, microwaves and ultrasound are all not only efficient and green, but also scalable, which is of utmost importance to move from the laboratory research stage towards industrial implementation. Thus, further work needs to be conducted specifically with AlgaeCytes Ltd. to attempt pilot-scale extractions and purifications on the order of using several kg of ALG01 instead of just 10 g in order to assess not only efficiency and scalability, but also financial optimisation and the limits to which operations can be scaled up to. Especially technology such as microwaves will prove to be a limiting factor for expansion at some point, which will need to be assessed.

4.2.4 Future Work – Defibrillated Cellulose Hydrogel Testing

Testing of the hydrogel formation capabilities of the DFC samples showed, that a comparatively short-lived gel can be generated only using high concentrations of defibrillated cellulose samples (more than 3% of cellulose in water). Further experiments will have to be undertaken looking at the rheological properties of the hydrogels to see if they can be used for applications.

4.2.5 Future Work – Pyrolysis Bio-char properties

The bio-chars obtained from microwave pyrolysis have already been analysed with regards to their composition and thermal degradation profiles. However, further research will have to be conducted to characterise their porosity, ability to adsorb biomolecules as well as to evaluate their potential use as solid-state catalysts for chemical reactions.

4.2.6 Future Work – Algaenan Research

Isolated algaenan from the DFC samples has shown, that the samples still contain impurities in the form of residual cellulose. Future work will attempt to further purify the algaenan fraction and determine its monomer composition by subjecting it to Mass Spectrometry.

4.2.7 Future Work – Fucoxanthin biorefinery from ALG15

Fucoxanthin is a xanthophyll pigment which is predominantly found in the chloroplasts of brown macroalgae as well as diatoms with it contributing to around 10% of global carotenoids. [37,103] This major carotenoid pigment (constituting around 10% of all natural carotenoids[38]) is of high commercial value, fetching prices of around 11 Euro/ mg.[38] Its structural uniqueness stems from the presence of allenic bonds, conjugated carbons, epoxides and acetyl groups (Figure 4-8).

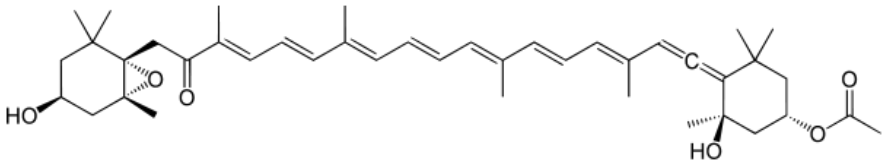

Figure 4-8 Molecular structure of fucoxanthin

Fucoxanthin behaves as a radical-scavenging antioxidant, exhibits anti-inflammatory, anti-cancer and anti-diabetic properties as well as protecting cardiovascular health amongst many more. [294]

The main role of fucoxanthin in microalgal cells is the function of a light-harvesting pigment working as an effective scavenger of singlet oxygen ($^1O_2$) as well as peroxy radicals ($ROO^{\cdot}$).[45] It is reported to scavenge these radicals better than other pigments such as lutein or *beta*-carotene with a high energy transfer efficiency of around 80%. [36,295,296]

Fucoxanthin extraction optimisation has been a prime focus of algal research. Traditional methods utilise a wide variety of solvents such as acetone, chloroform or methanol which generate a lot of solvent waste and are not ideal when trying to establish a green and sustainable extraction process. Recent publications [294,297] have shifted the focus towards methods such as subcritical extraction which managed to achieve yields of 0.69 +/- 0.05 mg/g of wet cell weight. [297] However, extraction optimisation highly depends on the used species as well as different needs and requirements with regards to the final product

including purity and further application. Therefore a 'one-size fits all' method has not been described in the literature before. Overall fucoxanthin content depends on various factors such as seasonality and species but oscillates between 0.05 – 2.96 mg/g of dry biomass. [38] *T. Lutea* has been shown to be the microalgal species with the highest amount of fucoxanthin production at 18.23 mg/ g.[296] Its lack of a cell wall also aides the ease of extraction with rigid microalgal cell walls often inhibiting any extraction from microalgae.

In addition to difficulties choosing the appropriate extraction method the stability of fucoxanthin is weak upon commercial production as it is sensitive to light, heat and low pH degradation which requires it to be stored in the dark at cooler temperatures.[38] Recently the focus has shifted away from macroalgae towards microalgae in terms of industrial extraction of fucoxanthin, as microalgae are easier and less complicated organisms in terms of their structure and cultivation and harvesting, but also their extractability. [296]

Amongst the most significant parts of this body of work, which is to be extended within future work, is the extraction of fucoxanthin from the marine diatom species ALG15, and its biorefinery potential combining fucoxanthin extraction with protein extraction, determining the impact of different fucoxanthin extraction methods on the proteins and vice-versa. The 'waste' biomass subsequently will have to be valorised either through microwave pyrolysis or the conversion to defibrillated cellulose.

Research has already been started on optimising the fucoxanthin extraction itself, with fucoxanthin extraction yield and purity the two determining factors. This work was curtailed due to time lost during Covid. Extraction of fucoxanthin has been performed in ethanol using ultrasound as a pre-treatment followed by extraction at 40^{o}C and gradient elution silica gel column chromatography to obtain the red fraction, which contains the fucoxanthin. The silica column containing the fucoxanthin fraction is shown in Figure 4-10. Various extraction parameters have been varied, such as the biomass to solvent ratio as well as the extraction time. The already obtained results are summarised in Figure 4-9.

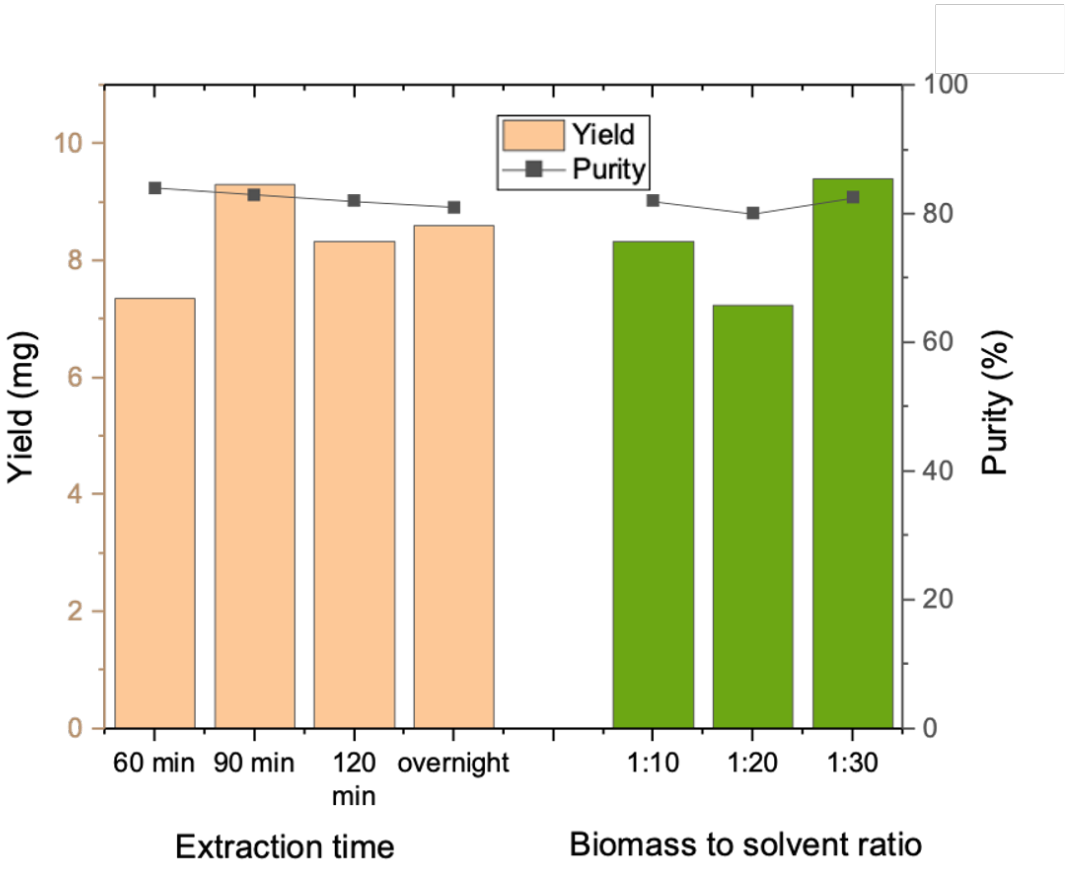

Figure 4-9 Fucoxanthin yield and purity depending on extraction time and biomass to solvent ratio, obtained from ALG15, a diatom species.

It can be seen that purity values (obtained from HPLC) appear to be very constant and do not fluctuate excessively, mainly staying between 80% and 85%. Yield, however, varies slightly more with maximum yields obtained for 90 min extractions (9.3 mg/ 10 g biomass) and a biomass to solvent ratio of 1:30 (9.3 mg/ 10 g biomass). The results have shown that there is no extraction time under which the yield drastically increases or decreases suggesting that even at short extraction times most of the contained fucoxanthin is collected and that the additional reward of extending the stirring time does not outweigh the energy and time constraints put on the method. An extraction time of 90 min is therefore assumed to be the optimal time period. These two parameters therefore suggest being ideal for method optimisation regarding the extraction of fucoxanthin from ALG15, as they show both high yields as well as purities being close to the maximum purity (82% for both).

The HPLC chromatograms of the pure fucoxanthin standard as well as the red fraction

containing fucoxanthin from extraction are shown in Figure 4-10, along with the appearance of the silica gel column with the fucoxanthin fraction circled in red.

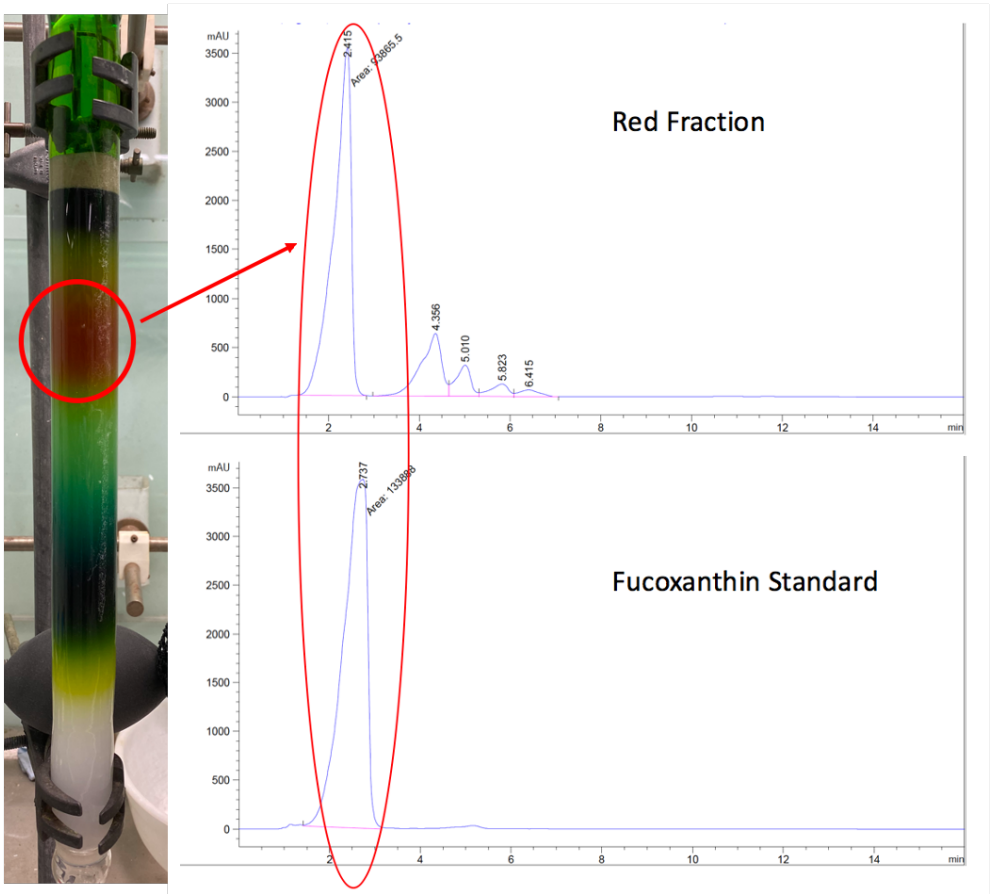

Figure 4-10 HPLC chromatograms of red fraction obtained from silica column chromatography (shown in the left) using gradient elution of ALG15 ethanol extract upon ultrasonication, as well as the pure fucoxanthin standard

As can be seen, apart from fucoxanthin various other pigments co-elute upon extraction, most of which are carotenoids as well as chlorophyll. These, adhering to the general picture of a zero-waste biorefinery, can be further sold as pigments and platform molecules to various industrial companies for different applications.

In addition to optimising the extraction of fucoxanthin, more work needs to be put in to identify possible isomers within the mixture as well as to identify the remaining 17% of contaminants within the fucoxanthin containing fraction, which is necessary in case further commercialisation is to be pursued regarding fucoxanthin from ALG15. The used method involving ultrasonic pre-treatment instead of no pre-treatment has already been shown to

generate fucoxanthin which possesses higher antioxidant and ABTS radical scavenging activity than standard fucoxanthin, as shown in Figure 4-11.

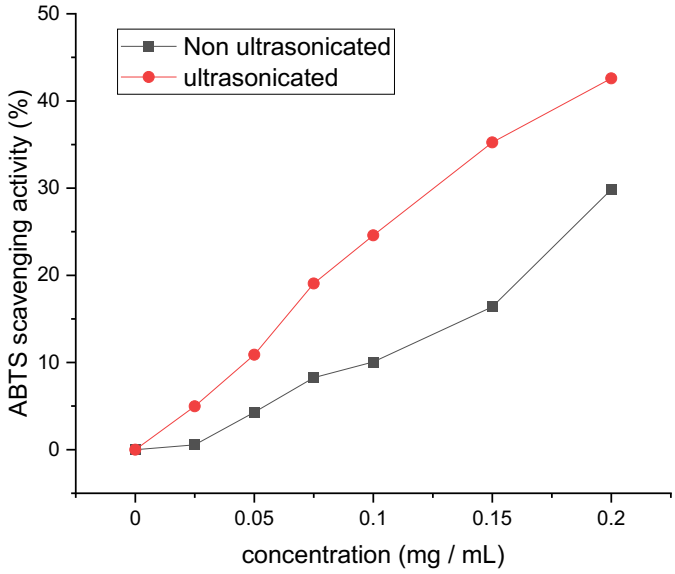

Figure 4-11 ABTS scavenging activity of both ultrasonicated and non-ultrasonicated fucoxanthin from ALG15

Appendix

Section 1 – Protein Extraction Using DES

The following section details the experimental methodology for protein extraction using DES.

A.1 Protein Extraction using Deep Eutectic Solvents

A1.1 Protein Extraction Using Deep Eutectic Solvents (DES)

A.1.2 Preparation of DES

Choline Chloride (hydrogen bond acceptor), 1,4-butanediol (hydrogen bond donor) and deionised water were mixed according to a molar ratio of 1:3:1 and heated to 100°C for one hour under constant stirring in order to ensure mixing and formation of the desired DES.

A.1.3 Protein Extraction using DES

The desired ALG01 (10 g) was mixed with the choline chloride : 1,4-butanediol : water DES (100 mL) and heated under stirring for 80 minutes at a temperature of 80°C. The resulting mixture was cooled to room temperature and centrifuged as previously at 3900 rpm for 10 minutes. The resulting supernatant was isolated, vacuum filtered, collected and combined with the supernatant resulting from the centrifugation of another wash of the pellet with fresh DES. An excess amount of deionised water (300 mL) was added to the combined and filtered supernatant, and the mixture was left to effect protein precipitation. Ammonium Sulfate (saturated solution) was added to salt-out the proteins to aid precipitation but without any success. Thus, in order to separate proteins from the DES, an aqueous solution of K_3PO_4 (0.5 mg/ mL, 70 mL) was added to the DES/protein mixture, shaken in a separating funnel and left to separate after which the aqueous phase was run off and freeze dried to afford a crystalline, white solid, which was analysed by CHN and ATR-IR.

Section 2 – Fucoxanthin Extraction

The following section details the experimental methodology for fucoxanthin extraction as well as its characterisation

A2. Fucoxanthin Extraction from Diatom ALG15

A2.1 Fucoxanthin Extraction with ultrasound pre-treatment

Diatom samples (1 g) were immersed in ethanol (10 mL). The mixture was ultrasonicated with a Sonics Vibra Cell probe by placing it in an ice bath an irradiating it for 30 minutes with a 3 second pulse followed by a 1 second pause. Amplitude was set at 75%. The sample was subsequently stirred for various times at 40°C, filtered via vacuum filtration and the filtrate concentrated using rotary evaporation. The times that were used in the method optimisation were 60 minutes, 90 minutes, 120 minutes and overnight. For the 120 minute run upon ultrasonication the solvent to biomass ratio was varied from 1:10 to 1:20 and 1:30 by adding the necessary amount of ethanol before the stirring phase at 40°C.

A2.2 Silica Column Chromatography Pigment Purification

The concentrated pigment sample was loaded onto a silica-gel column and eluted with gradient elution using a mixture of hexane and ethyl acetate starting with a 2:1 ratio to separate beta-carotene as well as chlorophyll before eluting the fucoxanthin fraction with a 1:1 ratio followed by the collection of it with 1:2 hexane : ethyl acetate.
The different coloured fractions were collected and submitted for HPLC analysis.

The yield of fucoxanthin was calculated using Equation 2.12:

Equation A.1:

Fucoxanthin yield (%) = (Weight of fucoxanthin/ Weight of raw dried biomass) x 100
Equation 2.12

Upon obtaining the red fucoxanthin containing fraction a second further purification via column chromatography was performed by loading the fucoxanthin fraction onto another column and eluting it using a solvent mixture of hexane : ethyl acetate of 1:1 followed by a final wash with a 1:2 ratio. Collected fraction were submitted for HPLC service.

A2.3 ABTS Antioxidant Assay

ABTS stock solution (7mM in dH_20) was mixed with potassium persulfate (2.45mM) in a 1:1 ratio and incubated in the dark overnight at room temperature.

This mixture was then diluted with Ethanol until absorption on a Jasco 550 UV-vis spectrometer reached 0.700 +/- 0.05 at 734 nm.

Two types of fucoxanthin were used for the assay: ultrasonicated and purified fucoxanthin as well as non-ultrasonicated and purified fucoxanthin. Each sample was prepared in the following concentrations:

0 mg/mL, 0.025 mg/mL, 0.05 mg/mL, 0.075 mg/mL, 0.100 mg/mL, 0.150 mg/mL, 0.175 mg/mL and 0.200 mg/mL.

For analysis, each sample (20µL) was mixed with the prepared ABTS mixture (980 µL), incubated at room temperature for 30 minutes and the absorbance was read at 734 nm.

A2.4 HPLC for fucoxanthin analysis

The purified fucoxanthin was analysed using high performance liquid chromatography equipped with a UV-vis detector. Separation was carried out using an analytical column, C18 (250mmA, 4.6mm, 5µm) was maintained at 30^{o}C. Sample volume of 1µL was injected to the column followed by elution solvent methanol : water (90:10 v/v). The elution parameters were fixed as follows: flow rate of 1 mL/ min, isocratic elution for 20 min and detection wavelength at 449 nm. HPLC was run by Dr Richard Gammons at the GCCE, University of York.

Section 3 – Appendix Experimental & Results and Discussion

A3-1 – Bioactivity Testing Protocol for spent microwaved and enzymatically hydrolysed peptides

Pepsin and trypsin modulation were assessed in the trinitrobenzenesulfonic acid, n-terminal assay.[232] Cell viability and cytokine release were assessed using Caco-2 cells grown in a 24 well flat plate format. Cell viability was assessed using the Promega Cell Titre Blue method.

Cytokine release was assessed using the following methods:

- IL-8 – DuoSet ELISA Human IL-8/CXCL8 (R&D Systems)
- IL-6 - DuoSet ELISA Human IL-6 (R&D Systems)
- TNF-α – DuoSet ELISA Human TNF-α (R&D Systems)

All peptides were assessed using a concentration of 0.1 mg/ mL.

A3-2 – Bioactivity Testing Protocol for spent microwaved peptides

For this second round of testing, 3 plates of Caco-2 cells were grown in 24 well transwell plates, for at least 21 days. Cells were exposed apically to Peptide Extract Samples or controls at the concentrations indicated as follows: Test samples were incubated for 120 minutes with the cells and apical and basolateral samples were collected and analysed for:

- o IL-8
- o IL-6
- o TNF-α o IL-10

Samples and positive controls were tested at the following concentrations in Table A1.

Table A1 Peptide samples and positive controls along their tested concentrations

Sample Type	Reporting Nomenclature	Tested Concentrations
Peptide Extracts	Spent 160	0.5, 0.125 and 0.03125 mg/ ml
	Spent 180	0.5, 0.125 and 0.03125 mg/ ml
	Spent 200	0.5, 0.125 and 0.03125 mg/ ml
	Spent 220	0.5, 0.125 and 0.03125 mg/ ml
Untreated Samples	Untreated Control	0.5, 0.125 and 0.03125 mg/ ml
	Lipopolysaccharide	100 ug/ mL
Positive Controls	Flagellin	33.3. ug/ mL

The results of the assays are summarised in Figure 3-62.

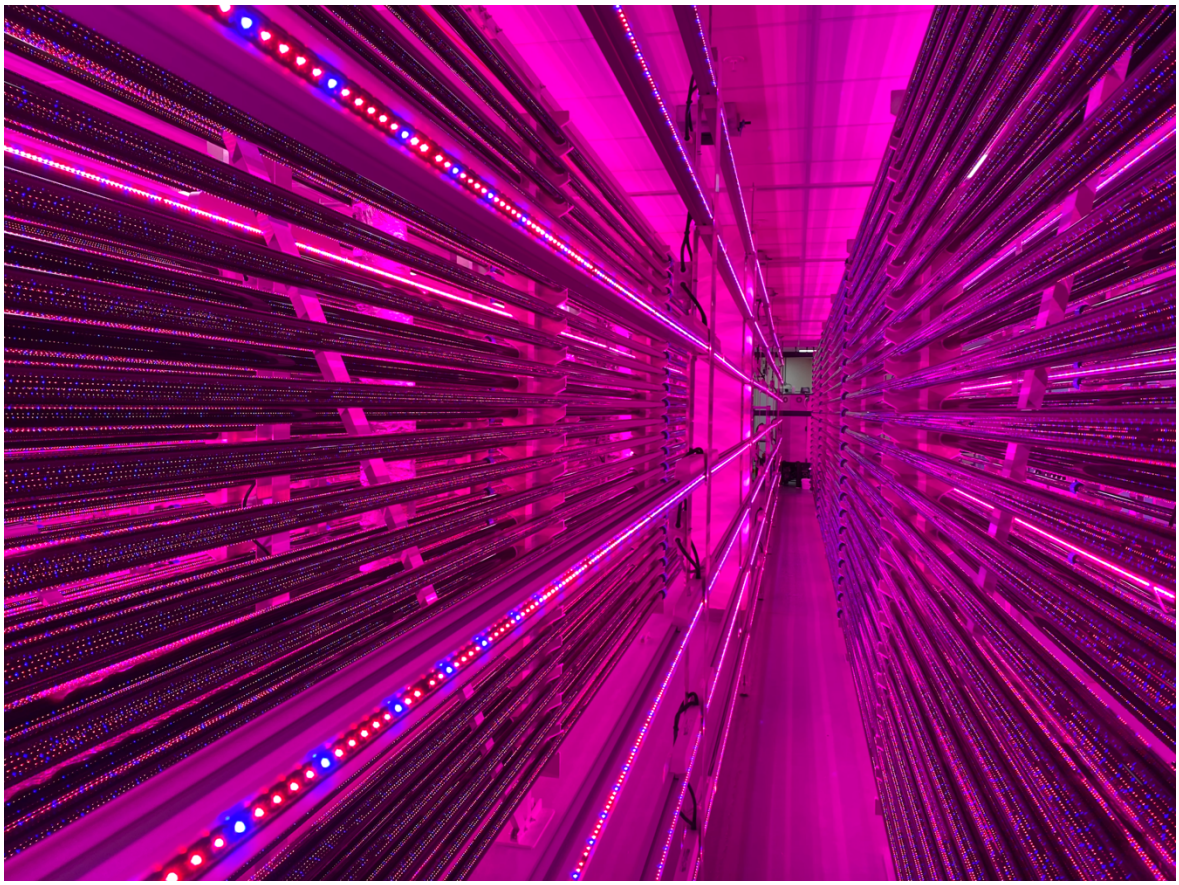

Figure A1 Tubular reactor for ALG01 at AlgaeCytes Ltd., Discovery Park, Sandwich, UK

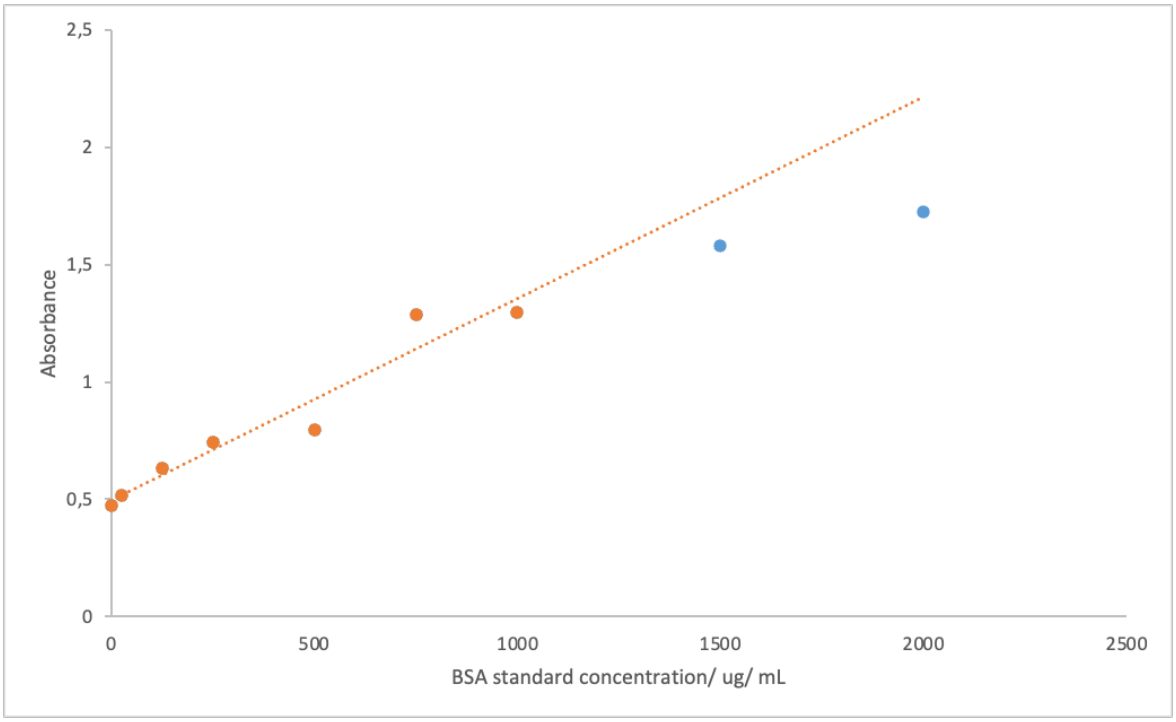

Figure A2 Bradford Assay calibration curve

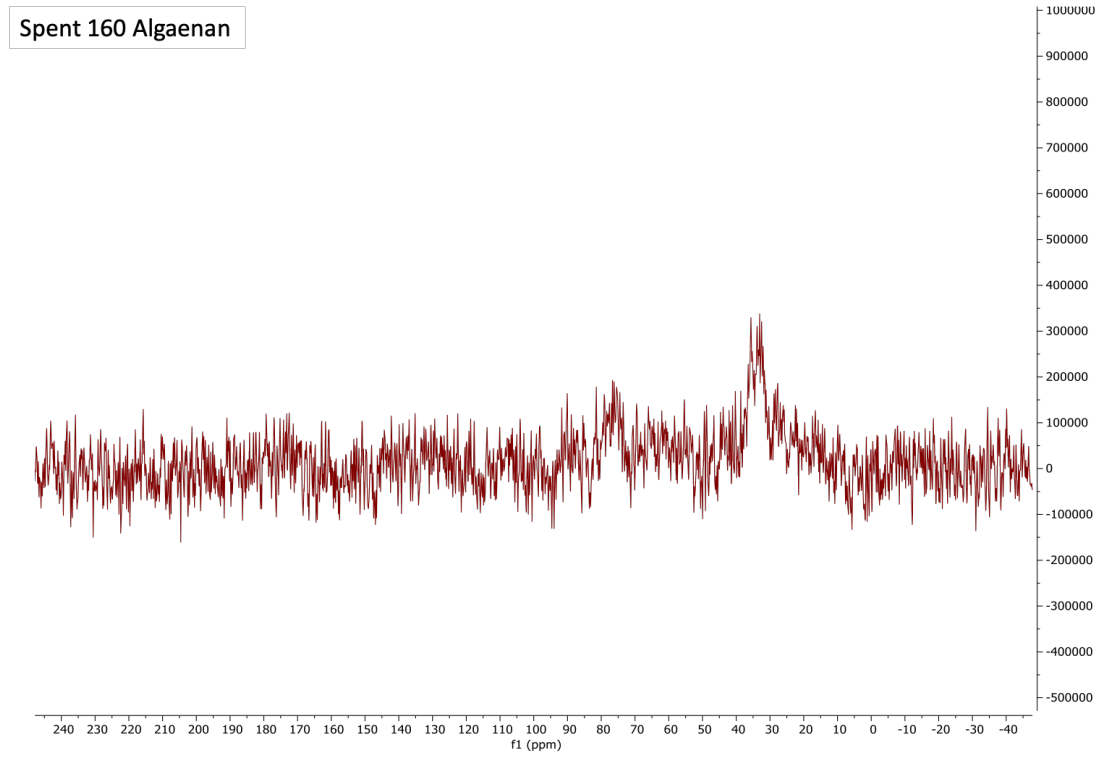

Figure A3 Solid State NMR spectrum of Spent 160 Algaenan

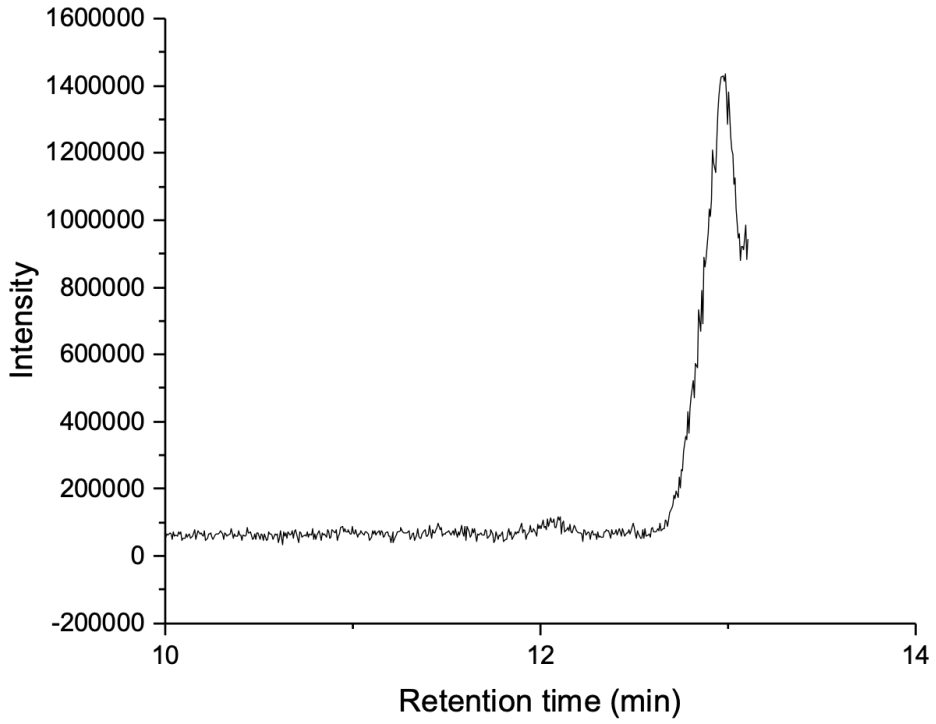

Figure A4 GC-MS spectrum of pure Vitamin E standard

References

1 F. Cherubini, *Energy Convers. Manage.*, 2010, **51**, 1412–1421.
2 N. L. Panwar, S. C. Kaushik and S. Kothari, *Renewable Sustainable Energy Rev.*, 2011, **15**, 1513–1524.
3 T. Searchinger, R. Waite, C. Hanson, P. Dumas, E. Matthews and C. Klirs, Creating a sustainable food future: A menu of solutions to feed nearly 10 billion people by 2050. Final report, https://agritrop.cirad.fr/593176/1/WRR_Food_Full_Report_0.pdf, (accessed 19 December 2022).
4 P. W. Griffin, G. P. Hammond and J. B. Norman, *Appl. Energy*, 2018, **227**, 587–602.
5 B. D. Solomon and K. Krishna, *Energy Policy*, 2011, **39**, 7422–7431.
6 R. Fouquet, *Energy Policy*, 2010, **38**, 6586–6596.
7 P. T. Anastas and M. M. Kirchhoff, *Acc. Chem. Res.*, 2002, **35**, 686–694.
8 C. Wang, S. A. Raza, T. S. Adebayo, S. Yi and M. I. Shah, *Energy*, 2023, **262**, 125303.
9 R. K. Srivastava, N. P. Shetti, K. R. Reddy, E. E. Kwon, M. N. Nadagouda and T. M. Aminabhavi, *Environ. Pollut.*, 2021, **276**, 116731.
10 Y. Duan, A. Tarafdar, V. Kumar, P. Ganeshan, K. Rajendran, B. Shekhar Giri, R. Gómez-García, H. Li, Z. Zhang, R. Sindhu, P. Binod, A. Pandey, M. J. Taherzadeh, S. Sarsaiya, A. Jain and M. Kumar Awasthi, *Fuel*, 2022, **325**, 124846.
11 Anastas, P.T. and Warner, J.C. (1998) Green Chemistry: Theory and Practice. Oxford University Press, New York, 29-56.
12 D. Griggs, M. Stafford-Smith, O. Gaffney, J. Rockström, M. C. Öhman, P. Shyamsundar, W. Steffen, G. Glaser, N. Kanie and I. Noble, *Nature*, 2013, **495**, 305–307.
13 T. Hák, S. Janoušková and B. Moldan, *Ecol. Indic.*, 2016, **60**, 565–573.
14 D. Le Blanc, *Sustain. dev.*, 2015, **23**, 176–187.
15 H. van Asselt and F. Green, *Wiley Interdiscip. Rev. Clim. Change*, 2022, DOI: 10.1002/wcc.816doi.org/10.1002/wcc.816
16 R. L. Ibrahim, *Environ. Sci. Pollut. Res.*, 2022, **29**, 86759–86770.
17 G. Halkos and E.-C. Gkampoura, *Econ. Anal. Policy*, 2021, **70**, 94–122.
18 P. Kaparaju, M. Serrano, A. B. Thomsen, P. Kongjan and I. Angelidaki, *Bioresour. Technol.*, 2009, **100**, 2562–2568.
19 S. Liu, L. P. Abrahamson and G. M. Scott, *Biomass Bioenergy*, 2012, **39**, 1–4.
20 A. Rehman, H. Ma, M. Ahmad, M. Irfan, O. Traore and A. A. Chandio, *Ecol. Indic.*, 2021, **125**, 107460.
21 J. H. Mussgnug, V. Klassen, A. Schlüter and O. Kruse, *J. Biotechnol.*, 2010, **150**, 51–56.
22 L. Goswami, R. Kayalvizhi, P. K. Dikshit, K. C. Sherpa, S. Roy, A. Kushwaha, B. S. Kim, R. Banerjee, S. Jacob and R. C. Rajak, *Chem. Eng. J.*, 2022, **448**, 137677.
23 Z. Yang, D. D. Leero, C. Yin, L. Yang, L. Zhu, Z. Zhu and L. Jiang, *Bioresour. Technol.*, 2022, **361**, 127656.
24 A. Saravanan, P. Senthil Kumar, M. Badawi, G. Mohanakrishna and T. M. Aminabhavi, *Chem. Eng. J.*, 2023, **453**, 139754.
25 A. T. Ubando, E. Anderson S Ng, W.-H. Chen, A. B. Culaba and E. E. Kwon, *Bioresour. Technol.*, 2022, **360**, 127615.
26 E. S. Okeke, O. Ejeromedoghene, C. O. Okoye, T. P. C. Ezeorba, R. Nyaruaba, C. K. Ikechukwu, A. Oladipo and J. I. Orege, *Energy Converse. Manage.*, 2022, **16**, 100323.

27 J. Remón, S. H. Danby, J. H. Clark and A. S. Matharu, *ACS Sustainable Chem. Eng*, 2020, **8**, 12493–12510.
28 R. Madadi, H. Maljaee, L. S. Serafim and S. P. M. Ventura, *Mar. Drugs*, 2021, **19**, 466.
29 S. Y. A. Siddiki, M. Mofijur, P. S. Kumar, S. F. Ahmed, A. Inayat, F. Kusumo, I. A. Badruddin, T. M. Y. Khan, L. D. Nghiem, H. C. Ong and T. M. I. Mahlia, *Fuel*, 2022, **307**, 121782.
30 D. C. Elliott, P. Biller, A. B. Ross, A. J. Schmidt and S. B. Jones, *Bioresour. Technol.*, 2015, **178**, 147–156.
31 P. Biller, B. K. Sharma, B. Kunwar and A. B. Ross, *Fuel*, 2015, **159**, 197–205.
32 G. Venkata Subhash, M. Rajvanshi, G. Raja Krishna Kumar, U. Shankar Sagaram, V. Prasad, S. Govindachary and S. Dasgupta, *Bioresour. Technol.*, 2022, **343**, 126155.
33 D. Zhuang, N. He, K. S. Khoo, E.-P. Ng, K. W. Chew and T. C. Ling, *Chemosphere*, 2022, **291**, 132932.
34 M. De Luca, I. Pappalardo, A. R. Limongi, E. Viviano, R. P. Radice, S. Todisco, G. Martelli, V. Infantino and A. Vassallo, *Cosmet. Toiletries*, 2021, **8**, 52.
35 J. Wu, X. Gu, D. Yang, S. Xu, S. Wang, X. Chen and Z. Wang, *Food Sci Nutr*, 2021, **9**, 5279–5292.
36 S. C. Foo, N. M. H. Khong and F. Yusoff, *Algal Res.*, 2020, **51**, 102061.
37 C. Lourenço-Lopes, M. Fraga-Corral, C. Jimenez-Lopez, M. Carpena, A. G. Pereira, P. Garcia-Oliveira, M. A. Prieto and J. Simal-Gandara, *Trends Food Sci. Technol.*, 2021, **117**, 163-181
38 A. Zarekarizi, L. Hoffmann and D. Burritt, *J. Appl. Phycol.*, 2019, **31**, 281–299.
39 K. Skjånes, R. Aesoy, L. Herfindal and H. Skomedal, *Physiol. Plant.*, 2021, **173**, 612–623.
40 R. Kumar, A. S. Hegde, K. Sharma, P. Parmar and V. Srivatsan, *Food Res. Int.*, 2022, **157**, 111338.
41 *https://www.intechopen.com/chapters/48245 (last accessed 29/01/2023)*
42 L. Zhu, *Renewable Sustainable Energy Rev.*, 2015, **41**, 1376–1384.
43 S. Khanra, M. Mondal, G. Halder, O. N. Tiwari, K. Gayen and T. K. Bhowmick, *Food Bioprod. Process.*, 2018, **110**, 60–84.
44 K. W. Chew, J. Y. Yap, P. L. Show, N. H. Suan, J. C. Juan, T. C. Ling, D.-J. Lee and J.-S. Chang, *Bioresour. Technol.*, 2017, **229**, 53–62.
45 S. C. Foo, K. S. Khoo, C. W. Ooi, P. L. Show, N. M. H. Khong and F. M. Yusoff, *Front Bioeng Biotechnol*, 2020, **8**, 546067.
46 D. Bilanovic, A. Andargatchew, T. Kroeger and G. Shelef, *Energy Convers. Manage.*, 2009, **50**, 262–267.
47 E. B. Sydney, W. Sturm, J. C. de Carvalho, V. Thomaz-Soccol, C. Larroche, A. Pandey and C. R. Soccol, *Bioresour. Technol.*, 2010, **101**, 5892–5896.
48 A. Asghari, M. Fazilati, A. M. Latifi, H. Salavati and A. Choopani, A review on antioxidant properties of Spirulina, http://www.biotechrep.ir/article_69007_cf87ec6a3acc0e69c330b2086d8ecdd0.pdf, (accessed 23 December 2022).
49 M. I. Khan, J. H. Shin and J. D. Kim, *Microb. Cell Fact.*, 2018, **17**, 36.
50 B. Porto, A. L. Gonçalves, A. F. Esteves, S. M. A. G. U. de Souza, A. A. U. de Souza, V. J. P. Vilar and J. C. M. Pires, *Chem. Eng. J.*, 2021, **413**, 127546.
51 H. Jia and Q. Yuan, *Cogent Environ. Sci.*, 2016, **2**, 1275089.
52 M. Ras, J.-P. Steyer and O. Bernard, *Rev. Environ. Sci. Technol.*, 2013, **12**, 153–164.
53 T. M. Mata, A. A. Martins and N. S. Caetano, *Renewable Sustainable Energy Rev.*, 2010, **14**, 217–232.

54 W. Moomaw, I. Berzin and A. Tzachor, *Ind. Biotechnol.* , 2017, **13**, 234–243.
55 M. Sprague, J. R. Dick and D. R. Tocher, *Sci. Rep.*, 2016, **6**, 1–9.
56 T. C. Adarme-Vega, D. K. Y. Lim, M. Timmins, F. Vernen, Y. Li and P. M. Schenk, *Microb. Cell Fact.*, 2012, **11**, 96.
57 D. J. Hibberd and G. F. Leedale, *Taxon*, 1971, **20**, 523–525.
58 R. Amaral, T. Ševčíková, M. Eliáš and L. M. A. Santos, *Eur. J. Phycol.*, 2021, **56**, 186–202.
59 M. W. Fawley, K. P. Fawley and A. B. Cahoon, *J. Phycol.*, 2021, **57**, 1636–1647.
60 M. Stoyneva-Gärtner, P. Stoykova, B. Uzunov, I. Dincheva, I. Atanassov, P. Draganova, C. Borisova and G. Gärtner, *Biotechnol. Biotechnol. Equip.*, 2019, **33**, 250–267.
61 E. T. Chua and P. M. Schenk, *Bioresour. Technol.*, 2017, **244**, 1416–1424.
62 B. P. Nobre, F. Villalobos, B. E. Barragán, A. C. Oliveira, A. P. Batista, P. A. S. Marques, R. L. Mendes, H. Sovová, A. F. Palavra and L. Gouveia, *Bioresource Technology*, 2013, **135**, 128–136.
63 L. M. P. Valente, M. Custódio, S. Batista, H. Fernandes and V. Kiron, *Fish Physiol. Biochem.*, 2019, **45**, 1067–1081.
64 A. F. Ferreira, L. A. Ribeiro, A. P. Batista, P. A. S. S. Marques, B. P. Nobre, A. M. F. Palavra, P. P. da Silva, L. Gouveia and C. Silva, *Bioresour. Technol.*, 2013, **138**, 235–244.
65 N. Bongiovani, C. A. Popovich, A. M. Martínez, D. Constenla and P. I. Leonardi, *Bioenergy Res.*, 2020, **13**, 518–529.
66 C. Ribeiro, E. T. Santos, L. Costa, C. Brazinha, P. Saraiva and J. G. Crespo, *Membranes,* 2022*,* **12**, 401
67 M. Mitra and S. Mishra, in *Application of Microalgae in Wastewater Treatment: Volume 2: Biorefinery Approaches of Wastewater Treatment*, eds. S. K. Gupta and F. Bux, Springer International Publishing, Cham, 2019, pp. 123–145.
68 J. K. Volkman, M. R. Brown, G. A. Dunstan and S. W. Jeffrey, *J. Phycol.*, 1993, **29**, 69–78.
69 T. M. M. Bernaerts, L. Gheysen, I. Foubert, M. E. Hendrickx and A. M. Van Loey, *Biotechnol. Adv.*, 2019, **37**, 107419.
70 S. Weber, P. M. Grande, L. M. Blank and H. Klose, *PLoS One*, 2022, **17**, e0262500.
71 C.-Y. Chen, X.-Q. Zhao, H.-W. Yen, S.-H. Ho, C.-L. Cheng, D.-J. Lee, F.-W. Bai and J.-S. Chang, *Biochem. Eng. J.*, 2013, **78**, 1–10.
72 A. Gille, A. Trautmann, C. Posten and K. Briviba, *Int. J. Food Sci. Nutr.*, 2015, **67**, 507–513.
73 P.-H. Baudelet, G. Ricochon, M. Linder and L. Muniglia, *Algal Research*, 2017, **25**, 333–371.
74 S. Derenne, C. Largeau and P. G. Hatcher, *Org. Geochem.*, 1992, **18**, 417–422.
75 M. Alhattab, A. Kermanshahi-Pour and M. S.-L. Brooks, *J. Appl. Phycol.*, 2019, **31**, 61–88.
76 N. A. H. Fetyan, A. E.-K. B. El-Sayed, F. M. Ibrahim, Y. A. Attia and M. W. Sadik, *Environ. Sci. Pollut. Res. Int.*, 2022, **29**, 2588–2597.
77 W. Obeid, E. Salmon and P. G. Hatcher, *Org. Geochem.*, 2014, **76**, 259–269.
78 J. L. Zelibor, L. Romankiw, P. G. Hatcher and R. R. Colwell, *Appl. Environ. Microbiol.*, 1988, **54**, 1051–1060.
79 B. Allard, J. Templier and C. Largeau, *Org. Geochem.*, 1998, **28**, 543–548.
80 I. L. Ross, S. Shah, B. Hankamer and N. Amiralian, *Trends Plant Sci.*, 2021, **26**, 924–939.
81 D. Lavanya, P. K. Kulkarni, M. Dixit, P. K. Raavi and L. N. V. Krishna, *International Journal of Drug Formulation and Research*, 2011, **2**, 19–38.
82 H. V. Lee, S. B. A. Hamid and S. K. Zain, *ScientificWorldJournal*, 2014, **2014**, 631013.

83 R. Ravindran and A. K. Jaiswal, *Bioresour. Technol.*, 2016, **199**, 92–102.
84 C. Yan, R. Wang, J. Wan, Q. Zhang, S. Xue, X. Wu, J. Zhang, J. Zhang, Y. Lu and W. Cong, *Algal Res.*, 2016, **20**, 135–141.
85 A. Mihranyan, *J. Appl. Polym. Sci.*, 2011, **119**, 2449–2460.
86 G. Markou, I. Angelidaki and D. Georgakakis, *Appl. Microbiol. Biotechnol.*, 2012, **96**, 631–645.
87 D. W. Templeton, M. Quinn, S. Van Wychen, D. Hyman and L. M. L. Laurens, *J. Chromatogr. A*, 2012, **1270**, 225–234.
88 G. A. Colusse, J. Carneiro, M. E. R. Duarte, J. C. de Carvalho and M. D. Noseda, *Crit. Rev. Biotechnol.*, 2021, **42**, 1–16.
89 D. Cheng, D. Li, Y. Yuan, L. Zhou, X. Li, T. Wu, L. Wang, Q. Zhao, W. Wei and Y. Sun, *Biotechnol. Biofuels*, 2017, **10**, 75.
90 S. Wahidin, A. Idris and S. R. M. Shaleh, *Bioresour. Technol.*, 2013, **129**, 7–11.
91 K. K. Sharma, H. Schuhmann and P. M. Schenk, *Energies*, 2012, **5**, 1532–1553.
92 L. Rodolfi, G. Chini Zittelli, N. Bassi, G. Padovani, N. Biondi, G. Bonini and M. R. Tredici, *Biotechnol. Bioeng.*, 2009, **102**, 100–112.
93 I. L. D. Olmstead, D. R. A. Hill, D. A. Dias, N. S. Jayasinghe, D. L. Callahan, S. E. Kentish, P. J. Scales and G. J. O. Martin, *Biotechnol. Bioeng.*, 2013, **110**, 2096–2104.
94 H. Taher, S. Al-Zuhair, A. H. Al-Marzouqi, Y. Haik and M. Farid, *Biomass Bioenergy*, 2014, **66**, 159–167.
95 J.-Y. Lee, C. Yoo, S.-Y. Jun, C.-Y. Ahn and H.-M. Oh, *Bioresour. Technol.*, 2010, **101**, S75-7.
96 S. P. Cuellar-Bermudez, I. Aguilar-Hernandez, D. L. Cardenas-Chavez, N. Ornelas-Soto, M. A. Romero-Ogawa and R. Parra-Saldivar, *Microb. Biotechnol.*, 2015, **8**, 190–209.
97 E. A. Ehimen, Z. F. Sun and C. G. Carrington, *Fuel*, 2010, **89**, 677–684.
98 E. Lopez-Huertas, *Pharmacol. Res.*, 2010, **61**, 200–207.
99 A. R. Fajardo, L. E. Cerdán, A. R. Medina, F. G. A. Fernández, P. A. G. Moreno and E. M. Grima, *Eur. J. Lipid Sci. Technol.*, 2007, **109**, 120–126.
100 S. Tang, C. Qin, H. Wang, S. Li and S. Tian, *J. Supercrit. Fluids*, 2011, **57**, 44–49.
101 K. Sudhakar, R. Mamat, M. Samykano, W. H. Azmi, W. F. W. Ishak and T. Yusaf, *Renewable Sustainable Energy Rev.*, 2018, **91**, 165–179.
102 F. Fernand, A. Israel, J. Skjermo, T. Wichard, K. R. Timmermans and A. Golberg, *Renewable and Sustainable Energy Rev.*, 2017, **75**, 35–45.
103 M. Øverland, L. T. Mydland and A. Skrede, *J. Sci. Food Agric.*, 2019, **99**, 13–24.
104 H.-W. Yen, S.-C. Yang, C.-H. Chen, Jesisca and J.-S. Chang, *Bioresour. Technol.*, 2015, **184**, 291–296.
105 S. Obeid, N. Beaufils, S. Camy, H. Takache, A. Ismail and P.-Y. Pontalier, *Algal Res.*, 2018, **34**, 49–56.
106 M. Mathur, N. Hans, F. Naaz, S. N. Naik, K. K. Pant and A. Malik, *J. Clean. Prod.*, 2022, **373**, 133925.
107 A. Y. Prosekov and S. A. Ivanova, *Geoforum*, 2018, **91**, 73–77.
108 K. Govindan, *Int. J. Prod. Econ.*, 2018, **195**, 419–431.
109 J. G. Conijn, P. S. Bindraban, J. J. Schröder and R. E. E. Jongschaap, *Agric. Ecosyst. Environ.*, 2018, **251**, 244–256.
110 F. Boukid, C. M. Rosell, S. Rosene, S. Bover-Cid and M. Castellari, *Crit. Rev. Food Sci. Nutr.*, 2022, **62**, 6390–6420.
111 M. P. Caporgno and A. Mathys, *Front Nutr*, 2018, **5**, 58.
112 J. de Boer and H. Aiking, *Food Qual. Prefer.*, 2021, **88**, 104098.

113 Z. W. Wong, *The Ingredients and Challenge of Plant-Based Meat Patty: a Narrative Review.* Final Year Project (Bachelor), Tunku Abdul Rahman University College., 2022
114 Y.-C. Lai, C.-H. Chang, C.-Y. Chen, J.-S. Chang and I.-S. Ng, *Bioresour. Technol.*, 2019, **289**, 121625.
115 A. Niccolai, G. C. Zittelli, L. Rodolfi, N. Biondi and M. R. Tredici, *Algal Res.*, 2019, **42**, 101617.
116 J. Ampofo and L. Abbey, *Foods* 2022, ***11***,1744
117 P. Geada, C. Moreira, M. Silva, R. Nunes, L. Madureira, C. M. R. Rocha, R. N. Pereira, A. A. Vicente and J. A. Teixeira, *Bioresour. Technol.*, 2021, **332**, 125125.
118 R. B. Draaisma, R. H. Wijffels, P. M. E. Slegers, L. B. Brentner, A. Roy and M. J. Barbosa, *Curr. Opin. Biotechnol.*, 2013, **24**, 169–177.
119 Y. Li, C. Lammi, G. Boschin, A. Arnoldi and G. Aiello, *J. Agric. Food Chem.*, 2019, **67**, 11825–11838.
120 L. Soto-Sierra, P. Stoykova and Z. L. Nikolov, *Algal Res.*, 2018, **36**, 175–192.
121 Y. Wang, S. M. Tibbetts and P. J. McGinn, *Foods*, 2021, **10**, 3002
122 A.-V. Ursu, A. Marcati, T. Sayd, V. Sante-Lhoutellier, G. Djelveh and P. Michaud, *Bioresour. Technol.*, 2014, **157**, 134–139.
123 E. Günerken, E. D'Hondt, M. H. M. Eppink, L. Garcia-Gonzalez, K. Elst and R. H. Wijffels, *Biotechnol. Adv.*, 2015, **33**, 243–260.
124 P. Prabakaran and A. D. Ravindran, *Lett. Appl. Microbiol.*, 2011, **53**, 150–154.
125 C. Safi, A. V. Ursu, C. Laroche, B. Zebib, O. Merah, P.-Y. Pontalier and C. Vaca-Garcia, *Algal Res.*, 2014, **3**, 61–65.
126 E. S. Garcia, E. Suarez Garcia, J. van Leeuwen, C. Safi, L. Sijtsma, M. H. M. Eppink, R. H. Wijffels and C. van den Berg, *Bioresour. Technol.*, 2018, **268**, 197–203.
127 N. Grimi, A. Dubois, L. Marchal, S. Jubeau, N. I. Lebovka and E. Vorobiev, *Bioresour. Technol.*, 2014, **153**, 254–259.
128 K.-Y. Show, D.-J. Lee, J.-H. Tay, T.-M. Lee and J.-S. Chang, *Bioresour. Technol.*, 2015, **184**, 258–266.
129 J. A. Gerde, T. Wang, L. Yao, S. Jung, L. A. Johnson and B. Lamsal, *Algal Res.*, 2013, **2**, 145–153.
130 M. Demuez, A. Mahdy, E. Tomás-Pejó, C. González-Fernández and M. Ballesteros, *Biotechnol. Bioeng.*, 2015, **112**, 1955–1966.
131 P. Spolaore, C. Joannis-Cassan, E. Duran and A. Isambert, *J. Biosci. Bioeng.*, 2006, **101**, 87–96.
132 R. Castro-Muñoz and O. García-Depraect, *Membranes* , 2021, **11**, 585
133 N. I. Md Saleh, W. A. Wan Ab Karim Ghani, S. M. Mustapa Kamal and R. Harun, *Processes*, 2021, **9**, 610.
134 A. E.-M. M. R. Afify, G. S. El Baroty, F. K. El Baz, H. H. Abd El Baky and S. A. Murad, *J. Genet. Eng. Biotechnol.*, 2018, **16**, 399–408.
135 J. Stack, A. V. Le Gouic, P. R. Tobin, F. Guihéneuf, D. B. Stengel and R. J. FitzGerald, *Journal of Food Bioactives*, 2018, **1**, 153-165-153–165.
136 H. J. Morris, A. Almarales, O. Carrillo and R. C. Bermúdez, *Bioresour. Technol.*, 2008, **99**, 7723–7729.
137 K. Samarakoon and Y.-J. Jeon, *Food Res. Int.*, 2012, **48**, 948–960.
138 R. Sathya, D. Mubarak-Ali, M. G. Mehboob, N. Vasimalai, N. Tahjuddin and J.-W. Kim, *Appl. Biochem. Biotechnol.*, 2022,**194**, 5580-5593
139 I.-C. Sheih, T.-K. Wu and T. J. Fang, *Bioresour. Technol.*, 2009, **100**, 3419–3425.

140 S. L. Minic, D. Stanic-Vucinic, J. Mihailovic, M. Krstic, M. R. Nikolic and T. Cirkovic Velickovic, *J. Proteomics*, 2016, **147**, 132–139.
141 R. Sathya, D. MubarakAli, J. MohamedSaalis and J.-W. Kim, *Sustain. Sci. Pract. Policy*, 2021, **13**, 3262.
142 J. Pekkoh, K. Ruangrit, C. Pumas, K. Duangjan, S. Chaipoot, R. Phongphisutthinant, I. Jeerapan, K. Sawangrat, W. Pathom-aree and S. Srinuanpan, *Biomass Convers. Biorefin.*, 2021, doi.org/10.1007/s13399-021-01622-7
143 E. M. Rojo, I. Piedra, A. M. González, M. Vega and S. Bolado, *Bioresour. Technol.*, 2021, **335**, 125256.
144 V. Timira, K. Meki, Z. Li, H. Lin, M. Xu and S. N. Pramod, *Crit. Rev. Food Sci. Nutr.*, 2022, **62**, 4309–4325.
145 Y. Liu, X. Liu, Y. Cui and W. Yuan, *Ultrason. Sonochem.*, 2022, **87**, 106054.
146 F. A. Khawli, F. J. Martí-Quijal, N. Pallarés, F. J. Barba and E. Ferrer, *NATO Adv. Sci. Inst. Ser. E Appl. Sci.*, 2021, **11**, 1701.
147 L. Machado, G. Carvalho and R. N. Pereira, *Biomass*, 2022, **2**, 80–102.
148 M. Zamani, H. Shokrkar and S. Ebrahimi, *Iran. J.Chem. Chem. Eng.,* 2021, **19**, 18-27
149 S. R. Motlagh, A. A. Elgharbawy, R. Khezri, R. Harun and R. Omar, *Biomass Convers. Biorefin.*, 2021, DOI:10.1007/s13399-021-01778-2.
150 S. Rezaei Motlagh, R. Harun, D. R. Awang Biak, S. A. Hussain, R. Omar, R. Khezri and A. A. Elgharbawy, *J. Appl. Phycol.*, 2021, **33**, 2015–2029.
151 M. K. Sarma, K. Saha, R. Choudhury, S. Pabbi, D. Madamwar and S. Subudhi, *Biofuels Bioprod. Biorefin.*, 2022, **16**, 698–709.
152 N. Flórez, E. Conde and H. Domínguez, *J. Chem. Technol. Biotechnol.*, 2015, **90**, 590–607.
153 K. W. Chew, S. R. Chia, S. Y. Lee, L. Zhu and P. L. Show, *Chem. Eng. J.*, 2019, **367**, 1–8.
154 P. S. Saravana, V. Ummat, P. Bourke and B. K. Tiwari, *Crit. Rev. Biotechnol.*, 2022, 1–16.
155 E. Barbarino and S. O. Lourenço, *Journal of Applied Phycology*, 2005, **17**, 447–460.
156 S. O. Lourenço, E. Barbarino, P. L. Lavín, U. M. Lanfer Marquez and E. Aidar, *Eur. J. Phycol.*, 2004, **39**, 17–32.
157 C. Safi, M. Charton, O. Pignolet, F. Silvestre, C. Vaca-Garcia and P.-Y. Pontalier, *J. Appl. Phycol.*, 2013, **25**, 523–529.
158 M. van der Spiegel, M. Y. Noordam and H. J. van der Fels-Klerx, *Compr. Rev. Food Sci. Food Saf.*, 2013, **12**, 662–678.
159 E. W. Becker, *Biotechnol. Adv.*, 2007, **25**, 207–210.
160 P. D. Patil, K. P. R. Dandamudi, J. Wang, Q. Deng and S. Deng, *J. Supercrit. Fluids*, 2018, **135**, 60–68.
161 P. Boelen, R. van Dijk, J. S. Sinninghe Damsté, W. I. C. Rijpstra and A. G. Buma, *AMB Express*, 2013, **3**, 26.
162 R. J. Winwood, *OCL*, 2013, **20**, D604.
163 R. Ghosh and Z. F. Cui, *J. Memb. Sci.*, 2000, **167**, 47–53.
164 C. Baldasso, T. C. Barros and I. C. Tessaro, *Desalination*, 2011, **278**, 381–386.
165 N. Rossignol, L. Vandanjon, P. Jaouen and F. Quéméneur, *Aquacult. Eng.*, 1999, **20**, 191–208.
166 C. Denis, A. Massé, J. Fleurence and P. Jaouen, *Sep. Purif. Technol.*, 2009, **69**, 37–42.
167 M. Frappart, A. Massé, M. Y. Jaffrin, J. Pruvost and P. Jaouen, *Desalination*, 2011, **265**, 279–283.
168 K. J. Howe and M. M. Clark, *Environ. Sci. Technol.*, 2002, **36**, 3571–3576.

169 A. D. Marshall, P. A. Munro and G. Trägårdh, *Desalination*, 1993, **91**, 65–108.
170 S. Moaveni, M. Salami, M. Khodadadi, M. McDougall and Z. Emam-Djomeh, *LWT*, 2022, **154**, 112468.
171 F. L. Zitzmann, E. Ward, X. Meng and A. S. Matharu, *Molecules*, 2021, ***26***, 4972
172 F. L. Zitzmann, E. Ward and A. S. Matharu, *Gels*, 2022, ***8***, 383
173 A. Kumar, V. Gupta and K. K. Gaikwad, *Biomass Conversion and Biorefinery*, 2021, DOI:10.1007/s13399-021-01794-2.
174 Y. Gao, M. Z. Ozel, T. Dugmore, A. Sulaeman and A. S. Matharu, *J. Hazard. Mater.*, 2021, **401**, 123400.
175 E. M. de Melo, J. H. Clark and A. S. Matharu, *Green Chem.*, 2017, **19**, 3408–3417.
176 L. E. Silva, A. de A. Dos Santos, L. Torres, Z. McCaffrey, A. Klamczynski, G. Glenn, A. R. de Sena Neto, D. Wood, T. Williams, W. Orts, R. A. P. Damásio and G. H. D. Tonoli, *Carbohydr. Polym.*, 2021, **252**, 117165.
177 K. Li, D. Mcgrady, X. Zhao, D. Ker, H. Tekinalp, X. He, J. Qu, T. Aytug, E. Cakmak, J. Phipps, S. Ireland, V. Kunc and S. Ozcan, *Carbohydr. Polym.*, 2021, **256**, 117525.
178 H.-R. Lee, K. Kim, S. C. Mun, Y. K. Chang and S. Q. Choi, *Carbohydr. Polym.*, 2018, **180**, 276–285.
179 Y. Gao, H. Xia, A. P. Sulaeman, E. M. de Melo, T. I. J. Dugmore and A. S. Matharu, *ACS Sustainable Chem. Eng.*, 2019, **7**, 11861–11871.
180 T. Owoyokun and C. M. P. Berumen, *Res. Appl. Chem.* 2021, **11**, 11797 - 11816
181 C. O. Kappe, *Angew. Chem. Int. Ed Engl.*, 2004, **43**, 6250–6284.
182 P. Biller, C. Friedman and A. B. Ross, *Bioresour. Technol.*, 2013, **136**, 188–195.
183 I. L. Choi, S. J. Choi, J. K. Chun and T. W. Moon, *J. Food Process. Preserv.*, 2006, **30**, 407–419.
184 J. Iqbal and C. Theegala, *Algal Res.*, 2013, **2**, 34–42.
185 V. Pasquet, J.-R. Chérouvrier, F. Farhat, V. Thiéry, J.-M. Piot, J.-B. Bérard, R. Kaas, B. Serive, T. Patrice, J.-P. Cadoret and L. Picot, *Process Biochem.*, 2011, **46**, 59–67.
186 Z. Du, Y. Li, X. Wang, Y. Wan, Q. Chen, C. Wang, X. Lin, Y. Liu, P. Chen and R. Ruan, *Bioresour. Technol.*, 2011, **102**, 4890–4896.
187 W.-H. Chen, B.-J. Lin, M.-Y. Huang and J.-S. Chang, *Bioresour. Technol.*, 2015, **184**, 314–327.
188 D. Beneroso, J. M. Bermúdez, A. Arenillas and J. A. Menéndez, *Bioresour. Technol.*, 2013, **144**, 240–246.
189 S.-S. Kim, H. V. Ly, J. Kim, E. Y. Lee and H. C. Woo, *Chem. Eng. J.*, 2015, **263**, 194–199.
190 K. Azizi, M. Keshavarz Moraveji and H. Abedini Najafabadi, *Renewable Sustainable Energy Rev.*, 2018, **82**, 3046–3059.
191 N. H. Zainan, S. C. Srivatsa, F. Li and S. Bhattacharya, *Fuel*, 2018, **223**, 12–19.
192 M. Zych, J. Burczyk, W. Borymska and I. Kaczmarczyk-Sedlak, *Algal Res.*, 2022, **62**, 102598.
193 S. A. Channiwala and P. P. Parikh, *Fuel*, 2002, **81**, 1051–1063.
194 M. F. L. Olsen, J. S. Pedersen, S. T. Thomsen, H. J. Martens, A. Petersen and P. E. Jensen, *Physiol. Plant.*, 2021, **173**, 483–494.
195 J. Song, H. Fan, J. Ma and B. Han, *Green Chem.*, 2013, **15**, 2619–2635.
196 Z. Yan, J. Lian, Y. Feng, M. Li, F. Long, R. Cheng, S. Shi, H. Guo and J. Lu, *Fuel*, 2021, **289**, 119969.
197 E. Agcam, *Food Anal. Methods*, 2022, **15**, 1286–1299.
198 J. Fábregas, A. Maseda, A. Domínguez and A. Otero, *World J. Microbiol. Biotechnol.*, 2004, **20**, 31–35.

199 X.-N. Ma, T.-P. Chen, B. Yang, J. Liu and F. Chen, *Mar. Drugs*, 2016, **14**, 61
200 T. Lafarga, A. Sánchez-Zurano, S. Villaró, A. Morillas-España and G. Acién, *Trends Food Sci. Technol.*, 2021, **116**, 176–185.
201 S. K. Ali and A. M. Saleh, *Int. J. Pharm. Pharm. Sci.*, 2012, **4**, 9–15.
202 Babadzhanov and Abdusamatova, *Chem. Nat. Compd.* 2004, **40**, 3, 2004
203 C. Safi, B. Zebib, O. Merah, P.-Y. Pontalier and C. Vaca-Garcia, *Renewable Sustainable Energy Rev.*, 2014, **35**, 265–278.
204 S.-H. Ho, S.-W. Huang, C.-Y. Chen, T. Hasunuma, A. Kondo and J.-S. Chang, *Bioresour. Technol.*, 2013, **135**, 157–165.
205 R. Nguyen, H. Harvey, X. Zang and J. Heemst, *Org. Biomol. Chem.,* 2003, **34**, 483-497
206 A. Simpson, X. Zang, R. Kramer and P. Hatcher, *Phytochemistry*., 2003, **62**, 783-796
207 P. Biller, A. B. Ross and S. C. Skill, *Org. Geochem.*, 2015, **81**, 64–69.
208 N. Ghassemi, A. Poulhazan, F. Deligey, F. Mentink-Vigier, I. Marcotte and T. Wang, *Chem. Rev.*, 2021, **122**, 10036-10086
209 S. M. Tibbetts, W. J. Bjornsson and P. J. McGinn, *Anim. Feed Sci. Technol.*, 2015, **204**, 62–71.
210 P. Lunven, Le Clement de St Mar, E. Carnovale and A. Fratoni, *Br. J. Nutr.*, 1973, **30**, 189–194.
211 C. G. Zarkadas, C. Gagnon, S. Gleddie, S. Khanizadeh, E. R. Cober and R. J. D. Guillemette, *Food Res. Int.*, 2007, **40**, 129–146.
212 T. Zor and Z. Selinger, *Anal. Biochem.*, 1996, **236**, 302–308.
213 S. J. Compton and C. G. Jones, *Anal. Biochem.*, 1985, **151**, 369–374.
214 C. G. Jones, J. Daniel Hare and S. J. Compton, *J. Chem. Ecol.*, 1989, **15**, 979–992.
215 C. D. Georgiou, K. Grintzalis, G. Zervoudakis and I. Papapostolou, *Anal. Bioanal. Chem.*, 2008, **391**, 391–403.
216 N. P. Bonjoch and P. R. Tamayo, in *Handbook of Plant Ecophysiology Techniques*, ed. M. J. Reigosa Roger, Springer Netherlands, Dordrecht, 2001, pp. 283–295.
217 N. J. Kruger, in *The Protein Protocols Handbook*, ed. J. M. Walker, Humana Press, Totowa, NJ, 2009, pp. 17–24.
218 M. Aminian, F. Nabatchian, A. Vaisi-Raygani and M. Torabi, *Anal. Biochem.*, 2013, **434**, 287–291.
219 R. Seevaratnam, B. P. Patel and M. J. Hamadeh, *J. Biochem.*, 2009, **145**, 791–797.
220 K. Zocher, J.-W. Lackmann, J. Volzke, L. Steil, M. Lalk, K.-D. Weltmann, K. Wende and J. F. Kolb, *Algal Res.*, 2019, **39**, 101416.
221 K. Zocher, R. Banaschik, C. Schulze, T. Schulz, J. Kredl, C. Miron, M. Schmidt, S. Mundt, W. Frey and J. F. Kolb, *PMED*, 2016, **6**, 273-302
222 S. Lucakova, I. Branyikova and M. Hayes, *NATO Adv. Sci. Inst. Ser. E Appl. Sci.*, 2022, **12**, 4402.
223 F. Apone, A. Barbulova and M. G. Colucci, *Front. Plant Sci.*, 2019, **10**, 756.
224 J. A. Callejo-López, M. Ramírez, J. Bolívar and D. Cantero, *J. Chem. Chem. Eng.*, 2019, **2019**, 10
225 T. Tang, H. Du, S. Tang, Y. Jiang, Y. Tu, M. Hu and M. Xu, *Innov. Food Sci. Emerg. Technol.*, 2021, **72**, 102742.
226 Z. Wan, X. Yang and L. M. C. Sagis, *Langmuir*, 2016, **32**, 8092–8101.
227 L. Amagliani, J. V. C. Silva, M. Saffon and J. Dombrowski, *Trends Food Sci. Technol.*, 2021, **118**, 261–272.
228 C. Malabat, R. I. S. nchez-Vioque, C. Rabiller and J. Gu guen, *J. Am. Oil Chem. Soc.*, 2001, **78**, 235–242.

229 Z. Karami and B. Akbari-Adergani, *J. Food Sci. Technol.*, 2019, **56**, 535–547.
230 S. Ebert, L. Grossmann, J. Hinrichs and J. Weiss, *Food Funct.*, 2019, **10**, 754–764.
231 S. Kamiloglu, G. Sari, T. Ozdal and E. Capanoglu, *Food Frontiers*, 2020, **1**, 332–349.
232 P. I. Chater, M. D. Wilcox, I. A. Brownlee and J. P. Pearson, *Carbohydr. Polym.*, 2015, **131**, 142–151.
233 P. J. Van Soest, *Nutritional Ecology of the Ruminant*, Cornell University Press, 1994.
234 A. T. Quitain, T. Kai, M. Sasaki and M. Goto, *Ind. Eng. Chem. Res.*, 2013, **52**, 7940–7946.
235 M. Rokicka, M. Zieliński, M. Dudek and M. Dębowski, *Bioenergy Res.*, 2020, **14**, 752-760
236 G. Canelli, P. Murciano Martínez, S. Austin, M. E. Ambühl, F. Dionisi, C. J. Bolten, R. Carpine, L. Neutsch and A. Mathys, *J. Agric. Food Chem.*, 2021, **69**, 2226–2235.
237 A. Shchukarev, Z. Gojkovic, C. Funk and M. Ramstedt, *Appl. Surf. Sci.*, 2020, **526**, 146538.
238 B. Rashidi and L. M. Trindade, *Algal Res.*, 2018, **35**, 152–159.
239 S. Nam, A. D. French, B. D. Condon and M. Concha, *Carbohydr. Polym.*, 2016, **135**, 1–9.
240 N. Terinte, R. Ibbett and K. C. Schuster, *Lenzinger Berichte*, 2011, **89**, 118–131.
241 P. Ahvenainen, I. Kontro and K. Svedström, *Cellulose*, 2016, **23**, 1073–1086.
242 M. Hajir, R. Graf and W. Tremel, *Chem. Commun.* , 2014, **50**, 6534–6536.
243 A. Synytsya, J. Opíková and J. Brus, *Czech Journal of Food Sciences; Prague*, 2003, **21**, 1–12.
244 A. P. Sulaeman, Y. Gao, T. Dugmore, J. Remón and A. S. Matharu, *Cellulose*, 2021, **28**, 7687–7705.
245 A. A. Arnold, J.-P. Bourgouin, B. Genard, D. E. Warschawski, R. Tremblay and I. Marcotte, *J. Biomol. NMR*, 2018, **70**, 123–131.
246 A. A. Arnold, B. Genard, F. Zito, R. Tremblay, D. E. Warschawski and I. Marcotte, *Biochimica et Biophysica Acta (BBA) - Biomembranes*, 2015, **1848**, 369–377.
247 S. Park, D. K. Johnson, C. I. Ishizawa, P. A. Parilla and M. F. Davis, *Cellulose*, 2009, **16**, 641–647.
248 O. D. Bernardinelli, M. A. Lima, C. A. Rezende, I. Polikarpov and E. R. deAzevedo, *Biotechnol. Biofuels*, 2015, **8**, 110.
249 T. Kumar, R. R. G. Soares, L. Ali Dholey, H. Ramachandraiah, N. A. Aval, Z. Aljadi, T. Pettersson and A. Russom, *Nanoscale*, 2020, **12**, 21788–21797.
250 F. X. Choong, L. Lantz, H. Shirani, A. Schulz, K. P. R. Nilsson, U. Edlund and A. Richter-Dahlfors, *Cellulose*, 2019, **26**, 4253–4264.
251 E. Lahchaichi, Degree Project in Biotechnology, University of Stockholm, 2021, https://www.diva-portal.org/smash/get/diva2:1586225/FULLTEXT01.pdf (last accessed 29/01/2023)
252 A. Petrova, T. Gorshkova and L. Kozlova, *J. Exp. Bot.*, 2021, **72**, 1764–1781.
253 A. Petrova, G. Sibgatullina, T. Gorshkova and L. Kozlova, *Planta*, 2022, **255**, 108.
254 P. Blokker, S. Schouten, H. van den Ende, J. W. de Leeuw, P. G. Hatcher and J. S. Sinninghe Damsté, *Org. Geochem.*, 1998, **29**, 1453–1468.
255 O. Spain, M. Plöhn and C. Funk, *Physiol. Plant.*, 2021, **173**, 526–535.
256 M. J. Scholz, T. L. Weiss, R. E. Jinkerson, J. Jing, R. Roth, U. Goodenough, M. C. Posewitz and H. G. Gerken, *Eukaryot. Cell*, 2014, **13**, 1450–1464.
257 A. Sannino, C. Demitri and M. Madaghiele, *Materials* , 2009, **2**, 353–373.
258 R. Cha, Z. He and Y. Ni, *Carbohydr. Polym.*, 2012, **88**, 713–718.

259 H. Du, W. Liu, M. Zhang, C. Si, X. Zhang and B. Li, *Carbohydr. Polym.*, 2019, **209**, 130–144.
260 M. Bahram and N. Mohseni, *Emerging concepts in analysis and applications of hydrogels*, 2016, doi.org/10.5772/61692
261 F. Mariotti, D. Tomé and P. P. Mirand, *Crit. Rev. Food Sci. Nutr.*, 2008, **48**, 177–184.
262 L. Garcia Alba, C. Torri, C. Samorì, J. van der Spek, D. Fabbri, S. R. A. Kersten and D. W. F. (wim) Brilman, *Energy Fuels*, 2012, **26**, 642–657.
263 W.-H. Chen, Y.-S. Chu, J.-L. Liu and J.-S. Chang, *Energy Convers. Manage.*, 2018, **160**, 209–219.
264 T. Tang, J. Liu, S. Tang, N. Xiao, Y. Jiang, Y. Tu and M. Xu, *LWT*, 2022, **153**, 112503.
265 M. Zhang, X. Fan, F. Ye, J. Xue, S. Fan and L. Cheng, *J. Mater. Sci.: Mater. Electron.*, 2022, **33**, 6411–6420.
266 K. Li, G. Chen, J. Chen, J. Peng, R. Ruan and C. Srinivasakannan, *Bioresour. Technol.*, 2019, **291**, 121838.
267 Z. Hu, X. Ma and C. Chen, *Bioresour. Technol.*, 2012, **107**, 487–493.
268 A. Kumar, B. Yan, Z. Cheng, J. Tao, M. Hassan, J. Li, L. Kumari, B. T. Oba, M. A. Aborisade, I. A. Jamro and Others, *Fuel*, 2023, **331**, 125814.
269 F. Li, S. C. Srivatsa and S. Bhattacharya, *Renewable Sustainable Energy Rev.*, 2019, **108**, 481–497.
270 X. Gong, B. Zhang, Y. Zhang, Y. Huang and M. Xu, *Energy Fuels*, 2014, **28**, 95–103.
271 C. Chen, Q. Qi, D. Huang, T. Zeng, X. Bu, Y. Huang and H. Huang, *Energy*, 2021, **229**, 120752.
272 C. Yang, R. Li, B. Zhang, Q. Qiu, B. Wang, H. Yang, Y. Ding and C. Wang, *Fuel Process. Technol.*, 2019, **186**, 53–72.
273 Y. Hong, W. Chen, X. Luo, C. Pang, E. Lester and T. Wu, *Bioresour. Technol.*, 2017, **237**, 47–56.
274 F. Huang, A. Tahmasebi, K. Maliutina and J. Yu, *Bioresour. Technol.*, 2017, **245**, 1067–1074.
275 X. Wang, L. Sheng and X. Yang, *Bioresour. Technol.*, 2017, **229**, 119–125.
276 R. Re, N. Pellegrini, A. Proteggente, A. Pannala, M. Yang and C. Rice-Evans, *Free Radic. Biol. Med.*, 1999, **26**, 1231–1237.
277 P. Hernández-Rodríguez, L. P. Baquero and H. R. Larrota, in *Bioactive Compounds*, ed. M. R. S. Campos, Woodhead Publishing, 2019, pp. 265–288.
278 A. Paiva, R. Craveiro, I. Aroso, M. Martins, R. L. Reis and A. R. C. Duarte, *ACS Sustain. Chem. Eng.*, 2014, **2**, 1063–1071.
279 Y. Dai, J. van Spronsen, G.-J. Witkamp, R. Verpoorte and Y. H. Choi, *Anal. Chim. Acta*, 2013, **766**, 61–68.
280 Y. Liu, J. B. Friesen, J. B. McAlpine, D. C. Lankin, S.-N. Chen and G. F. Pauli, *J. Nat. Prod.*, 2018, **81**, 679–690.
281 K. Xu, Y. Wang, Y. Huang, N. Li and Q. Wen, *Anal. Chim. Acta*, 2015, **864**, 9–20.
282 J. F. Zayas, in *Functionality of Proteins in Food*, ed. J. F. Zayas, Springer Berlin Heidelberg, Berlin, Heidelberg, 1997, pp. 260–309.
283 F. J. Marti-Quijal, S. Zamuz, I. Tomašević, B. Gómez, G. Rocchetti, L. Lucini, F. Remize, F. J. Barba and J. M. Lorenzo, *LWT*, 2019, **110**, 316–323.
284 K. Dooleweerdt, H. Birkedal, T. Ruhland and T. Skrydstrup, *J. Org. Chem.*, 2008, **73**, 9447–9450.
285 V. Stefov, B. Šoptrajanov, F. Spirovski, I. Kuzmanovski, H. D. Lutz and B. Engelen, *J. Mol. Struct.*, 2004, **689**, 1–10.

286 S. Zhang, H.-S. Shi, S.-W. Huang and P. Zhang, *J. Therm. Anal. Calorim.*, 2013, **111**, 35–40.
287 Cicci, Sed and Bravi, *Chem. Eng. Trans.* 2017, **57**
288 C. A. Suarez Ruiz, J. Kwaijtaal, O. C. Peinado, C. van den Berg, R. H. Wijffels and M. H. M. Eppink, *ACS Sustainable Chem. Eng.*, 2020, **8**, 2441–2452.
289 R. K. Desai, M. S. Fernandez, R. H. Wijffels and M. H. M. Eppink, *Front Bioeng Biotechnol*, 2019, **7**, 284.
290 S. Y. Lee, P. L. Show, T. C. Ling and J.-S. Chang, *Biochem. Eng. J.*, 2017, **124**, 26–35.
291 D. Moldes, E. M. Rojo, S. Bolado, P. A. García-Encina and B. Comesaña-Gándara, *NATO Adv. Sci. Inst. Ser. E Appl. Sci.*, 2022, **12**, 2391.
292 J. Pang, X. Sha, Y. Chao, G. Chen, C. Han, W. Zhu, H. Li and Q. Zhang, *RSC Adv.*, 2017, **7**, 49361–49367.
293 N. Li, Y. Wang, K. Xu, Y. Huang, Q. Wen and X. Ding, *Talanta*, 2016, **152**, 23–32.
294 N. Nunes, J. M. Leça, A. C. Pereira, V. Pereira, S. Ferraz, M. C. Barreto, J. C. Marques and M. A. A. P. de Carvalho, *Algal Research*, 2019, **42**, 101603.
295 T. Nomura, M. Kikuchi, A. Kubodera and Y. Kawakami, *Biochem. Mol. Biol. Int.*, 1997, **42**, 361–370.
296 S. Mohamadnia, O. Tavakoli, M. A. Faramarzi and Z. Shamsollahi, *Aquaculture*, 2020, **516**, 734637.
297 B. Aslanbay Guler, I. Deniz, Z. Demirel, O. Yesil-Celiktas and E. Imamoglu, *Biochem. Eng. J.*, 2020, **153**, 107403.